Optimization of red fluorescent marker proteins guided by evaluation of structure-function relations

Ph.D. thesis

Dissertation

zur Erlangung des Doktorgrades Dr. rer. nat.
an der Fakultät für Naturwissenschaften
der Universität Ulm

vorgelegt von

Diplom-Biologin Silke Gundel

aus Dillingen/Donau

2009

Optimization of red fluorescent marker proteins guided by evaluation of structure-function relations

Ph.D. thesis

Titelbild (von oben nach unten):
1. Fotografische Aufnahme von *Anemonia sulcata* var. *rufescens*
2. Fluoreszenzmikroskopische Aufnahme von *E. coli* Kolonien (BL21DE3), die das Chromoprotein apCP558 (rechts) und dessen fluoreszierende Mutante apCP558-L13M/C143S (links) rekombinant exprimieren
3. Mikroskopische Aufnahme von psRFP-Kristallen nach Anregung der roten Fluoreszenz (links) und im Durchlicht (rechts)
4. Schematische Darstellung des schaltbaren Chromophors von psRFP im An-Zustand (*cis* Konformation, magenta) und Aus-Zustand (*trans* Konformation, blau)
5. Schematische Darstellung der Struktur eines asRFP-Monomers

Der besten Familie

Die Hartnäckigen gewinnen die Schlachten.

Napoleon I. Bonaparte

Amtierender Dekan der Fakultät für Naturwissenschaften:

Prof. Dr. Peter Bäuerle

Erstgutachter:

Prof. Dr. Klaus-Dieter Spindler

Zweitgutachter:

Prof. Dr. Wolfgang Weidemann

Tag der mündlichen Prüfung :

27. November 2009

Eidesstattliche Erklärung

Ich erkläre hiermit, dass ich die Arbeit selbstständig und nur mit den angegebenen Hilfsmitteln angefertigt habe, und dass alle Stellen, die dem Wortlaut oder dem Sinn nach anderen Werken entnommen sind, durch Angabe der Quellen als Entlehnung kenntlich gemacht worden sind.

Ulm, den 27.07.2009

Table of contents

I. Introduction

1. A short story of nearly everything from bioluminescence to fluorescence

A popular speculation among scientists is the idea of bioluminescent light signals being a widespread form of communication on the Earth. Bioluminescence is the production and emission of light in the visible band of electromagnetic spectrum by a living organism. This luminous effect is the result of a chemical reaction during which chemical energy is converted to light energy. Its name is a hybrid word, originating from the Greek word *bios* for "living" and the Latin phrase for *lumen* "light". This form of luminescence is also called "cold light" because the light emission occurs almost 100 % efficient, nearly without loosing energy as heat. In the bioluminescent organisms typal components have to come together to produce light in an enzymatic oxidative reaction – the enzyme luciferase and its substrate luciferin (named after Lucifer, the fallen angel of light), oxygen and other factors depending on the organism, for instance ATP, Ca^{2+} or Mg^{2+}.

In this connection, valence electrons of the luciferin are raised up to an excited energy state. When they fall back in their ground state, light will be emitted. After the reaction, the exhausted substrate luciferin must be new delivered.

In nature, there is an amazing diversity of organisms that emit light including bacteria (Miller et al., 2005; Nealson & Hastings, 1979, 2006), fungi (Molitoris, 1999), phytoplankton (Malkiel et al., 1999), molluscs (Ohmyia et al., 2005; Shimomura et al., 1972), fishes (Herring, 1978) and insects (Case, 1984). Bioluminescent signals serve as multifaceted functions. They are used for recognition of members of their own species for reproduction purpose (Lloyd, 1977), for prey attraction (Harvey, 1952) or for defence against predators (Hastings et al., 2005). Using light signals allow the organisms to camouflage themselves and escape or enable them to see in the dark (Herring, 1978). As pervasive as bioluminescent species are on Earth, there are no glowing plants or higher vertebrates known (excepting fish) and only few of freshwater bioluminescent organisms noted. Most frequently appearance of living light is in the oceans (Herring, 1977). One fascinating example of bioluminescence which appeals to observers from ancient up to present times is shown by some cnidarian species.

The first description of the bioluminescence of jellyfish was bequeathed from Pliny the Elder (23-79 CE). He depicted the light of *pulmo marinus* (sea lung), a

purple jellyfish and demonstrated the first application of glowing jellyfish: "Rub a piece of wood with the fish called Pulmo Marinus, it will seeme as though it were on fire; in so much as a staffe so rubbed or besmeared with it, may serve instead of a torch to give light before one" (Harvey, 1957). Most cnidarian bioluminescence is used as an aposematic signal to frighten or deter predators such as fishes and crustaceans (Harvey, 1952; Herring 1978; Morin 1976, 1983). The most prominent bioluminescent system arises from the jellyfish *Aequorea victoria* and will be highlighted regarding its green glowing secondary emitter. In this case, the green glow is caused by another fascinating light phenomenon widespread within cnidarian species: fluorescence. It is generally defined as a photoluminescent event, according to light as trigger for luminescence. The absorbed energy is supplied by electromagnetic radiation. This light absorption elevates an electron of an atom from a lower energy state into an "excited" higher energy state. When it falls back to a lower energy state, then the electron releases the energy in the form of light (luminescence) of longer, red-shifted wavelengths. George Gabriel Stokes (1819-1903) invented the term "fluorescence" in his 1852 publication. The term was given as a description of the characteristic of the mineral fluorite, composed of calcium fluoride, which emits light in the visible part oft the electromagnetic spectrum when illuminated with "invisible radiation" (UV radiation).

With the first description of this green fluorescent substance in the hydromedusa *Aequorea victoria* (Murbach & Shearer, 1902) the unique success story of green fluorescent protein (GFP) started (Davenport & Nicol, 1955). This bioluminescent hydrozoan jellyfish, which is responsible for the "glowing genes" revolution, is generally found off the West Coast of North America in the Pacific Ocean. The medusa part of life cycle can grow up to 7-10 cm in diameter and lives only for six months or less. Its preferred diet is other jellies and as a cruising predator they swim a lot to catch prey using a rowing mode of propulsion. This jellyfish species is capable to fluoresce when they are agitated. *Aequorea victoria* is able to produce flashes of blue light in a bioluminescent reaction by a fast release of calcium (Ca^{2+}) which interacts with the photoprotein aequorin. The blue light emitted is in turn converted to green by the now famous green fluorescent protein of Aequorea victoria (avGFP). This species is an example for combined bioluminescent and fluorescent reaction. Both aequorin and avGFP are important tools used in fields of cell biology research.

The "glowing genes" encoding for fluorescent proteins (FPs) provide several advantages in comparison with procedures using luciferases. They possess the exclusive capability to synthesize their chromophores (part of the protein that is responsible for its colour) in autocatalytic reactions in the absence of additional cofactors or substrates aside from molecular oxygen (Chalfie et al., 1994; Cubitt et al., 1995; Heim et al., 1994; Inouye & Tsuji, 1994; Prasher et al., 1992; Tsien, 1998). Only light radiation of specific wavelength is required to let them glow. The usefulness of FPs is caused by their potential to be fused to target molecules, producing fluorescence without limiting their capability to function or moving behaviour in living cells. Scientists are enabled to monitor and image biological processes in genetics, medicine research, molecular and cellular biology or biotechnology. Their significance as "microscopes of the new millennium" (Zimmer, 2005) becomes obvious regarding the number of peer-reviewed publications during the last 15 years. In 1994 only ten papers released in all had "green fluorescent protein" (GFP) in the title and/or abstract. After Chalfie's milestone paper in 1994 about "Green fluorescent proteins as a marker for gene expression" (nowadays one of the 20 most-cited publications in the field of molecular biology and genetics) the revolution had been started. Within four years the number of papers increased up to 500 in 1998 concerning this topic. In 2005 more than 9,000 articles have been published with reference to this domain, up to round about 20,000 in these days of genesis of this PhD thesis.

The story of GFP revolution has several acts: the discovery of GFP (Shimomura et al., 1962), its cloning (Prasher et al., 1992) the expression of fluorescing GFP in a key model organism (Chalfie et al., 1994) and the development of GFP-like proteins into a universal set of genetic tags (Tsien, 1998).

Therefore, in 2008, Osamu Shimomura, Martin Chalfie and Roger Tsien awarded the chemistry Nobel Prize "for the discovery and development of the green fluorescent protein, GFP" (press release of the Royal Swedish Academy of Sciences, 8. October 2008).

2. Overall three-dimensional structure of GFP-like proteins

From the first protein crystals of avGFP in 1974 (Morise et al., 1974) over reported diffraction patterns 14 years later (Perozzo et al., 1988), it totally took 22 years until the structure of wild-type avGFP was solved (Yang et al., 1996).

Furthermore, the solution of avGFP S65T mutant was achieved in 1996 (Ormö et al., 1996). Figure 1 shows a regular β-barrel structure, consisting of 11 antiparallel β-sheets revealed by X-ray crystallography studies (Ormö et al., 1996; Tsien, 1998; Yang et al., 1996). The dimension of the cylinder is about 30 Å in diameter and about 40 Å in length. A central α-helix pervades the β-can between β-sheet 3 and 4 from the top to the ground and contains in its middle the fluorescent chromophore (Phillips, 2006; Shaner et al., 2007). In the geometric centre of the container and flanked by α-helices and loops that form caps on the end of the cylinder, the chromophore is well-protected against unfolding by heat or denaturants (Phillips, 2006). It can be predicted that all homologous group members within the GFP-like protein family represent the same highly conserved overall three-dimensional structure of β-can (Nienhaus & Wiedenmann, 2009).
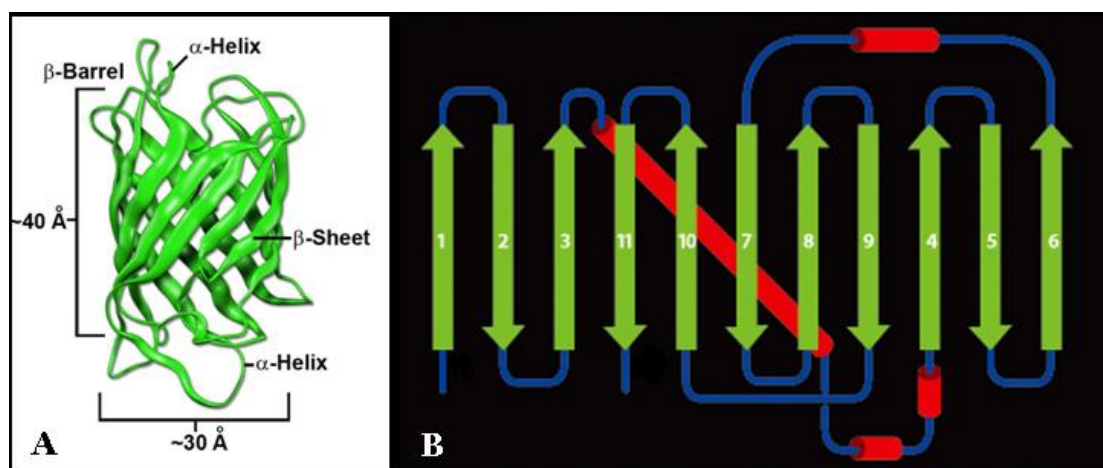
Figure 1. Overall three-dimensional structure of avGFP (A) and a topology diagram of the folding pattern (B). The β-barrel structure consists of 11 antiparallel β-sheets (green coloured in A and B). Four α-helices are indicated in red (B). The α-helix between β-sheet 3 and 4 contains in its middle the chromophore (figure A modified from Shaner et al., 2007; figure B modified from Zimmer, www.conncoll.edu/ccacad/zimmer/GFP-ww/GFP-1.htm).

Structural homologs of GFP-like proteins can be found in porin, which has not 11 but 16 antiparallel β-strands and no caps at the ends of the cylinder (Kreusch et al., 1994). Furthermore, streptavidin is formed by an eight-stranded β-barrel (Hendrickson et al., 1989). The extracellular matrix protein nidogen from mammalian cells also resembles in its overall structure the 11-stranded β-can fold (Hopf et al., 2001; Kvansakul et al., 2001; Liddington, 2001). The absence of a

chromophore results in non-existence of colour. Thus, in the following chapters the "light in the can", its formation and variations of the chromophore will be illustrated.

3. GFP chromophore: formation and properties

GFP technology offers a unique feature: its outstanding capability to synthesize the chromophore in an autocatalytic reaction in the absence of additional cofactors or substrates aside from molecular oxygen (Chalfie et al., 1994; Cubitt et al., 1995; Heim et al., 1994; Inouye & Tsuji, 1994; Prasher et al., 1992; Tsien, 1998). Residues Ser65-Gly66-Tyr67 are forming the chromophore of avGFP (Cody et al., 1993; Ormö et al., 1996). In figure 2 is the assembly of the green chromophore shown, a 4-(p-hydroxybenzylidene)-5-imidazolinone, which occurs by successional cyclization, dehydration and oxidation steps within typical time scale (Tsien, 1998).
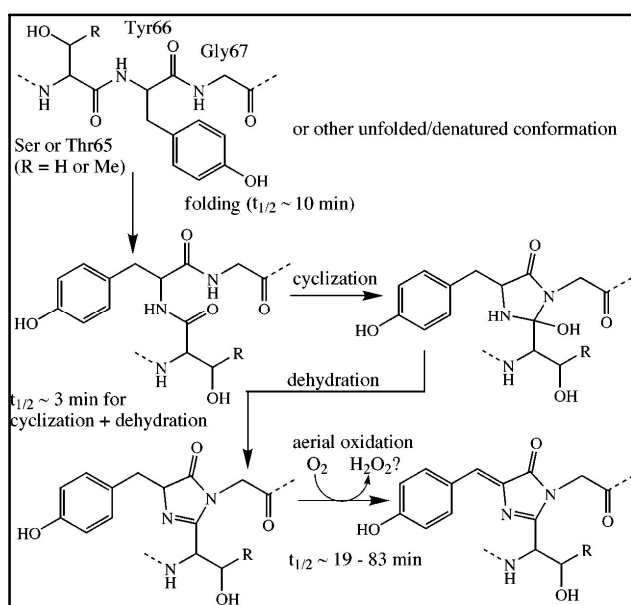
Figure 2. Formation mechanism for the avGFP chromophore. After folding of the peptide chain in native conformation, heterocyclization to imidazolinone occurs and a water molecule is released. Within this intermediate the Cα-Cβ bond of Tyr66 is oxidized with hydrogen peroxide discharge and the conjugated π-electron-system of the green chromophore is formed (figure from Tsien, 1998).

First, the peptide chain folds into a native conformation, so that the amide of Gly67 is in close proximity of the carbonyl group of Ser65 (Barondeau et al., 2003). Thereby, the nucleophilic attack is eased, the imidazolinone could be formed and a water molecule is released. Then, the occurring intermediate after cyclization is dehydrogenated at the Cα-Cβ bond of Tyr66 under the influence of molecular oxygen. Finally, the p-hydroxybenzyl-ring of Tyr66 is conjugated with the imidazolinone and the π-electron-system of the green chromophore is built up (Cubitt et al., 1995; Tsien, 1998). Essential for a high fluorescence quantum yield is the coplanar fixation of the

two-ring-system within the chromophore provided by bound water molecules and circumjacent residues (Nienhaus & Wiedenmann, 2009). Important residues for the autocatalytic reaction are Arg96 and Glu222 (Barondeau et al., 2005; Sniegowski et al., 2005; Wachter et al., 2007; Wood et al., 2005).

Regarding the spectral properties of avGFP, two absorption bands are described, a major peak at 395 nm and a minor peak at 475 nm representing the neutral/protonated and anionic/deprotonated form of the chromophore. Excitation of the anionic chromophore leads to green fluorescence emission at 508 nm. Surprisingly, excitation of the neutral form also results in green emission of the anionic chromophore instead of expected blue light emission. The reason is excited state proton transfer, where the excited neutral *p*-hydroxybenzyl-ring of Tyr66 releases a proton, which is transferred to acceptor residue Glu222. In this way, the π-electron-system is enlarged and the green emission results from anionic chromophore (Brejc, et al., 1997; Chattoraj et al., 1996; Nienhaus & Wiedenmann, 2009; Remington, 2006; Stepanenko et al., 2008; Tsien, 1998).

4. Variations of the chromophore among GFP-like proteins

Besides the avGFP chromophore, nowadays seven chemically distinct chromophores have been identified. Figure 3 presents their different structural displays.
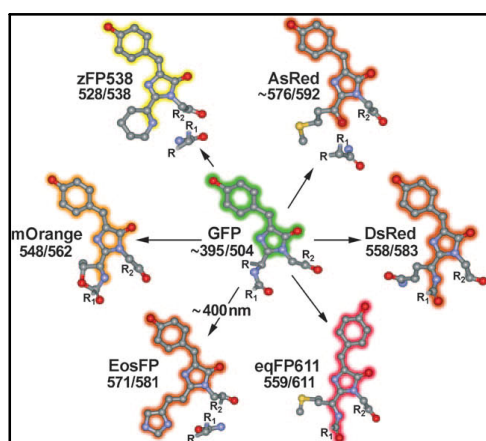
Figure 3. Variations of the GFP chromophore. Among several GFP-like proteins with different colours variety of chromophore architecture can be observed. According to their emission colour the conjugated π-electron systems are coloured. Below the common names of GFP-like proteins, their excitation and emission wavelengths are indicated in nanometres (figure from Nienhaus & Wiedenmann, 2009).

The mechanism of chromophore formation is highly conserved among GFP-like proteins. First of all, the basic green chromophore is synthesized as described above, which is afterwards modified. The tripeptide Ser-Tyr-Gly forms the chromophore, whereas the first amino acid can be altered, but the other two should be preserved as

tyrosine and glycine (Nienhaus & Wiedenmann, 2009; Remington, 2006; Shaner et al., 2007).

DsRed (Matz et al., 1999) shows in contrast to avGFP red-shifted spectra caused by an enlarged system of conjugated double bonds within its Gln-Tyr-Gly chromophore. This extended GFP-like chromophore, with two strongly electron-withdrawing double bonds results from an additional autocatalytic dehydrogenation of the α C-N bond of Gln65 and is in *cis* conformation (Gross et al., 2000; Wall et al., 2000; Yarbrough et al., 2001).

The non-fluorescent chromoprotein Rtms5 from *Montipora efflorescens* reveals the DsRed-like chromophore in unusual *trans* conformation and is nonplanar (Prescott et al., 2003).

In far-red fluorescent protein eqFP611 (Wiedenmann et al., 2002b) the DsRed-like chromophore (here Met-Tyr-Gly) also adopts a *trans* configuration, but it is coplanar in contrast to Rtms5 chromophore (Petersen et al., 2003).

Other modifications just as UV-light irradiation can also cause red emitting chromophore. In the photoconvertible proteins Kaede (Ando et al., 2002) and EosFP (Nienhaus et al., 2005, 2006; Wiedenmann et al., 2004b) with His-Tyr-Gly chromophore, strong illumination results in cleavage of protein backbone followed by formation of an additional double bond (Mizuno et al., 2003) (detailed description in chapter 6.2).

The yellow fluorescent protein zFP538 from *Zoanthus* contains a three-ring chromophore (Remington et al., 2005). Lys65, the first position of the chromophore triplet, autocatalytically forms a third heterocycle. It is supposed, that the polypeptide backbone is cleaved after a transimination reaction in which a transiently appearing DsRed-like acylimine is attacked by the terminal amino group of Lys65 (Nienhaus & Wiedenmann, 2009; Remington, 2006).

In mOrange, a monomeric DsRed variant emitting at 562 nm (Shaner et al., 2004), the Thr-Tyr-Gly chromophore also undergoes a second oxidation step to produce an acylimine linkage in the polypeptide backbone. The cyclization of Thr66 forms an oxazole ring. Within the nonplanar chromophore the hydroxyl group of Thr66 attacks the preceding carbonyl group (Nienhaus & Wiedenmann, 2009; Shu et al., 2006).

Crystallography studies of AsRed, (asFP595 A143S mutant; Yanushevich et al., 2002) and KFP display a break in the peptide backbone between Cys64 and Met65

within chromophore maturation, which leads to a novel *trans* nonplanar chromophore structure: C=O group at Cα of Met65 in conjugation with GFP-like chromophore (Andresen et al., 2005; Quillin et al., 2005; Wilmann et al., 2005; Yampolsky et al., 2005).

Generally, the DsRed-like chromophore seems to be widespread among red-shifted fluorescent proteins in coplanar orientation with high fluorescence quantum yield and in non-fluorescent chromoproteins with *trans* nonplanar conformation.

Spectral variety of GFP-like proteins is induced by a few chemically different chromophores in combination with interactions to the surrounding, which leads to an effect on the π-electron-system resulting in influences on absorption and emission spectra. Depending on the chromophore environment, there are existing different conformations (*cis/trans*) and protonation states. Chromophore charge is responsible for the colouration (Malo et al., 2008; Matz et al., 1999; Wachter et al., 1998), whereas fluorescence quantum yield depends on conformation state (Adam et al., 2008; Andresen et al., 2005; Stiel et al., 2008; Vogt et al., 2008).

5. Red fluorescent GFP-like proteins

Even though Tsien created an extended colour palette of GFP variants, he was not able to design an avGFP with a red chromophore. Red fluorescent proteins (RFPs) are indispensable for utilization because some properties of *Aequorea victoria* GFP and its variants are disadvantageous for wide application and demand further improvement. In particular, excitation by cytotoxic light and the restricted range of emission wavelengths pose severe limitations for many applications. For cellular studies, red fluorescent proteins are particularly desirable, because background fluorescence of cellular tissue, media, culture ware and certain chemical compounds is markedly reduced in the red spectral region. Accordingly, the FP emission can be more easily distinguished from the background. The longer wavelengths of red light cause less scattering, and thus the light is transmitted more efficiently through tissue, resulting in clearer images especially in whole-body imaging experiments (Deliolanis et al., 2008; Shcherbo et al., 2007, 2009a). Low-energy excitation light is also less cytotoxic and therefore ideal suitable for long-term monitoring studies (Schäfer et al., 2008; Stadtfeld et al., 2008). Finally, semiconductor detection systems are more sensitive in the red spectral region. Another attractive possibility is the application of red FPs in combination with other

coloured FPs in FRET experiments (Fluorescence or Förster Resonance Energy Transfer; Förster, 1948) or multicolour labelling (Campbell et al., 2002; Fradkov et al., 2002; Kredel et al., 2009; Merzlyak et al., 2007; Shcherbo et al., 2009a/b). Hence, red fluorescent proteins have in addition to well-established FPs a great potential to be used as *in vivo* markers of protein localization and interaction and gene activity in many fields of cell biology research (Kiessling, 2008; Stepanenko et al., 2008; Zhang et al., 2002).

The demand for RFPs motivated explorers to give this direction to their research. But the question was: "How to reach the goal of allocation RFPs?" Two main reasons retarded their discovery: First, fluorescent pigments of corals were classified spuriously to biliproteins from algae like phycocyanin or phycoerythrin. Due to their specific chromophore structure (tetrapyrroles added to heteromultimeric apoproteins), these dyes were not considered to be applied effortlessly as marker proteins. Second, the scientific community was convinced, that GFP-like proteins appear merely as green secondary emitters in bioluminescent organisms. For instance, other similar green fluorescent proteins that operate as light emitter of *in vivo* bioluminescence were found in a number of bioluminescent coelenterates, e.g. the hydroid *Obelia*, the sea pansy *Renilla* and the sea pens *Ptilosarcus* and *Pennatula* (Hastings & Morin, 1969; Morin & Hastings, 1971a/b; Wampler et al., 1971, 1973; Cormier et al., 1973, 1974; Morin, 1976). All these publications endorsed the widespread conception that GFPs, in general, serve as secondary emitters in the bioluminescence reaction of marine cnidarians. Thus, the search has been limited to species exhibiting bioluminescence. Therefore, red fluorescent pigments in non-bioluminescent cnidarians were not taken into account as promising candidates for marker proteins at that time.

In 1999, the only known GFP homolog was the green fluorescent protein from *Renilla reniformis* at that time (Ward & Cormier, 1979), Matz and co-workers published their milestone paper about "Fluorescent proteins from nonbioluminescent Anthozoa species" (Matz et al., 1999) and paved the way for GFP-like proteins that are not obligatory functionally linked to bioluminescence and exhibit different colours. For the first time, a red emitting fluorescent protein (drFP583, also called "DsRed") was demonstrated. They also hypothesized that the fluorescence of reef corals could be attributed to GFP-like proteins. Contemporaneous, GFP-like proteins were cloned from non-bioluminescent sea anemones, from the Mediterranean Sea.

These proteins included red fluorescent and non-fluorescent chromoproteins (Wiedenmann, 1997, 2000; Wiedenmann & Lorenz, 2000; Wiedenmann et al., 1999, 2000a, 2000b, 2002a).

There are existing two different strategies to obtain red-emitting FPs: A) Screening of naturally occurring fluorescent proteins to discover promising candidates with extraordinary properties in potential applications as marker proteins. Besides DsRed, another promising RFP, eqFP611, was cloned from the sea anemone *Entacmaea quadricolor* and is the so far most red-shifted natural emitter with an emission maximum at 611 nm (Wiedenmann et al., 2002b). Other sources for orange-red fluorescing proteins were identified among scleractinian corals (Dove et al., 2001; Karasawa et al., 2004; Labas et al., 2002), ceriantharians (Ip et al., 2004) and actiniarian sea anemones (Wiedenmann et al., 2004a, 2007).

B) Evolution of red fluorescent proteins by mutagenesis of chromoproteins is another promising strategy to develop novel tools for life science research. Non-fluorescent, red absorbing chromoproteins were used as a source of far-red fluorescent proteins emitting between 615-645 nm (Gurskaya et al., 2001a). This group also generated a mutant of cyan emitter dsFP483 that demonstrated dual colour (cyan and red) fluorescence (Gurskaya et al., 2001b). The farthest red-shifted fluorescence described to date for GFP-like proteins shows a variant from a blue chromoprotein emitting at 663 nm. Unfortunately, its fluorescence is highly sensitive to light irradiation (Shkrob et al., 2005).

However, the utility of anthozoan RFPs is currently still compromised by disadvantageous properties such as tetramerization, aggregation, temperature-sensitivity of folding and photostability as well as the presence of green emitting states (Shkrob et al., 2005; Wiedenmann et al., 2002b; Yanushevich et al., 2002). To fully exploit the superior potential of RFPs, further optimization of these novel markers is necessary. An improvement of DsRed was the transformation of the obligate tetramer using extensive mutagenesis into a monomer keeping its fluorescence properties (Baird et al., 2000; Campbell et al., 2002). Deriving from this new monomeric protein, Tsien and his associates generated novel "fruit" FPs ranging their colours in the visible light spectrum from "honeydew" to "plum" by *in vitro* (Shaner et al., 2004) and *in vivo* (Wang et al., 2004) directed evolution. Furthermore, folding optimized, dimeric or rather monomeric and more red-shifted mutants of eqFP611 could be generated (Kredel et al., 2008, 2009; Nienhaus et al.,

2008; Wiedenmann et al., 2005). Moreover, 16 years after its cloning, the first substantially red emitting variant of avGFP (emission maximum at 585 nm) could be created via mutagenesis (Mishin et al., 2008). Nevertheless, the end of the rope in the field of marker protein technology has not yet been reached. Further developments in the area of novel tools for life science research are optical highlighter proteins.

6. Advanced optical highlighters – The next generation of GFP-like proteins

A widely used technique for live cell imaging is avGFP photobleaching, e.g. FRAP (**F**luorescence **R**ecovery **A**fter **P**hotobleaching) and FLIP (**F**luorescence **L**oss **I**n **P**hotobleaching) (White & Stelzer, 1999; Lippincott-Schwartz et al., 2001, 2003). These techniques only allow general monitoring of intracellular protein movement, but no direct tracking of change of location within a living cell. For the first time, this demand could be satisfied with the introduction of optical highlighter fluorescent proteins. This next generation of GFP-like proteins reacts in different manners to light-induction. Therefore, they can be classified according to the underlying mechanisms in three main rubrics:

6.1 Photoactivatable fluorescent proteins (PAFPs)

This class of monomeric fluorescent proteins changes its fluorescence intensity partially in combination with a shift to longer wavelength emission in response to irradiation with light of a specific wavelength and intensity. Figure 4 illustrates exemplified for PA-GFP the process of photoactivation that is based on irreversible change from the neutral (protonated) to anionic (deprotonated) chromophore form.
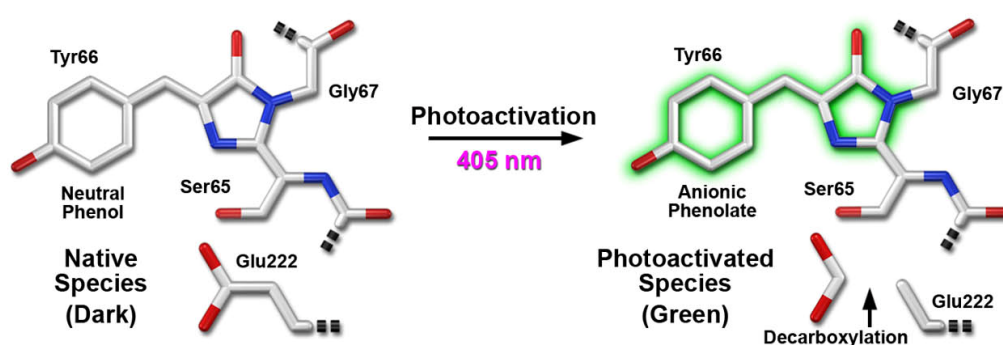
Figure 4. Schematic diagram of photoactivation mechanism in PA-GFP. Intense UV-light exposure (~ 400 nm) results in decarboxylation of Glu222 and irreversible conversion of the neutral to anionic chromophore state (figure from Shaner et al., 2007).

The first photoactivatable FP was generated by mutating avGFP. The predominantly, non-fluorescent neutral status of the chromophore of the PA-GFP (for **p**hoto and **a**ctivatable) is caused by the substitution of histidine for threonine at position 203 (Thr203His) (Patterson & Lippincott-Schwartz, 2002). Almost no fluorescence can be observed when PA-GFP is excited at wavelengths corresponding to the excitation spectrum of the anionic chromophore form (480-510 nm). Intense UV-light illumination (~ 400 nm) leads to decarboxylation of Glu222 and causes irreversible conversion of the chromophore from the neutral to anionic state with excitation and emission maximum at 504 and 517 nm and a 100-fold increase in the green fluorescence of the anionic form (Henderson et al., 2009; Henderson & Remington, 2006; Lukyanov et al., 2005; Shaner et al., 2007; Stepanenko et al., 2008; Wiedenmann & Nienhaus, 2006).

A **p**hoto**s**witching **c**yan **f**luorescent **p**rotein, designated PS-CFP, was created by the introduction of 9 mutations in the monomeric, colourless *Aequorea coerulescens* protein (Chudakov et al., 2004; Gurskaya et al., 2003). In contrast to PA-GFP, PS-CFP shows a significant level of fluorescence in non-activated state (emission maximum = 468 nm). Intense UV-light irradiation (~ 400 nm) switches emission from predominantly cyan to mainly green (511 nm), yielding a 300-fold increase in the green emission and a 5-fold decrease in cyan emission for a 1500-fold change in the optical contrast (Chudakov et al., 2004; Henderson & Remington, 2006). The irreversible photoactivation mechanism is suspected to be the same as in PA-GFP (Shaner et al., 2007).

PAmRFPs are three red **p**hoto**a**ctivatable variants of **mRFP**1 (Campbell et al., 2002) with substitutions at positions 148, 165 and 203 (numbering is based on avGFP). PAmRFP1-1 is the brightest variant and shows initially weak cyan fluorescence. Upon stimulation with 380 nm light, it presents with excitation and emission maxima at 578 and 605 nm a 70-fold increase in red fluorescence. The photoactivation mechanism has not been completely understood. It may be involved a *cis-trans* isomerization of the chromophore resulting in conformational change from non-fluorescent (*trans*) to fluorescent (*cis*) state. Concerning the fluorescent state the anionic chromophore might be stabilized through a mechanism suggested for PA-GFP (Verkusha & Sorkin, 2005).

Based on **mCherry** (Shaner et al., 2004), an improved variant of mRFP1, other red fluorescent **p**hoto**a**ctivatable proteins were produced. The best evaluated mutant PAmCherry1 contains 10 mutations compared to mRFP1 and shows after UV-light illumination (~ 400 nm) red fluorescence with excitation and emission maximum at 564 and 595 nm. Substitutions are carried out amongst others at positions 148, 165, 168 and 203 (numbering is in accordance to avGFP), which are spatially close to the chromophore (Subach et al., 2009). Compared to PAmRFP1, it shows 10-fold increase in brightness after photoactivation, besides fast maturation, high pH- and photostability. Regarding the photoactivation mechanism it is supposed that also a pH-dependent decarboxylation of Glu222 is involved.

6.2 Photoconvertible fluorescent proteins (PCFPs)

This process results in red-shifted emission caused by irreversible conversion of the green to a red chromophore after illumination with UV- or blue light. The emission maxima of PCFPs range between 507-519 nm before and 573-593 nm after photoconversion. The chromophore of these PCFPs is always formed by the tripeptide His62-Tyr63-Gly64 (the residue numbering relates to EosFP; Wiedenmann et al., 2004b). The unique positioning of His62 is the structural basis for the photoconversion (Nienhaus et al., 2005). As illustrated for the photoconverter EosFP, figure 5 shows that UV-light irradiation induces a cleavage of protein backbone between the amide nitrogen and the Cα of His62. Thus, a double bond could be formed between the Cα and Cβ of His62. This leads to an extended π-electron conjugation of Tyr63 to the imidazole ring of His62 and results in red shift of emission maximum (Lukyanov et al., 2005; Shaner et al., 2007; Stepanenko et al.,

2008; Wiedenmann & Nienhaus, 2006). Except for a few (Chudakov et al., 2007; Gurskaya et al., 2006; Nienhaus et al., 2006), this type of fluorescent proteins usually possesses a tetrameric oligomerization state (Adam et al., 2008; Ando et al., 2002; Labas et al., 2002; Shagin et al., 2004; Tsutsui et al., 2005; Wiedenmann et al., 2004b).
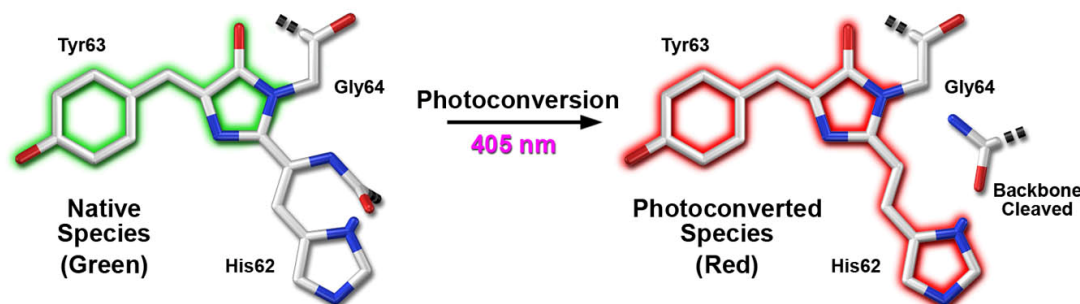
Figure 5. Schematic diagram of photoconversion mechanism in EosFP. Intense UV-light exposure (~ 400 nm) results in cleavage of protein backbone between the amide nitrogen and the Cα of His62. A double bond could be formed between the Cα and Cβ of His62. This extends the π-electron system of Tyr63 to the imidazole ring of His62 and leads to a red shift of fluorescence (figure from Shaner et al., 2007).

The first published representative of PCFPs was Kaede (named after the Japanese maple leaf), cloned from the stony coral *Trachyphyllia geoffroyi* (Ando et al., 2002). Complete photoconversion results in a more than 2000-fold increase in the red/green fluorescence ratio.

Based on Kaede as lead structure, another PCFP was generated: KikGR. This protein is derived from a stony coral parent fluorescent protein KikG, which was cloned from *Favia favus*, the Japanese name of which is "**Kik**ume-ishi" and shows **g**reen fluorescence. KikGR fluorescence is several-fold brighter than Kaede fluorescence when recombinant expressed. Furthermore, it demonstrates 3-fold faster photoconversion in contrast to Kaede (Tsutsui et al., 2005).

Cloned from the stony coral *Lobophyllia hemprichii*, EosFP bears the name of the goddess of dawn in Greek mythology. EosFP, its dimeric and monomeric variants and tandem dimers show similar spectroscopic properties as Kaede. However, the expression of monomeric EosFP variant is limited to 30°C. That is the reason why pseudomonomeric tandem dimers have been developed, which overcomes this disadvantage in application. (Nienhaus et al., 2005, 2006; Wiedenmann et al., 2004b; Wiedenmann & Nienhaus, 2006).

Recently, a new variant of tetrameric EosFP was introduced: IrisFP, named after the Greek goddess of the rainbow, possesses the single mutation Phe173Ser. Additionally to known photoconversion from green to red, it incorporates *cis-trans* phototransformation of the chromophore. Both green and red form of IrisFP can be reversible photoswitched by light illumination between a fluorescent on- and a non-fluorescent off-state as later described for photoswitchable fluorescent proteins. After irradiation of the anionic chromophore (488 nm and 532 nm for the green and the red form) the fluorescence is turned off. Fluorescence is switched on again by excitation of the neutral chromophore (405 nm for the green and 440 nm for the red form) (Adam et al., 2008; Nienhaus & Wiedenmann, 2009).

Other UV-converted red FPs have been found in *Montastrea cavernosa* (mcavRFP), *Ricordea florida* (rfloRFP) and *Dendronephtyha* sp. (dendRFP) (Labas et al., 2002; Shagin et al., 2004; Verkusha & Lukyanov, 2004). Hence, they exhibit "fluorescent timer" phenotype like DsRed mutant E5 (changing fluorescence colour from green to red over time) (Terskikh et al., 2000), it is not surprisingly that dendRFP originally was described as a green fluorescent protein (Labas et al., 2002).

Dendra (named after **Dend**ronephthya sp., **r**ed **a**ctivatable) is a monomeric variant from dendRFP described above. It combines high photoconversion contrast (1000-4500-fold) from green to red with high photostability and the capability to be converted by less phototoxic blue light (488 nm). It is supposed that residue 116 could be involved in the convertibility by blue light. Comparison with Kaede, EosFP and KikGR shows that only Dendra has Gln instead of Asn in position 116 with a longer side chain, which can contact the protein backbone near the chromophore-forming residue His62 (the residue numbering is in accordance to EosFP). In this way, the contact possibly facilitates a break of the peptide backbone and the red chromophore formation after low-energy blue light illumination (Gurskaya et al., 2006; Stepanenko et al., 2008). The improved version Dendra2 comprises single mutation Ala224Val, which results in a brighter fluorescence both before and after photoconversion and an efficient chromophore maturation (Chudakov et al., 2007).

6.3 Photoswitchable fluorescent proteins (PSFPs)

Characteristic for this class of optical highlighters is the reversible on- and off-switching between a fluorescent and a non-fluorescent chromophore state. This occurrence is attributed to protonation/deprotonation in combination with

conformational changes between *cis-* and *trans* state of the chromophore. The reversibility can depend in some cases on the intensity and duration of light illumination (Chudakov et al., 2003a). Positive PSFPs switch from a dark state to a bright fluorescent state (Andresen et al., 2008; Chudakov et al., 2003a/b; Lukyanov et al., 2000; Stiel et al., 2008), whereas negative PSFPs show a decrease of fluorescence intensity after irradiation (Ando et al., 2004; Andresen et al., 2008; Henderson et al., 2007; Shaner et al., 2008; Stiel et al., 2007, 2008; Vogt et al., 2008). Furthermore, PSFPs can be distinguished between A) green and B) red emission colour.

A) Green-emitting PSFPs: Dronpa, a mutant of a GFP-like fluorescent protein that was cloned from *Pectiniidae* sp. coral, was named on the capacity of its fluorescence to vanish and reappear. "**Dron**" is a ninja term for vanishing and "**pa**" stands for **p**hoto**a**ctivation. Initially, this monomeric marker fluoresces green with excitation and emission maximum at 503 and 518 nm, respectively. When irradiated with blue light (470-510 nm) the anionic chromophore emits fluorescence at simultaneously quenching to non-fluorescent neutral chromophore. The green fluorescence emission vanishes upon further excitation. Dronpa is an example for a negative PSFP, in which the excitation wavelength for fluorescence emission is also inducing off-switching. Figure 6 shows that Dronpa can reversibly be switched on to the fluorescent form over 100-times by illumination with 405 nm light (Ando et al., 2004; Andresen et al., 2007; Habuchi et al., 2005; Henderson & Remington, 2006; Lukyanov et al., 2005; Shaner et al., 2007; Stepanenko et al., 2008; Wiedenmann & Nienhaus, 2006).
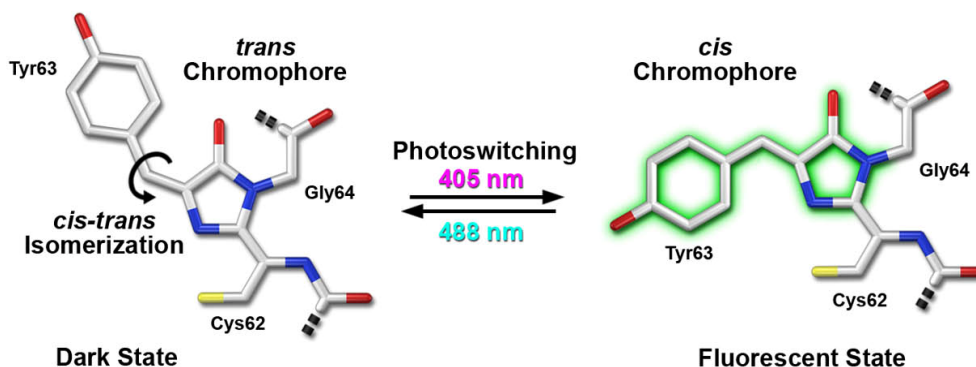
Figure 6. Schematic diagram of photoswitching mechanism in Dronpa. *Cis-trans* conformation changes of chromophore are induced by light irradiation with 405 and 488 nm, respectively. The *cis* conformation corresponds to the fluorescent state, whereas the *trans* conformation is related to the non-fluorescent dark state of chromophore. (figure from Shaner et al., 2007).

16

Developing monomeric teal FP (mTFP1) as a bright and stable version of the *Clavularia* cyan FP cFP484 (Ai et al., 2006), an intermediate known as mTFP0.7 was obtained, which shows similar photoswitching behaviour as Dronpa (Henderson et al., 2007).

rsFastLime, bsDronpa and Padron are improved genetically engineered variants of Dronpa, which combine excellent spectral properties as accelerated switching-off kinetics (~ 50-fold), enhanced optical contrast, considerably reduced photobleaching (~ 90%), but show only ~ 30% of Dronpa's fluorescence brightness (Andresen et al., 2008; Stiel et al., 2007). rsFastLime (Dronpa Val157Gly) and bsDronpa are both negative PSFPs. Characteristic and eponymous for bsDronpa is the blue-shifted, **b**road absorption **s**pectrum, that allows both excitation with 405 and 488 nm resulting in the same bright fluorescence. However, Padron is a positive PSFP and displays a reversed switching behaviour to that of Dronpa and its other variants. Due to this fact, Dronpa's name was also reversed into Padron (Andresen et al., 2008).

A reversible protonation of the chromophore is also involved in negative photoswitching process of cerFP505 from a deep-sea **cer**iantharian emitting at **505** nm. Blue light irradiation (~ 450 nm) causes a fast decrease of the green fluorescence. Adjacent illumination with UV-light (~ 400 nm) leads to on-switching. Its brightness and switching rate is comparable to that of Dronpa variants, but only 15% of all molecules can be switched off (Vogt et al., 2008).

B) Red-emitting PSFPs: Most prominent red emitting PSFPs are asFP595 (also known as asCP; Bulina et al., 2002 and asulCP; Labas, et al., 2002) and its genetically engineered variants KFP (asFP595 Ala148Gly) and KFP1 with 7 amino acid substitutions (Chudakov et al., 2003a/b). They all offer positive switching behaviour. The initial protein isolated from sea anemone *Anemonia sulcata* (Lukyanov et al., 2000) is non-fluorescent and becomes weakly red fluorescent ("kindles") upon less phototoxic green light irradiation (530-550 nm). The kindled protein then switches back to a non-fluorescent form or can be quenched by blue light illumination (~ 450 nm). The mutants present the same switching manner with improved brightness. But irradiation with on-switching light of great intensity or long duration causes irreversible kindling, reaching 50% of reversibly kindled protein brightness (Chudakov et al., 2003a). In contrast to PAmRFP1, kindled KFP1 is 5-fold brighter, but only half as bright as PAmCherry1 (Shaner et al., 2007; Stepanenko et al., 2008; Subach et al., 2009).

The kindling properties could be transferred to non-fluorescent chromoproteins from Anthozoa species *Heteractis crispa* (hcCP) and *Condylactis gigantea* (cgCP) (Gurskaya et al., 2001a). The variants show similar properties to KFP (Chudakov et al., 2003a; Stepanenko et al., 2008).

mApple0.5, an intermediate while evolving monomeric red fluorescent mApple from mRFP1 (Campbell et al., 2002), shows negative photoswitching capabilities repeatable over many cycles without substantial irreversible bleaching. The photoswitching illumination leads to a reduction in fluorescence emission ~ 50% (Shaner et al., 2008).

Additionally, two monomeric red emitting (~ 610 nm) PFSPs were published recently: rsCherry and rsCherryRev (Stiel et al., 2008), deriving from mCherry (Shaner et al., 2004). In rsCherry, excitation light (~ 550 nm) absorbed by the anionic chromophore leads to on-switching of fluorescence. This positive switching FP is turned off by irradiation with blue light (~ 450 nm), which is absorbed by the neutral chromophore. The negative PFSPs rsCherryRev reacts reversed towards the switching wavelengths (Stiel et al., 2008; Nienhaus & Wiedenmann, 2009). Nevertheless, both proteins are maximal as half as bright as KFP1 and have minimal 5-fold decreased brightness in contrast to non-switching PAmCherry1 (Shaner et al., 2007; Stepanenko et al., 2008; Subach et al., 2009).

7. Applications of optical highlighters – Shedding light on life science research

In addition to hitherto existing fluorescent marker proteins and their versatile applications, optical highlighters constitute a new class of probes, that will expand the field of applications, especially concerning protein dynamic experiments in live cell imaging (Gurskaya et al., 2006; Lippincott-Schwartz et al., 2003; Lukyanov et al., 2005; Remington, 2006). First, they offer direct and constricted highlighting of definite molecules within cells (Nienhaus & Wiedenmann, 2009; Shaner et al., 2007; Stepanenko et al., 2008). Besides, they allow tracking without the demand for continual visualization by constant imaging, which reduces photobleaching and phototoxicity difficulties (Lukyanov et al., 2005). The realization of repeated activation events is the most useful benefit of photoswitchable fluorescent proteins. The observations obtain more validity, if within the same examination area replicated measurements can be performed instead of different study regions. In this

case, effects of the surrounding area have no influence. Above all, the photolabeling of several subcellular regions one after another is allowed. These capabilities are necessary for the most important application of PSFPs: protein tracking. Diffusion or transport of signalling molecules can be monitored in living cells (Ando et al., 2004; Chudakov et al., 2006). The high optical contrast, especially after irreversible photoactivation and -conversion can be used for real-time *in vivo* tracking movements of marked cells, organelles or proteins to study cellular migration behaviour developmental biology problems (Chudakov et al., 2004; Nienhaus et al., 2006; Patterson & Lippincott-Schwartz, 2002, 2003; Stark & Kulesa, 2005; Theis-Febvre et al., 2005; Wiedenmann & Nienhaus, 2006).

Moreover, experiments are not constrained by non-converted or newly synthesized markers, which furthermore emit at the original wavelength (Adam et al., 2008; Ando et al., 2002; Chudakov et al., 2007; Gurskaya et al., 2006; Nienhaus et al., 2005, 2006; Tsutsui et al., 2005; Wiedenmann et al., 2004b; Wiedenmann & Nienhaus, 2006).

Colour-changing properties of UV-converted red-emitting FPs (Labas et al., 2002) offer a mighty labelling technique just as "fluorescent timer" DsRed variant E5 (Terskikh et al., 2000) for distinguishing of aging cells and organelles or differentiation of promoter activities.

In addition, the spatio-temporal limits of studies of dynamic processes are extraordinary extended. Likewise, they open new opportunities for the study of complex protein-protein interactions (Adam et al., 2008) using specific FRET methods, e.g. PA-FRET or PC-FRET (Lukyanov et al., 2005).

Furthermore, photoconvertible and -switchable fluorescent proteins could become a versatile device for data-storage applications (Andresen et al., 2005; Sauer, 2005) for which reversibility is important if not mandatory.

Optical highlighter proteins are beneficial tools for superresolution microscopy. Using these modern techniques, spatial resolution beyond the diffraction barrier of optical microscopy can be attained (Bates et al., 2007; Chi, 2009; Gustafsson, 2008; Hell, 2003, 2007; Hofmann et al., 2005; Walter et al., 2008). The new class of probes provides novel instruments of non-invasive microscopy inventions as RESOLFT (**RE**versible **S**aturable **O**ptica**L** **F**luorescence **T**ransitions; Hell, 2003; Hell et al., 2003; Schwentker et al., 2007) or STED (**ST**imulated **E**mission **D**epletion; Hell & Wichmann, 1994; Hell, 2007). Further innovative single-molecule microscopy

concepts are PALM (**P**hoto**a**ctivated **L**ocalization **M**icroscopy; Betzig et al., 2006; Shroff et al., 2008), FPALM (**F**luorescence **P**hoto**a**ctivation **L**ocalization **M**icroscopy; Gould et al., 2009; Hess et al., 2006), STORM (**ST**ochastic **O**ptical **R**econstruction **M**icroscopy; Huang et al., 2008a/b; Rust et al., 2006) or PALMIRA (**PALM** with **I**ndependently **R**unning **A**cquistion; Bock et al., 2007; Egner et al., 2007). These techniques rely on detection of emission of individual molecules and the afterwards calculation of the exact coordinates of the single fluorescent molecules.

By using optical highlighters with different colours, it should be possible to study dynamics of several target proteins simultaneously *in vivo*, e.g. in automated high content screening applications (Nienhaus et al., 2006). Monomeric representatives among optical highlighters provide optimal performance as fusion tags (Ando et al., 2004; Andresen et al., 2008; Chudakov et al., 2004, 2007; Gurskaya et al., 2006; Henderson et al., 2007; Nienhaus et al., 2006; Patterson & Lippincott-Schwartz, 2002; Shaner et al., 2008; Stiel et al., 2007, 2008; Subach et al., 2009; Verkusha & Sorkin, 2005).

Although, existing optical highlighter proteins offer advantageous properties, further development of this class of fluorescent marker proteins concerning colour, brightness, contrast, aggregation and oligomerization state is required and will greatly expand the potential applications.

8. *Anemonia sulcata* var. *rufescens* – Source of a new optical highlighter?

Being on the prowl for a new optical highlighter protein, several Mediterranean Anthozoa species were scrutinised. The already known, barely fluorescent photoswitchable protein asFP595 was isolated from the non-bioluminescent sea anemone *Anemonia sulcata* (Lukyanov et al., 2000). Regarding this animal's phenotype with brownish tentacles and red non-fluorescent tips (Lukyanov et al., 2000), it could eventually be classified as the colour morph *Anemonia sulcata* var. *vulgaris* (Wiedenmann et al., 1999). Therefore, it was supposed to find such a type of GFP-like protein in colour variety *Anemonia sulcata* var. *rufescens* (Andres, 1883), because this organism is very similar to the described source of the photoswitchable protein asFP595.

First descriptions of pigmented varieties of sea anemones took place nearly 150 years ago (Gosse, 1860; Andres, 1881, 1883). Figure 7 shows the characteristic

colouration of the morph *Anemonia sulcata* var. *rufescens*: a green fluorescent upside and a red fluorescent underside of the tentacles with pink non-fluorescent tips. Three GFP-like proteins located in the ectodermal are causing this pigmentation: green fluorescent asFP499, highly red fluorescent asFP595 (starting from now named "asRFP.b" to avoid confusion with asFP595 published by Lukyanov et al., 2000) and pink non-fluorescent asCP562 (Gundel, 2004; Wiedenmann, 1997, 2000; Wiedenmann et al., 1999, 2000b, 2002a). These pigments are predominating the brown tone of additionally occupied symbiotic algae, so-called zooxanthellae, which are located in the entoderm (Wiedenmann & Lorenz, 2000; Wiedenmann et al., 1999).

Figure 7. Characteristic colouration of *Anemonia sulcata* var. *rufescens*. The upside of the tentacles shows green fluorescence, whereas the underside is red fluorescent. The tentacle tips are pink coloured and exhibit no fluorescence. This colouration is brought about three GFP-like proteins: asFP499 (green), asFP595 (red) and asCP562 (pink) (figure from Gundel, 2004).

Different colour morphs of *Anemonia sulcata* occur frequently on rocky shores of the Mediterranean Sea in shallow water of a sheltered bay together (Wiedenmann et al., 1999). Due to the easy outdoor accessibility and the content of different GFP-like proteins, *Anemonia sulcata* and its colour morphs are predestined for field studies concerning the biological function of GFP-like proteins.

9. Motivation and aims of the thesis

A) Determination of the influence of structural variability among GFP-like proteins from *Anemonia sulcata* var. *rufescens* on the fluorescence intensity

Comparing the non-fluorescent protein asCP562 and the highly fluorescent protein asRFP.b from *Anemonia sulcata* var. *rufescens*, key residues responsible for high fluorescence intensity can be identified and transferred to other non-fluorescent chromoproteins for RFP-evolution. By this thorough exploration of structure-function relations, a rational design of fluorescent marker proteins for the use in life science research will be accomplished.

B) Discovery and characterization of a new optical highlighter protein for application in live cell imaging

Since the first application as *in vivo* markers in 1994 (Chalfie et al., 1994), GFP-like proteins have become the microscope of the 21st century. Especially optical highlighter technology allows unexpected before variety of experiments, above all photoswitchable fluorescent proteins, e.g. in high-resolution microscopy. Therefore, new representatives of this class of GFP-like proteins must be obtained.

C) Indications towards biological function of GFP-like proteins from *Anemonia* spp.

Field studies concerning two different *Anemonia* species in combination with investigation of host pigmentation and several biomarkers could suggest possible considerations of *in vivo* scope of GFP-like proteins.

II. Summary of results and discussion

A) Determination of the influence of structural variability among GFP-like proteins from *Anemonia sulcata* var. *rufescens* on the fluorescence intensity

Red fluorescent proteins (RFPs) attract particular attention from both scientific and practical points of view. In practice, they have in addition to well-established FPs a great potential to be used as *in vivo* markers in multicolour labelling and FRET-based applications (Campbell et al., 2002; Fradkov et al., 2002; Kredel et al., 2009; Merzlyak et al., 2007; Shcherbo et al., 2009a/b). Since long-wave light penetrates tissue more easily, far-red FPs provide an excellent tool for whole-body imaging (Deliolanis et al., 2008; Shcherbo et al., 2007, 2009a).

Besides the discovery of naturally occurring RFPs, they can also be generated by mutagenesis of non-fluorescent chromoproteins. However, the key residues responsible for a bright red FP have to be identified. Therefore, we investigated both non-fluorescent and high fluorescent GFP-like proteins from *Anemonia sulcata* var. *rufescens*.

Key residues responsible for high fluorescence intensity are identified among GFP-like proteins from *Anemonia sulcata* var. *rufescens* and transferred to chromoprotein apCP558 from *Adamsia palliata*.

Reference:

Gundel, S., Kachalova, G. S., Bartunik, H. D., Fuchs, J., Nienhaus, G. U. & Wiedenmann, J. (2009a). Identification of key residues responsible for high fluorescence intensity in GFP-like proteins. *prepared for publication*.

Comparing both non-fluorescent and highly fluorescent proteins of *Anemonia sulcata* var. *rufescens*, it could be noticed that they have an eminent sequence identity of ~ 90%. Therefore, only a difference of ~ 10% of the amino acid sequence causes differences in fluorescence intensity (see reference: table 4).

Via mutagenesis and structure analysis the key residues responsible for the immense difference in fluorescence intensity between asCP562 (non-fluorescent chromoprotein) and asRFP.b (bright fluorescent protein) were determined. Sequence

analysis of 35 generated mutants was carried out in combination with investigation of spectral properties of selected mutants (see reference: table S1, S2). Thereby, the amino acids at position 13, 143 and 144 were determined as key residues for fluorescence intensity (see reference: table 5). X-ray crystallography confirmed influence of internal residue 13, chromophore-interacting residue 143 and interface residue 144 (see reference: figure 6). The Met-Tyr-Gly chromophore of asRFP exclusively adopts the *cis* conformation, which is stabilized by surrounding residues. Space is opened for the *cis* isomerization of the chromophore through amino acids in position 13, 143 and 144. Ser143 is hydrogen-bonded to the chromophore positioning the observed *cis* form of the fluorescent chromophore. Furthermore, Cys144 exerts a stabilizing function on Ser143. Due to interaction of Cys62 with Met63 of the chromophore, influence of Met13 on high fluorescence intensity (*cis* conformation of the chromophore) is facilitated (see reference: figure 7).

In the next step, we transferred these results to chromoprotein apCP558 from *Adamsia palliata* and produced a mutant with 4 to 5-fold increased fluorescence brightness (see reference: figure 8). Therefore, a new concept for generating red FPs could be demonstrated.

Evolution of red fluorescent proteins by mutagenesis of chromoproteins is a promising strategy to develop novel tools for life science research. Consequently, non-fluorescent, red absorbing chromoproteins can be used as a source of red fluorescent proteins, which should be continued to further development. Due to still increasing popularity of GFP-like proteins in cell biology, a comprehension of structure-function relations has both a scientific and a practical significance, highlighting new opportunities to attain preferable protein properties artificially.

B) Discovery and characterization of a new optical highlighter protein for application in live cell imaging

Genetically encoded fusions of cellular structures with a member of the GFP-like protein family have become indispensable tools in cell biology. Starting from avGFP and its multicoloured variants, a broad diversity of novel marker proteins was discovered in recent years. In the course of further development of fluorescent proteins, a new class of probes opened up advances in dynamic cellular imaging.

These optical highlighters are able to modify their fluorescence emission colour and intensity, respectively, due to wavelength-dependent illumination.

The reversible on- and off-switching between a fluorescent and a non-fluorescent chromophore state is characteristic for a specific class of optical highlighters (Shaner et al., 2007; Stepanenko et al., 2008). A big advantage of these photoswitchable fluorescent proteins (PSFPs) is the fact that their chromophores can attend the switching cycle many times until they are bleached or transferred to a permanent non-switchable state in contrast to chromophores of photoactivatable or photoconvertible FPs, respectively. A *cis-trans* isomerization of the chromophore was revealed as key event in the switching process in recent studies concerning the molecular switching mechanism of PSFPs (Andresen et al., 2005, 2007; Chudakov et al., 2003b; Henderson et al., 2007; Stiel et al., 2007).

PSFPs are important imaging tools enlarging possible applications of optical highlighter FPs. A promising area of application for PSFPs is their usage in high resolution fluorescence imaging, where the spatial resolution of fluorescence microscopy is optimized (Betzig et al., 2006; Egner et al., 2007; Hell, 2007; Hess et al., 2006).

Due to the increasing demand for novel PSFPs, we investigated various red FPs from Anthozoa to obtain a new member of this class of optical highlighters.

A new photoswitchable red fluorescent protein (psRFP) could be evolved from red FP of *Anemonia sulcata*.

Reference:

Gundel, S., Kachalova, G. S., Bartunik, H. D., Fuchs, J., Nienhaus, G. U., Oswald, F. & Wiedenmann, J. (2009b). psRFP – a new photoswitchable red fluorescent protein from *Anemonia sulcata*. *prepared for publication*.

Several RFPs from sea anemones common to the Mediterranean Sea were screened concerning their photoswitching properties. The red FP asRFP.b from *Anemonia sulcata* var. *rufescens* was the only investigated protein that displays switching behaviour upon illumination. This naturally occurring photoswitchable red fluorescent protein can be switched off to 84% of its maximum fluorescence, which can be compared to recently published green PSFP cerFP505 with an reduced

fluorescence intensity of 15% after photoswitching (Vogt et al., 2008). Introduction of non-aggregation mutations in the N-terminal region of further optimized asRFP results in 28% of maximum fluorescence in the off-state. Finally, we succeeded in developing a new optical highlighter, named psRFP. Due to the amino acid exchange of the chromophore interacting residue Ser143Gly, psRFP shows a further reduction of rest fluorescence in the off-state of 9% (see reference: figure 8).

In summary, psRFP and its precursors show in its initial state bright red fluorescence and can be switched off almost completely by blue light illumination (~ 450 nm). On-switching is performed due to thermal relaxation in the absence of light. Therefore, they display a negative switching mode (decrease of fluorescence intensity after irradiation) (Ando et al., 2004; Andresen et al., 2008). This switching type is advantageous in comparison with positive switching mode (switch from a dark state to a bright fluorescent state) (Chudakov et al., 2003b; Stiel et al., 2008) because initial localization of cellular structures is simplified when the marker protein is fluorescent after expression in cells.

Structural analysis of psRFP before and after illumination revealed a *cis-trans* isomerization of the chromophore involved in photoswitching mechanism. The non-fluorescent chromophore in the off-state represents the *trans* conformation, whereas the *cis* conformation is adopted by the fluorescent on-state chromophore (see reference: figure 12). Besides, a substantial change in chromophore planarity is associated with the conformational switch. Moreover, a pH-dependent characterization of spectral properties will reveal more detailed information about chromphore protonation states and their influence on switching.

A half-life of 70 s for psRFP off-switching was determined, which is indeed faster than Dronpa (263 s), but not as fast as cerFP505 (30 s) or rsFastLime (5 s), the fast switching derivative of Dronpa (Henderson et al., 2007; Stiel et al., 2007). In addition, psRFP only acquires low-energy light illumination for inducement of photoswitching in contrast to KFP1 (Andresen et al., 2005). Moreover, irradiation of KFP1 with on-switching light of greater intensity, longer duration, or both causes irreversible kindling (Chudakov et al., 2003b) which could never be observed for psRFP. In contrast to green PSFPs the new candidate displays advantages of red fluorescent proteins (Ex$_{max}$ 582 nm, Em$_{max}$ 601 nm) and can be excited with low-cytotoxic wavelengths for imaging. All current available red PSFPs (KFP1, rsCherry and rsCherryRev) (Chudakov et al., 2003b; Stiel et al., 2008) show distinct lower

brightness in their on-state (3 to 30-fold reduced) and higher background fluorescence in their off-state in comparison to psRFP (see reference: table 1). Accordingly, psRFP has the best on-/off-ratio, which is required for remarkable contrast in microscopy applications. The successful performance of psRFP as marker protein in live cell imaging applications was shown by fusing it C-terminally to the mitochondrial localization signal of subunit VIII of humane cytochrome-c-oxidase (Rizzuto et al., 1995). psRFP can be overexpressed in mammalian cells without exhibiting cytotoxic effects and shows strong red fluorescence. Mitochondrial localization of psRFP can be observed after functional expression of the fusion protein in living cells (see reference: figure 13). A single mitochondrion could be repeatedly switched off to ~ 5% of initial fluorescence. Absence of green emitting states of psRFP offers the attractive possibility of multicolour labelling in combination with green-to-red photoconvertible FPs (Adam et al., 2008; Ando et al., 2002; Gurskaya et al., 2006; Tsutsui et al., 2005; Wiedenmann et al., 2004b) and green photoswitchable FPs (Ando et al., 2004; Andresen et al., 2008; Henderson et al., 2007; Stiel et al., 2007). However, the tetrameric oligomerization state could be a limitation when performing protein tracking and subdiffraction resolution microscopy. Nevertheless, efficiency of psRFP in high resolution microscopy should be tested. Beyond that, monomerization of new optical highlighter protein psRFP should take centre stage in subsequent studies.

In summary, we successfully developed a novel photoswitchable red fluorescent protein, which combines properties preferably applicable for live cell imaging.

C) Indications towards biological function of GFP-like proteins from *Anemonia* spp.

GFP-like proteins from representatives of the phylum Cnidaria can be classified into four colour types: green, yellow, and orange-red fluorescent as well as purple-blue non-fluorescent chromoproteins (Labas et al., 2002). They were isolated both from animals containing symbiotic algae, the so-called zooxanthellae, and non-symbiotic organisms. The widespread distribution of GFP-like proteins in zooxanthellate and azooxanthellate cnidarians and their impressive colour diversity indicates different specific biological functions, which are still not completely understood (Dove et al., 2001; Fradkov et al., 2000; Karasawa et al., 2004; Labas et al., 2002; Matz et al., 1999; Mazel et al., 2003; Oswald et al., 2007; Wiedenmann, 1997, 2000;

Wiedenmann et al., 1999, 2000b, 2002a, 2002b, 2004a, 2004b). Therefore, own contributions were made to enlighten the purpose of the whole light show of GFP-like proteins *in vivo*. For this reason, field studies concerning two different *Anemonia* species in combination with investigation of host pigmentation and several biomarkers were performed during this thesis.

1. GFP-like proteins have no influence on the degree of a bleaching event occurred to the sea anemones *Anemonia rustica* and *Anemonia sulcata* var. *smaragdina.*

Reference:

Leutenegger, A., Kredel, S., Gundel, S., D'Angelo, C., Salih, A. & Wiedenmann, J. (2007). Analysis of fluorescent and non-fluorescent sea anemones from the Mediterranean Sea during a bleaching event. *Journal of Experimental Marine Biology and Ecology*, 353, 221-234.

Bleaching phenomena accompanied by loosing overall colouration are caused by expulsion of symbiotic zooxanthellae during stressful conditions. These incidents are well studied among tropical anthozoans. On the contrary, there is only scant information available about bleaching of temperate anthozoans.

Therefore, the aim of the study was to compare the physiological responses of two different pigmented *Anemonia* species to a bleaching event occurred in the Mediterranean Sea considering the host pigmentation and several biomarkers.

We documented a bleaching event among the two shallow water sea anemone species *Anemonia rustica* and *Anemonia sulcata* var. *smaragdina* common to the Mediterranean Sea. Both of them are symbiotic cnidarians, which can be distinguished by the colouration of their host animals due to GFP-like proteins homologous to the green fluorescent protein from *Aequorea victoria* (see reference: figure 3). In case of *Anemonia sulcata* var. *smaragdina,* a green fluorescent protein (asFP499) is colouring the tentacles and a non-fluorescent chromoprotein (asulCP) pigments the tentacle tips (see reference: figure 4). Since little amounts of the transcripts for both GFP-like proteins were detected in tentacles of the non-fluorescent *Anemonia rustica*, differences in colouration occur on altered expression levels of GFP-like proteins. For bleached individuals of *A. sulcata* we observed a decrease by ~ 30% in tissue fluorescence (see reference: figure 4).

Besides the host pigments (GFP-like proteins) and photosynthetic symbiont pigments (chlorophyll a, c and peridinin) also the contents of mycosporine-like aminoacids (MAAs) and the activity of anti-oxidant enzymes, e.g. superoxide dismutase (SOD), catalase (CAT), and peroxidase (POD) were determined.

It could be shown that comparable numbers of zooxanthellae with similar contents of photosynthetic pigments were hosted in the tentacles of both fluorescent and non-fluorescent *Anemonia* spp. (see reference: figure 5). It is a known fact that *A. sulcata* releases zooxanthellae as a response to experimental heat stress (Miller et al., 1992; Richier et al., 2006). Linked to increased water temperatures a mass bleaching event occurred and ~ 30% of the *Anemonia* spp. population exhibited uncharacteristic white tentacle colouration. Bleaching proceeds in both species via the loss of ~ 90% of the zooxanthellae (see reference: figure 5), this indicates that the host pigmentation did not influence the degree of bleaching of *Anemonia* spp.. Moreover, the content of photosynthetic pigments of zooxanthellae was not affected by the bleaching event. Eventually, the individual degree of bleaching was comparable between both species (see reference: figure 5).

Mycosporine-like aminoacids (MAAs) are UV-screening compounds and widespread in many marine cnidarians, also in sea anemones (Dunlap & Shick, 1998). The tissue concentration is often positively correlated with the radiation intensity in the habitat (Shick et al., 1995). Both studied sea anemone species were living in the same depth under same light conditions. However, in fluorescent *Anemonia sulcata* var. *smaragdina*, MAA levels were significantly increased compared to *Anemonia rustica*. In bleached specimens, the content of MAAs was basically unchanged (see reference: figure 6). For this reason, a reduced MAA level can presumably be excluded as cause for the bleaching.

Stressful circumstances might lead to cellular damage due to increased levels of reactive oxygen species (Downs et al., 2002; Lesser & Shick, 1989; Smith et al., 2005; Tchernov et al., 2004). Especially highlighted is H_2O_2, which has a relatively long lifetime and is able to cross organelle and cell borders via diffusion (Downs et al., 2002; Smith et al., 2005). Elevated H_2O_2 concentration can provoke exocytosis of symbiotic algae via a mitogen-activated protein kinase-signalling cascade (Smith et al., 2005). Anti-oxidant enzymes, e.g. superoxide dismutase (SOD), catalase (CAT), and peroxidase (POD) are defence systems of the animals against oxidative stress (Hawkridge et al., 2000; Richier et al., 2003). Non-significant differences between

unbleached individuals of both species indicate a similar sensitivity of fluorescent and non-fluorescent *Anemonia* spp. to oxidative stress. Though, SOD level was increased by a factor > 2 after bleaching resulting in a high intracellular H_2O_2 level, which is further intensified by a decreased CAT activity after bleaching (see reference: figure 7). The studied sea anemone specimens showed increased SOD and decreased CAT activity resulting from oxidative stress that might be a direct cause for bleaching. Concerning the POD content, there were no differences between bleached and non-bleached individuals within the species (see reference: figure 7).

In our study, both loss of zooxanthellae and GFP-like proteins is responsible for bleached appearance of sea anemones. Nevertheless, it still remains unclear, if the decreased contents of host pigments are a cause or a consequence of the loss of zooxanthellae and should be further scrutinised. Considering the results of anti-oxidant enzyme activity, it is possible that oxidative stress will be relevant in the occurred bleaching of *Anemonia rustica* and *Anemonia sulcata* var. *smaragdina*.

2. GFP-like proteins may serve a photoprotective function in *Anemonia sulcata* var. *smaragdina* when competing for space under highlight conditions.

Reference:

Wiedenmann, J., Leutenegger, A., Gundel, S., Schmitt, F., D'Angelo, C., & Funke, W. (2007). Longterm monitoring of space competition among fluorescent and non-fluorescent sea anemones in the Mediterranean Sea. *Journal of the Marine Biological Association of the United Kingdom*, 87, 851-852.

The evaluation whether pigmented sea anemones possess a selective advantage in a bright light habitat took the centre stage in this field study. Therefore, competition for space between fluorescent due to GFP-like pigments *Anemonia sulcata* var. *smaragdina* and non-fluorescent *Anemonia rustica* was monitored over a period of 11 years in a shallow-water habitat in the Mediterranean Sea.

The observations of *Anemonia* spp. populations in the sun-exposed rocky slope within a restricted area started with only a few *Anemonia rustica* specimens in 1994. Four years later, their number increased and additionally *Anemonia sulcata* var. *smaragdina* representatives appeared (see reference: figure 2). Each species formed distinct clusters and increased their number of individuals presumably due to asexual

reproduction via longitudinal fission, because direct contact between individuals is only tolerated within the same genotype (Sauer, 1986; Wiedenmann, 2000). In 2002, almost all representatives descended from *Anemonia sulcata* var. *smaragdina*. The *Anemonia rustica* population did not increase anymore. Until 2005, the number of *Anemonia sulcata* var. *smaragdina* individuals further raised up and can be explained by an exponential rate of growth with a doubling time of approximately two years (see reference: figure 2). Consequently, these results suggest that representatives of *Anemonia sulcata* var. *smaragdina* possess increased fitness when competing for space in sun-exposed shallow-water surroundings.

Other fluorescent morphs of this sea anemone species (*viridis* and *rufescens*) also show maximal abundance close to the surface in other habitats (Wiedenmann et al., 1999).

The positive correlation between superior condition of *Anemonia sulcata* colour morphs under highlight conditions and the expression of GFP-like pigments in tentacle tissues can be interpreted as support for the hypothesis that these proteins possess a photoprotective function and can increase competitive ability in anthozoans. This assumption should be further investigated. Certainly, enhanced fitness may also be mediated by other UV-protective compounds like mycosporine-like aminoacids or several anti-oxidant enzymes (Furla et al., 2005; Leutenegger et al., 2007; Shick, 1991).

3. Possible functions of GFP-like proteins

3.1 Bioluminescent organisms

As already introduced, green fluorescent proteins play a role as secondary emitter in the jellyfish *Aequorea victoria* and several other bioluminescent Hydrozoa and Anthozoa species (Johnson et al., 1962; Morin & Hastings, 1971b; Szent-Gyorgyi et al., 2001; Ward & Cormier, 1979). In a radiationless energy transfer (Morin & Hastings 1971b; Ward & Cormier, 1979), they accept the energy from a primary light-producing protein and reemit it, thereby changing the colour from blue to green (Morin & Hastings, 1971b; Morise et al., 1974; Ward & Cormier, 1976). This suggests that their task must be associated with the bioluminescence function, but their biological significance is not completely understood. Green light becomes less attenuated compared to blue light and therefore, it achieves better penetration of

emission light through oceanic water (Jerlov, 1976; Miyawaki, 2002). From this standpoint, it seems obvious that coastal-water organisms show green colour of bioluminescence. Because many photoreceptors possess a high sensitivity in the green spectral region (Patridge, 1990; Patridge & Cummings, 1999), their luminescence can act as deterring response to predator behaviour. An astonishing light flash might scare off a potential assaulter, enabling the prey to flee away into the darkness (Hastings, 1995; Labas, 1977; Mackie, 1995a; Morin, 1976).

Most importantly, light emission is triggered by mechanical stimulation, meaning that the raider has to contact the organism. So, there seems to be no intrinsic need for the enhanced light transmission through the ocean unless with the intention to warn other conspecific representatives. Such intraspecific signalling is known for planktonic tunicates (Mackie, 1995b) and some ctenophores (Labas, 1980), but there is nothing known about it in GFP-possessing Cnidaria. To support the hypothesis of increased transmission, it can be assumed that green light emission serves as "burglar alarm" (Burkenroad, 1943), which exists to uncover the whereabout of primary predator to top-predators (Fleisher & Case, 1995).

Considering the point of defence against predators, cnidarians are quite well protected using their eponymous cnidae loaded with efficient toxins. Nevertheless, a few cnidarian enemies, e.g. nudibranchs are specialized in feeding on them (Clark, 1975; Todd, 1981, 1983). It is very unlikely that these attackers are chased away by a light flash.

A more plausible explanation of GFPs attendance in bioluminescent animals could be the improvement of the efficiency of bioluminescence, implying that their function is not directly linked to the change in emission colour. Accordingly, the luminescence quantum yield can be raised because of energy transfer to an efficient chromophore before the energy is squandered into heat. For instance, the luminescence quantum yield of *Renilla* luciferase is approximately 3-fold higher in complex with GFP than in absence of green fluorescent protein (Ward & Cormier, 1979). However, in *Aequorea* system no change in quantum yield could be measured after complexing with GFP (Gorokhovatsky et al., 2003; Morise et al., 1974).

Nonetheless, it still remains unclear whether GFP is a member of bioluminescence-system right from the start or it was recruited later. Hence, studying fluorescent, but non-bioluminescent, Anthozoa and the function of their fluorescent

proteins is essential and since their discovery in 1999 even possible (Matz et al., 1999).

3.2 Non-bioluminescent organisms

Most anthozoa species containing GFP-like proteins are non-bioluminescent. The broad spectrum of emitted colours in co-existence with non-fluorescent GFP-like proteins raises the question about the biological significance of this variety and is discussed controversially.

Originally, it was considered that GFP-like proteins might serve as UV-blocking substances (Catala, 1959). However, the majority of these pigments are characterized by a minor absorption in the UV-region (Mazel et al., 2003). Therefore, it seems rather doubtful that FPs can operate as efficient UV-filter.

Furthermore, it was suggested that green fluorescent proteins convert detrimental UV-light into low-energy radiation, which can be used for photosynthesis reaction by symbiotic zooxanthellae (Kawaguti, 1944, 1969). Salih et al. (2000) extended this photoprotection hypothesis by describing a positive correlation between the content of fluorescent proteins and the efficiency of photosystem II of zooxanthellae under light stress conditions. The photoprotective role of FPs also seems to be supported by the localization of the fluorescent granules in the ectoderm above the zooxanthellae in corals from sun-exposed habitats (Salih et al., 2000). Scattering, reflectance and absorption of excess visible and UV-light (Salih et al., 2000) might achieve this effect. This function fits best the spectral properties of cyan or rather green fluorescent proteins. Their excitation maxima are located in the wavelength area near the one of the maxima of photosynthesis action spectrum (400-480 nm). For this reason, they are qualified to reduce the photosynthetically active radiation (PAR). In contrast, Mazel et al. (2003) suggested that in Caribbean corals (*Montastrea* sp.) the effect of FPs must have minor impact on the level of PAR reaching the zooxanthellae, so that the photoprotection mechanisms intrinsic to the photosystems of symbiotic algae would be much more capable (Gorbunov et al., 2001). Nevertheless, FP-containing organisms seem to be more resistant against heat and oxidative stress (Salih et al., 2000; Wiedenmann et al., 2007).

Only the biological function of green fluorescent proteins can be explained with the photoprotection hypothesis, because merely their absorption/excitation properties match the peaks of photosynthesis action spectrum. In 2000, Salih and co-

workers suggested that non-green fluorescent proteins could serve as enhancers of the photoprotection function of the green FPs: Incoming light might be transferred from green to yellow-red pigments, resulting in further conversion of PAR into wavelengths scarcely influencing photosynthesis of zooxanthellae. The physiological impact of this system remains to be investigated.

In addition to their photoprotection assumption, Salih et al. (2000) also debated the prospect that in low-light environment FPs may possess the opposite function and act as light-collecting device. In this case, the fluorescent layer is positioned below the symbiotic algae instead of above them. Accordingly, it was suggested that GFP-like pigments increase PAR by reflectance, back-scattering and wavelength conversion (Kawaguti, 1969; Salih et al., 1998, 2000; Schlichter et al., 1986). Conversely, Gilmore et al. (2003) pointed out that, although the energy of the absorbed light is abundantly transferred between different FPs within the coral, it never reaches the photosynthetic pigments of zooxanthellae - which confutes the photosynthetic-aid function.

Another discussed alternative function of GFP-like proteins is photoreception. Low-light photoreception was studied in stony coral *Montastrea cavernosa*, for which GFP-like proteins are well characterized (Kelmanson & Matz, 2003). However, the action spectrum for tentacle retraction does not match either absorption or emission maxima of any of its known GFP-like pigments. The overall shape of the photosensitivity spectrum in some hydroid medusae is still very unlike to GFP characteristics (Arkett, 1985; Weber, 1982). For these reasons, it can be concluded that published data do not support GFP-like proteins' significance in photoreception.

Finally, the function of non-fluorescent chromoproteins remains in complete obscurity. These proteins are widespread among sea anemones and Indo-Pacific corals and mainly localized to terminal parts of the animal, such as tentacle tips or branch. They are characterized by intense absorption, but no fluorescence emission at all. Under the name "pocilloporin" they were first described in the stony coral *Pocillopora damicornis*. However, they do not work neither as photoprotectant, nor UV-screen, nor as photosynthetic accessory pigment (Dove et al., 1995).

A possible explanation for colouration of corals might be found at a larval or juvenile stage and not in adult animals. GFP-like proteins may play a role in the negotiation between coral and zooxanthellae when establishing the symbiotic

relationships, which happens during immediate post-settlement period (van Woesik, 2000).

An alternative annotation for colour diversity in corals may be the unique colourful appearance aimed to an observer, e.g. for attraction of fish weeding out the fouling algae of the corals (Ward, 2002). Distribution of reef organisms could be affected by colour diversity and strong visual effects (Mazel & Fuchs, 2003), which may indirectly improve complexity of the habitat when ecological niches and biodiversity increase.

3.3 Functions of other GFP-like proteins

Fluorescent pigments are not restricted to cnidarians. They are also described for the phylum Arthropoda. The yellow fluorescent spots on male Mantis shrimp *Lysiosquillina glabriuscula,* found in the western Atlantic Ocean, e.g. accentuate the appearance when confronting predators or rivals (Mazel et al., 2004). Furthermore, Shagin et al. characterized six green fluorescent pigments from planktonic Copepoda of the *Pontellidae* family (2004). Concerning their spectral and biochemical properties, they are very similar to avGFP and regarding their function, they might be used for visual recognition of conspecific individuals.

Recently, Deheyn et al. (2007) were the first of all reporting the occurrence of fluorescence in three species of amphioxus (Chordata: Cephalochordata), namely *Branchiostoma floridae*, *B. lanceolatum* and *B. belcheri.* For the lancelet *B. floridae*, the "glowing genes" causing the fluorescence were even specified in detail (Baumann et al., 2008), but their biological significance is still unknown.

Surprisingly, G2F (Globular-2 fragment) domains of extracellular matrix proteins exhibit a similar three-dimensional structure to cnidarian GFP-like proteins (Hopf et al., 2001). This fact could give a hint for homologous development of these proteins within the same protein family. These proteins, which are named nidogen or entactin (Hohenester & Engel, 2002), show a protein-binding function. G2F domains appear in all bilaterian genomes sequenced hitherto: Humane extracellular matrix proteins (Yanagisawa et al., 2002), *C. elegans* hemicentin (Vogel & Hedgecock, 2001), a protein from tunicates (Nakae et al., 1993) and in *Drosophila* (Hoskins, et al., 2007). The sequence identity with cnidarian fluorescent proteins is less than 10% and G2F domains are neither fluorescent nor coloured because they have no chromophore. Obviously, the capability of fluorescence is not the special feature, which unites all

members of the GFP-like protein family. The binding surface of G2F domains is well conserved among them, suggesting that they have a similar function (Hopf et al., 2001). The conserved regions correspond to β-strands 1, 2, 3 and 11 in GFP-like proteins, which are exposed on the surface of tetrameric structures (Wall et al., 2000; Yarbrough et al., 2001). Therefore, it can be speculated that protein binding by these β-strands was the most ancient function of GFP-like proteins, followed by the ability of fluorescence.

III. Deutschsprachige Zusammenfassung

Innerhalb des letzten Jahrzehntes haben fluoreszierende Proteine (FPs) immer mehr Einzug in viele Bereiche der lebenswissenschaftlichen Forschung gehalten. Das grün fluoreszierende Protein (GFP) aus der im Pazifik beheimateten Qualle *Aequorea victoria* nimmt im Bereich der Markerproteine die Pionierrolle ein. Nach seiner Entdeckung vor über 40 Jahren wurde der Fluoreszenzfarbstoff im Laufe der Zeit näher charakterisiert (Chalfie et al., 1994; Prasher et al., 1992; Shimomura et al., 1962; Tsien, 1998). Darüber hinaus wurden die Fluoreszenzeigenschaften von FPs optimiert bzw. natürlich vorkommende besser als Marker geeignete Varianten mit neuen spektralen Eigenschaften gesucht und gefunden. Auf diese Art und Weise konnten neue Anwendungsgebiete in der biologischen und medizinischen Grundlagenforschung erschlossen werden.

A) Bestimmung des Einflusses von Stukturvariabilität auf die Fluoreszenzintensität innerhalb natürlich vorkommender GFP-ähnlicher Proteine aus *Anemonia sulcata* var. *rufescens*

Rot fluoreszierende Proteine (RFPs) sind generell sowohl von wissenschaftlicher als auch anwendungsbezogener Seite interessant. Sie können im Vergleich zu grünen FPs mit energieärmerem Licht zur Emission angeregt werden. Im roten Spektralbereich ist die zelluläre Autofluoreszenz reduziert und die Gewebetransparenz erhöht, weshalb sie als leistungsfähige Werkzeuge für Untersuchungen in lebenden Geweben bzw. im Tiermodell eingesetzt werden können (Deliolanis et al., 2008; Shcherbo et al., 2007, 2009a). Außerdem besitzen RFPs ein großes Anwendungspotential als *in vivo* Marker in Mehrfarbmarkierungs-experimenten sowie FRET-basierten Untersuchungen (Campbell et al., 2002; Fradkov et al., 2002; Kredel et al., 2009; Merzlyak et al., 2007; Shcherbo et al., 2009a/b). Neben der Entdeckung natürlich vorkommender RFPs stellt die Mutagenese von nicht-fluoreszierenden Chromoproteinen eine Erfolg versprechende Alternative auf der Suche nach neuen RFPs dar. Hierfür müssen allerdings die Schlüsselpositionen identifiziert werden, die für ein helles RFP verantwortlich sind. Damit soll letztendlich eine Optimierungsstrategie entwickelt werden, um natürlich vorkommende, nicht-fluoreszierende Chromoproteine als *in vivo* Marker nutzen zu können. In der vorliegenden Arbeit wurden deshalb sowohl nicht-fluoreszierende als

auch fluoreszierende GFP-ähnliche Proteine aus *Anemonia sulcata* var. *rufescens* untersucht.

Schlüsselpositionen wurden identifiziert, die verantwortlich sind für die hohe Fluoreszenzintensität innerhalb natürlich vorkommender GFP-ähnlicher Proteine aus *Anemonia sulcata* var. *rufescens* und auf das Chromoprotein apCP558 aus *Adamsia palliata* übertragen.

Referenz:

Gundel, S., Kachalova, G. S., Bartunik, H. D., Fuchs, J., Nienhaus, G. U. & Wiedenmann, J. (2009a). Identification of key residues responsible for high fluorescence intensity in GFP-like proteins. *prepared for publication.*

Aus *Anemonia sulcata* var. *rufescens* sind sowohl fluoreszierende als auch nicht fluoreszierende Proteine bekannt, deren Sequenz zu ~ 90 % übereinstimmt (siehe Referenz: Tabelle 4). Dies bedeutet, dass ein Unterschied von ~ 10% dafür verantwortlich ist, ob ein Protein nicht oder aber sehr stark fluoreszent ist. Ziel war es, die Schlüsselpositionen in der Aminosäuresequenz zu ermitteln, die entscheidend dafür sind, ob ein Protein fluoresziert oder nicht. Mittels Mutagenese-Experimenten und Röntgenstrukturanalyse wurden die Schlüsselpositionen bestimmt, die für den beträchtlichen Unterschied der Fluoreszenzintensität zwischen dem Chromoprotein asCP562 und dem rot fluoreszierenden Protein asRFP.b verantwortlich sind. Eine Sequenzanalyse von 35 erzeugten Varianten wurde in Verbindung mit der Untersuchung der spektralen Eigenschaften von ausgewählten Mutanten durchgeführt (siehe Referenz: Tabelle S1, S2). Dadurch konnten die Aminosäuren in Position 13, 143 und 144 als Schlüsselpositionen für die Fluoreszenzintensität bestimmt werden (siehe Referenz: Tabelle 5). Die Röntgenstrukturanalyse bestätigte den Einfluss der Aminosäurereste an den Positionen 13, 143 und 144 auf die *cis* Konformation des Chromophors, welche charakteristisch für den fluoreszenten Zustand ist (siehe Referenz: Abbildung 6). Diese Aminosäuren bieten ausreichend Platz, um die *cis* Chromophor-Konformation zu ermöglichen. Ser143 ist über Wasserstoffbrücken mit dem Chromophor verbunden, wodurch die *cis* Konformation des fluoreszenten Chromophors in Position gehalten wird. Cys144 übt eine stabilisierende Funktion auf Ser143 aus. Die Interaktion von Cys62 mit Met63 des

Chromophors bedingt den Einfluss von Met13 auf die *cis* Konformation des Chromophors (siehe Referenz: Abbildung 7).

Im anschließenden Schritt wurden diese Ergebnisse auf das Chromoprotein apCP558 aus *Adamsia palliata* übertragen und auf diesem Weg eine Mutante mit 4 bis 5-fach höherer Fluoreszenzintensität erzeugt (siehe Referenz: Abbildung 8). Folglich konnte ein neuer Ansatz zur Bereitstellung von roten FPs vorgestellt werden, der durch Mutagenese weiterer CPs in Zukunft fortgeführt werden sollte.

Die Entwicklung eines roten FPs durch Mutagenese eines Chromoproteins stellt eine viel versprechende Strategie dar, neue Werkzeuge für die lebenswissenschaftliche Forschung bereitzustellen. Infolgedessen können nicht-fluoreszierende Chromoproteine als Quelle für rot fluoreszierende Proteine verwendet werden. Aufgrund der weiterhin zunehmenden Beliebtheit von GFP-ähnlichen Proteinen im Bereich der Zellbiologie ist ein Verständnis von Struktur-Funktions-Beziehungen sowohl von wissenschaftlicher als auch praktischer Bedeutung. Dadurch können neue Möglichkeiten erschlossen werden, um erwünschte Proteineigenschaften künstlich zu erzielen.

B) Entdeckung und Charakterisierung eines neuen Markerproteins für die Anwendung im Bereich des *live cell imaging*

Im Zuge der Verbesserungen von FPs wurde eine neue Klasse an fluoreszierenden Proteinen für spezielle Anwendungen des *live cell imaging* im Bereich von optischen Nachweismethoden entdeckt, wie z. B die Hochauflösungsmikroskopie in lebenden Zellen (Hell et al., 2007). Diese reversibel schaltbaren fluoreszierenden Proteine (RSFPs) sind in der Lage nach Bestrahlung mit Licht bestimmter Wellenlängen ihre Emissionsintensität umkehrbar zu ändern (Shaner et al., 2007; Stepanenko et al., 2008). Aufgrund der Reversibilität des Schaltens können wiederholt Subpopulationen von Fusionsproteinen in Zellen untersucht werden, wodurch die Aussagekraft des Experiments erhöht wird (Ando et al., 2004; Chudakov et al., 2006; Stiel et al., 2008). Darüber hinaus besitzen RSFPs durch die einzigartige Eigenschaft der Schaltbarkeit ein großes Potential in der Entwicklung und Anwendung neuer hoch auflösender Bildgebungsverfahren mit einer Auflösung jenseits der Beugungsgrenze (Betzig et al., 2006; Egner et al., 2007; Hess et al., 2006).

Ein neues schaltbares rot fluoreszierendes Protein (psRFP) wurde entwickelt aus einem roten FP aus *Anemonia sulcata.*

Referenz:

Gundel, S., Kachalova, G. S., Bartunik, H. D., Fuchs, J., Nienhaus, G. U., Oswald, F. & Wiedenmann, J. (2009b). psRFP – a new photoswitchable red fluorescent protein from *Anemonia sulcata. prepared for publication.*

Auf der Suche nach neuen RSFPs wurden verschiedene rote FPs von Seeanemonen aus dem Mittelmeer bezüglich ihrer Schalteigenschaften untersucht. Nur das rote FP asRFP.b aus *Anemonia sulcata* var. *rufescens* reagierte mit reversiblem Schaltverhalten auf Lichtbestrahlung. Dieses natürlich vorkommende RSFP kann bis zu 84% seiner Ausgangsfluoreszenzintensität ausgeschaltet werden. Das Einbringen von Mutationen im N-terminalen Bereich des Proteins führte zu einer Verbesserung der Schaltbarkeit und bewirkte zusätzlich eine Verringerung der Aggregationstendenz. Dieses optimierte Protein asRFP zeigte im ausgeschalteten Zustand maximal 28% seiner anfänglichen Fluoreszenzintensität. Schlussendlich konnte durch die Mutation Ser143Gly die Variante psRFP erzielt werden, welche nur noch über 9% Restfluoreszenz nach Lichtbestrahlung verfügt (siehe Referenz: Abbildung 8). Anhand des Verhaltens nach Bestrahlung konnte festgestellt werden, dass psRFP und seine Vorläufer einen negativen Schaltmechanismus aufweisen. Dies bedeutet, dass der initiale rot fluoreszierende Zustand durch Bestrahlung mit blauem Licht (~ 450 nm) beinahe komplett ausgeschaltet werden kann. Das Anschalten erfolgt durch thermische Relaxation in Abwesenheit von Licht. Der negative Schaltmechanismus ist im Gegensatz zum positiven (Zunahme der Fluoreszenzintensität nach Lichtbestrahlung) von Vorteil, weil die initiale Lokalisation von zellulären Strukturen vereinfacht ist, wenn das Markerprotein nach Expression in lebenden Zellen fluoreszent ist (Ando et al., 2004; Andresen et al., 2008; Chudakov et al., 2003b; Stiel et al., 2008).

Zur Untersuchung des Schaltens auf molekularer Ebene wurde das Protein kristallisiert und im Kristall in den nicht fluoreszierenden Zustand geschaltet, um strukturelle Unterschiede zu bestimmen. Die Röntgenstrukturanalyse von psRFP vor und nach Lichtbestrahlung ließ eine *cis-trans* Isomerisierung des Chromophors als grundlegenden Mechanismus für das reversible Schalten deutlich erkennen. Der

nicht-fluoreszierende Chromophor im Aus-Zustand repräsentiert den *trans* Chromophor, wohingegen die *cis* Konformation vom fluoreszierenden Chromophor im An-Zustand eingenommen wird (siehe Referenz: Abbildung 12). Darüber hinaus geht eine beachtliche Änderung der Chromophor-Planarität mit der Konformationsänderung einher. Eine pH-abhängige spektrale Charakterisierung könnte zusätzlich detaillierte Informationen liefern bezüglich der Protonierungszustände des Chromophors und deren Einfluss auf die Schaltbarkeit.

Für das Ausschalten von psRFP wurde eine Halbwertszeit von 70 s bestimmt, womit dieses Protein zu den schnell schaltbaren Varianten zählt (Henderson et al., 2007; Stiel et al., 2007). Außerdem wird für das Ausschalten von psRFP nur energiearmes Licht benötigt, welches nicht zu irreversiblem Anschalten des Proteins führt, wie es für andere RSFPs beobachtet wurde (Andresen et al., 2005; Chudakov et al., 2003b). Im Gegensatz zu grünen RSFPs besitzt psRFP die Vorteile von rot fluoreszierenden Proteinen und deshalb kann die Fluoreszenzemission mit wenig-cytotoxischem, längerwelligen Licht angeregt werden. Im Vergleich zu psRFP zeigen alle derzeit verwendeten roten RSFPs eine deutlich verringerte Helligkeit im An-Zustand (3 bis 30-fach), sowie eine höhere Hintergrund-Fluoreszenz im Aus-Zustand (Chudakov et al., 2003b; Stiel et al., 2008) (siehe Referenz: Tabelle 1). Demzufolge besitzt psRFP die beste An-/Aus-Ratio, die für einen deutlichen Kontrast in mikroskopischen Anwendungen nötig ist. Der erfolgreiche Einsatz von psRFP als *in vivo* Markerprotein konnte mittels eukaryotischer Expression eines Fusionskonstruktes aus psRFP und dem mitochondrialen Lokalisationssignal der Untereinheit VIII der humanen Cytochrom-c-Oxidase gezeigt werden (Rizzuto et al., 1995). Nach Überexpression in Säugetierzellen wurden keine zytotoxischen Effekte festgestellt. Die mitochondriale Lokalisation von psRFP in lebenden Zellen konnte anhand heller Rotfluoreszenz deutlich beobachtet werden (siehe Referenz: Abbildung 13). Ein einzelnes Mitochondrium konnte wiederholt bis zu einem maximalen Wert von 5% der Anfangsfluoreszenz ausgeschaltet werden. Da psRFP keine störenden zusätzlichen grün fluoreszierende Zustände besitzt, stellen Mehrfarbmarkierungen mit grünen RSFPs (Ando et al., 2004; Andresen et al., 2008; Henderson et al., 2007; Stiel et al., 2007) oder grün-rot-photokonvertierbaren FPs (Adam et al., 2008; Ando et al., 2002; Gurskaya et al., 2006; Tsutsui et al., 2005; Wiedenmann et al., 2004b) einen möglichen Einsatzbereich dar. Bei psRFP handelt es sich um ein Erfolg versprechendes Reportermolekül für Genaktivitäts-Studien und für die Markierung

von Zellen und Geweben im Tiermodell. Bei diesen Anwendungsbeispielen besteht aufgrund des tetrameren Oligomerisierungszustandes kein Nachteil. Allerdings kann die Oligomerisierung bei Fusionsexperimenten in Abhängigkeit des Fusionspartners limitierend wirken, indem die korrekte intrazelluläre Lokalisation sowie die Funktionalität des Zielproteins beeinträchtigt werden. Nichtsdestotrotz könnte die Anwendbarkeit im Bereich der Hochauflösungsmikroskopie jenseits der Beugungsgrenze bereits zum momentanen Zeitpunkt getestet werden. Darüber hinaus sollte dennoch die Monomerisierung von psRFP im Mittelpunkt zukünftiger Studien stehen.

Zusammenfassend kann gesagt werden, dass im Rahmen dieser Doktorarbeit ein neues RSFP entwickelt wurde, welches die Eigenschaften kombiniert, die für *live cell imaging* insbesondere im Bereich von hochauflösenden mikroskopischen Verfahren erforderlich sind. Darüber hinaus wurden Untersuchungen zum molekularen Mechanismus des optimierten reversibel schaltbaren fluoreszierenden Proteins durchgeführt.

C) Hinweise bezüglich der biologischen Funktion von GFP-ähnlichen Proteinen aus *Anemonia* spp.

Bezüglich der biologischen Funktion von GFP-ähnlichen Proteinen in ihren Ursprungsorganismen besteht großer Aufklärungsbedarf. Es ist davon auszugehen, dass diesen Proteinen auch hier elementare Aufgaben zukommen. GFP-ähnliche Proteine wurden sowohl in Tieren entdeckt, die symbiontische Algen (Zooxanthellen) besitzen als auch in Organismen ohne symbiontische Algen. Das weit verbreitete Vorkommen von GFP-ähnlichen Proteinen sowohl in zooxanthellaten wie auch in azooxanthellaten Nesseltieren und ihre beeindruckende Farbvielfalt weist auf verschiedene spezifische Funktionen hin, die bis dato aber nicht vollständig verstanden sind und kontrovers diskutiert werden (Dove et al., 2001; Fradkov et al., 2000; Karasawa et al., 2004; Labas et al., 2002; Matz et al., 1999; Mazel et al., 2003; Oswald et al., 2007; Wiedenmann, 1997, 2000; Wiedenmann et al., 1999, 2000b, 2002a, 2002b, 2004a, 2004b).

Deshalb wurden eigene Untersuchungen angestellt, um „Licht ins Dunkel" bezüglich der Aufgabe von GFP-ähnlichen Proteinen *in vivo* zu bringen. Aus diesem Grund wurden im Rahmen dieser Arbeit Freilanduntersuchungen an zwei

verschiedenen *Anemonia*-Arten in Kombination mit einer Analyse der GFP-ähnlichen Proteine und verschiedener Biomarker durchgeführt.

1. GFP-ähnliche Proteine haben keinen Einfluss auf den Grad des Bleichereignisses, welches den Seeanemonen *Anemonia rustica* und *Anemonia sulcata* var. *smaragdina* widerfahren ist.

Referenz:

Leutenegger, A., Kredel, S., Gundel, S., D'Angelo, C., Salih, A. & Wiedenmann, J. (2007). Analysis of fluorescent and non-fluorescent sea anemones from the Mediterranean Sea during a bleaching event. *Journal of Experimental Marine Biology and Ecology*, 353, 221-234.

Bleichphänomene werden unter Stressbedingungen durch den Ausstoß der symbiontischen Zooxanthellen hervorgerufen. Hierbei wird ein Verlust der Färbung beobachtet. Diese Ereignisse sind bei tropischen Anthozoen gut untersucht. Im Gegensatz dazu gibt es allerdings nur wenige Informationen über das Bleichen von Anthozoen in gemäßigten Zonen.

Daher wurden im Rahmen dieser Studie die physiologischen Reaktionen zweier unterschiedlich pigmentierter *Anemonia*-Arten auf ein Bleichereignis unter Berücksichtigung der Wirtstier-Pigmentation und verschiedener Biomarker untersucht.

Hierfür wurde ein Bleichereignis dokumentiert, welches den im Mittelmeer weit verbreiteten Seeanemonen *Anemonia rustica* und *Anemonia sulcata* var. *smaragdina* widerfahren ist. Beide Spezies gehören zu den symbiontischen Nesseltieren und können anhand ihrer Färbung unterschieden werden (siehe Referenz: Abbildung 3). Die Färbung der Wirtstiere ist auf GFP-ähnliche Proteine zurückzuführen, welche homolog zu dem GFP aus *Aequorea victoria* sind. Im Fall von *Anemonia sulcata* var. *smaragdina* beruht die Färbung der Tentakel auf einem grün fluoreszierenden Protein (asFP499) und die der Tentakelspitzen auf einem nicht-fluoreszierenden Chromoprotein (asulCP; siehe Referenz: Abbildung 4). Zwar wurden geringe Transkriptmengen beider GFP-ähnlicher Proteine in den Tentakeln von *Anemonia rustica* ermittelt, diese sind aber nicht fluoreszent. Demzufolge beruhen die Farbunterschiede auf veränderten Expressionslevels der GFP-ähnlichen Proteine. In gebleichten Individuen von *Anemonia sulcata* var. *smaragdina* konnte

eine Abnahme der Gewebefluoreszenz um 30% festgestellt werden (siehe Referenz: Abbildung 4).

Außer den Wirtspigmenten (GFP-ähnliche Proteine) und den photosynthetischen Pigmenten der Symbionten (Chlorophyll a, c und Peridinin) wurde ebenso der Gehalt an Mycosporin-ähnlichen Aminosäuren (MAAs) sowie die Aktivität von antioxidativ wirkenden Enzymen, wie z.B. Superoxid-Dismutase (SOD), Katalase (KAT) und Peroxidase (POD) bestimmt.

Es konnte gezeigt werden, dass in den Tentakeln beider *Anemonia*-Arten eine vergleichbare Anzahl an Zooxanthellen mit jeweils ähnlichem Gehalt an photosynthetischen Pigmenten enthalten sind. Verbunden mit erhöhten Wassertemperaturen ereignete sich ein Bleichereignis und 30% der *Anemonia* spp. Population wies eine untypische weiße Tentakelfärbung auf. Das Bleichen erfolgte in beiden Spezies aufgrund des Verlustes von 90% der Zooxanthellen (siehe Referenz: Abbildung 5). Bekanntermaßen stößt *Anemonia sulcata* bei experimentellem Hitzestress ihre Zooxanthellen aus (Miller et al., 1992; Richier et al., 2006). Diese Tatsache weist darauf hin, dass die Wirtstier-Pigmentation den Grad des Bleichens bei *Anemonia* spp. nicht beeinflusst. Darüber hinaus wurde der Gehalt an photosynthetischen Pigmenten der Zooxanthellen durch das Bleichereignis ebenfalls nicht beeinträchtigt. Letztendlich ist der individuelle Grad des Bleichens vergleichbar zwischen beiden Spezies (siehe Referenz: Abbildung 5).

Mycosporin-ähnliche Aminosäuren (MAAs) sind UV-absorbierende Verbindungen und in vielen marinen Nesseltieren weit verbreitet, so auch in Seeanemonen (Dunlap & Shick, 1998). Die Gewebekonzentration steht häufig in positivem Zusammenhang mit der Strahlungsintensität im Habitat (Shick et al., 1995). Beide untersuchten Anemonen-Arten kommen in derselben Tiefe bei gleichen Lichtbedingungen vor. In der fluoreszenten *Anemonia sulcata* var. *smaragdina* ist jedoch der MAA-Gehalt erhöht im Vergleich zu *Anemonia rustica*. In gebleichten Vertretern blieb der MAA-Gehalt im Wesentlichen unverändert (siehe Referenz: Abbildung 6). Deshalb kann ein reduzierter MAA-Gehalt als Grund für das Bleichen vermutlich ausgeschlossen werden.

Ein erhöhter Gehalt an reaktiven Sauerstoffspezies hervorgerufen durch Stressbedingungen kann zu Zellschäden führen (Downs et al., 2002; Lesser & Shick, 1989; Smith et al., 2005; Tchernov et al., 2004). Besonders hervorgehoben wird in diesem Zusammenhang H_2O_2, welches eine relative lange Lebenszeit besitzt und in

der Lage ist Grenzen von Organellen und Zellen mittels Diffusion zu überwinden (Downs et al., 2002; Smith et al., 2005). Eine erhöhte H_2O_2-Konzentration kann die Exozytose von symbiontischen Algen hervorrufen (Smith et al., 2005). Antioxidative Enzyme wie z.B. Superoxid-Dismutase (SOD), Katalase (KAT) und Peroxidase (POD) sind Verteidigungssysteme der Tiere gegen oxidativen Stress (Hawkridge et al., 2000; Richier et al., 2003). Nicht-signifikante Unterschiede zwischen ungebleichten Vertretern beider Arten weisen auf eine ähnliche Sensivität gegenüber oxidativem Stress hin. Allerdings war der SOD-Gehalt um mehr als das Doppelte nach dem Bleichen erhöht, was zu einer hohen intrazellulären H_2O_2-Konzentration führt, welche wiederum weiter gesteigert wird durch die erniedrigte KAT-Aktivität nach dem Bleichen (siehe Referenz: Abbildung 7). Dieser Umstand resultiert aus oxidativem Stress, welcher vielleicht ein direkter Grund für das Bleichen sein könnte. Bezüglich des POD-Gehaltes konnten keine Unterschiede zwischen gebleichten und ungebleichten Individuen innerhalb der Arten festgestellt werden (siehe Referenz: Abbildung 7).

Laut diesen Ergebnissen ist sowohl der Verlust von Zooxanthellen als auch von GFP-ähnlichen Proteinen für das gebleichte Erscheinungsbild von Seeanemonen verantwortlich. Nichtsdestotrotz bleibt es weiterhin unklar, ob der erniedrigte Gehalt an Wirtstier-Pigmenten Grund oder Folge des Zooxanthellenverlustes ist. Hinsichtlich dieser offenen Frage sollten weitere Untersuchungen angestellt werden. In Anbetracht der Ergebnisse zur Aktivität der antioxidativ wirkenden Enzyme ist es möglich, dass der oxidative Stress von Bedeutung ist im Zusammenhang mit dem Bleichen von *Anemonia sulcata* var. *smaragdina* und *Anemonia rustica*.

2. GFP-ähnliche Proteine können bezüglich der Standortkonkurrenz bei Starklichtbedingungen eine photoprotektive Funktion in *Anemonia sulcata* var. *smaragdina* ausüben.

Referenz:

Wiedenmann, J., Leutenegger, A., Gundel, S., Schmitt, F., D'Angelo, C., & Funke, W. (2007). Longterm monitoring of space competition among fluorescent and non-fluorescent sea anemones in the Mediterranean Sea. *Journal of the Marine Biological Association of the United Kingdom*, 87, 851-852.

Untersuchungen hinsichtlich eines selektiven Vorteils von pigmentierten Seeanemonen in einem lichtexponierten Standort standen im Mittelpunkt einer weiteren Studie. Aus diesem Grund wurde die Tiefenverteilung zwischen der fluoreszierenden *Anemonia sulcata* var. *smaragdina* und der nicht-fluoreszierenden *Anemonia rustica* über einen Zeitraum von 11 Jahren in einem Flachwasserhabitat im Mittelmeer beobachtet.

Die Beobachtungen der *Anemonia* spp.-Populationen begannen 1994. Zu diesem Zeitpunkt befanden sich innerhalb einer abgegrenzten Fläche nur wenige Exemplare von *Anemonia rustica*. Vier Jahre später hatte ihre Anzahl zugenommen und zusätzlich hatten sich Vertreter von *Anemonia sulcata* var. *smaragdina* angesiedelt (siehe Referenz: Abbildung 2). Jede Art bildete eindeutige Gruppen und vergrößerte ihre Anzahl an Individuen vermutlich durch ungeschlechtliche Vermehrung per Längsteilung, da direkter Kontakt zwischen den Individuen nur innerhalb desselben Genotyps toleriert wird (Sauer, 1986; Wiedenmann, 2000). Im Jahr 2002 stammten beinahe alle Vertreter von *Anemonia sulcata* var. *smaragdina* ab, während die Population von *Anemonia rustica* nicht weiter anstieg. Bis zum Jahr 2005 nahm die Anzahl an Individuen von *Anemonia sulcata* var. *smaragdina* weiterhin zu. Diese Tatsache kann durch eine exponentielle Wachstumsrate mit einer ungefähren Verdopplungszeit von zwei Jahren erklärt werden (siehe Referenz: Abbildung 2). Angesichts der Verteilung in lichtexponierten Flachwasserhabitaten lassen diese Resultate vermuten, dass *Anemonia sulcata* var. *smaragdina* an diese Bedingungen besser angepasst ist.

Andere fluoreszente Farbmorphen dieser Seeanemonenart (*viridis* und *rufescens*) zeigen ebenso maximale Häufigkeit an der Wasseroberfläche in anderen Habitaten (Wiedenmann et al., 1999).

Der positive Zusammenhang zwischen Überlegenheit von *Anemonia sulcata*-Farbmorphen bei Starklichtbedingungen und der Expression von GFP-ähnlichen Pigmenten im Tentakelgewebe kann hinsichtlich der Hypothese unterstützend interpretiert werden, dass diese Proteine eine photoprotektive Funktion besitzen und somit die Wettbewerbseigenschaften in Anthozoen verbessern. Diese Annahme sollte allerdings weiter untersucht werden. Sicherlich kann die verbesserte Eignung ebenso durch andere UV-schützende Verbindungen, wie z.B. Mycosporin-ähnliche Aminosäuren oder verschieden antioxidativ wirkende Enzyme vermittelt werden.

IV. References

Adam, V., Lelimousin, M., Boehme, S., Desfonds, G., Nienhaus, K., Field, M. J., Wiedenmann, J., McSweeney, S., Nienhaus, G. U. & Bourgeois, D. (2008). Structural characterization of IrisFP, an optical highlighter undergoing multiple photo-induced transformations. *Proc Natl Acad Sci U S A*, 105, 47, 18343-18348.

Ai, H.-W., Henderson, J. N., Remington, S. J. & Campbell, R. (2006). Directed evolution of a monomeric, bright and photostable version of Clavularia cyan fluorescent protein: structural characterization and applications in fluorescence imaging. *Biochem. J.*, 400, 531-540.

Ando, R., Hama, H., Yamamoto-Hino, M., Mizuno, H. & Miyawaki A. (2002). An optical marker based on the UV-induced green-to-red photoconversion of a fluorescent protein. *Proc Natl Acad Sci U S A*, 99, 20, 12651-12656.

Ando, R., Mizuno, H. & Miyawaki, A. (2004). Regulated fast nucleocytoplasmic shuttling observed by reversible protein highlighting. *Science*, 306, 1370-1373.

Andres, A. (1881). *Mitth. Zool. Stat. Neapel.*, 2. Bd., Heft 3, 313-314.

Andres, A. (1883). Le Attinie. In: *Reale Accademia Dei Lincei* (serie 3, Memorie della Classe di scienze fisiche, matematiche e natvrali), vol. XIV, 211-674.

Andresen, M., Wahl, M. C., Stiel, A. C., Gräter, F., Schäfer, L. V., Trowitzsch, S., Weber, G., Eggeling, C., Grubmüller, H., Hell, S. W. & Jakobs, S. (2005). Structure and mechanism of the reversible photoswitch of a fluorescent protein. *Proc Natl Acad Sci U S A*, 102, 37, 13070-13074.

Andresen, M., Stiel, A. C., Trowitzsch, S., Weber, G., Eggeling, C., Wahl, M. C., Hell, S. W. & Jakobs, S. (2007). Structural basis for reversible photoswitching in Dronpa. *Proc Natl Acad Sci U S A,* 104, 32, 13005-13009.

Andresen, M., Stiel, A. C., Fölling, J., Wenzel, D., Schönle, A., Egner, A., Eggeling, C., Hell, S. W. & Jakobs, S. (2008). Photoswitchable fluorescent proteins enable monochromatic multilabel imaging and dual color fluorescence nanoscopy. *Nature Biotechnol.*, 26, 9, 1035-1040.

Arkett, S. A. (1985). The shadow response of a hydromedusan (*Polyorchis penicillatus*): Behavioral mechanisms controlling diel and ontogenic vertical migration. *Biol. Bull.*, 169, 297-312.

Baird, G. S., Zacharias, D. A. & Tsien, R. Y. (2000). Biochemistry, mutagenesis, and oligomerization of DsRed, a red fluorescent protein from coral. *Proc Natl Acad Sci U S A*, 97, 22, 11984-11989.

Barondeau, D. P., Putnam, C. D., Kassmann, C. J., Tainer, J. A. & Getzoff, E. D. (2003). Mechanism and energetics of green fluorescent protein chromophore synthesis revealed by trapped intermediate structures. *Proc Natl Acad Sci U S A*, 100, 21, 12111-12116.

Barondeau, D. P., Kassmann, C. J., Tainer, J. A. & Getzoff, E. D. (2005). Understanding GFP chromophore biosynthesis: controlling backbone cyclization and modifying posttranslational chemistry. *Biochemistry*, 44, 6, 1960-1970.

Bates, M., Huang, B., Dempsey, G. T. & Zhuang, X. (2007). Multicolor Super-Resolution Imaging with Photo-Switchable Fluorescent Probes. *Science,* 317, 1749-1753.

Baumann, D., Cook, M., Ma, L., Mushegian, A., Sanders, E., Schwartz, J. & Yu, C. R. (2008). A family of GFP-like proteins with different spectral properties in lancelet *Branchiostoma floridae. Biology Direct*, 3, 28.

Betzig, E., Patterson, G. H., Sougrat, R., Lindwasser, O. W., Olenych, S., Bonifacino, J. S., Davidson, M. W., Lippincott-Schwartz, J. & Hess, H. F. (2006). Imaging intracellular fluorescent proteins at nanometer resolution. *Science*, 313, 5793, 1642-1645.

Bock, H., Geisler, C., Wurm, C. A., Jakobs, S., Schönle, A., Egner, A., Hell , S. W. & Eggeling, C. (2007). Two-color far-field fluorescence nanoscopy based on photoswitching emitters. *Appl. Phys. B*, 88, 161-165.

Brejc, K., Sixma, T. K., Kitts, P. A., Kain, S. R., Tsien, R. Y., Ormo, M. & Remington, S. J. (1997). Structural basis for dual excitation and photoisomerization of the *Aequorea victoria* green fluorescent protein. *Proc Natl Acad Sci U S A*, 94, 6, 2306-2311.

Bulina, M. E., Chudakov, D. M., Mudrik, N. N. & Lukyanov, K. A. (2002). Interconversion of Anthozoa GFP-like fluorescent and non-fluorescent proteins by mutagenesis. *BMC Biochemistry*, 3, 7.

Burkenroad, M. D. (1943). A possible function of bioluminescence. *J. Mar. Res.*, 5, 161-164.

Campbell, R. E., Tour, O., Palmer, A. E., Steinbach, P. A., Baird, G. S., Zacharias, D. A. & Tsien, R. Y. (2002). A monomeric red fluorescent protein. *Proc Natl Acad Sci U S A*, 99, 7877-7882.

Case, J. (1984). Firefly behavior and vision. In: *Insect Communication*, Lewis, T., Ed. Harcourt, Brace, Jovanovich, London, 195-222.

Catala, R. (1959). Fluorescence effects from corals irradiated with ultra-violet rays. *Nature*, 183, 949.

Chalfie, M., Tu, Y., Euskirchen, G., Ward, W. W. & Prasher, D. C. (1994). Green fluorescent proteins as a marker for gene expression. *Science*, 263, 802-805.

Chattoraj, M., King, B.A., Bublitz, G. U. & Boxer, S. G. (1996). Ultra-fast excited state dynamics in green fluorescent protein: multiple states and proton transfer. *Proc Natl Acad Sci U S A,* 93, 8362-8367.

Chi, K. R. (2009). Super-resolution microscopy: breaking the limits. *Nature Methods*, 6, 15-18.

Chudakov, D. M., Feofanov, A. V., Mudrik, N. N., Lukyanov, S. & Lukyanov, K. A. (2003a). Chromophore environment provides clue to "kindling fluorescent protein" riddle. *J Biol Chem*, 278, 9, 7215-7219.

Chudakov, D. M., Belousov, V. V., Zaraisky, A. G., Novoselov, V. V., Staroverov, D. B., Zorov, D. B., Lukyanov, S. & Lukyanov, K. A. (2003b). Kindling fluorescent protein for precise *in vivo* photolabeling. *Nat. Biotechnol.*, 21, 191-194.

Chudakov, D. M., Verkusha, V. V., Staroverov, D. B., Souslova, E. A., Lukyanov, S. & Lukyanov, K. A. (2004). Photoswitchable cyan fluorescent protein for protein tracking. *Nat. Biotechnol.*, 22, 1435-1439.

Chudakov, D. M., Chepurnykh, T. V., Belousov, V. V., Lukyanov, S. & Lukyanov, K. A. (2006). Fast and precise protein tracking using repeated reversible photoactivation. *Traffic*, 7, 10, 1304-1310.

Chudakov, D. M., Lukyanov, S., Lukyanov, K. A. (2007). Tracking intracellular protein movements using photoswitchable fluorescent proteins PS-CFP2 and Dendra2. *Nat Protoc.*, 2 ,8, 2024-32.

Clark, K. B. (1975). Nudibranch life cycles in the northwest Atlantic and their relationship to the ecology of fouling communities. *Helgoländer Meeresuntersuchungen*, 27, 28-69.

Cody, C. W., Prasher, D. C., Westler, W. M., Pendergast, F. G. & Ward, W. W. (1993). Chemical Structure of the hexapeptide chromophore of the *Aequorea* Green fluorescent protein. *Biochemistry* 32, 1212-18.

Cormier, M. J., Hori, K., Karkhanis, Y. D., Anderson, J. M., Wampler, J. E., Morin, J. G. & Hastings, J. W. (1973). Evidence for similar biochemical requirements for bioluminescence among coelenterates. *J. Cell. Physiol.* 81, 291-298.

Cormier, M. J., Hori, K. & Anderson, J. M. (1974). Bioluminescence in coelenterates. *Biochim. Biophys. Acta* 364, 137-164.

Cubitt, A. B., Heim, R., Adams, S. R., Boyd, A. B., Gross, L. A. & Tsien, R. Y., (1995). Understanding, improving and using green fluorescent proteins. *TIBS,* 20, 448-455.

Davenport D., Nicol, J. A .C. (1955). Luminescence of hydromedusae. *Proc. R. Soc. London, Ser. B* 144, 399-411.

Deheyn, D. D., Kubokawa, K., McCarthy, J. K., Murakami, A., Porrachia, M., Rouse, G. W. & Holland, N. D. (2007). Endogenous Green Fluorescent Protein (GFP) in Amphioxus. *Biol. Bull.*, 213, 95-100.

Deliolanis, N. C., Kasmieh, R., Wurdinger, T., Tannous, B. A., Shah, K. & Ntziachristos, V. (2008). Performance of the red-shifted fluorescent proteins in deep-tissue molecular imaging applications. *J Biomed Opt.*, 13, 4, 044008.

Dove, S. G., Takabayashi, M. & Hoegh-Guldberg, O. (1995). Isolation and partial characterization of the pink and blue pigments of pocilloporid and acroporid corals. *Biol. Bull.*, 189, 288-297.

Dove, S. G., Hoegh-Guldberg, O. & Ranganathan, S. (2001). Major colour patterns of reef-building are due to a family of GFP-like protein. *Coral Reefs* 19, 197-204.

Downs, C. A., Fauth, J. E., Halas, J. C., Dustan, P., Bemiss, J. & Woodley, C. M. (2002). Oxidative stress and seasonal coral bleaching. *Free Radic. Biol. Med.*, 33, 533-543.

Dunlap, W. C. & Shick, J.M. (1998). Ultraviolet radiation-absorbing mycosporine-like amino acids in coral reef organisms: a biochemical and environmental perspective. *J. Phycol.*, 34, 418-430.

Egner, A., Geisler, C., von Middendorff, C., Bock, H., Wenzel, D., Medda, R., Andresen, M., Stiel, A. C., Jakobs, S., Eggeling, C., Schonle, A. & Hell, S. W. (2007). Fluorescence nanoscopy in whole cells by asnychronous localization of photoswitching emitters. *Biophys J.*, 93, 9, 3285-3290.

Fleisher, K. J. & Case, J. F. (1995). Cephalopod predation facilitated by dinoflagellates luminescence. *Biol. Bull.*, 189, 263-271.

Förster, T. (1948). Zwischenmolekulare Energiewanderung und Fluoreszenz. *Annalen der Physik*, 437, 55-75.

Fradkov, A. F., Chen, Y., Ding, L., Barsova, E. V., Matz, M. V. & Lukyanov, S. A. (2000). Novel fluorescent protein from *Discosoma* coral and its mutants possesses a unique far- red fluorescence. *FEBS Letters*, 479, 127-30.

Fradkov, A. F., Verkusha, V. V., Staroverov, D. B., Bulina, M. E., Yanushevich, Y. G., Martynov, V. I., Lukyanov, S. & Lukyanov, K. A. (2002). Far-red fluorescent tag for protein labelling. *Biochem. J.*, 368, 17-21.

Furla, P., Allemand, D., Shick, J. M., Ferrier-Pagès, C., Richier, S., Plantivaux, A., Merle, P. L. & Tambutté, S. (2005). The symbiotic anthozoan: a physiological chimera between alga and animal. *Integrative and Comperative Biology*, 45, 595-604.

Gilmore, A. M., Larkum, A. W. D., Salih, A., Itoh, S., Shibata, Y., Bena, C., Yamasaki, H., Papina, M. & Van Woesik, R. (2003). Simultaneous time resolution of the emission spectra of fluorescent proteins and zooxanthellar chlorophyll in reef- building corals. *Photochem Photobiol.*, 77, 515-23.

Gorbunov, M. Y., Kolber, Z. S., Lesser, M. P. & Falkowski, P. G. (2001). Photosynthesis and photoprotection in symbiotic corals. *Limnol. Oceanogr.*, 46, 75-85.

Gorokhovatsky, A. Y., Rudenko, N. V., Marchenkov, V. V., Skosyrev, V. S., Arzhanov, M. A., Burkhardt, N., Zakharov, M. V., Semisotnov, G. V., Vinokurov, L. M. & Alakhov, Y. B. (2003). Homogenous assay for biotin based on *Aequorea victoria* bioluminescence resonance energy transfer system. *Anal. Biochem.*, 313, 68-75.

Gosse, P.H. (1860). *A History Of The British Sea-Anemones and Corals*, London: Van Voorst, Paternoster Row. 1860, 160-169.

Gould, T. J., Verkhusha, V. V. & Hess. S. T. (2009). Imaging Biological Structures with Fluorescence Photoactivation Localization Microscopy. *Nature Protocols*, 4, 291-308.

Gross, L. A., Baird, G. S., Hoffman, R. C., Baldridge, K. K. & Tsien, R. Y. (2000). The structure of the chromophore within DsRed, a red fluorescent protein from coral. *Proc Natl Acad Sci U S A*, 97, 22, 11990-11995.

Gundel, S. (2004). Charakterisierung von neuartigen GFP-ähnlichen Proteinen aus *Anemonia sulcata* var. *rufescens* Andres, 1883 und *Adamsia palliata* Bohadsch, 1761 (Cnidaria, Anthozoa), *Diplomarbeit*, Universitätsbibliothek Ulm.

Gundel, S., Kachalova, G. S., Bartunik, H. D., Fuchs, J., Nienhaus, G. U. & Wiedenmann, J. (2009a). Identification of key residues responsible for high fluorescence intensity in GFP-like proteins. *prepared for publication*.

Gundel, S., Kachalova, G. S., Bartunik, H. D., Fuchs, J., Nienhaus, G. U., Oswald, F. & Wiedenmann, J. (2009b). psRFP – a new photoswitchable red fluorescent protein from Anemonia sulcata. *prepared for publication*.

Gurskaya, N. G., Fradkov, A. F., Terskikh, A., Matz, M. V., Labas, Y. A., Martynov, V. I., Yanushevich, Y. G., Lukyanov, K. A. & Lukyanov, S. A. (2001a). GFP-like chromoproteins as a source of far-red fluorescent proteins. *FEBS Letters*, 507, 16-20.

Gurskaya, N. G., Savitsky, A. P., Yanushevich, Y. G., Lukyanov, S. A. & Lukyanov, K. A. (2001b). Color transitions in coral's fluorescent proteins by site-directed Mutagenesis. *BMC Biochem.*, 2, 6.

Gurskaya, N. G., Fradkov, A. F., Pounkova, N. I., Staroverov, D. B., Bulina, M. E., Yanushevich, Y. G., Lukyanov, K. A. & Lukyanov, S. A. (2003). A colourless green fluorescent protein homologue from the non-fluorescent hydromedusa *Aequorea coerulescens* and its fluorescent mutants. *Biochem. J.*, 373, 403-408.

Gurskaya, N. G., Verkusha, V. V., Shcheglov, A. S., Staroverov, D. B., Chepurnykh, T. V., Fradkov, A. F., Lukyanov, S. & Lukyanov, K. A. (2006). Engineering of a monomeric green-to-red photoactivatable fluorescent protein induced by blue light. *Nature Biotechnology*, 24, 461-465.

Gustafsson, M. G. L. (2008). Super-resolution microscopy goes live. *Nature Methods,* 5, 385-387.

Habuchi, S., Ando, R., Dedecker, P., Verheijen, W., Mizuno, H., Miyawaki, A. & Hofkens, J. (2005). Reversible single-molecule photoswitching in the GFP-like fluorescent protein Dronpa. *Proc Natl Acad Sci U S A*, 102, 27, 9511-9516.

Harvey, E. N. (1952). *Bioluminescence*. Academic, New York.

Harvey, E. N. (1957). *A History of Luminescence from the Earliest Times until 1900*. Philadelphia: American Philosophical Society.

Hastings, J. W. & Morin, J. G. (1969). Comparative biochemistry of calcium-activated photoproteins from the ctenophore, *Mnemiopsis*, and the coelenterates *Aequorea*, *Obelia*, *Pelagia* and *Renilla. Biol. Bull.* 137, 402.

Hastings, J. W. (1995). Bioluminescence. In: *Cell Physiology Source Book*, Sperelakis, N., Ed., Academic Press, San Diego, CA.

Hastings, J. W., Liu, L. & Schultz, W. (2005). Dinoflagellate Bioluminescence and its Circadian Regulation. In: *Bioluminescence* (John Lee, Editor).

Hawkridge, J. M., Pipe, R. K. & Brown, B. E. (2000). Localization of antioxidant enzymes in the cnidarians *Anemonia viridis* and *Goniopora stokesi. Mar. Biol.*, 137, 1-9.

Heim, R, Prasher, D. C. & Tsien, R. Y. (1994). Wavelength mutations and posttranslational autoxidation of green fluorescent protein. *Proc Natl Acad Sci U S A,* 91, 12501-12504.

Hell, S. W. (2003). Toward fluorescence nanoscopy. *Nat Biotechnol*, 21, 11, 1347-1355.

Hell, S. W. (2007). Far-field optical nanoscopy. *Science*, 316, 5828, 1153-1158.

Hell, S. W. & Wichmann, J. (1994). Breaking the Diffraction Resolution Limit by Stimulated-Emission - Stimulated-Emission-Depletion Fluorescence Microscopy. *Optics Letters*, 19, 11, 780-782.

Hell, S. W., Jakobs, S. & Kastrup, L. (2003). Imaging and writing at the nanoscale with focused visible light through saturable optical transitions. *Applied Physics A: Materials Science & Processing* , 77, 7, 859-860.

Henderson, J. N. & Remington, S. J. (2006). The kindling fluorescent protein: A transient photoswitchable marker. *Physiology*, 21, 162-170.

Henderson, J. N., Ai, H.-W., Campbell, R. E. & Remington, S. J. (2007). Structural basis for reversible photobleaching of a green fluorescent protein homologue. *Proc Natl Acad Sci U S A*, 104, 16, 6672-6677.

Henderson, J. N., Gepshtein, R., Heenan, J. R., Kallio, K., Huppert, D. & Remington, S. J. (2009). Structure and mechanism of the photoactivatable green fluorescent protein. *J. Am. Chem. Soc.*, 131, 4176-4177.

Hendrickson, W. A., Pahler, A., Smith, J. L., Satow, R., Meritt, E. A. & Phizackerley, R. D. (1989). Crystal structure of core streptavidin determined from multiwavelength anomalous diffraction of synchrotron radiation. *Proc Natl Acad Sci U S A*, 86, 2190-3194.

Herring, P. J. (1977). Bioluminescence of marine organisms. *Nature*, Vol. 267, 788-793.

Herring, P. J. Ed. (1978). *Bioluminescence in Action*. Academic, New York, 570 pp.

Hess, S. T., Girirajan, T. P. & Mason, M. D. (2006). Ultra-high resolution imaging by fluorescence photoactivation localization microscopy. *Biophys. J.*, 91, 4258-4272.

Hofmann, M., Eggeling, C., Jakobs, S. & Hell, S. W. (2005). Breaking the diffraction barrier in fluorescence microscopy at low light intensities by using reversibly photoswitchable proteins. *Proc Natl Acad Sci U S A*, 102, 49, 17565-17569.

Hohenester, E. & Engel, J. (2002). Domain structure and organization in extracellular matrix proteins. *Matrix Biol.*, 21, 115-128.

Hopf, M., Göhring, W., Ries, A., Timpl, R. & Hohenester, E. (2001). Crystal structure and mutational analysis of a perlecan-binding fragment of nidogen-1. *Nature Struct. Biol.*, 8, 634-640.

Hoskins, R. A., Carlson, J. W., Kennedy, C., Acevedo, D., Evans-Holm, M., Frise, E., Wan, K. H., Park, S., Mendez-Lago, M., Rossi, F., Villasante, A., Dimitri, P., Karpen, G. H. & Celniker, S. E. (2007). Sequence finishing and mapping of *Drosophila melanogaster* Heterochromatin. *Science*, 316, 5831, 1625-1628.

Huang, B., Wang, W., Bates, M. & Zhuang, X. (2008a). Three-dimensional super-resolution imaging by stochastic optical reconstruction microscopy. *Science*, 319, 5864, 810-813.

Huang, B., Jones, S. A., Brandenburg, B. & Zhuang, X. (2008b). Whole-cell 3D STORM reveals interactions between cellular structures with nanometer-scale resolution. *Nature Methods*, 5, 1047-1052.

Inouye, S. & Tsuji, F.I. (1994). *Aequorea* green fluorescent protein: expression of the gene and fluorescence characteristics of the recombinant protein. *FEBS Lett.*, 341, 277-280.

Ip, D. T., Chan, S. H., Allen, M. D., Bycroft, M., Wan, D. C. & Wong, K. B. (2004). Crystallization and preliminary crystallographic analysis of a novel orange fluorescent protein from the Cnidaria tube anemone *Cerianthus* sp.. *Acta Crystallogr.*, D60, 340-341.

Jerlov, N. G. (1976). *Marine Optics*. Elsevier, Amsterdam.

Johnson, F. H., Shimomura, O., Saiga, Y., Gershman, L. C., Reynolds, G. T. & Waters, J. R. (1962). Quantum efficiency of *Cypridina* luminescence, with a note on that of *Aequorea. J. Cell. Comp. Physiol.*, 60, 85-104.

Karasawa, S., Araki, T., Nagai, T., Mizuno, H. & Miyawaki, A. (2004). Cyan-emitting and orange-emitting fluorescent proteins as a donor/acceptor pair for fluorescence resonance energy transfer. *Biochem. J.*, 381, 307-312.

Kawaguti, S. (1944). On the physiology of reef corals VI. Study on the pigments. *Palao Trop. Biol. Stn. Stud.*, 2, 617-674.

Kawaguti, S. (1969). Effect of the green fluorescent pigment on the productivity of reef corals. *Micronesia*, 5, 313.

Kiessling, F. (2008). Noninvasive cell tracking. In: *Handb Exp Pharmacol.*, *Molecular Imgaging II*, 185, 2, 305-321.

Kelmanson, I. V. & Matz, M. V. (2003). Molecular basis and evolutionary origins of color diversity in great star coral *Montastraea cavernosa* (Scleractinia: Faviida). *Molecular Biology and Evolution*, 20, 1125-33.

Kredel, S., Nienhaus, K., Oswald, F., Wolff, M., Ivanchenko, S., Cymer, F., Jeromin, A., Michel, F. J., Spindler, K.-D., Heilker, R., Nienhaus, G. U. & Wiedenmann, J. (2008). Optimized and Far-Red-Emitting Variants of Fluorescent Protein eqFP611. *Chem Biol.* 15, 224-33.

Kredel, S., Oswald, F., Nienhaus, K., Deuschle, K., Röcker, C., Wolff, M., Heilker, R., Nienhaus, G. U. & Wiedenmann, J. (2009). mRuby, a Bright Monomeric Red Fluorescent Protein for Labeling of Subcellular Structures. *PLoS ONE,* 4, 2, e4391. doi:10.1371/journal.pone.0004391.

Kreusch, A., Neubuser, A., Schlitz, E., Weckesser, J. & Schulz, G. E. (1994). The structure of the membrane channel porin from *Rhodopseudomonas blastica* at 2.0 Å resolution. *Protein Sci.*, 3, 58-63.

Kvansakul, M., Hopf, M., Ries, A., Timpl, R. & Hohenester, E. (2001). Structural basis for the high-affinity interaction of nidogen-1 with immunoglobulin-like domain 3 of perlecan. *EMBO J.*, 20, 19, 5342-5346.

Labas, Y. A. (1977). Triggering and regulatory mechanisms of ciliary beating in Ctenophores. I. Coordination of ciliary beating with intracellular luminescence and muscle contraction. *Tsitologya*, 19, 514-521.

Labas, Y. A. (1980). Luminescent signaling in the Ctenophores. In: *Theoretical and Practical Importance of Coelenterates*, Naumov, D. V. & Stepanjanc, S. D., Eds., Zoological Institute Academy Science USSR, Leningrad, 41-49.

Labas, Y. A., Gurskaya, N. G., Yanushevich, Y. G., Fradkov, A. F., Lukyanov, K. A., Lukyanov, S. A. & Matz, M. V. (2002). Diversity and evolution of the green fluorescent protein family. *Proc Natl Acad Sci U S A*, 99, 4256-4261.

Lesser, M. P. & Shick, J.M. (1989). Effects of irradiance and ultraviolet radiation on photoadaptation in the zooxanthellae of *Aiptasia pallida*: primary production, photoinhibition, and enzymic defenses against oxygen toxicity. *Mar. Biol.*, 102, 243-255.

Leutenegger, A., Kredel, S., Gundel, S., D'Angelo, C., Salih, A. & Wiedenmann, J. (2007). Analysis of fluorescent and non- fluorescent sea anemones from the Mediterranean Sea during a bleaching event. *Journal of Experimental Marine Biology and Ecology*, 353, 221-234.

Liddington, R. C. (2001). Mapping out the basement membrane. *Nature structural biology*, 8, 7, 573-574.

Lippincott-Schwartz, J., Snapp, E. & Kenworthy, A. (2001). Studying protein dynamics in living cells. Nat. *Rev. Mol. Cell Biol.*, 2, 444-456.

Lippincott-Schwartz, J., Altan-Bonnet, N. & Patterson, G. H. (2003). Photobleaching and photoactivation: following protein dynamics in living cells. *Nat. Cell Biol.*, 5, S7-S14.

Lloyd, J. E. (1977). Bioluminescence and communication. In: *How Animals Communicate*, Seboek, T. A., Ed., Indiana University Press, Bloomington, IN, 164-183.

Lukyanov, K. A., Fradkov, A. F., Gurskaya, N. G., Matz, M. V., Labas, Y. A., Savitsky A. P., Markelov M. L., Zaraisky A. G., Zhao X., Fang Y., Tan W. & Lukyanov S. A. (2000). Natural animal coloration can be determined by a nonfluorescent green fluorescent protein homolog. *Journal of Biological Chemistry*, 275, 25879-25882.

Lukyanov, K. A., Chudakov, D. M., Lukyanov, S. & Verkusha, V. V. (2005). Photoactivatable fluorescent proteins. *Nature Reviews*, 6, 885-891.

Mackie, G. O. (1995a). Defensive strategies in planktonic coelenterates. *Mar. Fresh. Behav. Physiol.*, 26, 119-129.

Mackie, G. O. (1995b). Unconventional signalling in Tunicates. *Mar. Fresh. Behav. Physiol.*, 26, 197-205.

Malkiel, E., Alquaddoomi, O. & Katz, J. (1999). Measurements of plankton distribution in the ocean using submersible holography. *Measurement Science and Technology*, 10, 1142-1152.

Malo, G. D., Wang, M., Wu, D., Stelling, A. L., Tonge, P. J. & Wachter, R. M. (2008). Crystal structure and Raman studies of dsFP483, a cyan fluorescent protein from *Discosoma striata*. *J Mol Biol*, 378, 4, 871-886.

Matz, M. V., Fradkov, A. F., Labas, Y. A., Savitsky, A. P., Zaraisky, A. G., Markelov, M. L. & Lukyanov, S. A. (1999). Fluorescent proteins from nonbioluminescent Anthozoa species. *Nature biotechnol.* 17, 969-973.

Mazel, C. H. & Fuchs, E. (2003). Contribution of fluorescence to the spectral signature and perceived color of corals. *Limnology and Oceanography*, 48, 390-401.

Mazel, C. H., Lesser, M. P., Gorbunov, M. Y., Barry, T.M., Farrell, J. H., Wyman, K. D. & Falkowski, P. G. (2003). Green- fluorescent proteins in Caribbean corals. *Limnology and Oceanography*, 48, 402-11.

Mazel, C. H., Cronin, T. W., Caldwell, R. L. & Marshall, N. J. (2004). Fluorescent Enhancement of Signaling in a Mantis Shrimp. *Science*, 303, 51.

Merzlyak, E. M., Goedhart, J., Shcherbo, D., Bulina, M. E., Shcheglov, A. S., Fradkov, A. F., Gaintzeva, A., Lukyanov, K. A., Lukyanov, S., Gadella, T. W. J. & Chudakov, D. M. (2007). Bright monomeric red fluorescent protein with an extended fluorescence lifetime. *Nature Methods*, 4, 555-557.

Miyawaki, A. (2002). Green fluorescent protein-like proteins in reef anthozoa animals. *Cell Struct. Funct.*, 27, 343-347.

Miller, D., Brown, B. E., Sharp, V. A. & Nganro, N. (1992). Changes in the expression of soluble proteins extracted from the symbiotic anemone *Anemonia viridis* accompany bleaching induced by hyperthermia and metal stressors. *J. Therm. Biol.*, 17, 217-223.

Miller, S. D., Haddock, S. H. D., Elvidge, C. D. & Lee, T. F. (2005). Detection of a bioluminescent milky sea from space. *Proc. Nat. Acad. Sci.*, 102, 14181-14184.

Mishin, A. S., Subach, F. V., Yampolsky, I. V., King, W., Lukyanov, K. A. & Verkhusha, V. V. (2008). The First Mutant of the *Aequorea Victoria* Green Fluorescent Protein That Forms a Red Chromophore. *Biochemistry*, 47, 4666-4673.

Mizuno, H., Mal, T. K., Tong, K. I., Ando, R., Furuta, T., Ikura, M. & Miyawaki, A. (2003). Photo-induced peptide cleavage in the green-to-red conversion of a fluorescent protein. *Mol. Cell*, 12, 1051-1058.

Molitoris, H. P. (1994). Mushrooms in Medicine. *Folia Microbiol.*, 39, 2, 91-98.

Morin, J. G. (1976). Probable functions of bioluminescence in the Pennatulacea (Cnidaria, Anthozoa). In: *Coelenterate Ecology and Behavior*, Mackie, G. O., Ed., Plenum, New York, 629-638.

Morin, J. G. (1983). Coastal bioluminescence: Patterns and functions. *Bull. Mar. Sci.*, 33, 787-817.

Morin, J. G. & Hastings, J. W. (1971a). Biochemistry of the bioluminescence of colonial hydroids and other coelenterates. *J. Cell. Physiol.* 77, 305-312.

Morin, J. G. & Hastings, J. W. (1971b). Energy Transfer in a bioluminescent system. *J. Cell Physiol.* 77, 313-318.

Morise, H., Shimomura, O., Johnson, F. H. & Winant, J. (1974). Intermolecular energy transfer in the bioluminescent system of *Aequorea. Biochemistry*. 13, 2656-2662.

Murbach, L. & Shearer, C. (1902). Preliminary report on a collection of medusae from the ocean of British Columbia and Alaska. *Ann. Mag. Nat. Hist. Ser. 7* 9, 71-73.

Nakae, H., Sugano, M., Ishimori, Y., Endo, T. & Obinata, T. (1993). Ascidian entactin/nidogen. Implication of evolution by shuffling two kinds of cysteine-rich motifs. *Eur. J. Biochem.*, 213, 1, 11-19.

Nealson, K. H. & Hastings, J. W. (1979). Bacterial bioluminescence: its control and ecological significance. *Microbiol. Rev.*, 43, 396-518.

Nealson, K. H. & Hastings, J. W. (2006). Quorum Sensing on a Global Scale: Massive Numbers of Bioluminescent Bacteria Make Milky Seas. *Applied and Environmental Microbiology*, 2295-2297.

Nienhaus, K., Nienhaus, G. U., Wiedenmann, J. & Nar, H. (2005). Structural basis for photo-induced protein cleavage and green-to-red conversion of fluorescent protein EosFP. *Proc Natl Acad Sci U S A*, 102, 26,9156-9159.

Nienhaus, G. U., Nienhaus, K., Hölzle, A., Ivanchenko, S., Renzi, F., Oswald, F., Wolff, M., Schmitt, F., Röcker, C., Vallone, B., Weidemann, W., Heilker, R., Nar, H., Wiedenmann, J. (2006). Photoconvertible Fluorescent Protein EosFP - Biophysical Properties and Cell Biology Applications. *Photochemistry and Photobiology*, 82, 2, 351-358.

Nienhaus, K., Nar, H., Heilker, R., Wiedenmann, J. & Nienhaus, G.U. (2008). Trans-Cis Isomerization is Responsible for the Red-Shifted Fluorescence in Variants of the Red Fluorescent Protein eqFP611. *J. Am. Chem. Soc.*, 130, 38, 12578-12579.

Nienhaus, G. U. & Wiedenmann, J. (2009). Structure, Dynamics and Optical Properties of Fluorescent Proteins: Perspectives for Marker Development. *Chem Phys Chem*, DOI: 10.1002/cphc.200800839.

Ohmiya, Y., Kojima, S., Nakamura, M. & Niwa, H. (2005). Bioluminescence in the limpet-like snail, *Latia neritoides. Bull. Chem. Soc. Japan*, 78, 1197-1205.

Ormö, M., Cubitt, A. B., Kallio, K., Gross, L. A., Tsien, R. Y. & Remington, S. J. (1996). Crystal structure of the Aequorea victoria green fluorescent protein. *Science,* 273,1392-1395.

Oswald, F., Schmitt, F., Leutenegger, A., Ivanchenko, S., D'Angelo, C., Salih, A., Maslakova, S., Bulina, M., Schirmbeck, R., Nienhaus, G.U., Matz, M.V. & Wiedenmann, J. (2007). Contributions of host and symbiont pigments to the coloration of reef corals. *FEBS Journal*, 274, 1102-09.

Partridge, J. C. (1990). The colour sensitivity and vision of fishes. In: *Light and Life in the Sea*, Herrin, P. J., Campbel, A. K., Whitfield, M. & Maddock, L., Eds. Cambridge University Press, Cambridge, 167-184.

Partridge, J. C. & Cummings, M. E. (1999). Adaptation of visual pigments to the aquatic environment. In: *Adaptation of visual pigments to the aquatic environment*. Arche, S. N., Djamgoz, M. B. A., Loew, E. R., Partridge, J. C. & Vallerga, S., Eds., Kluwer Academic Publishers, Dordrecht, 251-283.

Patterson, G. H. & Lippincott-Schwartz, J. (2002). A photoactivatable GFP for selective photolabeling of proteins and cells. *Science*, 297, 1873-1877.

Patterson, G. H. & Lippincott-Schwartz, J. (2003). Development and Use of Fluorescent Protein Markers in Living Cells. *Science*, 300, 87-91.

Perozzo, M. A., Ward, K. B., Thompson, R. B. & Ward, W. W. (1988). X-ray diffraction and time-resolved fluorescence analyses of *Aequorea* green fluorescent protein crystals. *J. Biol. Chem.*, 263, 7713-7716.

Petersen, J., Wilmann, P. G., Beddoe, T., Oakley, A. J., Devenish, R. J., Prescott, M. & Rossjohn, J. (2003). The 2.0-A crystal structure of eqFP611, a far red fluorescent protein from the sea anemone *Entacmaea quadricolor*. *J Biol Chem*, 278, 45, 44626-44631.

Phillips, G. N., Jr. (2006). The three-dimensional structure of green fluorescent protein and its implications for function and design. In: *Green fluorescent protein: properties, applications, and protocols*, M. Chalfie, and S. Kain, eds. (New York: Wiley-Liss), 67-82.

Prasher, D. C., Eckenrode, V. K., Ward, W. W., Prendergast, F. G. & Cormier , M. J. (1992). Primary structure of the *Aequorea victoria* green fluorescent protein. *Gene*, 111, 229-233.

Prescott, M., Ling, M., Beddoe, T., Oakley, A. J., Dove, S., Hoegh-Guldberg, O., Devenish, R. J. & Rossjohn, J. (2003). The 2.2 A crystal structure of a pocilloporin pigment reveals a nonplanar chromophore conformation. *Structure (Camb).*, 11, 275-284.

Quillin, M. L., Anstrom, D. M., Shu, X., O'Leary, S., Kallio, K., Chudakov, D. M. & Remington, S. J. (2005). The kindling fluorescent protein from *Anemonia sulcata*: Dark state structure at 1.38-Å resolution. *Biochemistry*, 44, 5774-5787.

Remington, S. J., Wachter, R. M., Yarbrough, D. K., Branchaud, B., Anderson, D. C., Kallio, K. & Lukyanov, K. A. (2005). zFP538, a yellow fluorescent protein from *Zoanthus*, contains a novel three-ring chromophore. *Biochemistry*, 44, 202-212.

Remington, S. J. (2006). Fluorescent proteins: maturation, photochemistry and photophysics. *Curr. Opin. Struct. Biol.*, 16, 714-721.

Richier, S., Merle, P. L., Furla, P., Pigozzi, D., Sola, F. & Allemand, D. (2003). Characterization of superoxide dismutases in anoxia- and hyperoxia-tolerant symbiotic cnidarians. *Biochim. Biophys. Acta*, 1621, 84-91.

Richier, S., Sabourault, C., Courtiade, J., Zucchini, N., Allemand, D. & Furla, P. (2006). Oxidative stress and apoptotic events during thermal stress in the symbiotic sea anemone, *Anemonia viridis*. *FEBS J.*, 273, 4186-4198.

Rizzuto, R., Brini, M., Pizzo, P., Murgia, M. & Pozzan, T. (1995). Chimeric green fluorescent protein as a tool for visualizing organells in living cells. *Curr. Biol.*, 5, 6, 635-642.

Rust, M. J., Bates, M. & Zhuang, X.W. (2006). Sub-diffraction-limit imaging by stochastic optical reconstruction microscopy (STORM). *Nature Methods*, 3, 10, 793-795.

Salih, A., Hoegh-Guldberg, O. & Cox, G. (1998). Photoprotection of symbiotic dinoflagellates by fluorescent pigments in reef corals, 217-230. In: J. G. Greenwood and N. J. Hall, Eds., *Proc. of the Australian Coral Reef Society 75th Anniversary Conference*.

Salih, A., Larkum, A., Cox, G. Kühl, M. & Hoegh-Guldberg, O. (2000). Fluorescent pigments in corals are photoprotective. *Nature*, 408, 850-853.

Sauer, K. P. (1986). Strategies in generating temporally and spatially different niches. *Verhandlungen der Deutschen Zoologische Gesellschaft*, 79, 11-30.

Sauer, M. (2005). Reversible molecular photoswitches: A key technology for nanoscience and fluorescence imaging. *Proc Natl Acad Sci U S A*, 102, 27, 9433-9434.

Schäfer, C., Krause, M., Fuhrhop, I., Schroeder, M., Algenstaedt, P., Fiedler, W., Rüther, W. & Hansen-Algenstaed, N. (2008). Time-course-dependent microvascular alterations in a model of myeloid leukemia *in vivo*. *Leukemia*, 22, 59-65.

Schlichter, D., Fricke H. W. & Weber, W. (1986). Light harvesting by wavelength transformation in a symbiotic coral of the Red Sea twilightzone. *Marine Biology*, 91, 403-07.

Schwentker, M. A., Bock, H., Hofmann, M., Jakobs, S., Bewersdorf, J., Eggeling, C. & Hell, S. W. (2007). Wide-field subdiffraction RESOLFT microscopy using fluorescent protein photoswitching. *Microsc Res Tech*, 70, 3, 269-280.

Shagin, D. A., Barsova, E. V., Yanushevich, Y. G., Fradkov, A. F., Lukyanov, K. A., Labas, Y. A., Semenova, T. N., Ugalde, J. A., Meyers, A., Nunez, J. M., Widder, E. A., Lukyanov, S. A. & Matz, M. V. (2004). GFP-like proteins as ubiquitous metazoan superfamily: evolution of functional features and structural complexity. *Mol Biol Evol.*, 5, 841-850.

Shaner, N. C., Campbell, R. E., Steinbach, P. A., Giepmans, B. N. G., Palmer, A. E. & Tsien, R. Y. (2004). Improved monomeric red, orange and yellow fluorescent proteins derived from *Discosoma* sp red fluorescent protein. *Nature Biotechnology*, 22, 1567-72.

Shaner, N. C., Patterson, G. H. & Davidson, M. W. (2007). Advances in fluorescent protein technology. *Journal of Cell Science*, 120, 24, 4247-4260.

Shaner, N. C., Lin, M. Z., McKeown, M. R., Steinbach, P. A., Hazelwood, K. L., Davidson, M. W. & Tsien, R. Y. (2008). Improving the photostability of bright monomeric orange and red fluorescent proteins. *Nature Methods*, 5, 6, 545-551.

Shcherbo, D., Merzlyak, E. M., Chepurnykh, T. V., Fradkov, A. F., Ermakova, G. V., Solovieva, E. A., Lukyanov, K. A., Bogdanova, E. A., Zaraisky, A. G., Lukyanov, S. & Chudakov, D. M. (2007). Bright far-red fluorescent protein for whole-body imaging. *Nature Methods*, 4, 741-746.

Shcherbo, D., Murphy, C. S., Ermakova, G. V., Solovieva, E. A., Chepurnykh, T. V., Shcheglov, A. S., Verkhusha, V. V., Pletnev, V. Z., Hazelwood K. L., Roche, P. M., Lukyanov, S., Zaraisky, A. G., Davidson, M. W. & Chudakov, D. M. (2009a). Far-red fluorescent tags for protein imaging in living tissues. *Biochem J.*, 418, 3, 567-74.

Shcherbo, D., Souslova, E. A., Goedhart, J., Chepurnykh, T. V., Gaintzeva, A., Shemiakina, I. I., Gadella, T. W. J., Lukyanov, S. & Chudakov, D. M. (2009b). Practical and reliable FRET/FLIM pair of fluorescent proteins. *BMC Biotechnology*, 9, 24.

Shick, J. M. (1991). *A functional biology of sea anemones*. London: Chapman & Hall.

Shick, J. M., Lesser, M. P., Dunlap, W. C. & Stochaj, W. R. (1995). Depthdependent responses to solar ultraviolet radiation and oxidative stress in the zooxanthellate coral *Acropora microphthalma*. *Mar. Biol.*, 122, 41-51.

Shimomura, O., Johnson, F. H. & Saiga, Y. (1962). Extraction, purification and properties of aequorin, a bioluminescent protein from the luminous hydromedusan *Aequorea. J. Cell. Comp. Physiol.*, 59, 223-239.

Shimomura, O., Johnson, F. H. & Kohama, Y. (1972). Reactions involved in bioluminescence systems of limpet (*Latia neritoides*) and limnious bacteria. *Proc Natl Acad Sci U S A*, 69, 2086-2089.

Shkrob, M. A., Yanushevich, Y. G., Chudakov, D. M., Gurskaya, N. G., Labas, Y. A., Poponov, S. Y., Mudrik, N. N., Lukyanov, S. & Lukyanov, K. A. (2005). Far-red fluorescent proteins evolved from a blue chromoprotein from *Actinia equina. Biochem. J.*, 392, 649-654.

Shroff, H., White, H. & Betzig, E. (2008). Photoactivated localization microscopy (PALM) of adhesion complexes. *Current protocols in cell biology*, chapter 4, unit 4.21.

Shu, X., Shaner, N. C., Yarbrough, C. A., Tsien, R. Y. & Remington, S. J. (2006). Novel Chromophores and Buried Charges Control Color in mFruits. *Biochemistry*, 45, 32, 9639-9647.

Smith, D. J., Suggett, D. J. & Baker, N. R. (2005). Is photoinhibition of zooxanthellae photosynthesis the primary cause of thermal bleaching in corals? *Glob. Chang. Biol.*, 11, 1-11.

Sniegowski, J. A., Lappe, J. W., Patel, H. N., Huffman, H. A. & Wachter, R. M. (2005). Base catalysis of chromophore formation in Arg96 and Glu222 variants of green fluorescent protein. *J Biol Chem*, 280, 28, 26248-26255.

Stadtfeld, M., Varas, F. & Graf, T. (2008). Fluorescent Protein–Cell Labeling and Its Application in Time-Lapse Analysis of Hematopoietic Differentiation. From: *Methods in Molecular Medicine*, Vol. 105: *Developmental Hematopoiesis: Methods and Protocols*, III, 5 395-412.

Stark, D. A. & Kulesa, P. M. (2005). Photoactivatable green fluorescent protein as a single-cell marker in living embryos. *Dev. Dyn.*, 233, 983-992.

Stepanenko, O. V., Verkusha, V. V., Kuznetsova, I. M., Uversky, V. N. & Turoverov, K. K. (2008). Fluorescent proteins as biomarkers and biosensors: Throwing color lights on molecular and cellular processes. *Current Protein and Peptide Science*, 9, 4, 1-32.

Stiel, A. C., Trowitzsch, S., Weber, G., Andresen, M., Eggeling, C., Hell, S. W., Jakobs, S. & Wahl, M. C. (2007). 1.8 A bright-state structure of the reversibly switchable fluorescent protein Dronpa guides the generation of fast switching variants. *Biochem J.*, 402, 1, 35-42.

Stiel, A. C., Andresen, M., Bock, H., Hilbert, M., Schilde, J., Schonle, A., Eggeling, C., Egner, A., Hell, S. W. & Jakobs, S. (2008). Generation of Monomeric Reversibly Switchable Red Fluorescent Proteins for Far-Field Fluorescence Nanoscopy. *Biophys J.*, 95, 6, 2989-2997.

Stokes, G. G. (1852). *On the Change of the Refrangibility of Light*, Phil. Trans. Roy. Soc., London, 142, 463-562.

Subach, F. V., Patterson, G. H., Manley, S., Gillette, J. M., Lippincott-Schwartz, J & Verkusha, V. V. (2009). Photoactivatable mCherry for high-resolution two-color fluorescence microscopy. *Nature Methods*, 6, 2, 153-159.

Szent-Gyorgyi, C. S. & Bryan, B. J. (2001). Luciferases, fluorescent proteins, nucleic acids encoding the luciferases and fluorescent proteins and the use thereof in diagnostics, high throughput screening and novelty items. *US Patent* 6232107-B.

Tchernov, D., Gorbunov, M. Y., de Vargas, C., Yadav, S. N., Milligan, A. J., Häggblom, M. & Falkowski, P. G. (2004). Membrane lipids of symbiotic algae are diagnostic of sensitivity to thermal bleaching in corals. *Proc Natl Acad Sci U S A,* 101, 13531-13535.

Terskikh, A., Fradkov, A., Ermakova, G., Zaraisky, A., Tan, P., Kajava, A. V., Zhao, X., Lukyanov, S., Matz, M., Kim, S., Weissmann, I. & Siebert, P. (2000). "Fluorescent Timer": Protein that changes color with time. *Science*, 290, 1585-1588.

Theis-Febvre, N., Martel, V., Laudet, B., Souchier, C., Grunwald, D., Cochet, C. & Filhol, O. (2005). Highlighting protein kinase CK2 movement in living cells. *Mol. Cell. Biochem.*, 274, 15-22.

Todd, C. D. (1981). The ecology of nudibranchs mollusks. *Annual Review of Oceanography and Marine Biology*, 19, 141-234.

Todd, C. D. (1983). Reproductive and trophic ecology of nudibranch mollusks. In: *The Mollusca*, Russell-Hunter, W. D., Ed., Volume 6, Ecology, Academic Press, New York, 225-259.

Tsien, R. Y. (1998). The green fluorescent protein. *Annu Rev Biochem*, 67, 509-44.

Tsutsui, H., Karasawa, S., Shimizu, H., Nukina, N. & Miyawaki, A. (2005) Semi-rational engineering of a coral fluorescent protein into an efficient highlighter. *EMBO reports*, 6, 3, 1-6.

van Woesik, R. (2000). Modelling process that generate and maintain coral community diversity. *Biodivers. Conserv.*, 9, 1219-1233.

Verkhusha, V. V. & Lukyanov, K. A. (2004). The molecular properties and applications of Anthozoa fluorescent proteins and chromoproteins. *Nature Biotechnology*, 22, 3, 289-296.

Verkusha, V. V. & Sorkin, A. (2005). Conversion of the monomeric red fluorescent protein into a photoactivatable probe. *Chemistry & Biology*, 12, 279-285.

Vogel, B. E. & Hedgecock, E. M. (2001). Hemicentin, a conserved extracellular member of the immunoglobulin superfamily, organizes epithelial and other cell attachments into oriented line-shaped junctions. *Development*, 128, 883-894.

Vogt, A., D'Angelo, C., Oswald, F., Denzel, A., Mazel, C. H., Matz, M., Ivanchenko, S., Nienhaus, G. U. & Wiedenmann, J. (2008). A green fluorescent protein with photoswitchable emission from deep sea. *PLoS ONE*, 3, 11, e3766.

Wachter, R. M., Elsliger, M. A., Kallio, K., Hanson, G. T. & Remington, S. J. (1998). Structural basis of spectral shifts in the yellow-emission variants of green fluorescent protein. *Structure*, 6, 10, 1267-1277.

Wachter, R. M. (2007). Chromogenic cross-link formation in green fluorescent protein. *Acc Chem Res*, 40, 2, 120-127.

Wall, M. A., Socolich, M. & Ranganathan R. (2000). The structural basis for red fluorescence in the tetrameric GFP homolog DsRed. *Nat Struct Biol.*, 12, 1133-1138.

Walter, N. G., Huang, C.-Y., Manzo, A. J. & Sobhy, M. A. (2008). Do-it-yourself guide: how to use the modern single-molecule toolkit. *Nature Methods*, 5, 6, 475-489.

Wampler, J. E., Hori, K., Lee, J. W. & Cormier, M. J. (1971). Structured bioluminescence. Two emitters during both the in vitro and the *in vivo* bioluminescence of the sea pansy, *Renilla. Biochemistry* 10, 2903-2909.

Wampler, J. E., Karkhanis, Y. D., Morin, J. G. & Cormier, M. J. (1973). Similarities in the bioluminescence from the *Pennatulacea. Biochim. Biophys. Acta* 314, 104-109.

Wang, L., Jackson, W. C., Steinbach, P. A. & Tsien, R. Y. (2004). Evolution of new nonantibody proteins via iterative somatic hypermutation. *Proc Natl Acad Sci U S A,* 101, 16745-49.

Ward, W. W. (2002). Fluorescent proteins: Who's got 'em and why? In: *Bioluminescence and Chemiluminescence*. Stanley, P. E. & Kricka, L. J., Eds., World Scientific, Cambridge, UK, 123-126.

Ward, W. W. & Cormier, M. J. (1976). *In vitro* energy-transfer in Renilla bioluminescence. *J. Phys. Chem.*, 80, 2289-2291.

Ward, W. W. & Cormier, M. J. (1979). An energy transfer protein in coelenterate bioluminescence: characterization, of the *Renilla* green-fluorescent protein. *J. Biol. Chem.*, 254, 781-788.

Weber, C. (1982). Electrical activities of a type of electroretinogram recorded from the ocellus of a jellyfish, *Polyorchis penicillatus* (Hydromedusae). *J. Exp. Zool.*, 223, 231-243.

White, J. & Stelzer, E. (1999). Photobleaching GFP reveals protein dynamics inside live cells. *Trends Cell Biol.*, 9, 61-65.

Wiedenmann, J. (1997). Die Anwendung eines orange fluoreszierenden Proteins und weiterer farbiger Proteine und der zugehörenden Gene aus der Artengruppe *Anemonia* sp. (*sulcata*) Pennant, (Cnidaria, Anthozoa, Actinaria) in Gentechnologie und Molekularbiologie. Offenlegungsschrift DE 197 18 640 A1. *Deutsches Patent- und Markenamt*. 1-18.

Wiedenmann, J. (2000). The identification of new proteins homologous to GFP from *Aequorea victoria* as coloring compounds in the morphs of *Anemonia sulcata* and their biological function. *PhD Thesis*. Universitätsbibliothek Ulm.

Wiedenmann, J., Röcker C. & Funke, W. (1999). The morphs of *Anemonia* aff. *sulcata* (Cnidaria, Anthozoa) in particular consideration of the ectodermal pigments. In *Verhandlungen der Gesellschaft für Ökologie*, Band 29, J. Pfadenhauer, ed., Heidelberg, Berlin: Spektrum Akademischer Verlag, 497-503.

Wiedenmann, J. & Lorenz, U. (2000). Fluoreszenz- und elektronenmikroskopische Untersuchungen an der Seeanemone *Anemonia sulcata* PENNANT (Cnidaria, Anthozoa). *Mikrokosmos*, 89, 1, 1-6.

Wiedenmann, J., Kraus, P., Funke, W. & Vogel, W. (2000a). The relationship between different morphs of *Anemonia sulcata* PENNANT (Anthozoa, Actinaria) evaluated by DNA fingerprinting. *Ophelia*, 52, 1, 57-64.

Wiedenmann, J., Elke, C., Spindler, K.-D. & Funke W. (2000b). Cracks in the β-can: fluorescent proteins from *Anemonia sulcata*. *Proc Natl Acad Sci U S A*, 97, 26, 14091-14096.

Wiedenmann, J., Elke, C., Spindler, K.-D. & Funke W. (2002a). Correction for vol. 97, 14091-14096, *Proc Natl Acad Sci U S A*, 99, 13357b.

Wiedenmann, J., Schenk, A., Röcker, C., Girod, A., Spindler, K.-D. & Nienhaus, G. U. (2002b). A far-red fluorescent protein with fast maturation and reduced oligomerization tendency from *Entacmaea quadricolor* (Cnidaria, Anthozoa, Actinaria). *Proc Natl Acad Sci U S A,* 99, 18, 11646-11651.

Wiedenmann, J., Ivanchenko, S., Oswald, F. & Nienhaus G.U. (2004a). Identification of GFP-like proteins in non-bioluminescent, azooxanthellate Anthozoa opens new perspectives for bioprospecting. *Marine Biotechnology*, vol. 6, no. 3, 270-277.

Wiedenmann, J., Ivanchenko, S., Oswald, F., Schmitt, F., Röcker, C., Salih, A., Spindler, K.-D., & Nienhaus, G.U. (2004b). EosFP, a fluorescent marker protein with UV- inducible green- to- red fluorescence conversion. *Proc Natl Acad Sci U S A*, 101, 15905-15910.

Wiedenmann, J., Vallone, B., Renzi, F., Nienhaus, K., Ivanchenko, S., Röcker, C. & Nienhaus, G. U. (2005). The red fluorescent protein eqFP611 and its genetically engineered dimeric variants. *J Biol Opt*. 10, 014003 / 1-7.

Wiedenmann, J. & Nienhaus, G. U. (2006). Live-cell imaging with EosFP and other photoactivatable marker proteins of the GFP family. Future Drugs Ltd., *Expert Rev. Proteomics*, 3, 3, 361-374.

Wiedenmann, J., Leutenegger, A., Gundel, S., Schmitt, F., D'Angelo, C., & Funke, W. (2007). Longterm monitoring of space competition among fluorescent and non- fluorescent sea anemones in the Mediterranean Sea. *Journal of the Marine Biological Association of the United Kingdom*, 87, 851-852.

Wilmann, P. G., Petersen, J., Devenish, R. J., Prescott, M. & Rossjohn, J. (2005). Variations on the GFP chromophore. A polypeptide fragmentation within the chromophore revealed in the 2.1-Å

crystal structure of a nonfluorescent chromoprotein from *Anemonia sulcata. Journal of Biological Chemistry*, 280, 4, 2401-2404.

Wood, T. I., Barondeau, D. P., Hitomi, C., Kassmann, C. J., Tainer, J. A. & Getzoff, E. D. (2005). Defining the role of arginine 96 in green fluorescent protein fluorophore biosynthesis. *Biochemistry*, 44, 49, 16211-16220.

Yampolsky, I. V., Remington, S. J., Martynov, V. I., Potapov, V. K., Lukyanov, S. & Lukyanov, K. A. (2005). Synthesis and properties of the chromophore of asFP595 chromoprotein from *Anemonia sulcata. Biochemistry*, 44, 5788-5793.

Yanagisawa, H., Davi, E. C., Starche, B. C., Ouchi, T., Yanagisawa, M., Richardson, J. A. & Olson, E. N. (2002). Fibulin-5 is an elastin-binding protein essential for elastic fibre development *in vivo. Nature*, 415, 168-171.

Yang, F., Moss, L. G. & Phillips, G. N., Jr. (1996). The molecular structure of green fluorescent protein. *Nature Biotechnol.*, 14, 1246-1256.

Yanushevich Y. G., Staroverov D. B., Savitsky A. P., Fradkov A. F., Gurskaya N. G., Bulina M. E., Lukyanov K. A. & Lukyanov S.A. (2002). A strategy for the generation of non-aggregating mutants of Anthozoa fluorescent proteins. *FEBS Lett*. 511, 1-3, 11-14.

Yarbrough, D., Wachter, R. M., Kallio, K., Matz, M. V. & Remington, S. J. (2001). Refined crystal structure of DsRed, a red fluorescent protein from coral, at 2.0-A resolution. *Proc Natl Acad Sci U S A.*, 16, 98, 2, 462-467.

Zhang, J., Campbell, R. E., Ting, A. Y. & Tsien, R. Y. (2002). Creating new fluorescent probes for cell biology. *Nat Rev Mol Cell Biol.*, 12, 906-918.

Zimmer, M. (2005). *Glowing Genes: A Revolution in Biotechnology*, New York: Prometheus Books.

V. Manuscripts and articles reprinted in this PhD thesis

Results of project A (*Determination of the influence of structural variability among GFP-like proteins from Anemonia sulcata var. rufescens on the fluorescence intensity*) are presented in a scientific manuscript prepared for publication.

Reference:

<u>Gundel, S.</u>, Kachalova, G. S., Bartunik, H. D., Fuchs, J., Nienhaus, G. U. & Wiedenmann, J. (2009a). Identification of key residues responsible for high fluorescence intensity in GFP-like proteins. *prepared for publication.* **p. 65**

Results of project B (*Discovery and characterization of a new optical highlighter protein for application in live-cell imaging*) are described in a scientific manuscript prepared for publication.

Reference:

<u>Gundel, S.</u>, Kachalova, G. S., Bartunik, H. D., Fuchs, J., Nienhaus, G. U., Oswald, F. & Wiedenmann, J. (2009b). psRFP – a new photoswitchable red fluorescent protein from *Anemonia sulcata. prepared for publication.* **p. 105**

In two peer-reviewed publications are the results of project C summarized (*Indications towards biological function of GFP-like proteins from Anemonia spp.*).

References:

Leutenegger, A., Kredel, S., <u>Gundel, S.</u>, D'Angelo, C., Salih, A. & Wiedenmann, J. (2007). Analysis of fluorescent and non-fluorescent sea anemones from the Mediterranean Sea during a bleaching event. *Journal of Experimental Marine Biology and Ecology*, 353, 221-234. **p. 143**

Wiedenmann, J., Leutenegger, A., <u>Gundel, S.</u>, Schmitt, F., D'Angelo, C., & Funke, W. (2007). Longterm monitoring of space competition among fluorescent and non-fluorescent sea anemones in the Mediterranean Sea. *Journal of the Marine Biological Association of the United Kingdom*, 87, 851-852. **p. 157**

Identification of key residues responsible for high fluorescence intensity in GFP-like proteins

Silke Gundel[1], Galina S. Kachalova[2], Hans D. Bartunik[2], Jochen Fuchs[3], Gerd U. Nienhaus[3,4], Jörg Wiedenmann[1,5]

[1] Institute of General Zoology and Endocrinology, University of Ulm, 89069 Ulm, Germany

[2] Max-Planck Research Unit for Structural Biology, Protein Dynamics Group, 22607 Hamburg, Germany

[3] Institute of Biophysics, University of Ulm, 89069 Ulm, Germany

[4] Department of Physics, University of Illinois at Urbana-Champaign, Urbana, Illinois 1801, United States of America

[5] School of Ocean and Earth Sciences, National Oceanography Center, University of Southampton, SO 14 ZH, United Kingdom

Keywords: red fluorescent protein, chromoprotein, *Anemonia sulcata*, mutagenesis

Corresponding author: PD Dr. Jörg Wiedenmann

School of Ocean & Earth Science

Room 566/18

University of Southampton

National Oceanography Centre, Southampton

European Way

SOUTHAMPTON, SO14 3ZH

United Kingdom

e-mail: joerg.wiedenmann@noc.soton.ac.uk

Abstract

We have cloned four novel GFP-like proteins from two Mediterranean Anthozoa species (*Anemonia sulcata* var. *rufescens* and *Adamsia palliata)*. Regarding to their spectral properties, they are assigned to red fluorescent and red non-fluorescent chromoproteins, respectively. We met the challenge to point out the key residues responsible for the huge difference in fluorescence intensity between a non-fluorescent chromoprotein (asCP562) and a bright fluorescent protein (asRFP.b) that are varying in only 10% of amino acid sequence and were both isolated from sea anemone *Anemonia sulcata* var. *rufescens*. Structural analysis and mutagenesis study confirmed the considerable influence of key residues M13 / S143 / C144 on bright fluorescence emission. Consequently, this knowledge was transferred to non-fluorescent chromoprotein apCP558 from sea anemone *Adamsia palliata* resulting in a mutant with 4 to 5-fold increased fluorescence intensity. Therefore, we might have employed a new approach to create a general strategy for designing novel fluorescent proteins from red absorbing chromoproteins.

Introduction

Green fluorescent protein (GFP) from the jellyfish *Aequorea victoria*, its mutants and homologues are used as *in vivo* marker in cell, developmental and molecular biology since years (1-3). To date they represent the only available fluorescent label fully encoded in a single gene. The serendipity of the first naturally occurring red fluorescent protein paved the way for discovery of GFP-like proteins that are not obligatory functionally linked to bioluminescence and exhibit different colors (4). In recent years a broad spectral diversity among Anthozoan GFP-like proteins was discovered including red fluorescent proteins (RFPs) and non-fluorescent chromoproteins (CPs; ref. 1). Especially RFPs are of specific interest concerning their application in live cell imaging. For cellular studies, RFPs are particularly desirable, because of reduced cellular autofluorescence in the red spectral region. Low-energy excitation light is less cytotoxic and therefore ideal suitable for long-term monitoring studies (5, 6). The longer wavelengths of red light are causing less scattering. Thus, the light is transmitted more efficiently through tissue, resulting in clearer images especially in whole-body imaging experiments (7-9). Finally, semiconductor detection systems are more sensitive in the red spectral region. Another attractive possibility is the application of RFPs in combination with other colored fluorescent proteins (FPs) in FRET-experiments or multicolor labeling (9-14). Hence, red fluorescent proteins have in addition to well-established FPs a great potential to be used as *in vivo* markers of protein localization and interaction and gene activity in many fields of cell biology research (3, 15, 16).

There are existing two different possibilities for successful obtaining of RFPs. First, screening of naturally occurring FPs to discover promising candidates with extraordinary properties in potential applications as marker proteins (17-21). Second, evolution of RFPs by mutagenesis of chromoproteins as another promising strategy to develop novel tools for life science research (22-24). Realizing the second strategy, knowledge of relevant adjustment screws for turning is a prerequisite. Structural studies simplify the implementation of knowledge-based protein engineering. Moreover, they disclose information about chromophore type and its environment. Crystallographic studies revealed different types of chromphores (25-30) with altered conformations (31-35) among red-shifted GFP-like proteins.

The present work describes screening of natural occurring red GFP-like proteins of two Anthozoa species (*Anemonia sulcata* var. *rufescens* and *Adamsia palliata*) from the Mediterranean Sea. Three novel RFPs and a non-fluorescent CP were discovered and characterized. Furthermore, key residues responsible for high fluorescence intensity were determined via mutagenesis and structural studies among proteins from *Anemonia sulcata* var. *rufescens* and successfully transferred to chromoprotein apCP558 from *Adamsia palliata*. On this account, we could demonstrate a strategy for generating RFPs by mutagenesis of non-fluorescent CPs.

Results & Discussion

Construction of cDNA libraries and screening

Being on the prowl for novel red fluorescent proteins, we cloned genes encoding for four new GFP-like proteins from Anthozoa: Three of them are fluorescent proteins; the other one has spectral characteristics as well as non-fluorescent chromoproteins (Figure 1).

All the mRNAs were isolated from non-bioluminescent sea anemones from the Mediterranean Sea, *Anemonia sulcata* var. *rufescens* (36) and *Adamsia palliata* (37) (Table 1). We have chosen this Anthozoa species, because in our group both red fluorescent proteins and nonfluorescent proteins of the GFP family were purified from their tissue homogenates (21, 38). However, these proteins were not cloned hitherto. Therefore, we decided to construct their cDNA libraries and characterize the obtained proteins regarding their spectral properties.

For each organism, cDNAs encoding the novel GFP-like proteins were cloned. cDNA libraries were constructed using the SMART cDNA Library Construction Kit (39) combined with an additional accumulation step only for the cDNAs encoding for the novel GFP-like proteins. Advantage of the PCR-based step is the minor amount of required RNA and the higher percentage of full length clones. In contrast to expression vector pBK-CMV of ZAP Express method (38), the inserted cDNA is expressed in all three reading frames in the now applied vector pTriplEx2. The successful choice of this method becomes obvious, when the number of positive clones is compared to them of previous cloning strategy (Table 2). For example, in former cDNA library construction from mRNA derived from tentacles of *Anemonia sulcata* var. *rufescens* no colony with the red fluorescent target protein could have been found. However, with the new established method one colony of 600 showed red fluorescence. In contrast to the ZAP Express cDNA library, the fluorescent clones obtained with new construction strategy could not so easily be detected under UV-light, but using a fluorescence microscope. This fact can be explained with simultaneous expression of cDNA in all reading frames that leads to a decreased overall expression level and therefore, a more sensitive detection system is required. The reduced protein expression level may also explain why less detectable chromoprotein asCP562 was not perceived. Nevertheless, the presented cloning method can be considered as alternative strategy for cDNA library construction.

Primary structure, spectral and biochemical properties of the novel proteins

Our approach yielded four new members of the GFP protein family. All these proteins show their emission/absorption maxima at 558 nm or at longer wavelengths and so they are assigned to red fluorescent and red non-fluorescent chromoproteins, respectively. Their spectral properties as well as their characteristic data are listed in table 3. For a clear identification of the novel proteins we used Matz' nomenclature proposed in 1999 (4). The alignment of the amino acid sequences of the novel proteins with asCP562 (38), asulCP (19) and eqFP611 (17) is shown in figure 2.

Both a fluorescent and a non-fluorescent protein were cloned from the sea anemone *Adamsia palliata*. In the chromoprotein apCP558 (absorption maximum at 558 nm) consisting of 227 amino acids, the chromophore is formed by the tripeptide A63-Y64-G65. According to its emission maximum at 585 nm the novel red fluorescent protein from the same organism is denoted apFP585. Its excitation and absorption maximum is at 568 nm and 566 nm, respectively. The quantum yield reaches with 0.50 the highest value of all new cloned proteins in this study. Characteristic for apFP585 is the altered first position of the chromophore to S63. In comparison with the spectral properties of GFP-like proteins isolated from tissue extracts of *Adamsia palliata* (21), for both proteins perceptible deviations were noticed. These differences may depend on the varying tissues used for RNA isolation and homogenate, respectively. They did not originate from the identical animal specimen, but the sea anemones were collected in the same Mediterranean Sea district. This could be a hint for individual differences concerning their equipment of proteins within a species or color morphs. Furthermore, discrepancies between recombinant expressed and from tissue purified proteins were published for other sea anemones (40).

From *Anemonia sulcata* var. *rufescens* we cloned two bright red fluorescent proteins with only ten different amino acid residues and a sequence identity of 95.3% (Table 4). Both new proteins have their emission maximum at ~ 600 nm. To differentiate between this novel real red fluorescent proteins and a formerly cloned rather dim fluorescent protein called asFP595 (41) (also named asulCP; ref.19 or asCP; ref. 42) also originated from *Anemonia sulcata*, we decided to designate them asRFP.a and asRFP.b. The chromophores of all GFP-like proteins from *Anemonia sulcata* are represented by the tripeptide M63-Y64-G65. The absorption and excitation maxima of asRFP.a and asRFP.b are very similar (Abs$_{max}$ 576/572 nm and Ex$_{max}$ 578/574 nm). These novel red fluorescent proteins are 200-fold brighter than

asFP595 (19, 41, 42) and 3 to 4-fold brighter than its variant KFP1 in the kindled form (43), respectively, resulting from their considerable higher quantum yields (0.29 = asRFP.a, 0.33 = asRFP.b). In SDS-Page analysis with heat-denatured samples, both proteins show a fragmentation pattern (~ 26 kDa, < 20 kDa, < 10 kDa) (data not shown) similar to that observed in asCP562 (38), EosFP (44), Kaede (45) and asFP595 (46). This fact suggests maturation processes during which the peptide backbone breaks in the immediate proximity of the chromophore (21, 38, 41, 45, 46). In addition, the calculated molecular mass of one monomer is for every novel protein ~ 26 kDa, which corresponds to the expected value of GFP-like proteins. Size exclusion chromatography shows the formation of tetrameric oligomers (data not shown). Oligomerization does not considerably limit the use of fluorescent proteins merely as reporters of gene expression, but can become a substantial limitation in potential applications when they are fused to a host protein (12, 13, 17). Furthermore, we could observe aggregation of novel proteins during overexpression in both bacterial and eukaryotic cells.

In summary, sequence comparison of novel FPs and CPs revealed conserved primary structures (Figure 2). The N- and C-termini vary slightly among different proteins concerning the length and composition. The core protein is characterized by alternating conserved and variable regions. Amino acids whose side chains form the inner part of the protein and the interfaces are predominantly conserved among these proteins. Regarding their chromophores, amino acids tyrosine and glycine are strictly preserved (47-49). Furthermore, the amino acids arginine and glutamine in corresponding positions to R96 and E222 in avGFP are thorough maintained. These amino acids are involved in the autocatalytic chromophore formation (50-53). However, the first residue of the chromophore-tripeptide seems to be variable among differently high fluorescent GFP-like proteins. Both high fluorescent and non-fluorescent proteins can possess methionine in this position. It is not secure to predict spectral properties based on the first chromophore residue, whereas amino acid residue 143 is indicative of the spectral properties. In non-fluorescent GFP-like proteins this position is formed by alanine, cysteine and aspartic acid, while in highly fluorescent proteins, this residue is occupied by serine (22, 24, 42). The proteins eqFP611 (17) and cmFP512 (21) are exceptions, because they are bright red or green fluorescent and show asparagine and alanine in the homologous residue, respectively.

Sequence analysis of GFP-like proteins from Anemonia sulcata

After cloning of the bright red fluorescent proteins asRFP.a and asRFP.b we could notice that *Anemonia sulcata* possesses both non-fluorescent and highly fluorescent proteins, which have an eminent sequence identity of ~ 90%. Among both chromoproteins only six amino acids are differing. The red fluorescent proteins asRFP.a and asRFP.b are varying in ten amino acid residues (Figure 2, Table 4). This fact means that only a difference of 10% of the amino acid sequence can be responsible for the high fluorescence intensity of a GFP-like protein. We met the challenge to point out the key residues responsible for the huge difference in fluorescence intensity between a non-fluorescent chromoprotein and a brilliant fluorescent protein with almost identical amino acid sequences isolated from the same organism with regard to transmit the results on other chromoproteins illuminating them. Therefore, we decided to determine the key residues that are in charge for the high fluorescence intensity of a GFP-like protein. For further experiments we chose asRFP.b as appropriate candidate, because it bears the highest resemblance to the chromoproteins asCP562 and asulCP (each 21 different amino acid residues) paired with a bright red fluorescence.

Mutagenesis study revealing key residues responsible for high fluorescence intensity

The aim of the mutagenesis study was a successive adjustment of the sequence of the chromoprotein asCP562 to this of the highly fluorescent protein asRFP.b. To this end site-directed, multi site-directed PCR mutagenesis and sexual PCR was performed. Libraries of mutants were generated that had to be investigated under the same conditions. Therefore, we dropped transformed *E. coli* (BL21DE3) cells on agar plates. Two drops side by side from the same transformed *E. coli* cells. After overnight expression at 37°C, the plates were incubated at 4°C for two weeks. Afterwards, visually screening occurred and pictures were taken under daylight and UV-light conditions to compare the new recombinantly expressed proteins. We produced some light colored mutants under VIS conditions, which only show a weak fluorescence. Other mutants showed a strong red coloration under daylight conditions and were brightly fluorescent under UV-light conditions. In table S1 the mutants are arranged according to their relative brightness in consideration of the mutated amino acid positions. A sequence analysis of the new variants of asCP562 pointed out that the mutagenic process affected all kinds of residues: external,

internal, internal residues interacting with the chromophore and interface residues. The number of introduced mutations ranges between 1 up to 20 amino acid exchanges. It is obviously, that the more mutations the sequence obtains the brighter fluorescent the protein is. Mutants were selected under UV-light conditions and their spectral properties were measured (Table S2).

After collecting data of the spectral properties, the mutants can be arranged according to their relative brightness and summarized in three groups. There is one group with absorption, excitation and emission maxima comparable to non-fluorescent chromoprotein asCP562, however, with distinctly increased quantum yields and accordingly higher relative brightness (highlighted in white). Their emission maxima are ~ 10 nm blue-shifted in comparison to the wildtype fluorescent protein asRFP.b. The second group of mutants shows absorption maxima as like as chromoprotein asCP562, but their excitation and emission maxima are similar to those of wildtype red fluorescent protein asRFP.b (shaded in light grey). Spectral properties of members of the third group are equivalent to values of asRFP.b (shaded in dark grey).

Variable spectral properties of mutants might be explained by different conformation states of the chromophore. We suppose that one can distinguish between mutants with different fractions of *trans* and *cis* isomerized chromophores, respectively.

Members of the "white group" might have a major *trans* isomerized chromophore, because their spectral properties have similar values to those of investigated chromoproteins (29, 30, 33, 35). Associates of second "light grey shaded group" might have both *cis* and *trans* isomerized chromophores, because their absorption maxima are as like as that of chromoprotein asCP562, but the predominantly extinction and emission maxima are comparable to the data of wildtype fluorescent protein. Appearance of both isomerization states within one protein is already documented (35). The third "dark grey shaded group" members might have a major *cis* isomerized chromophore due to the fact that the spectral properties are as like as them of red fluorescent protein asRFP, whose *cis* conformation of the chromophore was verified by X-ray crystallography experiments (see chapter *"Aggregation of asRFP.b and structural analysis of asRFP"*). Furthermore, *cis* isomerization of the chromophore is widespread among highly fluorescent proteins (25, 31, 32).

The molar extinction coefficients of generated mutants are in a range between 31,000 and 66,000 M^{-1} cm^{-1} and their quantum yields differ between 0.04 and 0.32.

The new variants could reach a relative brightness between 15-120% in contrast to asRFP.b. If we focus on the number of mutations, it is noticeable, that in the first (white) and second group (light grey) the number is lower than in the third group (dark grey), where a high number of mutations up to the maximum of 20 can be discerned. Surprisingly, in contrast to wildtype red fluorescent protein, there are two mutants (no. 31 and 35) with an increased relative brightness, although they do not possess all amino acids of asRFP.b. Therefore, enhanced fluorescence intensity might be caused by an optimal synergism of included mutations in these variants.

In this study we tried to identify a new protein with optimized fluorescence and as few as possible mutations. The favorite mutants are summarized in table 5. Mutant 2 with single mutation A143S has ~ 8-fold increased fluorescent intensity in contrast to chromoprotein asCP562. The importance of this residue for transformation of GFP-like chromoproteins into red fluorescent state was previously demonstrated and was now confirmed. In a far-red fluorescent protein evolved from a blue chromoprotein from *Actinia equina* (24), in the red-shifted fluorescent protein HcRed (optimized variant of *Heteractis crispa* chromoprotein; ref. 22) and in asFP595-A143S mutant from *Anemonia sulcata* (41, 42) the conversion to S143 invariably induced the appearance of red fluorescence. Concerning its spectral properties the mutant 27 is the "star-mutant" with only three changed amino acids and a relative brightness increased by a factor of ~ 40 in comparison to the chromoprotein. This denotes that residues 13, 143 and 144 might exert strong influence to the conformation state of the chromophore and the relative brightness of the protein. In this case the key mutations that are responsible for the bright red fluorescence of GFP-like proteins from *Anemonia sulcata* var. *rufescens* are: T13M / A143S / T144C.

Aggregation of asRFP.b and structural analysis of asRFP

In parallel to the mutagenesis studies, X-ray crystallography experiments were started to confirm the data. First of all, we had to prevent aggregation of asRFP.b while keeping bright red fluorescence for successful recombinant expression and purification. Aggregation generally occurs during heterologous overexpression of fluorescent proteins in both bacterial and eukaryotic cells. Large fluorescent conglomerates were formed inside 80% of transfected cells (Figure 3). Presumably, aggregation depends on protein concentration because brighter cells typically present more aggregates. Additionally, we could observe aggregation of purified

fluorescent protein *in vitro*. It partially precipitated from solution in phosphate-buffered saline without any loss of color or fluorescence. Therefore, it is expected that high molecular weight-aggregated proteins include correctly folded native protein molecules. In an attempt to decrease aggregation tendency, we mutated the basic residues F4L, K6T, K7E, K12R according to published results (43, 54). It is speculated that the positively charged amino acids in the N-terminal region can form salt bridges with adjacent tetramers, which leads to very stable conglomerates. The substitution of the same residues tested before in asFP595 evolved a non-aggregating variant of asRFP.b, called asRFP (Figure 3). After solving the problem of aggregation, asRFP could be expressed and purified in high amounts for the crystallization experiments. Having established purification and crystallization methods as described, the crystal structure of asRFP was solved with a resolution of 1.75 Å (PDB accession code 3CFA, tables S3-S5). In figure 4 are the excitation and emission spectra of crystallized asRFP shown. They are similar to those of protein in solution (data not shown) and identical to spectral properties of asRFP.b (Table 3). Interestingly, both asRFP.b and its variant asRFP show a reduced fluorescence intensity upon blue light illumination, which should be further investigated.

The structure of asRFP contains one tetramer, constituting a dimer of dimers, per asymmetric unit (Figure 5). The conformation of the individual subunits are closely similar to the structures of asFP595 (PDB accession code 2A50; ref. 35) and KFP (PDB accession code 1XMZ; ref. 29), which both include one dimer per asymmetric unit, forming tetramers through crystallographic symmetry operations. Two types of subunit interfaces can be distinguished. They are denoted as antiparallel (between subunits A/B and C/D) and perpendicular (between subunits A/C and B/D) interfaces according to the mutual orientations of the main axes of the ß-barrels. Both interfaces involve hydrophobic and hydrophilic interactions. Hydrophobic interface is composed by a central cluster of tightly packed hydrophobic residues surrounded by polar amino acids. Hydrophilic interface includes many salt bridges and hydrogen bonds between polar amino acid residues and bound water molecules. One of these interfaces takes part in homodimer formation (A/B), whereas the other interface binds the second homodimer (A/C). Every subunit contains a chromophore derived from M63-Y64-G65-tripeptide. The asRFP chromophore resides in a helical segment midst in an 11-stranded-barrel as described for all GFP-like proteins (27, 29-34, 55-57). The tripeptide M63-Y64-G65 rearranges to a chromophoric, conjugated 2-

iminomethyl-5-(4-hydroxybenzylidene) imidazolinone (MYG) system. Unlike most other GFP-like proteins, the protein backbone is broken between C62 and the chromophore (21, 24, 46). However, the former M63 Cα and backbone nitrogen atoms are in plane with the imidazolinone ring and, in consequence, part of the conjugated system. The conjugated system of MYG is expanded by the imino group, probably causing the shift of the absorption maximum toward a longer wavelength (572 nm) as compared with that of GFP (470 nm; ref. 58).

Amino acid residues located nearby the chromophore putatively influencing the fluorescence intensity were further investigated. Based on the mutagenesis study, the struggle for identification the key residues was located on the positions 13, 143 and 144 in the solved structure. Investigating the localization of these sites in the structure, we figured out that these amino acid positions are near to the chromophore. Residue 13 is an internal residue, position 143 depicts a chromophore-interacting residue and site 144 belongs to interface residues (Figure 6). The MYG chromophore of asRFP exclusively adopts the *cis* conformation, which is stabilized by surrounding residues (Figure 7). Space is opened for the *cis* isomerization of the chromophore through amino acids in position 13, 143 and 144. S143 is hydrogen-bonded to the chromophore positioning the observed *cis* form of the fluorescent chromophore. Furthermore, C144 exerts a stabilizing function on S143. Influence of M13 on high fluorescence intensity (*cis* conformation of the chromophore) is facilitated due to interaction of C62 with M63 of the chromophore. In contrast to wildtype red fluorescent protein, both non-fluorescent chromoproteins asCP562 and asFP595 possess amino acids T13, A143 and T144, which are supposed to favor *trans* isomerization of the chromophore. Indeed, in asFP595 a *trans* conformation (35) could be observed contrary to the *cis* orientation of the chromophore in asRFP (Figure 7).

Furthermore, chromophore planarity seems also to be involved in fluorescence intensity. The dihedral angle between the least-squares planes of the imidazolinone and *p*-hydroxybenzyl rings of the MYG chromophore is in its *cis* conformation in asRFP about 11°. Accordingly, it exhibits a similar flat geometry as other proteins with *cis* chromophores like, e.g. GFP and DsRed (29). The ring systems included in the chromophore are in general more coplanar in proteins with *cis* chromophores. In contrast, the dihedral angles of chromophores in the *trans* conformation display much less coplanarity (29, 33). Interestingly, the structure of red fluorescent eqFP611

provides a fundamental exception to the tendency in dihedral angles identified in *trans* chromophores (34). The overall dihedral angle in this protein is 4°, which is much closer to values revealed for *cis* conformation of the chromophore. So far, eqFP611 is the only known example of a fluorescent protein with a *trans* chromophore conformation. Therefore, it might be possible that the fluorescent properties are rather influenced by the degree of planarity than by the geometric isomer.

In summary, mutating the key residues for high fluorescence intensity in the chromoprotein asCP562, we could reach a bright fluorescent GFP-like protein and confirmed its spectral data by solving the crystal structure of asRFP with a chromophore in *cis* conformation.

Transfer of key residues to chromoprotein apCP558 from Adamsia palliata

In the next step we tried to transfer this result to another chromoprotein to also increase its fluorescence intensity. For this purpose we mutated the non-fluorescent GFP-like protein from the sea anemone *Adamsia palliata* (apCP558), which was cloned in this work. In contrast to asCP562, which possesses a methionine in its first chromophore position, it has an AYG chromophore. The sequence identity of apCP558 with the chromoprotein asCP562 is only 64%. The chromoprotein from *Adamsia palliata* shows an absorption maximum at 558 nm. Concerning their molar extinction coefficients and quantum yields, both chromoproteins show nearly identical values (asCP562: 72,000 M^{-1} cm^{-1}, 0.003; apCP558: 73,000 M^{-1} cm^{-1}, < 0.001). Interesting is the already existence of key amino acid C144 in apCP558. Therefore, we assumed that the additional introduction of M13 and S143 would let to an increase in fluorescence brightness. Indeed, a fluorescent optimized variant of apCP558 was generated after transfer of key mutations (Figure 8). There is a 4 to 5-fold increase in fluorescence intensity between the wildtype non-fluorescent chromoprotein and its mutant. Although, we tried to functionally express and purify the fluorescent mutant protein for measurement of spectral properties, we were not able to cope with this task. Due to this fact, the brightness comparison relies on pictures using fluorescence microscopy. Nevertheless, we could transfer the key residues responsible for high fluorescence intensity in GFP-like proteins from *Anemonia sulcata* var. *rufescens* to the chromoprotein found in *Adamsia palliata*. This study confirmed that the first chromophore position seems to be unimportant for

brightness. A major determinant for the spectral properties is the position 143, which is in highly fluorescent proteins principally occupied by serine instead of alanine, cysteine or aspartic acid in non-fluorescent proteins (22, 24, 42). Altogether, the occurred amino acid exchanges in mutant protein seem to benefit the major *cis* conformation of the chromophore. In consideration of the successful transfer of the before determined key residues for fluorescence intensity, we might have employed a new approach to create a general strategy for designing novel fluorescent proteins from red absorbing chromoproteins.

Concluding remarks

In summary, we have cloned and characterized several fluorescent and non-fluorescent GFP-like proteins from Anthozoa. Key residues responsible for high fluorescence intensity were determined among proteins from *Anemonia sulcata* var. *rufescens* and transferred to another chromoprotein. Furthermore, these results were confirmed by structural analysis.

Material & Methods

Construction of cDNA libraries and screening

Total RNA was isolated from 50-200 mg of fresh tissue of the actiniarian taxa *Anemonia sulcata* var. *rufescens* (36) and *Adamsia palliata* (37) according to the protocols of Matz (59) and co-workers (60). cDNA libraries were constructed using the SMART cDNA Library Construction Kit (39) with a slight modification: After amplification of the cDNA in the LD-PCR step, the cDNAs coding for GFP-like proteins were accumulated. Therefore, a specific oligonucleotide called "Actiniaria FP fisher" (5'-GGTCATCGAAGGAGGTCCTCTGCCATTTGCCTTCGACATTCTGTCA-3') was used, which encodes for frequently found amino acid sequences in a conserved region of GFP-like proteins of the taxon Actiniaria. For this purpose a mRNA-Isolation method (61) was modified. The "Actiniaria FP fisher" was 5'-biotin-labeled and combined via a biotin-streptavidin bond with magnetic particles. Using the magnetic separator, all cDNA-strands were enriched, which have bound to the immobilized oligonucleotide. This experiment was followed by a second LD-PCR step according to the manufacturer's protocol. The cDNA ligated into λTriplEx2-vector was packed and amplified by using the ZAP Express Gigapack III Gold Packaging Extract (17, 62). The conversion from λTriplEx2-vector in pTriplEx2-plasmid occurred after infection of *E. coli* (BM25.8) with recombinant phages. After incubation at 37°C overnight, the agar plates stayed at 4°C for three (*Anemonia sulcata* var. *rufescens*) or up to 16 days (*Adamsia palliata*) until the colonies were red and pink colored, respectively and GFP-like proteins were matured completely (17). The plates were visually screened for positive clones under daylight and UV-light conditions (365 nm, Benda, Wiesloch, Germany). In addition they were investigated using a fluorescence microscope (Zeiss-Axioplan I, Karl Zeiss Jena GmbH, Jena) equipped with a 150 W Hg lamp (Karl Zeiss Jena GmbH, Jena) and with filtersets for green (BP 450-490 nm, FT 510 nm, LP 520 nm) and red fluorescent proteins (BP 530-585 nm, FT 600 nm, LP 615 nm). *E. coli* cells expressing GFP-like proteins from *Adamsia palliata* have shown both non-fluorescent pinkish and red fluorescent colors. The colonies of the cDNA library from *Anemonia sulcata* var. *rufescens* exhibited green or red fluorescence (38). Plasmids were isolated and sent for sequencing by a commercial provider (MWG Biotech AG, Ebersberg, Germany).

Cloning and recombinant expression

For bacterial expression of novel GFP-like proteins and mutants, the full-length coding regions were amplified using specific primers and were cloned *Bam*HI/*Kpn*I or *Xma*I/*Hind*III into the pQE-32 vector (Qiagen, Hilden, Germany). All proteins fused to a N-terminal polyhistidine tag were expressed in *E. coli* (BL21DE3) and purified as described (21, 17, 63, 64) for measurement of spectral properties. *E. coli* cells expressing asCP562 mutants were screened using UV-light (365 nm, Benda, Wiesloch, Germany) and imaged with a digital camera (Olympus, Hamburg, Germany).

Encoding sequence for asRFP was cloned into pET-17b vector (EMD Bioscience Novagen, Merck, Darmstadt, Germany) in *BamH*I and *Nde*I sites. After IPTG-induced expression (final concentration 0.5 mM) in *E. coli* (BL21DE3, Invitrogen, Carlsbad, CA, USA) at 4°C for one week the protein was purified for crystallization experiments as described above, transferred to protein buffer (20 mM Tris-HCl pH 7,5; 120 mM NaCl; 1 mM β-Mercaptoethanol) and concentrated up to ~ 10 mg/ml for crystallization.

Mutagenesis

Site-directed mutagenesis of asCP562, apCP558 and asRFP.b was performed by PCR using overlap extension method, with primers containing appropriate target substitutions (65, 66). Generation of chimeras out of asCP562 and asRFP.b was also performed by overlap extension method. In this case of "sexual PCR method" several fragments each with the same length were generated in a first PCR step by using primers in conserved regions of both coding sequences. These fragments were recombined in a second PCR step. In the manner described coding sequences were produced consisting of two different origin sequences. Consequently, not only single or multi mutations were introduced, but complete regions of encoding sequences were mixed to determine the influence of complete different parts and not only of single amino acid positions (67-69). For multi site-directed mutagenesis of asCP562 QuikChange Multi Site-Directed Mutagenesis Kit (Stratagene, La Jolla, CA, USA) was used (12, 44). All mutants were cloned between *Bam*HI and *Kpn*I restriction sites of the pQE-32 vector (Qiagen, Hilden Darmstadt).

Spectroscopic analysis

Absorbance spectra were recorded on a Cary 1 and a Cary 50 UV-VIS spectrophotometer (Varian, Darmstadt, Germany), respectively, at a resolution of 1 nm. Purified proteins were solved in 50 mM sodium phosphate buffer (pH 7.0) supplemented with 300 mM NaCl and 300 mM imidazole. The molar extinction coefficients were estimated based on the method of alkaline denaturation (25). For this purpose, equal amounts of protein were diluted in same amounts of buffer solution and in NaOH (final concentration 0.1 M). Relation of the spectra in PBS buffer and in NaOH yields the molar extinction coefficient. The chromoprotein asCP562 was chosen as reference, because its chromophore matures almost completely.

Fluorescence spectra of proteins in solution were measured with a fluorescence spectrophotometer Cary Eclipse (Varian, Darmstadt, Germany) with a resolution of 1 nm. For measurements of asRFP crystal at the same resolution the fluorescence spectrophotometer was additionally equipped with fiber optics.

Emission spectra for calculation of fluorescent quantum yields were recorded with a Spex Fluorolog II (Spex Industries, Edison, NJ, USA) with 2.2 nm resolution at room temperature and corrected for the wavelength dependence of the detector efficiency. For quantum yield determination, the fluorescence of the new GFP-like proteins was compared to equally absorbing eqFP611 used as reference (quantum yield for eqFP611 was measured to be 0.45; ref. 17).

A fluorescent microscope (Zeiss-Axioplan I, Karl Zeiss Jena GmbH, Jena) equipped with a digital camera (Polaroid DMC Ie, Model PDMC-2, Polaroid Corp., Cambridge, Mass., USA), a 150 W Hg lamp (Karl Zeiss Jena GmbH, Jena) and a 560/50 nm band-pass excitation filter (595 nm long-pass suppression filter, 645/75 nm transmission) was used for imaging *E. coli* colonies expressing apCP558 and its fluorescent variant. The fluorescence intensity was analyzed using the ImageJ software (http://rsb.info.nih.gov/ij/).

Structural analysis of asRFP

Crystallization and data collection

The initial manual sitting drop crystallization setup was done using the identical conditions as previously described to grow crystals of other closely homologous

protein (2A50, asFP595; ref. 35). The full data set of such type of crystal was collected and the subsequent analysis of diffraction intensities has revealed the presence of pseudo-crystallographic translation and twinning of crystal lattice with four tetramers in unit cell, which made them inadequate for diffraction studies. Searching for alternative conditions, the next crystallization setup was done with Roxtal system using Nextal Kits (1152 different crystallization conditions) in 96 well microplates at 18°C in an automated robotic system. The drops were consisting of equal volumes (400 nl) of protein and reservoir solution. The protein solution contained ~ 10mg/ml protein in 120 mM NaCl, 20 mM Tris buffer at pH 7.5 with an admixture of ß-mercaptoethanol. The reservoir volume accounted 50 µl. After data processing crystallization conditions were identified to be suitable for the experiment as the untwinned crystals diffracted better than 1.8 Å and were found to belong to the same space group with closely similar cell parameters (table S3). The new crystallization conditions were 0.1 M Hepes buffer pH 7.5, 0.2 M Calcium chloride, 28% (w/v) PEG400. Cryoprotective properties of mother solution allowed to shock-freeze crystals without further additions.

The same buffer conditions were used for crystallization with hanging drop vapor method. These resulting crystals were taken for spectral measurements.

asRFP crystals of the full-length red fluorescent protein with 231 amino acids were grown in space group $C222_1$ with four molecules (tetramer) per asymmetric unit. X-ray diffraction data (table S3) were collected at the MPG beamline BW6, DESY/HASYLAB, Hamburg, using a 165 mm MarCCD detector at an X-ray wavelength of 1.05 Å. The loop-mounted crystals were shock-frozen and kept at 100 K in a nitrogen gas stream. The diffraction images were processed and scaled using the HKL program suite (70, 71). The data collection statistics are summarized in table S3.

Structure refinement

The structure of asRFP was solved by molecular replacement with MOLREP (72) using the crystal structure of the closely homologous kindling fluorescent protein KFP (PDB accession code 1XQM; ref. 30) as a search model. Apart from four disordered N-terminal residues, a complete model of asRFP was rebuilt using ARP/wARP (73) and COOT program (74). The refinement procedure of the intermediate models of each tetramer's monomer was done with REFMAC (75) without using non-

crystallographic symmetry. The refinement statistics are shown in table S4. The electron density distributions around cysteine residues 114 and 221 were modeled as s,s-(2-hydroxyethyl)thiocysteine, taking into account the presence of β-mercaptoethanol in the protein solution. Using the REFMAC dictionary of the individual peptide residues (M63, Y64 and G65) a model of the tripeptide chromophore conformation was initially built and subsequently modified according to characteristics of electron density maps analyzing the known conformations of the MYG chromophore in all available crystal structures with high resolution. The final model of asRFP was refined to a R-factor of 20.5% (Rfree = 23.1%). The other refinement statistics are summarized in table S4. Validation using the PDB Validation Suite showed good geometries for the structure. Molecular depictions were prepared with SWISS-MODEL (76).The coordinates and structure factors have been deposited in the RCSB Protein Data Bank under accession code 3CFA.

Online Supporting Information

The Supporting Information consists of five supplemental tables (tables S1-S5).

Acknowledgements

Funding

Author contributions

Conceived and designed the experiments: GUN HDB JW. Performed the experiments: GSK JF JW SG. Analyzed the data: GSK HDB JF JW SG. Contributed reagents/materials/analysis tools: HDB GUN JW. Wrote the paper: SG. Contributed to discussions: GSK HDB JF JW.

References

1. Verkhusha, V. V. & Lukyanov, K. A. (2004). The molecular properties and applications of Anthozoa fluorescent proteins and chromoproteins. *Nature Biotechnology*, 22, 3, 289-296.

2. Chudakov, D. M., Lukyanov, S. & Lukyanov, K. A. (2005). Fluorescent proteins as a toolkit for *in vivo* imaging. *Trends Biotechnol.*, 23, 605-613.

3. Stepanenko, O. V., Verkusha, V. V., Kuznetsova, I. M., Uversky, V. N. & Turoverov, K. K. (2008). Fluorescent proteins as biomarkers and biosensors: Throwing color lights on molecular and cellular processes. *Current Protein and Peptide Science*, 9, 4, 1-32.

4. Matz, M. V., Fradkov, A. F., Labas, Y. A., Savitsky, A. P., Zaraisky, A. G., Markelov, M. L. & Lukyanov, S. A. (1999). Fluorescent proteins from nonbioluminescent Anthozoa species. *Nature biotechnol.* 17, 969-973.

5. Schaefer, C., Krause, M., Fuhrhop, I., Schroeder, M., Algenstaedt, P., Fiedler, W., Rüther, W. & Hansen-Algenstaed, N. (2008). Time-course-dependent microvascular alterations in a model of myeloid leukemia *in vivo*. *Leukemia*, 22, 59–65.

6. Stadtfeld, M., Varas, F. & Graf, T. (2008). Fluorescent Protein–Cell Labeling and Its Application in Time-Lapse Analysis of Hematopoietic Differentiation. From: *Methods in Molecular Medicine, Vol. 105: Developmental Hematopoiesis: Methods and Protocols*, III, 5 395-412.

7. Deliolanis, N. C., Kasmieh, R., Wurdinger, T., Tannous, B. A., Shah, K. & Ntziachristos, V. (2008). Performance of the red-shifted fluorescent proteins in deep-tissue molecular imaging applications. *J Biomed Opt.*, 13, 4, 044008.

8. Shcherbo, D., Merzlyak, E. M., Chepurnykh, T. V., Fradkov, A. F., Ermakova, G. V., Solovieva, E. A., Lukyanov, K. A., Bogdanova, E. A., Zaraisky, A. G., Lukyanov, S. & Chudakov, D. M. (2007). Bright far-red fluorescent protein for whole-body imaging. *Nature Methods*, 4, 741 – 746.

9. Shcherbo, D., Murphy, C. S., Ermakova, G. V., Solovieva, E. A., Chepurnykh, T. V., Shcheglov, A. S., Verkhusha, V. V., Pletnev, V. Z., Hazelwood K. L., Roche, P. M., Lukyanov, S., Zaraisky, A. G., Davidson, M. W. & Chudakov, D. M. (2009). Far-red fluorescent tags for protein imaging in living tissues. *Biochem J.*, 418, 3, 567-74.

10. Campbell, R. E., Tour, O., Palmer, A. E., Steinbach, P. A., Baird, G. S., Zacharias, D. A. & Tsien, R. Y. (2002). A monomeric red fluorescent protein. *Proc Natl Acad Sci U.S.A.*, 99, 7877-7882.

11. Fradkov, A. F., Verkusha, V. V., Staroverov, D. B., Bulina, M. E., Yanushevich, Y. G., Martynov, V. I., Lukyanov, S. & Lukyanov, K. A. (2002). Far-red fluorescent tag for protein labelling. *Biochem. J.*, 368, 17-21.

12. Kredel, S., Oswald, F., Nienhaus, K., Deuschle, K., Röcker, C., Wolff, M., Heilker, R., Nienhaus, G. U. & Wiedenmann, J. (2009). mRuby, a Bright Monomeric Red Fluorescent Protein for Labeling of Subcellular Structures. *PLoS ONE*, 4, 2, e4391. doi:10.1371/journal.pone.0004391.

13. Merzlyak, E. M., Goedhart, J., Shcherbo, D., Bulina, M. E., Shcheglov, A. S., Fradkov, A. F., Gaintzeva, A., Lukyanov, K. A., Lukyanov, S., Gadella, T. W. J. & Chudakov, D. M. (2007). Bright monomeric red fluorescent protein with an extended fluorescence lifetime. *Nature Methods*, 4, 555–557.

14. Shcherbo, D., Souslova, E. A., Goedhart, J., Chepurnykh, T. V., Gaintzeva, A., Shemiakina, I. I., Gadella, T. W. J., Lukyanov, S. & Chudakov, D. M. (2009). Practical and reliable FRET/FLIM pair of fluorescent proteins. *BMC Biotechnology*, 9, 24.

15. Kiessling, F. (2008). Noninvasive cell tracking. In: *Handb Exp Pharmacol., Molecular Imgaging II*, 185, 2, 305-321.

16. Zhang, J., Campbell, R. E., Ting, A. Y. & Tsien, R. Y. (2002). Creating new fluorescent probes for cell biology. *Nat Rev Mol Cell Biol.*, 12, 906-918.

17. Wiedenmann, J., Schenk, A., Röcker, C., Spindler, K.-D. & Nienhaus, G. U. (2002). A far-red fluorescent protein with fast maturation and reduced oligomerization tendency from *Entacmaea quadricolor* (Cnidaria, Anthozoa, Actinaria). *Proc Natl Acad Sci U.S.A.*, 99 ,18, 11646-11651.

18. Dove, S. G., Takabayashi, M. & Hoegh-Guldberg, O. (1995). Isolation and partial characterization of the pink and blue pigments of pocilloporid and acroporid corals. *Biol. Bull.*, 189, 288-297.

19. Labas, Y. A., Gurskaya, N. G., Yanushevich, Y. G., Fradkov, A. F., Lukyanov, K. A., Lukyanov, S. A. & Matz, M. V. (2002). Diversity and evolution of the green fluorescent protein family. *Proc Natl Acad Sci U.S.A.*, 99, 7, 4256–4261.

20. Karasawa, S., Araki, T., Nagai, T., Mizuno, H. & Miyawaki, A. (2004). Cyan-emitting and orange-emitting fluorescent proteins as a donor/acceptor pair for fluorescence resonance energy transfer. *Biochem. J.*, 381, 307-312.

21. Wiedenmann, J., Ivanchenko, S., Oswald, F. & Nienhaus G. U., (2004). Identification of GFP-like proteins in non-bioluminescent, azooxanthellate Anthozoa opens new perspectives for bioprospecting. *Marine Biotechnology*, 6, 3 270-277.

22. Gurskaya, N. G., Fradkov, A. F., Terskikh, A., Matz, M. V., Labas, Y. A., Martynov, V. I., Yanushevich, Y. G., Lukyanov, K. A. & Lukyanov, S. A. (2001). GFP-like chromoproteins as a source of far-red fluorescent proteins. *FEBS Letters*, 507, 16-20.

23. Gurskaya, N. G., Savitsky, A. P., Yanushevich, Y. G., Lukyanov, S. A. & Lukyanov, K. A. (2001). Color transitions in coral's fluorescent proteins by site-directed Mutagenesis. *BMC Biochem.*, 2, 6.

24. Shkrob, M. A., Yanushevich, Y. G., Chudakov, D. M., Gurskaya, N. G., Labas, Y. A., Poponov, S. Y., Mudrik, N. N., Lukyanov, S. & Lukyanov, K. A. (2005). Far-red fluorescent proteins evolved from a blue chromoprotein from *Actinia equina. Biochem. J.*, 392, 649–654.

25. Gross, L. A., Baird, G. S., Hoffman, R. C., Baldridge, K. K. & Tsien, R. Y. (2000). The structure of the chromophore within DsRed, a red fluorescent protein from coral. *Proc Natl Acad Sci U S A.*, 97, 22, 11990-11995.

26. Mizuno, H., Mal, T. K., Tong, K. I., Ando, R., Furuta, T., Ikura, M. & Miyawaki, A. (2003). Photo-induced peptide cleavage in the green-to-red conversion of a fluorescent protein. *Mol. Cell*, 12, 1051-1058.

27. Remington, S. J., Wachter, R. M., Yarbrough, D. K., Branchaud, B., Anderson, D. C., Kallio, K. & Lukyanov, K. A. (2005). zFP538, a yellow-fluorescent protein from Zoanthus, contains a novel three-ring chromophore. *Biochemistry*, 44, 202-212.

28. Shu, X., Shaner, N. C., Yarbrough, C. A., Tsien, R. Y. & Remington, S. J. (2006). Novel Chromophores and Buried Charges Control Color in mFruits. *Biochemistry*, 45, 32, 9639-9647.

29. Quillin, M. L., Anstrom, D. M., Shu, X., O'Leary, S., Kallio, K., Chudakov, D. M. & Remington, S. J. (2005). The kindling fluorescent protein from *Anemonia sulcata*: Dark state structure at 1.38-Å resolution. *Biochemistry*, 44, 5774-5787.

30. Wilmann, P. G., Petersen, J., Devenish, R. J., Prescott, M. & Rossjohn, J. (2005). Variations on the GFP chromophore. A polypeptide fragmentation within the chromophore revealed in the 2.1-Å crystal structure of a nonfluorescent chromoprotein from *Anemonia sulcata. Journal of Biological Chemistry*, 280, 4, 2401–2404.

31. Wall, M. A., Socolich, M. & Ranganathan R. (2000). The structural basis for red fluorescence in the tetrameric GFP homolog DsRed. *Nat Struct Biol.*, 12, 1133-1138.

32. Yarbrough, D., Wachter, R. M., Kallio, K., Matz, M. V. & Remington, S. J. (2001). Refined crystal structure of DsRed, a red fluorescent protein from coral, at 2.0-A resolution. *Proc Natl Acad Sci U S A.*, 16, 98, 2, 462-467.

33. Prescott, M., Ling, M., Beddoe, T., Oakley, A. J., Dove, S., Hoegh-Guldberg, O., Devenish, R. J. & Rossjohn, J. (2003). The 2.2 A crystal structure of a pocilloporin pigment reveals a nonplanar chromophore conformation. *Structure (Camb).*, 11, 275-284.

34. Petersen, J., Wilmann, P. G., Beddoe, T., Oakley, A. J., Devenish, R. J., Prescott, M. & Rossjohn, J. (2003). The 2.0-A crystal structure of eqFP611, a far red fluorescent protein from the sea anemone *Entacmaea quadricolor. J Biol Chem*, 278, 45, 44626-44631.

35. Andresen, M., Wahl, M. C., Stiel, A. C., Gräter, F., Schäfer, L. V., Trowitzsch, S., Weber, G., Eggeling, C., Grubmüller, H., Hell, S. W. & Jakobs, S. (2005). Structure and mechanism of the reversible photoswitch of a fluorescent protein. *Proc. Natl. Acad. Sci. U S A.*, 102, 37, 13070-13074.

36. Andres, A. (1883). Le Attinie. In *Accad. Lincei* (3. Mem. Class. Scienz. Fis.), R. Atti, Tom. 14, 211-674.

37. Bohadsch, J. B. (1761). *De Quibusdam Animalibus Marinis*. Eds. Walter, G. C., S. 135-138.

38. Wiedenmann, J., Elke, C., Spindler, K.-D. & Funke W. (2000). Cracks in the β-can: fluorescent proteins from *Anemonia sulcata*. *Proc Natl Acad Sci U.S.A.*, 97, 26, 14091-14096.

39. BD Bioscience Clontech (2001). Manufacturer's protocol PT3000-1 (PR15738) for SMART cDNA Library Construction Kit.

40. Leutenegger, A., Kredel, S., Gundel, S., D'Angelo, C., Salih, A. & Wiedenmann, J. (2007). Analysis of fluorescent and non- fluorescent sea anemones from the Mediterranean Sea during a bleaching event. *Journal of Experimental Marine Biology and Ecology*, 353, 221-34.

41. Lukyanov, K. A., Fradkov, A. F., Gurskaya, N. G., Matz, M. V., Labas, Y. A., Savitsky A. P., Markelov M. L., Zaraisky A. G., Zhao X., Fang Y., Tan W. & Lukyanov S. A. (2000). Natural animal coloration can be determined by a nonfluorescent green fluorescent protein homolog. *Journal of Biological Chemistry*, 275, 25879-25882.

42. Bulina, M. E., Chudakov, D. M., Mudrik, N. N. & Lukyanov, K. A. (2002). Interconversion of Anthozoa GFP-like fluorescent and non-fluorescent proteins by mutagenesis. *BMC Biochemistry*, 3, 7.

43. Chudakov, D. M., Belousov, V. V., Zaraisky, A. G., Novoselov, V. V., Staroverov, D. B., Zorov, D. B., Lukyanov, S. & Lukyanov, K. A. (2003). Kindling fluorescent protein for precise *in vivo* photolabeling. *Nat. Biotechnol.*, 21, 191-194.

44. Wiedenmann, J., Ivanchenko, S., Oswald, F., Schmitt, F., Röcker, C., Salih, A., Spindler, K.-D., & Nienhaus, G. U. (2004). EosFP, a fluorescent marker protein with UV- inducible green- to- red fluorescence conversion. *Proc. Natl. Acad. Sci. U S A.*, 101, 15905- 15910.

45. Ando, R., Hama, H., Yamamoto-Hino, M., Mizuno, H. & Miyawaki A. (2002). An optical marker based on the UV-induced green-to-red photoconversion of a fluorescent protein. *Proc. Natl. Acad. Sci. U S A.*, 99, 20, 12651-12656.

46. Martynov, V. I., Savitsky, A. P., Martynova, N. Y., Savitsky, P. A., Lukyanov, K. A. & Lukyanov, S. A. (2001). Alternative cyclization in GFP-like proteins family. The formation and structure of the chromophore of a purple chromoprotein from *Anemonia sulcata*. *J Biol Chem*. 276, 24, 21012-21016.

47. Shaner, N. C., Patterson, G. H. & Davidson, M. W. (2007). Advances in fluorescent protein technology. *Journal of Cell Science*, 120, 24, 4247-4260.

48. Remington, S. J. (2006). Fluorescent proteins: maturation, photochemistry and photophysics. *Curr. Opin. Struct. Biol.*, 16, 714-721.

49. Nienhaus, G. U. & Wiedenmann, J. (2009). Structure, Dynamics and Optical Properties of Fluorescent Proteins: Perspectives for Marker Development. *Chem Phys Chem*, DOI: 10.1002/cphc.200800839.

50. Barondeau, D. P., Kassmann, C. J., Tainer, J. A. & Getzoff, E. D. (2005). Understanding GFP chromophore biosynthesis: controlling backbone cyclization and modifying posttranslational chemistry. *Biochemistry*, 44, 6, 1960-1970.

51. Sniegowski, J. A., Lappe, J. W., Patel, H. N., Huffman, H. A. & Wachter, R. M. (2005). Base catalysis of chromophore formation in Arg96 and Glu222 variants of green fluorescent protein. *J Biol Chem*, 280, 28, 26248-26255.

52. Wachter, R. M. (2007). Chromogenic cross-link formation in green fluorescent protein. *Acc Chem Res*, 40, 2, 120-127.

53. Wood, T. I., Barondeau, D. P., Hitomi, C., Kassmann, C. J., Tainer, J. A. & Getzoff, E. D. (2005). Defining the role of arginine 96 in green fluorescent protein fluorophore biosynthesis. *Biochemistry*, 44, 49, 16211-16220.

54. Yanushevich, Y. G., Staroverov D. B., Savitsky A. P., Fradkov A. F., Gurskaya N. G., Bulina, M. E., Lukyanov, K. A. & Lukyanov, S. A. (2002). A strategy for the generation of non-aggregating mutants of Anthozoa fluorescent proteins. *FEBS Lett.*, 511, 1-3,11-14.

55. Ormö, M., Cubitt, A. B., Kallio, K., Gross, L. A., Tsien, R. Y. & Remington, S. J. (1996). Crystal structure of the *Aequorea victoria* green fluorescent protein. *Science*, 273,1392-1395.

56. Yang, F., Moss, L. G. & Phillips, G. N., Jr. (1996). The molecular structure of green fluorescent protein. *Nature Biotechnol.*, 14, 1246-1256.

57. Henderson, J. N. & Remington, S. J. (2005). Crystal structures and mutational analysis of amFP486, a cyan fluorescent protein form *Anemonia majano. Proc Natl Acad Sci U.S.A.*, 102, 36, 12712-12717.

58. Tsien, R. Y. (1998). The green fluorescent protein. *Annu Rev Biochem*, 67, 509-44.

59. Matz, M. V. (2002). Amplification of representative cDNA samples from microscopic amounts of invertebrate tissue to search for new genes. In: *GFP: Methods in Molecular biology.* Hicks, B.W., (Ed.). Humana press.

60. Matz M., Usman, N., Shagin, D., Bogdanova, E., Lukyanov, S. (1997). Ordered differential display: a simple method for systematic comparison of gene expression profiles. *Nucleic Acids Res.* 25, 2541-2542.

61. Roche Molecular Biochemicals, (2003). Manufacturer`s protocol for mRNA Isolation Kit (catalogue number: 1 741 985). *Nucleic Acid Isolation and Purification Manual 2nd Edition.*

62. Stratagene (2004). *Manufacturer`s protocol for ZAP Express cDNA Gigapack III Gold Cloning Kit* (catalogue number: 200451) www.stratagene.com/manuals.

63. Ivanchenko, S., Röcker. C., Oswald. F., Wiedenmann, J. & Nienhaus. G. U. (2005). Targeted green-red photoconversion of EosFP, a fluorescent marker protein. *Journal of Biological Physics*, 31: 249-259.

64. Nienhaus, K., Vallone, B., Renzi, F., Wiedenmann, J. & Nienhaus, G. U. (2003). Crystallization and preliminary X-ray diffraction analysis of the red fluorescent protein eqFP611. *Acta Cryst.* D59, 1253-1255.

65. Ho, S. N., Hunt, H. D., Horton, R. M., Pullen, J. K. & Pease, L. R. (1989). Site-directed mutagenesis by overlap extension using the polymerase chain reaction. *Gene*, 77, 51–59.

66. Kredel, S., Nienhaus, K., Oswald, F., Wolff, M., Ivanchenko, S., Cymer, F., Jeromin, A., Michel, F. J., Spindler, K. D., Heilker, R., Nienhaus, G. U. & Wiedenmann, J. (2008). Optimized and Far-Red-Emitting Variants of Fluorescent Protein eqFP611. *Chem Biol.* 15:224-33.

67. Horton, R. M., Cai, Z.L, Ho, S. N. & Pease, L. R. (1990). Gene splicing by overlap extension: tailor-made genes using the polymerase chain reaction. *Biotechniques*, 5, 528-535.

68. Vallejo, A. N., Pogulis, R. J. & Pease, L.R. (1994). In vitro synthesis of novel genes: mutagenesis and recombination by PCR. *PCR Methods Appl.*, 4, 123-130.

69. Smith, G. P. (1994). The progeny of sexual PCR. *Nature,* 6488, 324-325.

70. Minor, W. (1993). *The HKL Manual.* HKL Research Inc., Charlottesville, VA, USA.

71. Otwinowski, Z. & Minor, W. (1997). Processing of X-ray diffraction data collected in oscillation mode. *Methods Enzymol.*, 276, 307-326.

72. Vagin, A. & Teplyakow, A. (1997) MOLREP: an automated program for molecular replacement. *J. Appl. Cryst.*, 30, 1022-1025.

73. Morris, R. J., Perrakis, A. & Lamzin, V. (2003) ARP/wARP and automatic interpretation of protein electron density maps. *Methods Enzymol.*, 374, 229-244.

74. Emsley, P. & Cowtan, K. (2004). COOT: model-building tools for molecular graphics. *Acta Crystallogr.* D60, 2126-2132.

75. Murshudov, G. N., Vagin, A. A. & Dodson, E. J. (1997) Refinement of macromolecular structures by the maximum-likelihood method. *Acta Crystallogr.* D Biol. Crystallogr., 53, 240-255.

76. Guex, N. & Peitsch, M. C. (1997) SWISS-MODEL and the Swiss-PdbViewer: An environment for comparative protein modeling. *Electrophoresis*, 18: 2714-2723. http://www.expasy.org/spdbv/
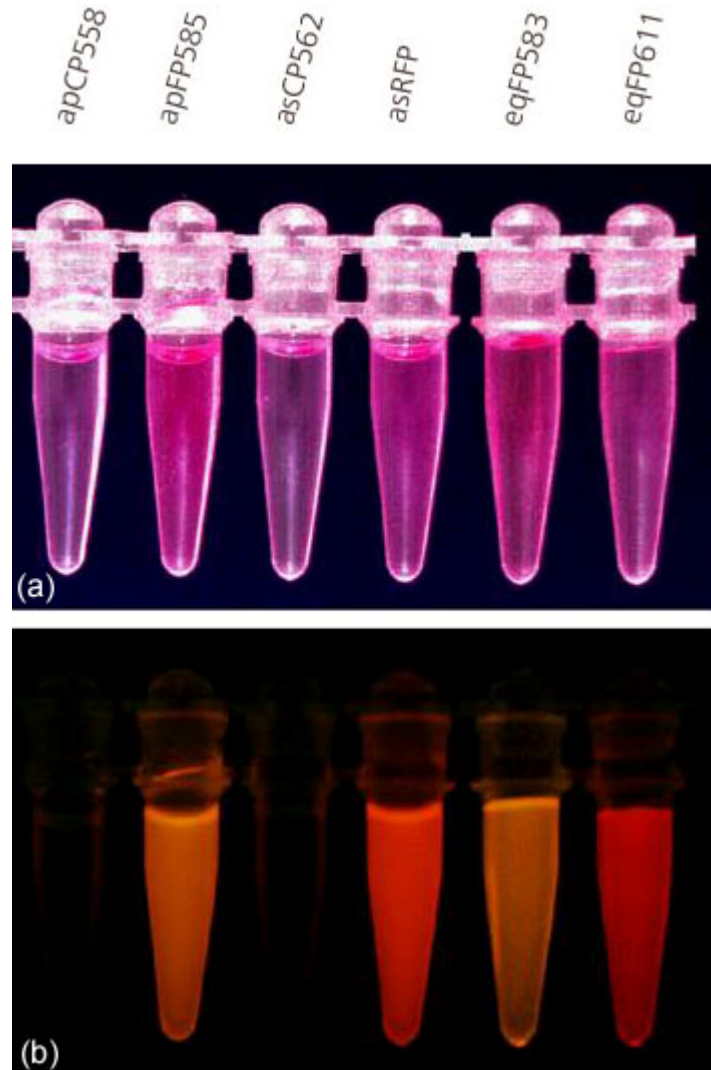
Figures

Figure 1. Overview: GFP-like proteins from Anthozoa. Novel proteins from *Adamsia palliata* (apCP558/apFP585) and *Anemonia sulcata* var. *rufescens* (asRFP) in comparison to known fluorescent proteins from *Entacmaea quadricolor* (eqFP583/eqFP611) and *Anemonia sulcata* var. *rufescens* (asCP562) under daylight (a) and UV-light conditions (b).
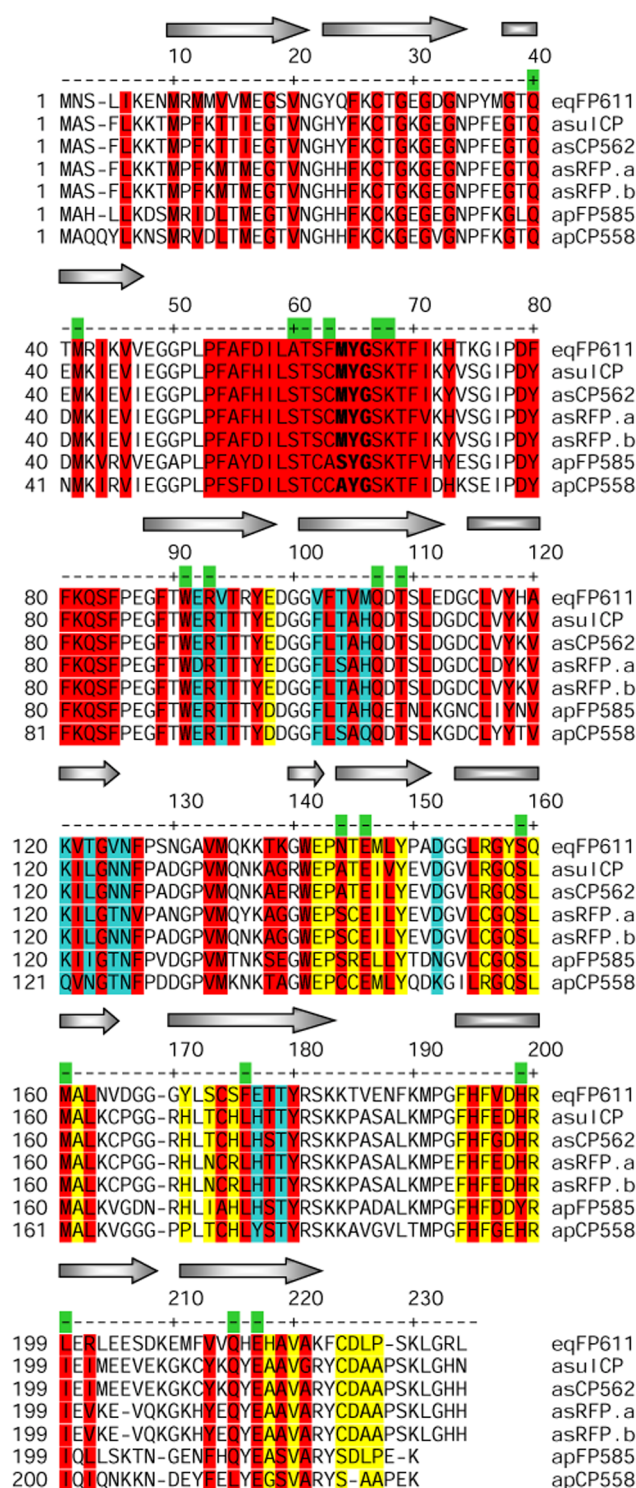
Figure 2. Multiple amino acid sequence alignment of the four new GFP-like proteins from *Anemonia sulcata* var. *rufescens* and *Adamsia palliata* with eqFP611, asulCP and asCP562. Residues forming the chromophore are printed in bold letters. Secondary structure is represented by β-sheets according to the structure of asRFP (RCSB Protein Data Bank accession code 3CFA). Amino acids whose side chains form the inner part of the protein are shaded in red. Residues forming the A/C-interface are marked in yellow, while amino acids that form the A/B-interface are shaded in cyan. The positions of amino acids, which are interacting with the chromophore, are labeled with green rectangles. Alignment gap is shown by hyphen (-). The sequence alignment was constructed using CLUSTAL V and edited manually.
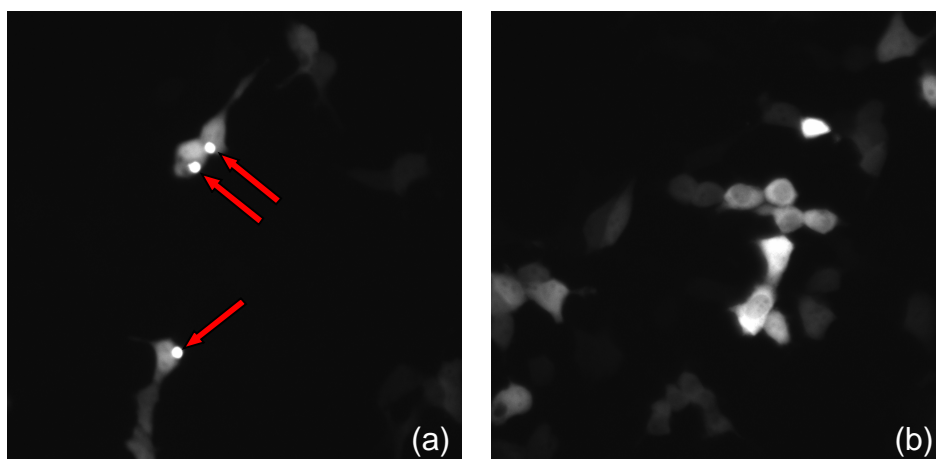
Figure 3. asRFP.b (a) and its non-aggregating variant asRFP (b) expressed in HEK 293-cells. The exposure time was 17 ms with a 40x magnification. Protein conglomerates of asRFP.b are marked with arrows in highly overexpressing cells.
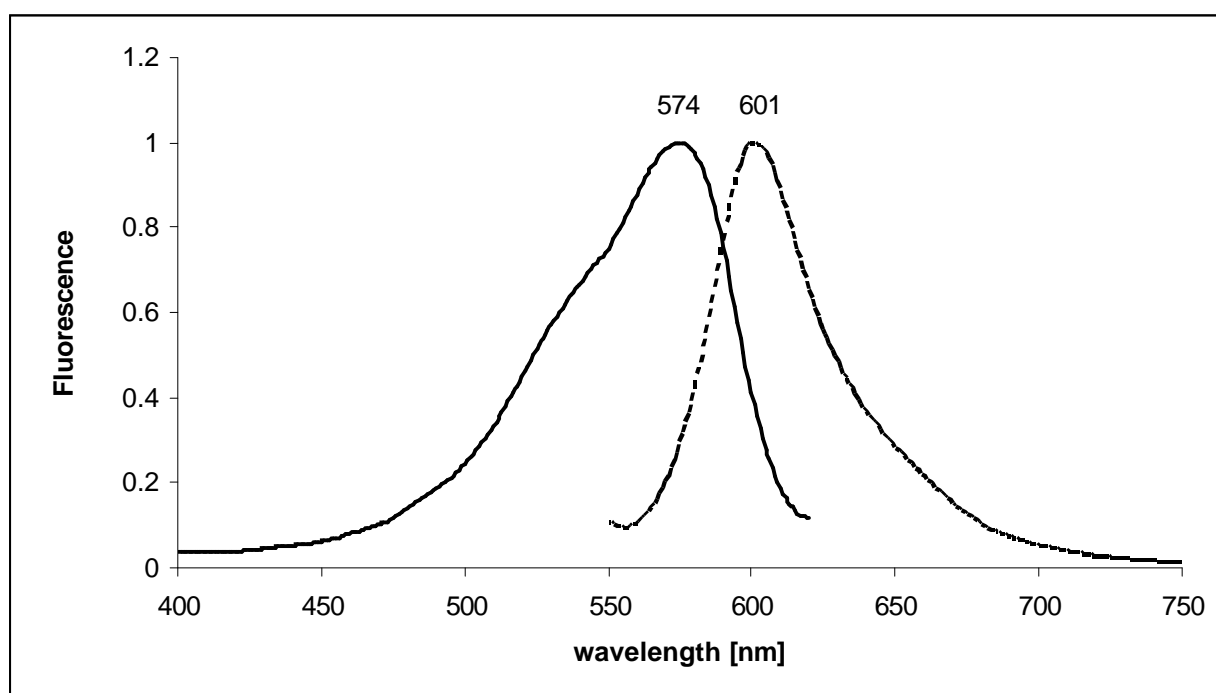
Figure 4. Excitation (solid line) and emission spectra (dashed line) of asRFP crystal.
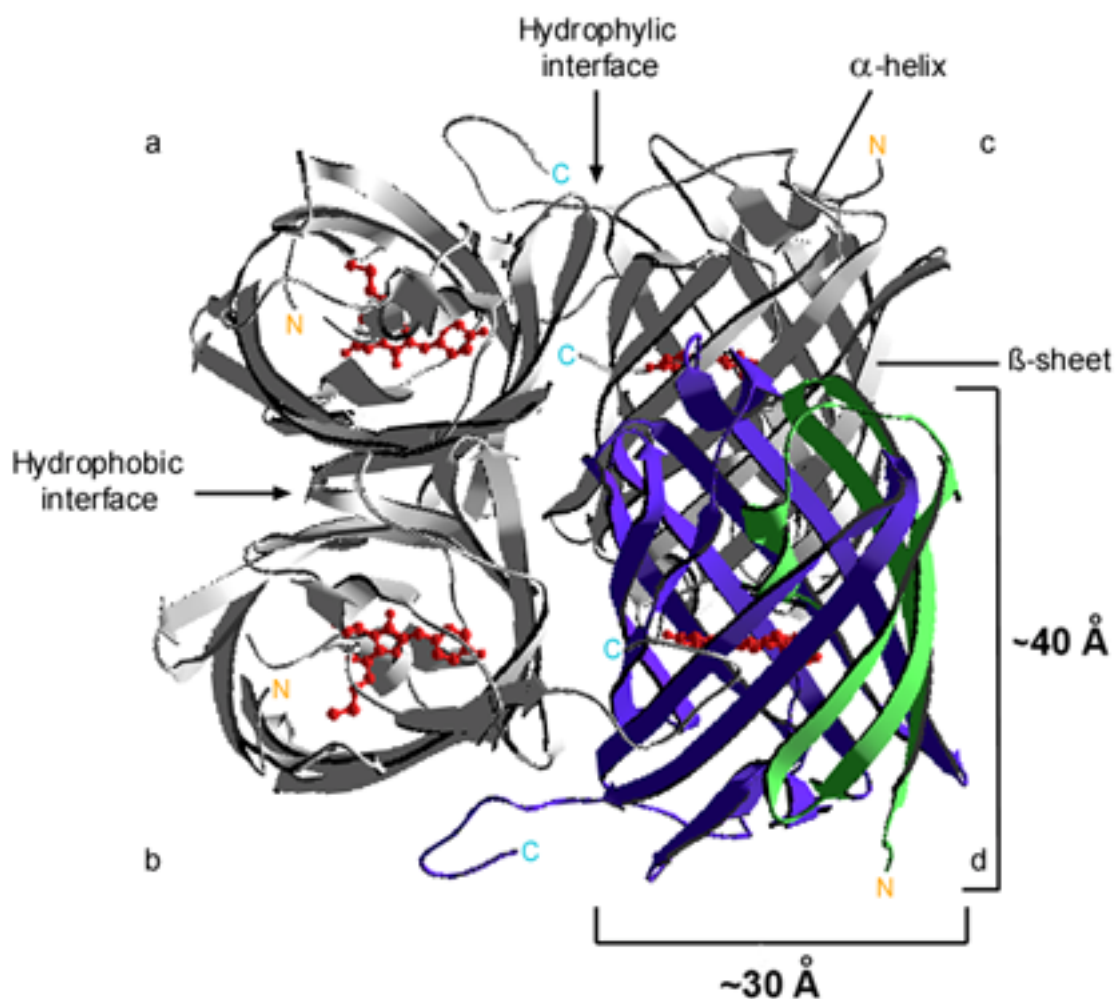
Figure 5. Overall structure of asRFP (PDB accession code 3CFA). A schematic ribbon representation of the quaternary tetrameric structure of asRFP shows the four monomers a-d. For one of the monomers (d), green and blue colors indicate the protein fragments created by break of the peptide backbone while maturation. The chromophores are highlighted in red. N- and C-termini for each monomer are designated in respective colored labeling. ß-barrel architecture and approximate dimensions are indicated.
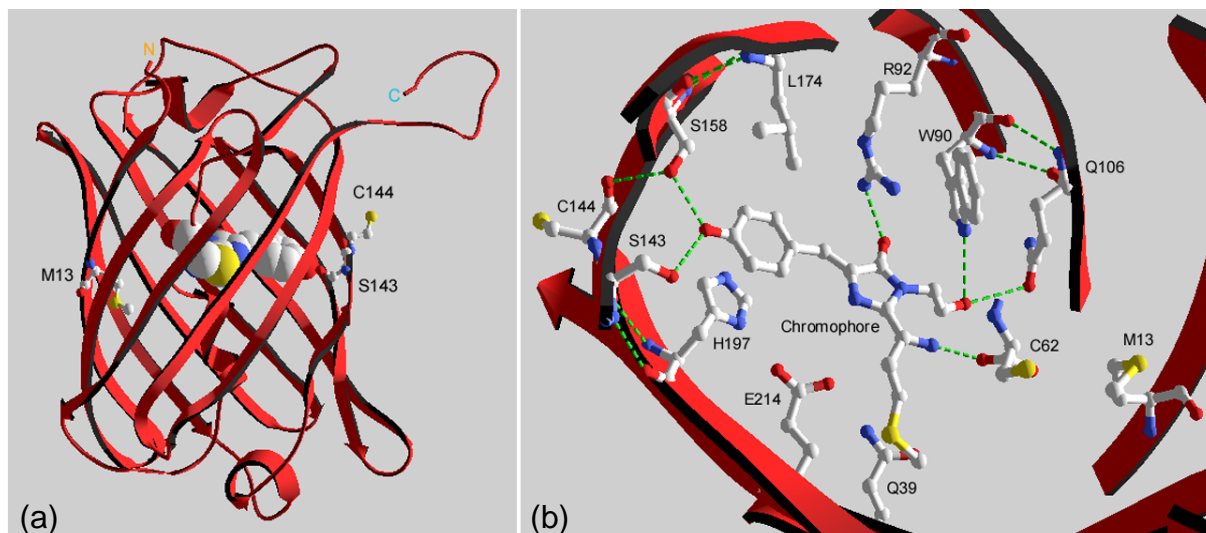
Figure 6. asRFP (PDB accession code 3CFA) chromophore and its environment including key residues for high fluorescence intensity (M13 / S143 / T144C). (a) shows a cartoon depiction of a monomeric subunit of the asRFP crystal structure. The chromophore is represented as a space-fill model. The key residues are illustrated as ball-and-sticks. (b) displays direct view of the chromophore and surrounding positions presented as ball-and-stick models. Hydrogen bonds are shown with dashed green lines. In both images atoms are color-coded: carbon atoms are white colored, oxygen atoms are represented in red, nitrogen atoms are blue labeled and sulfur atoms are indicated in yellow. ß-sheets are indicated in red.
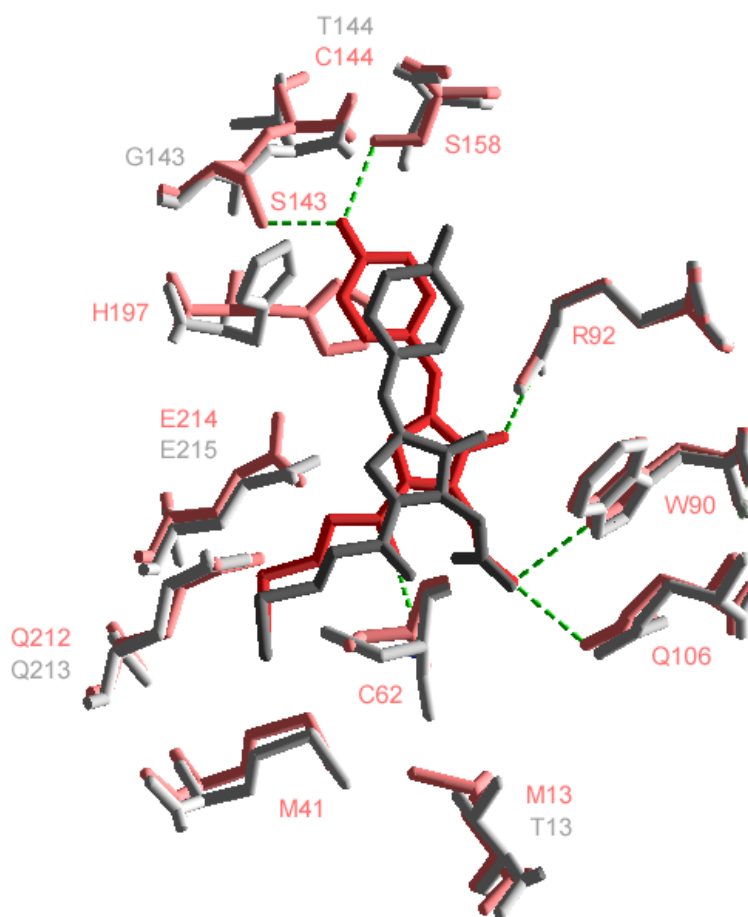
Figure 7. Overlay of chromophores and environments of asRFP (PDB accession code 3CFA; red) and KFP dark-state (PDB accession code 1XMZ; grey). Chromophores are exhibiting *cis* and *trans* conformation, respectively. Residues are shown in their major conformations. Hydrogen bonds are illustrated with dashed green lines.
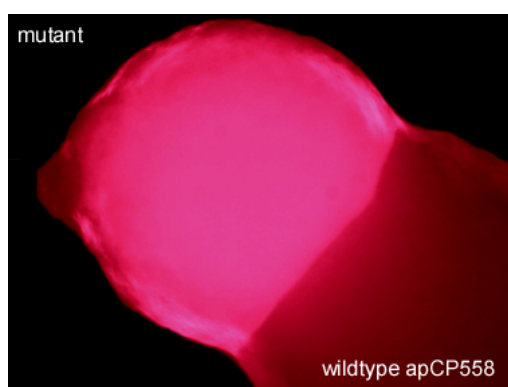
Fig. 8. Wildtype non-fluorescent chromoprotein apCP558 and its fluorescence intensity improved mutant (apCP558-L13M/C143S) recombinantly expressed in *E. coli* (BL21DE3) and viewed by fluorescence microscope.

Tables

Table 1. Anthozoa species used in this study

Species	Taxonomy	Coloration
Anemonia sulcata var. *rufescens*	*Zoantharia*, *Actiniaria*, *Actiniidae*	bright green (upside) and red (underside) fluorescent tentacles, pink tentacle tips
Adamsia palliata	*Zoantharia*, *Actiniaria*, *Hormathiidae*	red fluorescent dots on the scapulus-surface, bright red fluorescent ring around oral disk, pink acontia

Table 2. Efficiency of cDNA library construction systems

	ZAP Express cDNA Synthesis Kit [1]	SMART cDNA Library Construction Kit [2] + "Actiniaria FP fisher"-accumulation step
Anemonia sulcata var. *rufescens*	one of 700 colonies (0.14%) = asFP499 17 of 10^6 colonies (0.0017%) = asCP562 no red fluorescent colony	one of 300 colonies (0.33%) = asFP499 no non-fluorescent colony one of 600 colonies (0.17%) = asRFP.a/b
Adamsia palliata	-	no fluorescent colonies, only milky-white colored under daylight conditions

[1] Stratagene
[2] BD Bioscience Clontech

94

Table 3. Properties of identified fluorescent proteins in contrast to known GFP-like proteins

Species	Protein name	Number of amino acids	Calculated molecular mass [kDa]	Absorption maximum [nm]	Excitation maximum [nm]	Emission maximum [nm]	Extinction coefficient [M^{-1} cm^{-1}]	Quantum yield	Relative Brightness[a]	Chromophore
Anemonia sulcata var. *rufescens*	asRFP.a	231	25.77	576	578	600	50,000	0.29	0.41	MYG
Anemonia sulcata var. *rufescens*	asRFP.b	231	25.81	572	574	601	38,000	0.33	0.36	MYG
Adamsia palliata	apFP585	226	25.44	566	568	585	n. m.	0.50	n. c.	SYG
Adamsia palliata	apCP558	227	25.43	558	(568)	(584)	n. m.	0.01	n. c.	AYG
Entacmaea quadricolor	eqFP611	231	25.93	560	559	611	78,000	0.45	1.0	MYG
Anemonia sulcata	asFP595[b] asCP[c] asulCP[d]	232	25.92	572[b]	568[c, d]	595[b]	56,200[b, c]	<< 0.001[b, c]	< 0.002	MYG
Anemonia sulcata	KFP1 (initial)[e]	232	25.82	n. m.	580	600	123,000	< 0.001	< 0.004	MYG
Anemonia sulcata	KFP1 (kindled)[e]	232	25.82	n. m.	580	600	59,000	0.07	0.12	MYG

[a] = as compared to the brightness (extinction coefficient multiplied by quantum yield) of eqFP611.
[b] = Data are from ref. 41   [c] = Data are from ref. 42
[d] = Data are from ref. 19   [e] = Data are from ref. 43
n. m. = data not measured   n. c. = data not calculated

Table 4. Amino acid sequence analysis of GFP-like proteins from *Anemonia sulcata*

	asCP562	asulCP [a]	asRFP.a	asRFP.b	asFP499 [b]
asCP562		6 [c] 97,4 [d] 2,6 [e]	29 86,2 13,3	21 89,7 9,3	110 52,6 71,0
asulCP [a]	6 97,4 2,6		29 86,2 13,3	21 89,7 9,2	108 51,8 69,3
asRFP.a	29 86,2 13,3	29 86,2 13,3		10 95,3 4,5	105 51,8 64,7
asRFP.b	21 89,7 9,3	21 89,7 9,2	10 95,3 4,5		104 52,2 63,7
asFP499 [b]	110 52,6 71,0	108 51,8 69,3	105 51,8 64,7	104 52,2 63,7	

[a] = Data are from ref. 19
[b] = Data are from ref. 38
[c] = different amino acid residues
[d] = sequence identity (%)
[e] = divergence (nucleotide substitutions)

Divergence is calculated by comparing sequence pairs in relation to the phylogeny reconstructed by DNASTAR MegAlign. Percent identity compares sequences directly, without accounting for phylogenetic relationships. Note that divergence is not usually the inverse of percent identity (i.e. the sum of the percent identity and divergence values for a given pair is not usually 100).

Table 5. Key residues responsible for fluorescence intensity in GFP-like RFPs from *Anemonia sulcata* var. *rufescens*

Name	Mutations	Absorption maximum [nm]	Excitation maximum [nm]	Emission maximum [nm]	E_{mol} [M^{-1} cm^{-1}]	QY	Relative Brightness[a] [%]
asCP562	-	562	562	595	72,000	0.003	2
2	A143S	562	576	595	46,000	0.04	15
27	T13M A143S T144C	559	564	592	44,000	0.22	77
asRFP.b	total number of 21 mutations	572	574	601	38,000	0.33	100

[a] = as compared to the brightness (extinction coefficient multiplied by quantum yield) of asRFP.b

Table S1. Key residues responsible for high fluorescence intensity in GFP-like proteins from *Anemonia sulcata* var. *rufescens*

name	VIS	UV 302 nm	T13M	I15M	Y23H	E40D	H56D	E138G	R139G	A143S	T144C	R155C	T171N	H173R	S176T	G191E	G195E	I201V	M202K	E204-	E205Q	C209H	K211E
asCP562																							
1												■											
2										■	■												
3										■	■												
4					■					■	■					■							
5										■	■					■							
6										■	■					■							
7					■					■												■	■
8			■	■	■	■	■			■	■												
9			■	■						■	■	■	■	■	■	■	■	■	■	■	■	■	■
10								■		■	■												
11								■	■	■	■												
12								■	■	■													
13								■		■	■	■											
14					■					■	■	■											
15			■							■	■												
16	reddish, UV+-			■						■	■					■					■		
17	white-reddish, UV+-			■																	■		
18	white-reddish, UV+-		■							■											■		
19	reddish., UV+																						
20			■	■						■	■					■							
21										■	■												
22	pink, UV++		■	**I15L**						■	■					■							
23	red, UV+		■						**A137V**	■	■					■							
24	pink, UV+		■	**I15L**						■													
25	red, UV+			■						■	■	■											
26	red, UV++		■							■	■	■											
27	red, UV+									■	■												
28	red, UV+		■							■	■					■							
29					■	■		■		■	■												
30			■	■	■	■	■			■	■												
31			■	■	■	■	■	■		■	■							■	■	■	■	■	■
32			■	■	■	■	■	■	■	■	■		■		■		■	■	■	■	■	■	■
33			■	■	■	■	■	■	■	■	■		■	■	■	■	■	■	■	■	■	■	■
34			■	■	■	■	■	■	■	■	■	■	■	■	■	■	■	■	■	■	■	■	■
35			■	■				■	■	■	■	■	■	■	■	■	■	■	■	■	■	■	■
asRFP.b			■	■	■	■	■	■	■	■	■	■	■	■	■	■	■	■	■	■	■	■	■

Internal residue   **External residue**   **Internal residue interacting with the chromophor**   **Interface residue**

Table S1. Overview about generated mutants and their mutated amino acids. In the second column are pictures and comments, respectively, of the mutants expressed in *E.coli* under daylight and under UV-light conditions. The mutants are arranged according to their relative brightness in consideration of the mutated amino acid positions. In the headline are the mutated residues listed. The mutations affected all kinds of residues: external, internal, internal residues interacting with the chromophore and interface residues. The number of mutations ranges between 1 up to 20 amino acid exchanges. The more mutations the sequence obtains the brighter fluorescent the protein is.

Table S2. Spectral properties of selected mutants

Name	Abs$_{max}$ [nm]	Ex$_{max}$ [nm]	Em$_{max}$ [nm]	E$_{mol}$ [M^{-1} cm^{-1}]	Quantum yield	Relative Brightness[a]	Number of mutations compared to asCP562
asCP562	562	562	595	72,000	0.003	0.02	0
2	562	576	595	46,000	0.04	0.15	1
3	561	574	595	35,000	0.05	0.14	2
11	566	576	598	39,000	0.09	0.28	3
15	558	564	592	31,000	0.13	0.32	5
16	564	574	597	66,000	0.06	0.32	4
17	564	576	597	50,000	0.10	0.40	4
18	559	563	591	52,000	0.10	0.41	4
19	563	576	598	58,000	0.10	0.46	3
20	564	576	599	53,000	0.13	0.55	5
21	566	575	599	53,000	0.14	0.59	4
22	559	572	597	61,000	0.12	0.58	4 (with I15L: 5)
23	559	562	592	37,000	0.22	0.65	4 (with A137V: 5)
24	560	574	597	63,000	0.13	0.65	3 (with I15L: 4)
25	566	576	598	59,000	0.14	0.66	4
26	559	562	592	41,000	0.21	0.69	4
27	559	564	592	44,000	0.22	0.77	3
28	559	563	591	48,000	0.23	0.88	4
30	566	578	600	59,000	0.19	0.89	8
31	565	576	600	63,000	0.21	1.06	9
32	572	574	601	40,000	0.25	0.80	20
33	572	575	601	39,000	0.28	0.87	19
34	572	575	602	41,000	0.28	0.92	20
35	574	575	604	47,000	0.32	1.20	19
asRFP.b	572	574	601	38,000	0.33	1.0	21

[a] = as compared to the brightness (extinction coefficient multiplied by quantum yield) of asRFP.b

Table S2. Spectral properties (Abs$_{max}$, Ex$_{max}$, Em$_{max}$, E$_{mol}$, quantum yield and relative brightness) of selected mutants (listed in supplemental table 1). The mutants are arranged according to their relative brightness and summarized in three groups. There is one group with absorption, excitation and emission maxima comparable to non-fluorescent chromoprotein asCP562, but with distinctly increased quantum yields and accordingly higher relative brightness (highlighted in white). The second group of mutants shows absorption maxima as like as chromoprotein asCP562, but their excitation and emission maxima are similar to those of wildtype red fluorescent protein asRFP.b (shaded in light grey). Spectral properties of members of the third group are equivalent to values of asRFP.b (shaded in dark grey). The molar extinction coefficient is in a range between 31,000 and 66,000 M^{-1} cm^{-1} for all mutants. The quantum yield differs between 0.04 and 0.32. The mutants could reach a relative brightness between 15 and 120% in contrast to asRFP.b. Regarding the number of mutations, it can be noticed, that in the first and second group there is a low number and in the third group there is a high number of mutations up to the maximum of 20.

Table S3. Data collection statistics

Data set PDB entry	asRFP 3CFA
Space group	$C222_1$
Cell dimensions (Å)	
a	98.449
b	98.540
c	241.615
Wavelength (Å)	1.05
Resolution (Å)	20.0-1.75
	(1.78-1.75)
Completeness (%)	97.0 (98.9)
Redundancy	3.31 (3.25)
$<I/\sigma(I)>$	15.5 (4.5)
Rmerge[a]	0.08 (0.60)

Values in parentheses refer to data in the highest-resolution shell.
[a] Rmerge = $\Sigma |Iobs - <I>| / \Sigma <I>$.

Table S4. Refinement statistics

Data set PDB entry	asRFP 3CFA
Resolution (Å)	12.3-1.75
No. reflections	108505
Rcryst[a]	0.205
Rfree[a]	0.231
No. non-hydrogen atoms	
Protein	7336
Solvent	1012
Chromophore	4
Wilson *B* value (Å^2)	25.5
r.m.s. deviations from ideal geometry	
Bond lengths (Å)	0.022
Bond angles (º)	1.9
Ramachandran analysis	
Favored (%)	94.0
Allowed (%)	100.0

[a] R-factor = $\Sigma |F_{obs} - F_{calc}| / \Sigma F_{obs}$.

Table S5. Chromophore geometry and hydrogen-bonding contacts

Data set PDB entry	asRFP 3CFA
State	on
Conformation	*cis*
Occupancy	1
Dihedral angle (˚)	11
H-bonds (Å)	
OH-S143OG	2.51
OH-S158OG,A	2.75
OH-S158OG,B	3.23
N1-C62O	2.20
N3-T60O	2.90
O2-R92NH2	2.66
O3-W90NE1	3.19
O3-Q106OE1	3.05
SD-Q212NE2	3.01

psRFP – a new photoswitchable red fluorescent protein from *Anemonia sulcata*

Silke Gundel[1], Galina S. Kachalova[2], Hans D. Bartunik[2], Jochen Fuchs[3], Gerd U. Nienhaus[3,4], Franz Oswald[5], Jörg Wiedenmann[1,6]

[1] Institute of General Zoology and Endocrinology, University of Ulm, 89069 Ulm, Germany

[2] Max-Planck Research Unit for Structural Biology, Protein Dynamics Group, 22607 Hamburg, Germany

[3] Institute of Biophysics, University of Ulm, 89069 Ulm, Germany

[4] Department of Physics, University of Illinois at Urbana-Champaign, Urbana, Illinois 1801, United States of America

[5] Department of Internal Medicine I, University of Ulm, 89069 Ulm, Germany

[6] School of Ocean and Earth Sciences, National Oceanography Center, University of Southampton, SO 14 ZH, United Kingdom

Corresponding author: PD Dr. Jörg Wiedenmann

School of Ocean & Earth Science

Room 566/18

University of Southampton

National Oceanography Centre, Southampton

European Way

SOUTHAMPTON, SO14 3ZH

United Kingdom

e-mail: joerg.wiedenmann@noc.soton.ac.uk

Abstract

Photoswitchable fluorescent proteins are a new class of GFP-like proteins that are able to be repeatedly switched by light illumination from a fluorescent to a non-fluorescent state and vice versa. These genetically encoded probes have attracted widespread interest for many applications, in particular for new protein tracking concepts and superresolution microscopy projects. Using site-directed mutagenesis we evolved from precursor protein of *Anemonia sulcata* var. *rufescens* a reversible photoswitchable red fluorescent protein, psRFP, which displays negative switching mode. Off-switching to non-fluorescent state is induced by low-energy blue light illumination (~ 450 nm). Then, it switches back to the fluorescent state in a thermally driven process. To elucidate the molecular basis of the switching mechanism, we produced reversibly switchable psRFP protein crystals. The crystal structures of psRFP on- and off-state were solved with a resolution of 1.80 Å and 1.75 Å, respectively. After structural analysis, *cis-trans* isomerization is considered to be a key event for on- and off-switching of the protein. Moreover, a light-induced change in chromophore planarity may also be involved in switching process. However, the tetrameric oligomerization state could be a limitation when performing protein tracking. Nevertheless, after eukaryotic expression of fusion construct MLS-psRFP (mitochondrial localization signal) and successful realization of switching experiment psRFP offers great application potential in live cell imaging.

Introduction

In recent years, fluorescent proteins (FPs) from the green fluorescent protein (GFP) family have revolutionized cell biology as genetically encoded fluorescence marker tools (1-4). They open promising perspectives for tracking of proteins or cells, reporting of gene expression and promoter activity and for multifaceted studies of biochemical signals in living cells and organisms (5-7).

All known FPs possess the exclusive capability to synthesize their chromophores in autocatalytic reactions in the absence of additional cofactors or substrates aside from molecular oxygen, which is reasonable for their wide applicability (5, 8-12). Characteristic for them is also a universally conserved 11-stranded ß-barrel structure with an axial α-helix that contains the chromophore (13, 14). Although, GFP-like proteins from different species occupy high structural similarity, they vary considerably concerning their photophysical properties, e.g. emission color or fluorescence intensity. Both the influences of the whole protein on the chromophore surrounding and the unique chemical structure of the chromophore define these properties (15).

These structural effects are also involved in changes of the fluorescence emission properties after illumination. Considering their reactions towards light-induction, optical highlighter FPs can be classified in three major rubrics. Photoactivatable fluorescent proteins (PAFPs) change irreversibly their fluorescence intensity partially in combination with a shift to longer wavelength emission in response to irradiation with light of a specific wavelength and intensity (16-19). Red-shifted emission caused by irreversible conversion of the green to a red chromophore after illumination with UV- or blue light is specific for photoconvertible fluorescent proteins (PCFPs) (20-24). Characteristic for photoswitchable fluorescent proteins (PSFPs) is the reversible on- and off-switching between a fluorescent and a non-fluorescent chromophore state. A positive and a negative switching mode may be distinguished: Positive PSFPs switch from a dark state to a bright fluorescent state (25-30), whereas negative PSFPs show a decrease of fluorescence intensity after irradiation (26, 30-34). In contrast to PAFPs and PCFPs, respectively, the chromophores of this new class of optical highlighters can attend the switching cycle many times until they are bleached or transferred to a permanent non-switchable state. Recent studies concerning the molecular switching mechanism of PSFPs revealed a *cis-trans* isomerization of the

chromophore as key event in the switching process (25, 27, 31, 33, 35). The non-fluorescent chromophore in the off-state represents the *trans* conformation, whereas the *cis* conformation is adopted by fluorescent on-state chromophore.

PSFPs are important imaging tools that enlarge possible applications of optical highlighter FPs. A promising area of application for PSFPs of various colors is usage in superresolution microscopy concepts designed to break the traditional Abbe diffraction barrier (36-39). All these far-field fluorescence microscopy inventions rely on the switching between at least two states, one of which is fluorescent, whereas the other is dark.

So far, Dronpa and its variants are the most prominent green fluorescent PSFPs used for several applications (26, 31, 32, 40). Currently, asFP595 (29), its variant KFP1 (28), rsCherry and rsCherryRev (30) are the only known red fluorescent PSFPs. Indeed, they display all advantages of red fluorescent proteins, but they only have low brightness in their on-state and high background fluorescence in their off-state. Positive switching FPs (asFP595, KFP1 and rsCherry) are hardly to detect in their initial state after expression in cells, because they are non-fluorescent at that time. Disadvantegous for application is also the fact that irradiation of KFP1 with light of greater intensity, longer duration, or both causes irreversible fluorescent forms (28).

Therefore, we searched for an excellent photoswitchable red fluorescent protein combining the outstanding properties of bright red fluorescence, permanent photoswitching behavior, excellent contrast between on- and off-state and a long wavelength irradiaton with low-energy light causing photoswitching for facilitated subdiffraction imaging in superresolution microscopy.

Originating from a red fluorescent protein from *Anemonia sulcata* var. *rufescens* a novel photoswitchable fluorescent protein, psRFP, could be evolved displaying a negative switching mode. It shows increased brightness and optimized on-/off-ratio between fluorescent and non-fluorescent states in comparison to known red PSFPs. Structural analysis confirmed that *cis-trans* isomerization and changes in planarity of chromophore are involved in photoswitching. Application as fusion protein marker in live cell imaging could also be shown.

Results & Discussion

Discovery of a new red PSFP from Anemonia sulcata

Recently, we cloned two novel red fluorescent proteins, asRFP.a and asRFP.b from *Anemonia sulcata* var. *rufescens* (41). Interestingly, asRFP.b showed slight photoswitching behavior upon blue light illumination, whereas asRFP.a could not be influenced by this light irradiation. A remarkable certainty is the nearly non-switching behavior of protein extract purified directly from the sea anemone (only ~ 2% loss of fluorescence after switching; data not shown). In view of the fact that asRFP.a is not photoswitchable, we concluded that mainly this isoform of the two bright red fluorescent proteins is naturally expressed in the animal. Intriguingly, the already known, barely fluorescent photoswitchable protein asFP595 (also named asulCP; ref.42 or asCP; ref. 43) was also isolated from the non-bioluminescent sea anemone *Anemonia sulcata* (29). Regarding this animal's phenotype with brownish tentacles and red non-fluorescent tips (29), it could eventually be classified as the color morph *Anemonia sulcata* var. *vulgaris* (44). In comparison to similar color morph *Anemonia sulcata* var. *rufescens* with a green fluorescent upside and a red fluorescent underside of the tentacles and pink non-fluorescent tips, it was possible to hereby represent a new source of PSFPs (45). The alignment of the amino acid sequences of the red PSFPs from *Anemonia sulcata* is shown in figure 1. Analysis of amino acid sequences revealed an eminent sequence identity of ~ 90% between naturally occurring PSFPs asFP595 and asRFP.b. Furthermore, decreased fluorescence intensity after blue light illumination was also noticed for asRFP (non-aggregating variant of asRFP.b; ref. 41). On the basis of these initial observations, we decided to scrutinize in detail spectral properties concerning photoswitching of asRFP.b and its variant asRFP.

Optical switching of asRFP.b and asRFP

For spectral characterization of photoswitching properties of asRFP.b on- and off-cycles of emission and excitation spectra (Figure 2) were measured. In contrast to asFP595 and its mutant KFP1 that display a positive switching mode from dark state to a bright fluorescent state (27-29), this initial photoswitchable protein and its variants show a directly opposed fluorescence characteristic: The initial state is bright fluorescent and after irradiation with blue light it can be switched off. Therefore, these

new optical highlighters appertain to negative PSFPs that show a decrease of fluorescence intensity after irradiation (26, 30-34). The initial fluorescent state of negative PSFPs simplifies the localization of cellular structures of interest for high resolution microscopy concepts in contrast to positive PSFPs that are hardly detectable after expression in cells.

Figure 2 shows that the maximum remaining fluorescence of asRFP.b averages out at ∼ 76% after complete off-switching with blue light used for illumination with ∼ 25 mW cm^{-2}. Excitation and emission maxima remain during photoswitching at the same positions (Ex$_{max}$ 575 nm, Em$_{max}$ 597 nm). Additionally, repeated on- and off-switching was performed to investigate changes of fluorescence intensity after 10 switching cycles (Figure 3). Immediately after blue light illumination asRFP.b is switched off. The maximum remaining fluorescence in the off-state stays at ∼ 59% during the complete measurement using blue light with ∼ 80 mW cm^{-2}. This represents the non-switchable fraction in the protein sample. Differences between measurements shown in figure 2 and 3 concerning percentage of maximum remaining fluorescence in the off-state can be explained by varying irradiation energy (∼ 25 mW cm^{-2} vs. ∼ 80 mW cm^{-2}). In the on-state the maximum remaining fluorescence averages out ∼ 85% after 10 switching cycles. That means ∼ 15% of asRFP.b were bleached during the whole measurement, which lasts more than 80 min. At the beginning the on-/off-ratio is 1.7 and ends up in 1.5.

This important value for on-/off-ratio, which signifies an excellent contrast in microscopy applications, was increased in asRFP (non-aggregating variant of asRFP.b; ref. 41). Data of absorption, excitation and emission spectra of photoswitched asRFP were collected (Figure 4). The maximum remaining fluorescence averages out at ∼ 30% after complete switching with ∼ 25 mW cm^{-2} illumination. Absorption, excitation and emission maxima continue in position during photoswitching (Abs$_{max}$ 567 nm, Ex$_{max}$ 574 nm, Em$_{max}$ 596 nm). Furthermore, we measured repeated on- and off-switching cycles using blue light with ∼ 80 mW cm^{-2} (Figure 5). The maximum remaining fluorescence in the off-state is ∼ 14% after the first cycle and after the complete measurement ∼ 18%. Varying energy of illumination light explains differences between ratings (Figure 4 and 5). In comparison to its precursor protein asRFP.b the content of the non-switchable fraction is considerably reduced in asRFP. The slight increase in the baseline indicates the occurrence of a small fraction of fluorophores in a permanently fluorescent state upon several

switching cycles. After 10 switching cycles, asRFP shows in the on-state the same maximum remaining fluorescence (averaged out at ~ 85%) as well as asRFP.b. That means also ~ 15% of asRFP molecules were bleached during the whole measurement, which lasts more than 170 min. At the beginning the on-/off-ratio is 7.1 and ends up in 4.7. Therefore, asRFP possesses optimized on-/off-ration in comparison to asRFP.b.

Further optimization of red PSFP

The next step to improve this novel photoswitchable fluorescent label was to carry out site-directed mutagenesis of position S143. The amino acid exchange S143G was demonstrated to strongly influence fluorescence properties of asFP595 (29) and asCP (43), respectively. This S143G mutant of asRFP, named psRFP, is spectrally characterized by collecting data of absorption, excitation and emission spectra and the action spectrum upon blue light illumination with ~ 25 mW cm^{-2} (Figure 6). The wavelength for the optimal photoswitching effect is 440 nm. Absorption, excitation and emission maxima remain during photoswitching at the same positions (Abs$_{max}$ 562 nm, Ex$_{max}$ 582 nm, Em$_{max}$ 601 nm). The maximum remaining fluorescence averages out at ~ 11% after complete switching, that means mutation S143G decreases the off-state value of fluorescence 3-fold under these light conditions. Moreover, we measured repeated on- and off-switching cycles using blue light with ~ 80 mW cm^{-2} (Figure 7). The maximum remaining fluorescence in the off-state is ~ 5% after the first cycle and after the complete experiment ~ 4%. Diverse energy of illumination light explains divergences between measurement shown in figure 6 and 7. The amino acid exchange of chromophore interacting position 143 reduces the content of a non-switchable fraction in the whole protein sample of psRFP considerably in contrast to its precursor protein asRFP. In the on-state the maximum remaining fluorescence decreases ~ 20% and therefore, it averages out at ~ 80% after 10 switching cycles. While the whole measurement the on-/off-ratio remains 20. During the more than 180 min lasting measurement ~ 20% of psRFP were bleached.

The spectral data concerning absorption, excitation and emission of this novel red PSFPs are very similar, but they show respectable differences regarding their contrast between on- and off-state and brightness (Figure 8, Table 1). All this characterized proteins are fluorescent and can be switched to a dark state upon irradiation with 450 nm light. Subsequently without blue light illumination they switch

back to the fluorescent state in a thermally driven process. Under the light conditions used in this experiment, we determined a half-life of 50 s (asRFP.b), 70 s (psRFP) and 90 s (asRFP), respectively, for off-switching, which is indeed faster than Dronpa (263 s), but not as fast as cerFP505 (30 s; ref. 34) or rsFastLime (5 s), the fast switching derivative of Dronpa (31). The naturally occurring asRFP.b from *Anemonia sulcata* can be switched off to 84% of its maximum fluorescence. This unimpressive value can be compared with recently published PSFP cerFP505, which fluorescence intensity can be reduced only by ~ 15% (34). Introduction of non-aggregation mutations in asRFP are causing with 28% a more decreased remaining fluorescence after blue light irradiation. The S143G amino acid exchange in further evolved optical marker psRFP leads to stronger reduction of rest fluorescence in the off-state of 9%. In comparison to other photoswitchable fluorescent proteins, psRFP shows optimized characteristics. The new candidate can be excited with non-cytotoxic low-energy light in contrast to green PSFPs. Furthermore, psRFP could be used in two-color experiments with green optical highlighters, e.g. Dronpa and its variants (26, 31, 32, 35). Regarding available photoswitchable red fluorescent proteins, KFP1, rsCherry and rsCherryRev have to be compared with psRFP (28, 30). All of them have distinct lower brightness in their on-state (3 to 30-fold reduced) and higher background fluorescence in their off-state. Furthermore, psRFP shows the best on-/off-ratio which is required for remarkable contrast in microscopy applications. Initial localization of cellular structures of interest is handicapped when PSFPs with positive switching mode are used, because they show their non-fluorescent off-state after expression in cells. Therefore, a negative switching mode is preferred in live cell imaging. Further advantage of psRFP is the low-energy light illumination for inducement of photoswitching in contrast to KFP1. It was not possible to switch on KFP1 with the irradiaton energy we used for our experiments. Moreover, illumination of KFP1 with green light of greater intensity, longer duration, or both causes irreversible kindling (28) which could never be observed for psRFP. In summary, we successfully developed a novel photoswitchable red fluorescent protein, which combines properties preferably applicable for *in vivo* nanoscopy.

Structural analysis of on- and off-state of psRFP

Above all optimization of novel red PSFP we focused on comprehension of effects of introduced mutation on the structural level to be in a position to explain structure-function relationship. After protein purification crystals of psRFP were grown. The crystals appeared within a few days with a typically size of approximately 0.2 x 0.05 x 0.03 mm in numerous sitting drops. The crystallized protein psRFP can be switched by light illumination in the same way as the soluble protein (Figure 9). A 1000-fold lower intensity filtered light source was sufficient to achieve photoswitching in psRFP for structure determination, in contrast to high irradiation energy required for asFP595-A143S crystals (25). The spectral properties of psRFP crystals concerning absorption, excitation and emission in each buffer solution for on- and off-state structure determination are similar to protein in solution (Figures 6, 10, 11). The photoswitchable GFP-like protein psRFP can be reversibly switched between a fluorescent on- and a nonfluorescent off-state by irradiation with blue light. Without blue light illumination the off-state quickly and spontaneously relaxes back in a thermally driven process to the on-state, which is the initial ground state.

The structures of psRFP on- and off-state were solved with a resolution of 1.80 Å (on-state, PDB accession code 3CFF) and 1.75 Å (off-state, PDB accession code 3CFH) (Tables S1-S3). The structures of psRFP comprise one tetramer per asymmetric unit, which consists of a dimer of dimers. The structures of asFP595 (PDB accession code 2A50; ref. 25), KFP (PDB accession code 1XMZ; ref. 46) and asRFP (PDB accession code 3CFA; ref. 41) are closely similar to the conformation of the individual subunits. All these described structures also include one dimer per asymmetric unit, forming tetramers through crystallographic symmetry operations. The tetrameric subunit arrangement is held together by two different types of interfaces, denoted as antiparallel (between subunits A/B and C/D) and perpendicular (between subunits A/C and B/D) according to the relative orientations of the symmetry axes of the cylindrical subunit. Both interfaces involve hydrophobic and hydrophilic interactions. A chromophore derived from M63-Y64-G65-tripeptide is included in every subunit. In a helical segment embedded in an 11-stranded-barrel resides the psRFP chromophore. The chromophoric, conjugated 2-iminomethyl-5-(4-hydroxybenzylidene) imidazolinone system is autocatalytically rearranged by the tripeptide M63-Y64-G65. Interestingly, the protein backbone is cleaved between C62 and the chromophore in contrast to most other GFP-like proteins (47-49).

Nevertheless, the former M63 Cα and backbone nitrogen atoms are coplanar with the imidazolinone ring and, hence, part of the conjugated system. Furthermore, the conjugated system of MYG is expanded by the imino group, which likely effects the shift of the absorption maximum toward a longer wavelength (562 nm) as compared with that of GFP (470 nm; ref. 5).

The determined structures are similar to the asFP595-A143S structures solved by Andresen and co-workers (25). Our results show *cis* and *trans* conformation of the chromophore in both states, but in different proportion (Figure 12). In the on-state mainly the *cis* conformation exists, whereas blue light illumination shifts the equilibrium in favor of *trans* conformation of the chromophore. The non-illuminated equilibrium structure of psRFP (3CFF) corresponding to the fluorescent on-state, shows the *cis* conformation of the chromophore. In all known fluorescent GFP-like proteins the *cis* conformation was observed, except for eqFP611 which presents a *trans* chromophore conformation (50). After illumination with blue light, the off-state structure of psRFP (3CFH) did not show solely expected *trans* conformation, but a statistically distributed mixture of *cis* and *trans* populations. However, we observed a 70% population of the *cis* conformation and a 30% population of the *trans* conformation. After all, this result indicates a partial transition to the off-state after illumination. It can be speculated, that X-ray irradiation may influence structural behavior. Remington suggested oxidative damage to the chromophore and its environment with unknown effects on photoactivation caused by exposure to X-rays (15). On this account we experimented to determine the influence of X-rays on the chromophore conformation. Actually, there might be induced a (reversible) decrease of *trans* population. Therefore, X-ray irradiation seems to act like an on-switching device.

Associated with the conformational switch is a substantial change in planarity (Table S3). In its *cis* conformation is the dihedral angle between the least-squares planes of the imidazolinone and *p*-hydroxybenzyl rings of the MYG chromophore in psRFP with illumination about 4° (3CFH). Accordingly, it exhibits a similar flat geometry as other proteins with *cis* chromophores like, e.g. GFP and DsRed (46). The ring systems embracing the chromophore are in proteins with *cis* chromophores in general more coplanar than in proteins with *trans* chromophores. In the DsRed tetramer the chromophore conformation shows dihedral angles of less than 1° (51). Likewise, in GFP the dihedral angle between the ring systems is nearly 4° (13). The values for

dihedral angles in the *cis* chromophore conformations of asRFP (3CFA; 11°; ref. 41) and psRFP without illumination (3CFF; 9°) are comparable. In contrast, in the *trans* conformation the dihedral angles of chromophores are much less coplanar. The first description of the atomic resolution structure of a chromoprotein was performed with Rtms5 (52). It presents nonplanar chromophore formation with large dihedral angles of 35°. Similarly, the KFP chromophore shows dihedral angles with values of 20° (46). Corresponding to this angles of the *trans* isomerizations in the off-state structures of KFP (20°) and asFP595-A143S mutant (22°), the *trans* chromophore conformation presented in the psRFP off-state (3CFH) shows a dihedral angle of 19° (25, 46). Intriguingly, the structure of red fluorescent eqFP611 provides a fundamental exception to the tendency in dihedral angles identified in *trans* chromophores (50). The overall dihedral angle in this protein is 4°, which is much closer to values revealed for *cis* conformation of the chromophore. Hitherto, eqFP611 is the only known example of a fluorescent protein with a *trans* chromophore conformation. Therefore, it might be suggested that the fluorescent properties are rather determined by the degree of planarity than by the geometric isomer.

Further investigations of the chromophore reveals extensive contacts with neighboring residues (Table S3). A chromophore rotation by about 8° around C1 in comparison to its orientation in asRFP is caused by mutation of S143 to G143 in psRFP (41). Thus, the *p*-hydroxybenzyl ring of the chromophore remains stacked against the imidazole ring of H197. The stacking interaction is also seen in other fluorescent proteins from Anthozoa, e.g. eqFP611 (50), amFP486 (53), EosFP (54) and zFP538 (55). Although, H197 can statistically be distributed between two alternate conformations, it must be in the stacked configuration for the *cis* chromophore to be accommodated (46, 56). The impact of H197 can be outlined by the fact that the photoswitchable fluorescent protein Dronpa contains the corresponding histidine residue (32, 35). Furthermore, the conversion of GFP to PA-GFP requires only the mutation of T203H, again at the corresponding residue (16).

According to this movement, the *p*-hydroxybenzyl ring hydroxyl in psRFP is not further involved in H-bonding interactions (Figure 12). Moreover, introduction of glycine in position 143 is linked to reorientations of a number of side chains, especially H197 and marginal backbone movements of the segments 59-62, 143-144 and 195-197.

Illumination with blue light causes the transition to the off-state and orientates the *p*-hydroxybenzyl ring hydroxyl of the chromophore in close hydrogen bonding contact to the side chain of S158, which is also involved in *trans* chromophore conformation of eqFP611 (50). Numerous but significant changes in the direct surrounding of the chromophore are shown in the structures 3CFF and 3CFH. Reorientations of side chains (K67, E195) and backbone movements (C62, G143, H197-I199) are included. Light-induced structural changes are exhibited also in more distant areas including for instance the segment 225-231, which is located near the hydrophobic A/B-interface.

In summary, it can be hypothesized that *cis-trans* isomerization is necessary for the photoswitching effect of psRFP. Though, chromophore planarity analyses of fluorescent proteins and chromoproteins suggest, that coplanarity is more essential than isomer configuration in inducing the fluorescence intensity. Furthermore, the influence of the whole protein coating on the chromophore configuration is poorly understood.

Eukaryotic expression and fluorescence microscopy of psRFP

Photoswitching, the rapid and reversible conversion of photoswitchable molecules between a fluorescent and a non-fluorescent state by light irradiation, can be used in particular for high resolution microscopy. Other versatile applications like tracking of cells, subcellular organelles or proteins and local optical marking can naturally also be performed by PSFPs. Nowadays are mainly irreversible photoactivatable or photoconvertible GFP-like proteins available for live cell imaging, e.g. EosFP (22), Kaede (20), KikGR (21), PA-GFP (16), PS-CFP (17), PAmRFP1 (18), PAmCherry1 (19) or Dendra (24). All these proteins can be activated only once. If only low amounts of fluorescent proteins are expressed, the quorum of activation events needed to generate a superresolution image is hindered to be reached in contrast to reversibly photoswitchable proteins. Moreover, green and cyan emitting fluorescent proteins, respectively, require activation by cytotoxic UV-light. For the detection of new photoactivation events the fluorescent molecules have to be photobleached instead of being switched off to enable the detection of following photoactivation occurences. However, photobleaching induces cytotoxic reactive oxygen species that may cause cell damage. Currently, only few reversible photoswitchable fluorescent proteins are available as optical highlighters, merely three of them show

advantageous red fluorescence: cerFP505 (34), Dronpa (32), KFP1 (28) and rsCherry/rsCherryRev (30).

Therefore, we tested the performance of psRFP as marker in live cell imaging applications by fusing it C-terminally to the mitochondrial localization signal (MLS) of subunit VIII of humane cytochrome c-oxidase (57). Pictures of HEK-293 cells transfected with the eukaryotic expression vector were taken 24 h after and resulted in bright red fluorescence at 532 nm excitation. Transient expression in cells at 37°C showed the expected distribution without obvious signs of aggregation. psRFP can be overexpressed in cells without exhibiting cytotoxic effects and shows strong red fluorescence. Mitochondrial localization of psRFP can be observed after functional expression of the fusion protein in living cells (Figure 13a). Low-energy excitation light for red fluorescence imaging (532 nm) is less cytotoxic and therefore more suitable for long-term monitoring studies.

Three regions of interest were chosen (ROI 1-3) for analyzing the switching experiment and every second a picture was taken. The laser pulse (405 nm) at ROI 1 switched off a single mitochondrion (Figure 13b). Mitochondria in ROI 2 and 3 were not influenced by the laser pulse and therefore, they show no off-switching (Figures 13c, d). Altogether, three off-switching cycles were performed and psRFP can be switched off to maximum ~ 5% of initial fluorescence and reaches ~ 80% of maximum fluorescence after measurement. ROI 2 and 3 only show negligible loss in fluorescence intensity at the end of the measurement (Figure 13e). Concerning its photoswitching behavior, psRFP can be successful irradiated by minimal amounts of blue light and switched off almost completely comparable to switching properties of protein in solution. The new optical highlighter psRFP shows a high contrast between on- and off-states, which predestines it for application in live cell imaging. The fact of no additional green emitting states offers the attractive possibility of multicolor labeling in combination with green-to-red photoconvertible fluorescent proteins (20-24) and green photoswitchable FPs (26, 31-33). These properties make psRFP suitable as tool for superresolution microscopy, e.g. RESOLFT (**RE**versible **S**aturable **O**ptica**L** **F**luorescence **T**ransitions; 58-60) or STED (**ST**imulated **E**mission **D**epletion; 38, 61). Further innovative single-molecule microscopy concepts are PALM (**P**hoto**a**ctivated **L**ocalization **M**icroscopy; 36, 62), FPALM (**F**luorescence **P**hoto**a**ctivation **L**ocalization **M**icroscopy; 39, 63), STORM (**ST**ochastic **O**ptical **R**econstruction **M**icroscopy; 64-66) or PALMIRA (**PALM** with **I**ndependently **R**unning

Acquistion; 37, 67). These techniques rely on detection of emission of individual molecules and the afterwards calculation of the exact coordinates of the single fluorescent molecules. However, the tetrameric oligomerization state could be a limitation when performing protein tracking and subdiffraction resolution microscopy. Therefore, monomerization of new optical highlighter protein psRFP should take center stage in subsequent studies.

Concluding remarks

A reversible photoswitchable red fluorescent protein, psRFP, could be evolved and characterized in its on- and off-state. Structural analysis revealed light-induced *cis-trans* isomerization as a key event for switching process. Furthermore, a substantial change in chromophore planarity might also be relevant to on- and off-switching of the protein. psRFP performed well as marker for live cell imaging and therefore, it offers great potential for applications in recent superresolution concepts.

Material & Methods

Mutagenesis

The coding cDNAs of asRFP.b and asRFP were ligated in the pQE-32 vector (Qiagen, Hilden, Germany). Using site-directed mutagenesis with primers containing the appropriate target substitution, the amino acid exchange S143G was introduced in asRFP via overlap extension PCR (68, 69). Plasmids were isolated and sent for sequencing by a commercial provider (MWG Biotech AG, Ebersberg, Germany).

Cloning and recombinant expression

For bacterial expression of novel red PSFPs, all proteins were fused to a N-terminal polyhistidine tag and expressed in *E. coli* (BL21DE3). The proteins were purified using Talon^{TM} metal affinity resin (Clontech Laboratories, Inc., Mountain View, CA, USA) and gel filtration (Superdex 200, Äkta System, GE Healthcare Biosciences, Little Chalfont, UK) as previously described (47, 70-72) for measurement of spectral properties. Finally, purified proteins were solved in 50 mM sodium phosphate buffer (pH 7.0) supplemented with 300 mM NaCl.

Encoding sequence for psRFP was cloned into pET-17b vector (EMD Bioscience Novagen, Merck, Darmstadt, Germany) in *BamH*I and *Nde*I sites. After IPTG-induced expression (final concentration 0.5 mM) in *E. coli* (BL21DE3, Invitrogen, Carlsbad, CA, USA) at 4°C for one week the protein was purified for crystallization experiments as described above and transferred to protein buffer (20 mM Tris-HCl pH 7,5; 120 mM NaCl; 1 mM β-Mercaptoethanol) and concentrated up to ~ 10 mg/ml for crystallization.

Optical switching

Photoswitching experiments were performed on fluorescence spectrophotometer Cary Eclipse (Varian, Darmstadt, Germany) at a resolution of 1 nm. For off-switching the sample was irradiated with a Xe lamp (LOT-Oriel, Leatherhead, UK) equipped with a band pass filter 450/40 nm (center/bandwidth; Schott, Mainz, Germany). The light was focused on the sample by a lens system so that a uniform illumination of the sample could be assured. The protein solution was irradiated with an energy density of ~ 25 mW cm^{-2} for spectral measurements and an energy density of ~ 80 mW cm^{-2} for data collection of repeated photoswitching. The illumination was switched off as

soon as the fluorescence reached a constant value. The fluorescence then thermally recovered in the dark without additional light.

For measurements of fluorescence spectra of psRFP crystals the fluorescence spectrophotometer was additionally equipped with fiber optics.

The action spectrum of psRFP was determined in a range between 350-600 nm with a Spex Fluorolog II (Spex Industries, Edison, NJ, USA) with 2.2 nm resolution at room temperature and corrected for the wavelength dependence of the detector efficiency and the spectrum of the lamp. First, the protein sample was excited for 180 seconds with one single wavelength and after 40 seconds the fluorescence intensity at 600 nm was detected by excitation with 510 nm.

Data collection of absorption spectra in solution and in crystals was carried out on a Cary 1 spectrophotometer (Varian, Darmstadt, Germany) with a resolution of 1 nm. For protein in solution blue light illumination with an energy density of ~ 25 mW cm^{-2} was used. The illumination was switched off as soon as the fluorescence reached a constant value. The fluorescence then thermally recovered in the dark without additional light. The absorption measurements of psRFP crystal were accomplished using crystals squeezed between two quartz glasses until a suitable absorption value for measurements was attained. The sample was irradiated with 473 nm laser (65 mW cm^{-2}) until the spectra did not change any more. Then an absorption spectrum was measured. After complete recovery to the on-state next measurement took place. All experiments were performed at room temperature

Structural analysis psRFP

Crystallization and data collection

Crystallization was done with Roxtal system using Nextal Kits (1152 different crystallization conditions) in 96 well microplates at 18°C in an automated robotic system. These drops were consisting of equal volumes (400 nl) of protein and reservoir solution. The protein solution contained ~ 10 mg/ml protein in 120 mM NaCl, 20 mM Tris buffer at pH 7.5 with an admixture of ß-mercaptoethanol. The reservoir volume accounted 50 µl. Crystallization conditions were identified to be suitable for the experiment as crystals diffracted better than 1.8 Å and were found to belong to the same space group with closely similar cell parameters (Table S1). The crystallization conditions were for psRFP 0.2 M di-Sodium tartrate, 40% (w/v) MPD

for structure determination of protein without illumination and 0.1 M Tris buffer pH 8.0, 65% (w/v) MPD for structure determination of protein with illumination. Cryoprotective properties of all above mother solutions allowed to shock-freeze crystals without further additions.

The same buffer conditions were used for crystallization with hanging drop vapor method. These resulting crystals were taken for spectral measurements and fluorescence imaging pictures using a fluorescence microscope (Zeiss-Axioplan I, Karl Zeiss Jena GmbH, Jena) equipped with a digital camera (Polaroid DMC Ie, Model PDMC-2, Polaroid Corp., Cambridge, Mass., USA), a 150 W Hg lamp (Karl Zeiss Jena GmbH, Jena), a 560/50 nm band-pass excitation filter (595 nm long-pass suppression filter, 645/75 nm transmission) and a 470/40 nm filter for photoswitching, (495 nm long-pass suppression filter, 525-575 nm transmission).

psRFP crystals of the full-length red fluorescent protein with 231 amino acids were grown in space group $C222_1$ with four molecules (tetramer) per asymmetric unit. X-ray diffraction data (Table S1) were collected at the MPG beamline BW6, DESY/HASYLAB, Hamburg, using a 165 mm MarCCD detector at an X-ray wavelength of 1.05 Å. Native data sets for psRFP under dark-equilibrium conditions were measured without illumination. To obtain psRFP off-state, the crystals were illuminated in their mother solution immediately before shock-freezing using blue light. For irradiation a 150 W Xe lamp (LOT-Oriel, Leatherhead, UK) equipped with band pass filter (Schott, Mainz, Germany) with transmission at 450/40 nm (center/bandwidth) and a lens system for focusing the light beam was applied. The protein crystals experienced an energy density of ~ 45 mW cm^{-2}. In several trials the appropriate irradiation time (15 min) was found to induce substantial population of the off-state. This illumination time was experimentally determined by appearance of the chromophore off-state conformation on Fc-Fo electron density maps and allowed to avoid crystal damage and to keep the quality of crystal at the same resolution. Using this approach and slow relaxation, psRFP off-state crystals were measured. All loop-mounted crystals were shock-frozen and kept at 100 K in a nitrogen gas stream. The diffraction images were processed and scaled using the HKL program suite (73, 74). The data collection statistics are summarized in table S1.

Structure refinement

Molecular replacement with the program MOLREP (75) was accomplished to solve the structures of psRFP using the crystal structure of the closely homologous kindling fluorescent protein KFP (PDB accession code 1XQM; ref. 56) as a search model. Apart from four disordered N-terminal residues, a complete model of psRFP was rebuilt using ARP/wARP (76) and COOT program (77). The refinement procedure of the intermediate models of each tetramer's monomer was done with REFMAC (78) without using non-crystallographic symmetry. The refinement statistics are shown in table S2. The electron density distributions around cysteine residues 114 and 221 were modeled as s,s-(2-hydroxyethyl)thiocysteine, taking into account the presence of β-mercaptoethanol in the protein solution. The electron density maps have clearly confirmed the substitution of S143 residue by a Gly in psRFP. Using the REFMAC dictionary of the individual peptide residues (M63, Y64 and G65) a model of the tripeptide chromophore conformation was initially built and subsequently modified according to characteristics of electron density maps analyzing the known conformations of the MYG chromophore in all available crystal structures with high resolution. The final models of psRFP on-and off-state structures were refined to a R-factor of 19.8% and 20.4% (Rfree = 22.4%, 23.0%) respectively. The other refinement statistics are summarized in table S2. Validation using the PDB Validation Suite showed good geometries for all structures. Molecular depictions were prepared with SWISS-MODEL (79). The coordinates and structure factors have been deposited in the RCSB Protein Data Bank under accession codes 3CFF and 3CFH.

Vector construction

For eukaryotic expression experiment of psRFP-fusion protein, its coding sequence was inserted into the vector pcDNA3 (Invitrogen, Carlsbad, CA, USA). Coding sequence was introduced in *Xho*I and *Xba*I resctriction sites in front of the N-terminal region of the fusion partner. psRFP was fused to the mitochondrial localization signal (MLS) of subunit VIII of humane cytochrome c-oxidase (57).

Eukaryotic expression and fluorescence microscopy

HEK-293 cells were maintained in Dulbecco's Modified Eagle Medium (DMEM, Invitrogen, Carlsbad, CA, USA) supplemented with 10% fetal calf serum (FCS, Biochrom, Berlin, Germany) at 37°C in 5% CO_2. Cells (30,000) were seeded on

chambered cover glasses (Nalge Nunc International Corp., Rochester, NY, USA). After 16 h cells were transfected with 500 ng of plasmid DNA using the Nanofectine transfection reagent (PAA, Pasching, Austria) according to the manufacturer's instructions. The culture dishes were incubated at 37°C and expression of fluorescent proteins was monitored after 24 h of incubation. The fluorescent images of living cells were acquired using a spinning disk confocal microscope assembled from individual components, a CSU10 scan head (Yokogawa, Tokyo, Japan), an inverted microscope (Axio Observer, Zeiss, Göttingen, Germany) equipped with 63x oil immersion objective lens and with environmental control (PECON, Erbach, Germany), an image splitter unit (OptoSplit II, Cairn Research, Faversham, UK) and an EMCCD camera (DV-887, Andor, Belfast, UK) controlled by Andor IQ software. For photoswitching experiments 405 nm laser pulses were used, respectively to irradiate parts of living cells or whole cells for studying light-induced changes of red fluorescence. Every second a fluorescent image was taken at 532 nm laser excitation using filterset HQ585/80 with 545-625 nm transmission. The fluorescence intensity was analyzed using the ImageJ software (http://rsb.info.nih.gov/ij/).

Online Supporting Information

The Supporting Information consists of three supplemental tables (table S1-S3).

Acknowledgements

Funding

Author contributions

Conceived and designed the experiments: FO GUN HDB JW. Performed the experiments: FO GSK JF JW SG. Analyzed the data: FO GSK HDB JF JW SG. Contributed reagents/materials/analysis tools: FO HDB GUN JW. Wrote the paper: SG. Contributed to discussions: FO GSK HDB JF JW.

References

1. Matz, M. V., Fradkov, A. F., Labas, Y. A., Savitsky, A. P., Zaraisky, A. G., Markelov, M. L. & Lukyanov, S. A. (1999). Fluorescent proteins from nonbioluminescent Anthozoa species. *Nature biotechnol.* 17, 969-973.

2. Miyawaki, A. (2002). Green fluorescent protein-like proteins in reef anthozoa animals. *Cell Struct. Funct.*, 27, 343-347.

3. Verkhusha, V. V. & Lukyanov, K. A. (2004). The molecular properties and applications of Anthozoa fluorescent proteins and chromoproteins. *Nature Biotechnology*, 22, 3, 289-296.

4. Shaner, N. C., Patterson, G. H. & Davidson, M. W. (2007). Advances in fluorescent protein technology. *Journal of Cell Science*, 120, 24, 4247-4260.

5. Tsien, R. Y. (1998). The green fluorescent protein. *Annu Rev Biochem*, 67, 509-44.

6. Chudakov, D. M., Lukyanov, S. & Lukyanov, K. A. (2005). Fluorescent proteins as a toolkit for *in vivo* imaging. *Trends Biotechnol.*, 23, 605-613.

7. Stepanenko, O. V., Verkusha, V. V., Kuznetsova, I. M., Uversky, V. N. & Turoverov, K. K. (2008). Fluorescent proteins as biomarkers and biosensors: Throwing color lights on molecular and cellular processes. *Current Protein and Peptide Science*, 9, 4, 1-32.

8. Chalfie, M., Tu, Y., Euskirchen, G., Ward, W. W. & Prasher, D. C. (1994). Green fluorescent proteins as a marker for gene expression. *Science*, 263, 802-805.

9. Cubitt, A. B., Heim, R., Adams, S. R., Boyd, A. B., Gross, L. A. & Tsien, R. Y., (1995). Understanding, improving and using green fluorescent proteins. *TIBS*, 20, 448-455.

10. Heim, R., Prasher, D. C. & Tsien, R. Y. (1994). Wavelength mutations and posttranslational autoxidation of green fluorescent protein. *Proc Natl Acad Sci U.S.A.*, 91, 12501-4.

11. Inouye, S. & Tsuji, F. I. (1994). *Aequorea* green fluorescent protein: expression of the gene and fluorescence characteristics of the recombinant protein. *FEBS Lett.*, 341, 277-280.

12. Prasher, D. C., Eckenrode, V. K., Ward, W. W., Prendergast, F. G. & Cormier , M. J. (1992). Primary structure of the *Aequorea victoria* green fluorescent protein. *Gene*, 111, 229-233.

13. Ormö, M., Cubitt, A. B., Kallio, K., Gross, L. A., Tsien, R. Y. & Remington, S. J. (1996). Crystal structure of the *Aequorea victoria* green fluorescent protein. *Science*, 273,1392-1395.

14. Yang, F., Moss, L. G. & Phillips, G. N., Jr. (1996). The molecular structure of green fluorescent protein. *Nature Biotechnol.*, 14, 1246-1256.

15. Remington, S. J. (2006). Fluorescent proteins: maturation, photochemistry and photophysics. *Curr. Opin. Struct. Biol.*, 16, 714-721.

16. Patterson, G. H. & Lippincott-Schwartz, J. (2002). A photoactivatable GFP for selective photolabeling of proteins and cells. *Science*, 297, 1873-1877.

17. Chudakov, D. M., Verkusha, V. V., Staroverov, D. B., Souslova, E. A., Lukyanov, S. & Lukyanov, K. A. (2004). Photoswitchable cyan fluorescent protein for protein tracking. *Nat. Biotechnol.*, 22, 1435-1439.

18. Verkusha, V. V. & Sorkin, A. (2005). Conversion of the monomeric red fluorescent protein into a photoactivatable probe. *Chemistry & Biology*, 12, 279-285.

19. Subach, F. V., Patterson, G. H., Manley, S., Gillette, J. M., Lippincott-Schwartz, J & Verkusha, V. V. (2009). Photoactivatable mCherry for high-resolution two-color fluorescence microscopy. *Nature Methods*, 6, 2, 153-159.

20. Ando, R., Hama, H., Yamamoto-Hino, M., Mizuno, H. & Miyawaki A. (2002). An optical marker based on the UV-induced green-to-red photoconversion of a fluorescent protein. *Proc. Natl. Acad. Sci. U S A.*, 99, 20, 12651-12656.

21. Tsutsui, H., Karasawa, S., Shimizu, H., Nukina, N. & Miyawaki, A. (2005) Semi-rational engineering of a coral fluorescent protein into an efficient highlighter. *EMBO reports*, 6, 3, 1-6.

22. Wiedenmann, J., Ivanchenko, S., Oswald, F., Schmitt, F., Röcker, C., Salih, A., Spindler, K.-D., & Nienhaus, G. U. (2004). EosFP, a fluorescent marker protein with UV- inducible green- to- red fluorescence conversion. *Proc. Natl. Acad. Sci. U S A.*, 101, 15905- 15910.

23. Adam, V., Lelimousin, M., Boehme, S., Desfonds, G., Nienhaus, K., Field, M. J., Wiedenmann, J., McSweeney, S., Nienhaus, G. U. & Bourgeois, D. (2008). Structural characterization of IrisFP, an optical highlighter undergoing multiple photo-induced transformations. *Proc. Natl. Acad. Sci. U S A.*, 105, 47, 18343-18348.

24. Gurskaya, N. G., Verkusha, V. V., Shcheglov, A. S., Staroverov, D. B., Chepurnykh, T. V., Fradkov, A. F., Lukyanov, S. & Lukyanov, K. A. (2006). Engineering of a monomeric green-to-red photoactivatable fluorescent protein induced by blue light. *Nature Biotechnology*, 24, 461-465.

25. Andresen, M., Wahl, M. C., Stiel, A. C., Gräter, F., Schäfer, L. V., Trowitzsch, S., Weber, G., Eggeling, C., Grubmüller, H., Hell, S. W. & Jakobs, S. (2005). Structure and mechanism of the reversible photoswitch of a fluorescent protein. *Proc. Natl. Acad. Sci. U S A.*, 102, 37, 13070-13074.

26. Andresen, M., Stiel, A. C., Fölling, J., Wenzel, D., Schönle, A., Egner, A., Eggeling, C., Hell, S. W. & Jakobs, S. (2008). Photoswitchable fluorescent proteins enable monochromatic multilabel imaging and dual color fluorescence nanoscopy. *Nature Biotechnol.*, 26, 9, 1035-1040.

27. Chudakov, D. M., Feofanov, A. V., Mudrik, N. N., Lukyanov, S. & Lukyanov, K. A. (2003). Chromophore environment provides clue to "kindling fluorescent protein" riddle. *Journal of Biological Chemistry*, 278, 9, 7215-7219.

28. Chudakov, D. M., Belousov, V. V., Zaraisky, A. G., Novoselov, V. V., Staroverov, D. B., Zorov, D. B., Lukyanov, S. & Lukyanov, K. A. (2003). Kindling fluorescent protein for precise *in vivo* photolabeling. *Nat. Biotechnol.*, 21, 191-194.

29. Lukyanov, K. A., Fradkov, A. F., Gurskaya, N. G., Matz, M. V., Labas, Y. A., Savitsky A. P., Markelov M. L., Zaraisky A. G., Zhao X., Fang Y., Tan W. & Lukyanov S. A. (2000). Natural animal coloration can be determined by a nonfluorescent green fluorescent protein homolog. *Journal of Biological Chemistry*, 275, 25879-25882.

30. Stiel, A. C., Andresen, M., Bock, H., Hilbert, M., Schilde, J., Schonle, A., Eggeling, C., Egner, A., Hell, S. W. & Jakobs, S. (2008). Generation of Monomeric Reversibly Switchable Red Fluorescent Proteins for Far-Field Fluorescence Nanoscopy. *Biophys J.*, 95, 6, 2989-2997.

31. Stiel, A. C., Trowitzsch, S., Weber, G., Andresen, M., Eggeling, C., Hell, S. W., Jakobs, S. & Wahl, M. C. (2007). 1.8 A bright-state structure of the reversibly switchable fluorescent protein Dronpa guides the generation of fast switching variants. *Biochem J.*, 402, 1, 35-42.

32. Ando, R., Mizuno, H. & Miyawaki, A. (2004). Regulated fast nucleocytoplasmic shuttling observed by reversible protein highlighting. *Science*, 306, 1370-1373.

33. Henderson, J. N., Ai, H.-W., Campbell, R. E. & Remington, S. J. (2007). Structural basis for reversible photobleaching of a green fluorescent protein homologue. *Proc. Natl. Acad. Sci. U S A.*, 104, 16, 6672-6677.

34. Vogt, A., D'Angelo, C., Oswald, F., Denzel, A., Mazel, C. H., Matz, M., Ivanchenko, S., Nienhaus, G. U. & Wiedenmann, J. (2008). A green fluorescent protein with photoswitchable emission from deep sea. *PLoS ONE*, 3, 11, e3766.

35. Andresen, M., Stiel, A. C., Trowitzsch, S., Weber, G., Eggeling, C., Wahl, M. C., Hell, S. W. & Jakobs, S. (2007). Structural basis for reversible photoswitching in Dronpa. *Proc. Natl. Acad. Sci. U S A.*, 104, 32, 13005-13009.

36. Betzig, E., Patterson, G. H., Sougrat, R., Lindwasser, O. W., Olenych, S., Bonifacino, J. S., Davidson, M. W., Lippincott-Schwartz, J. & Hess, H. F. (2006). Imaging intracellular fluorescent proteins at nanometer resolution. *Science*, 313, 5793, 1642-1645.

37. Egner, A., Geisler, C., von Middendorff, C., Bock, H., Wenzel, D., Medda, R., Andresen, M., Stiel, A. C., Jakobs, S., Eggeling, C., Schonle, A. & Hell, S. W. (2007). Fluorescence nanoscopy in whole cells by asynchronous localization of photoswitching emitters. *Biophys J.*, 93, 9, 3285-3290.

38. Hell, S. W. (2007). Far-field optical nanoscopy. *Science*, 316, 5828, 1153-1158.

39. Hess, S. T., Girirajan, T. P. & Mason, M. D. (2006). Ultra-high resolution imaging by fluorescence photoactivation localization microscopy. *Biophys. J.*, 91, 4258-4272.

40. Ando, R., Flors, C., Mizuno, H., Hofkens, J. & Miyawaki, A. (2007). Highlighted generation of fluorescence signals using simultaneous two-color irradiation on Dronpa mutants. *Biophys. J.*, 92, L97-L99.

41. Gundel, S., Kachalova, G. S., Bartunik, H. D., Fuchs, J., Nienhaus, G. U. & Wiedenmann, J. (2009). Identification of key residues responsible for high fluorescence intensity in GFP-like proteins. *prepared for publication*.

42. Labas, Y. A., Gurskaya, N. G., Yanushevich, Y. G., Fradkov, A. F., Lukyanov, K. A., Lukyanov, S. A. & Matz, M. V. (2002). Diversity and evolution of the green fluorescent protein family. *Proc Natl Acad Sci U.S.A.*, 99, 7, 4256–4261.

43. Bulina, M. E., Chudakov, D. M., Mudrik, N. N. & Lukyanov, K. A. (2002). Interconversion of Anthozoa GFP-like fluorescent and non-fluorescent proteins by mutagenesis. *BMC Biochemistry*, 3, 7.

44. Wiedenmann, J., Röcker C. & Funke, W. (1999). The morphs of *Anemonia* aff. *sulcata* (Cnidaria, Anthozoa) in particular consideration of the ectodermal pigments. In *Verhandlungen der Gesellschaft für Ökologie*, Band 29, J. Pfadenhauer, ed., Heidelberg, Berlin: Spektrum Akademischer Verlag, 497-503.

45. Wiedenmann, J., Elke, C., Spindler, K.-D. & Funke W. (2000). Cracks in the β-can: fluorescent proteins from *Anemonia sulcata*. *Proc Natl Acad Sci U.S.A.*, 97, 26, 14091-14096.

46. Quillin, M. L., Anstrom, D. M., Shu, X., O'Leary, S., Kallio, K., Chudakov, D. M. & Remington, S. J. (2005). The kindling fluorescent protein from *Anemonia sulcata*: Dark state structure at 1.38-Å resolution. *Biochemistry*, 44, 5774-5787.

47. Wiedenmann, J., Ivanchenko, S., Oswald, F. & Nienhaus G. U., (2004). Identification of GFP-like proteins in non-bioluminescent, azooxanthellate Anthozoa opens new perspectives for bioprospecting. *Marine Biotechnology*, 6, 3 270-277.

48. Shkrob, M. A., Yanushevich, Y. G., Chudakov, D. M., Gurskaya, N. G., Labas, Y. A., Poponov, S. Y., Mudrik, N. N., Lukyanov, S. & Lukyanov, K. A. (2005). Far-red fluorescent proteins evolved from a blue chromoprotein from *Actinia equina. Biochem. J.*, 392, 649–654.

49. Martynov, V. I., Savitsky, A. P., Martynova, N. Y., Savitsky, P. A., Lukyanov, K. A. & Lukyanov, S. A. (2001). Alternative cyclization in GFP-like proteins family. The formation and structure of the chromophore of a purple chromoprotein from *Anemonia sulcata*. *J Biol Chem*. 276, 24, 21012-21016.

50. Petersen, J., Wilmann, P. G., Beddoe, T., Oakley, A. J., Devenish, R. J., Prescott, M. & Rossjohn, J. (2003). The 2.0-A crystal structure of eqFP611, a far red fluorescent protein from the sea anemone *Entacmaea quadricolor*. *J Biol Chem*, 278, 45, 44626-44631.

51. Yarbrough, D., Wachter, R. M., Kallio, K., Matz, M. V. & Remington, S. J. (2001). Refined crystal structure of DsRed, a red fluorescent protein from coral, at 2.0-A resolution. *Proc Natl Acad Sci U S A.*, 16, 98, 2, 462-467.

52. Prescott, M., Ling, M., Beddoe, T., Oakley, A. J., Dove, S., Hoegh-Guldberg, O., Devenish, R. J. & Rossjohn, J. (2003). The 2.2 A crystal structure of a pocilloporin pigment reveals a nonplanar chromophore conformation. *Structure (Camb).*, 11, 275-284.

53. Henderson, J. N. & Remington, S. J. (2005). Crystal structures and mutational analysis of amFP486, a cyan fluorescent protein form *Anemonia majano. Proc Natl Acad Sci U.S.A.*, 102, 36, 12712-12717.

54. Nienhaus, K., Nienhaus, G. U., Wiedenmann, J. & Nar, H. (2005). Structural basis for photo-induced protein cleavage and green-to-red conversion of fluorescent protein EosFP. *Proc Natl Acad Sci U.S.A.*, 102, 26,9156–9159.

55. Remington, S. J., Wachter, R. M., Yarbrough, D. K., Branchaud, B., Anderson, D. C., Kallio, K. & Lukyanov, K. A. (2005). zFP538, a yellow-fluorescent protein from Zoanthus, contains a novel three-ring chromophore. *Biochemistry*, 44, 202-212.

56. Wilmann, P. G., Petersen, J., Devenish, R. J., Prescott, M. & Rossjohn, J. (2005). Variations on the GFP chromophore. A polypeptide fragmentation within the chromophore revealed in the 2.1-Å crystal structure of a nonfluorescent chromoprotein from *Anemonia sulcata*. *Journal of Biological Chemistry*, 280, 4, 2401–2404.

57. Rizzuto, R., Brini, M., Pizzo, P., Murgia, M. & Pozzan, T. (1995). Chimeric green fluorescent protein as a tool for visualizing organells in living cells. *Curr. Biol.*, 5, 6, 635-642.

58. Hell, S. W. (2003). Toward fluorescence nanoscopy. *Nat Biotechnol.*, 21, 11, 1347-1355.

59. Hell, S. W., Jakobs, S. & Kastrup, L. (2003). Imaging and writing at the nanoscale with focused visible light through saturable optical transitions. *Applied Physics a-Materials Science & Processing* , 77, 7, 859-860.

60. Schwentker, M. A., Bock, H., Hofmann, M., Jakobs, S., Bewersdorf, J., Eggeling, C. & Hell, S. W. (2007). Wide-field subdiffraction RESOLFT microscopy using fluorescent protein photoswitching. *Microsc Res Tech*, 70, 3, 269-280.

61. Hell, S. W. & Wichmann, J. (1994). Breaking the Diffraction Resolution Limit by Stimulated-Emission - Stimulated-Emission-Depletion Fluorescence Microscopy. *Optics Letters*, 19, 11, 780-782.

62. Shroff, H., White, H. & Betzig, E. (2008). Photoactivated localization microscopy (PALM) of adhesion complexes. *Current protocols in cell biology*, chapter 4, unit 4.21.

63. Gould, T. J., Verkhusha, V. V. & Hess. S. T. (2009). Imaging Biological Structures with Fluorescence Photoactivation Localization Microscopy. *Nature Protocols*, 4, 291-308.

64. Huang, B., Wang, W., Bates, M. & Zhuang, X. (2008). Three-dimensional super-resolution imaging by stochastic optical reconstruction microscopy. *Science*, 319, 5864, 810-813.

65. Huang, B., Jones, S. A., Brandenburg, B. & Zhuang, X. (2008). Whole-cell 3D STORM reveals interactions between cellular structures with nanometer-scale resolution. *Nature Methods*, 5, 1047-1052.

66. Rust, M. J., Bates, M. & Zhuang, X.W. (2006). Sub-diffraction-limit imaging by stochastic optical reconstruction microscopy (STORM). *Nature Methods*, 3, 10, 793-795.

67. Bock, H., Geisler, C., Wurm, C. A., Jakobs, S., Schönle, A., Egner, A., Hell , S. W. & Eggeling, C. (2007). Two-color far-field fluorescence nanoscopy based on photoswitching emitters. *Appl. Phys. B*, 88, 161-165.

68. Ho, S. N., Hunt, H. D., Horton, R. M., Pullen, J. K. & Pease, L. R. (1989). Site-directed mutagenesis by overlap extension using the polymerase chain reaction. *Gene*, 77, 51–59.

69. Kredel, S., Nienhaus, K., Oswald, F., Wolff, M., Ivanchenko, S., Cymer, F., Jeromin, A., Michel, F. J., Spindler, K. D., Heilker, R., Nienhaus, G. U. & Wiedenmann, J. (2008). Optimized and Far-Red-Emitting Variants of Fluorescent Protein eqFP611. *Chem Biol.* 15:224-33.

70. Wiedenmann, J., Schenk, A., Röcker, C., Spindler, K.-D. & Nienhaus, G. U. (2002). A far-red fluorescent protein with fast maturation and reduced oligomerization tendency from *Entacmaea quadricolor* (Cnidaria, Anthozoa, Actinaria). *Proc Natl Acad Sci U.S.A.*, 99 ,18, 11646-11651.

71. Ivanchenko, S., Röcker. C., Oswald. F., Wiedenmann, J. & Nienhaus. G. U. (2005). Targeted green-red photoconversion of EosFP, a fluorescent marker protein. *Journal of Biological Physics*, 31: 249-259.

72. Nienhaus, K., Vallone, B., Renzi, F., Wiedenmann, J. & Nienhaus, G. U. (2003). Crystallization and preliminary X-ray diffraction analysis of the red fluorescent protein eqFP611. *Acta Cryst.* D59, 1253-1255.

73. Minor, W. (1993). *The HKL Manual.* HKL Research Inc., Charlottesville, VA, USA.

74. Otwinowski, Z. & Minor, W. (1997). Processing of X-ray diffraction data collected in oscillation mode. *Methods Enzymol.*, 276, 307-326.

75. Vagin, A. & Teplyakow, A. (1997) MOLREP: an automated program for molecular replacement. *J. Appl. Cryst.*, 30, 1022-1025.

76. Morris, R. J., Perrakis, A. & Lamzin, V. (2003) ARP/wARP and automatic interpretation of protein electron density maps. *Methods Enzymol.*, 374, 229-244.

77. Emsley, P. & Cowtan, K. (2004). COOT: model-building tools for molecular graphics. *Acta Crystallogr.* D60, 2126-2132.

78. Murshudov, G. N., Vagin, A. A. & Dodson, E. J. (1997) Refinement of macromolecular structures by the maximum-likelihood method. *Acta Crystallogr.* D Biol. Crystallogr., 53, 240-255.

79. Guex, N. & Peitsch, M. C. (1997) SWISS-MODEL and the Swiss-PdbViewer: An environment for comparative protein modeling. *Electrophoresis*, 18: 2714-2723. http://www.expasy.org/spdbv/
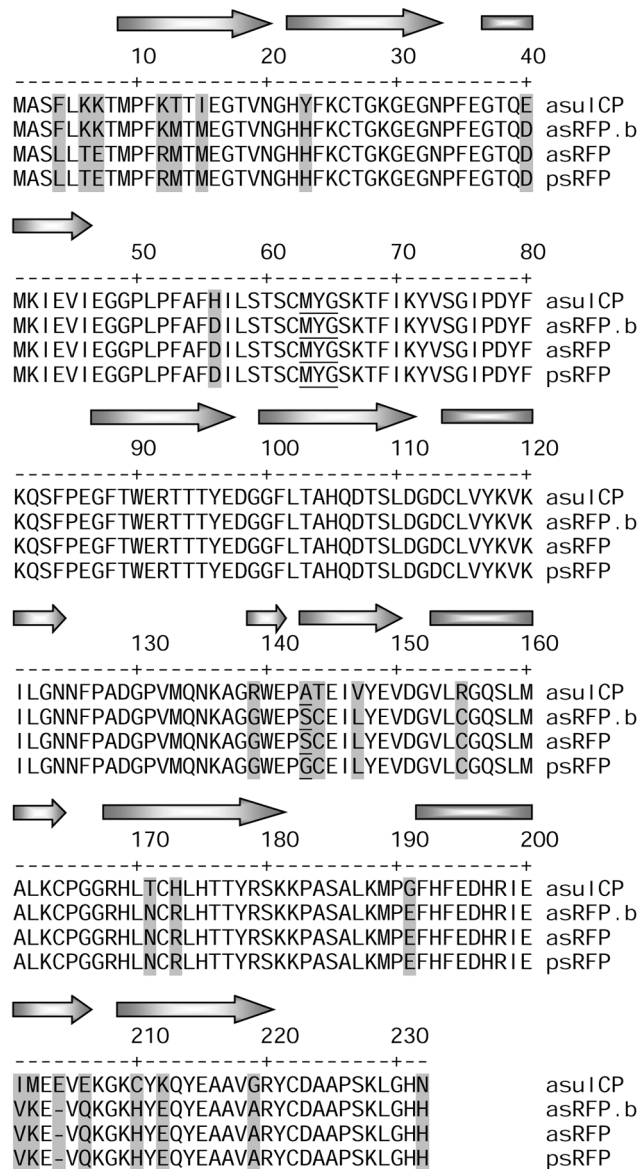
Figures

Figure 1. Multiple amino acid sequence alignment of PSFPs from *Anemonia sulcata*. Numbering is based on asulCP. Different amino acid residues between the four proteins are shaded in gray. Underlined residues are discussed in the text. Secondary structure is represented by β-sheets according to the structures of psRFP (RCSB Protein Data Bank accession code 3CFF, 3CFH). Alignment gap is shown by hyphen (-).The sequence alignment was constructed using CLUSTAL V and edited manually.
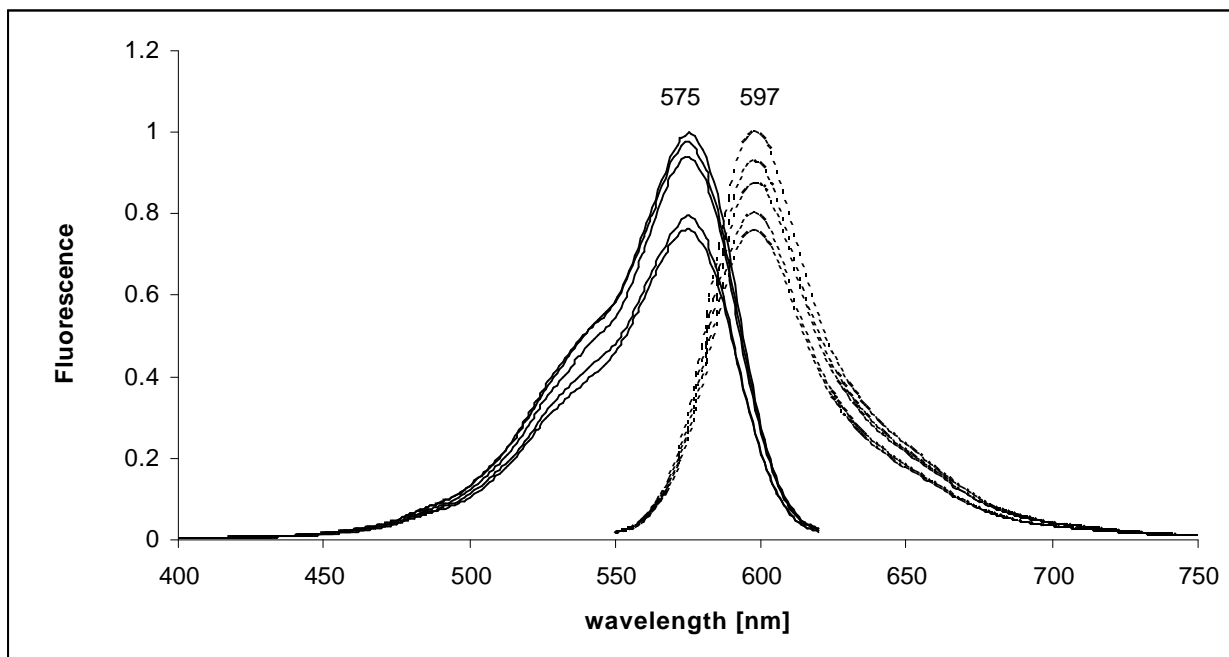
Figure 2. Excitation (solid lines) and emission (dashed lines) spectra of reversible photoswitched asRFP.b. For the excitation spectra, the emission was measured at 640 nm; for the emission spectra, fluorophores were excited at 510 nm. Light with 450/40 nm (center/bandwidth) was used for photoswitching irradiation with ~ 25 mW cm^{-2}. The maximum remaining fluorescence averages out at ~ 76% after complete switching. Excitation and emission maxima remain during photoswitching at the same positions (Ex$_{max}$ 575 nm, Em$_{max}$ 597 nm).
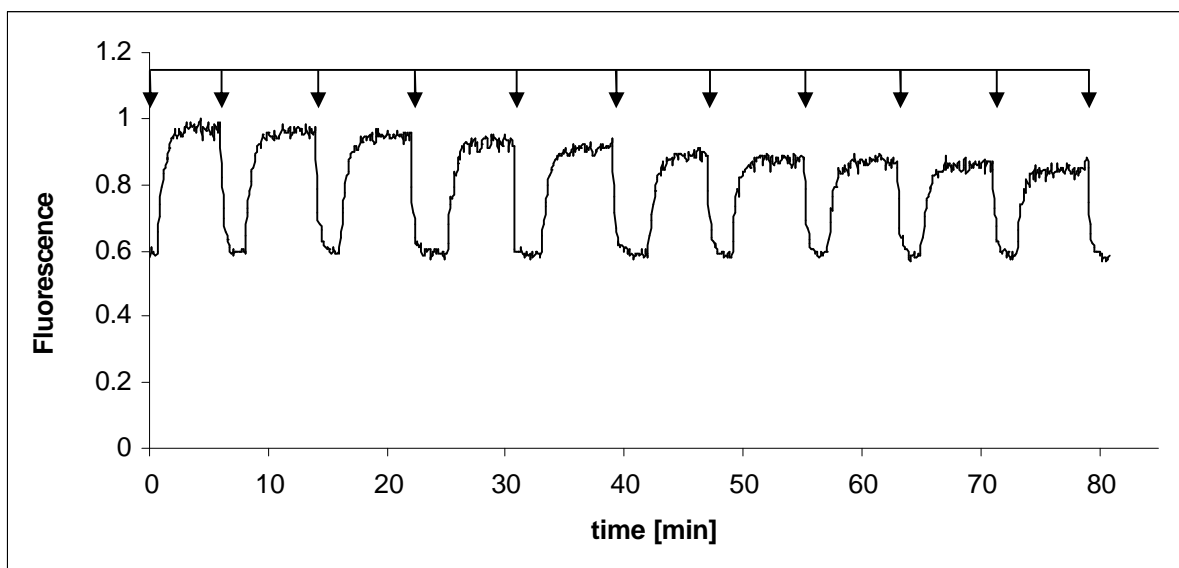
Figure 3. Reversible photoswitching of asRFP.b. Excitation was at 510 nm for fluorescence emission measurement at 600 nm. Light with 450/40 nm (center/bandwidth) was used for photoswitching irradiation with ~ 80 mW cm^{-2} (marked with arrows). At the starting point of the measurement asRFP.b was switched off. The maximum remaining fluorescence in the off-state stays at ~ 59% during the whole measurement. In the on-state the maximum fluorescence

decreases ~ 15% and averages out at ~ 85% after 10 switching cycles. At the beginning the on-/off-ratio is 1.7 and ends up in 1.5.
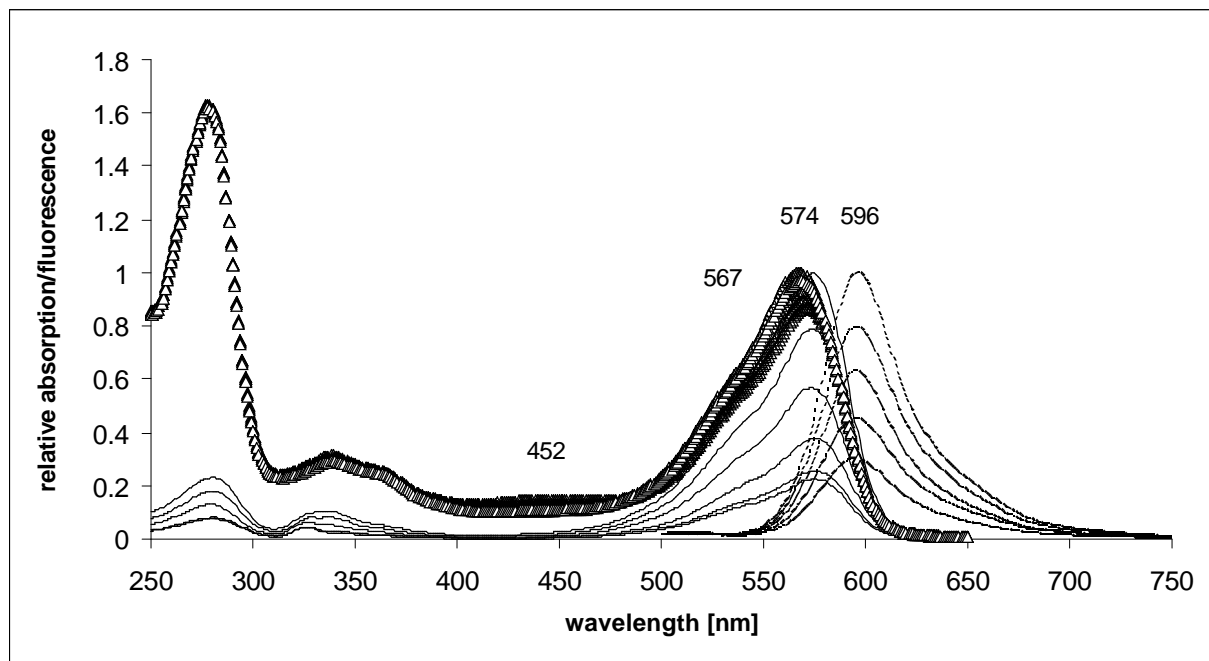

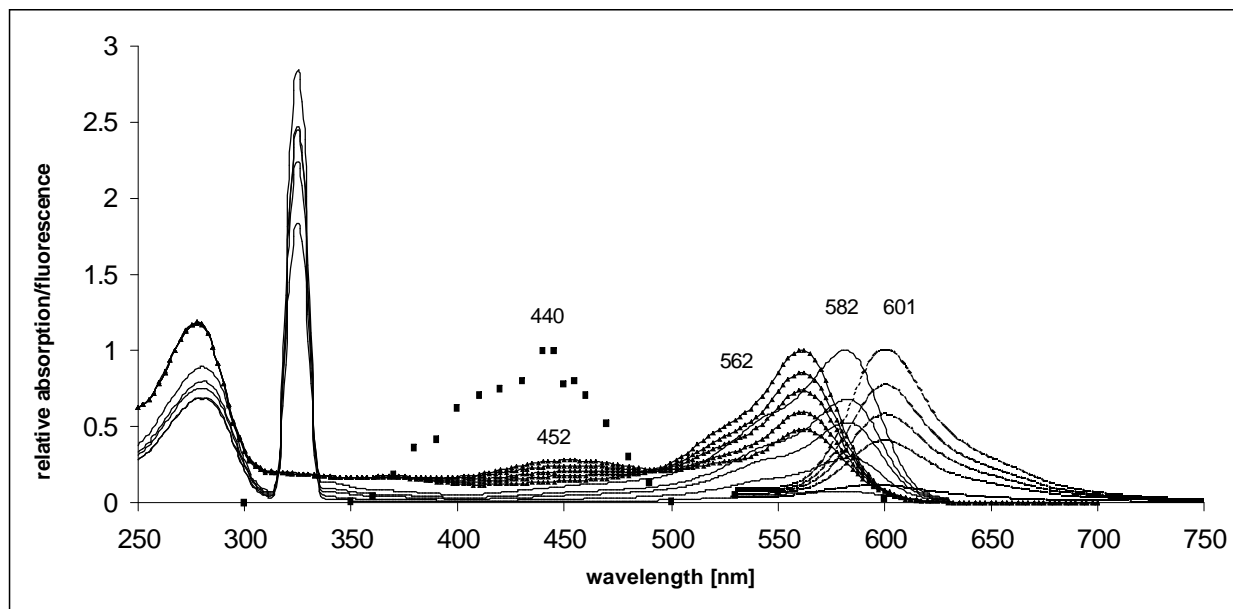**Figure 4.** Absorption (triangles), excitation (solid lines) and emission (dashed lines) spectra of reversible photoswitched asRFP. Fluorescence spectra were recorded using 480 nm light excitation for the emission spectra, whereas the excitation spectra were collected at emission wavelength 650 nm. Light with 450/40 nm (center/bandwidth) was used for photoswitching irradiation with ~ 25 mW cm^{-2}. The maximum remaining fluorescence averages out at ~ 30% after complete switching. Absorption, excitation and emission maxima remain during photoswitching at the same positions (Abs$_{max}$ 567 nm, Ex$_{max}$ 574 nm, Em$_{max}$ 596 nm).
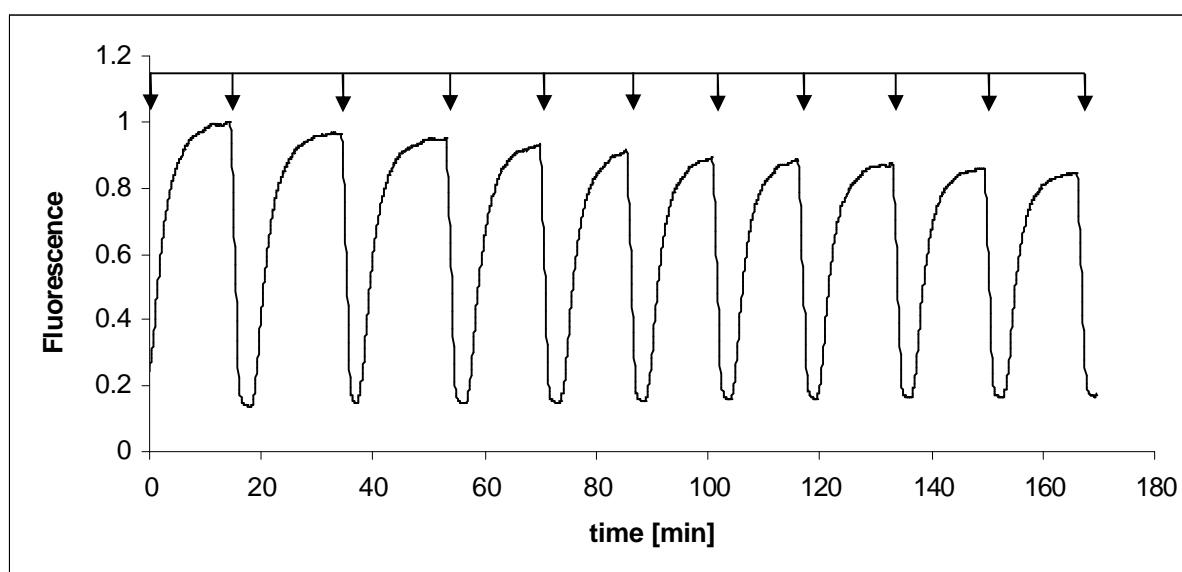
Figure 5. Reversible photoswitching of asRFP. Excitation was at 550 nm for fluorescence emission measurement at 600 nm. Light with 450/40 nm (center/bandwidth) was used for photoswitching irradiation with ~ 80 mW cm^{-2} (marked with arrows). The maximum remaining fluorescence in the off-state is ~ 14% after the first cycle and after the complete measurement ~ 18%. In the on-state the maximum remaining fluorescence decreases ~ 15% and averages out at ~ 85% after 10 switching cycles. At the beginning the on-/off-ratio is 7.1 and ends up in 4.7.

Figure 6. Absorption (thick solid lines with triangles), excitation (solid lines), emission (dashed lines) spectra and action spectrum (squares) of reversible photoswitched psRFP. Fluorescence spectra were recorded using 510 nm light excitation for the emission spectra, whereas the excitation spectra were collected at emission wavelength 650 nm. For the action spectrum the wavelength with the optimal photoswitching effect (440 nm) was determined. Light with 450/40 nm (center/bandwidth) was used for photoswitching irradiation with ~ 25 mW cm^{-2}. The maximum remaining fluorescence averages out at ~ 11% after complete switching. Absorption, excitation and emission maxima remain during photoswitching at the same positions (Abs$_{max}$ 562 nm, Ex$_{max}$ 582 nm, Em$_{max}$ 601 nm).
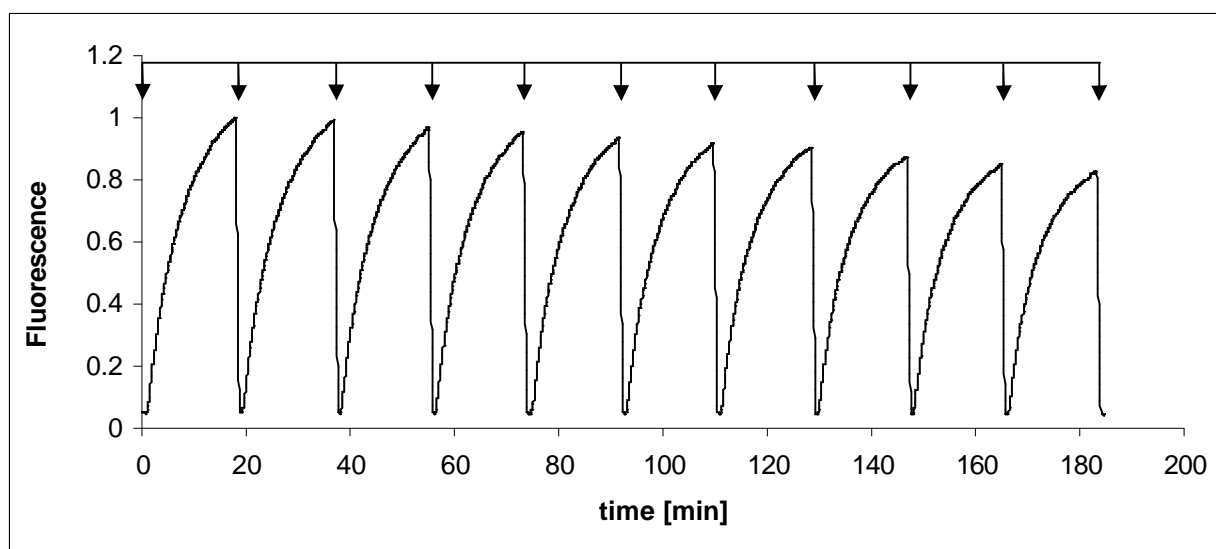
Figure 7. Reversible photoswitching of psRFP. Excitation was at 580 nm for fluorescence emission measurement at 600 nm. Light with 450/40 nm (center/bandwidth) was used for photoswitching irradiation with ~ 80 mW cm^{-2} (marked with arrows). At the starting point of the measurement psRFP was switched off. The maximum remaining fluorescence in the off-state is ~ 5% after the first cycle and after the complete measurement ~ 4%. In the on-state the maximum remaining fluorescence decreases ~ 20% and averages out at ~ 80% after 10 switching cycles. During the whole measurement the on-/off-ratio remains 20.
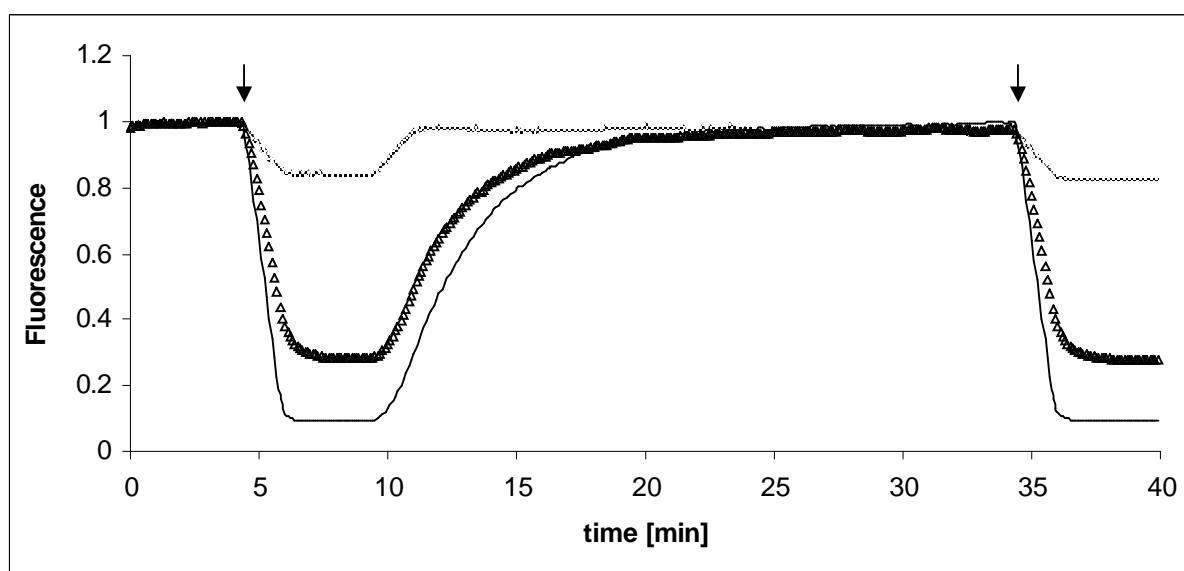

Figure 8. Comparison of photoswitching properties of asRFP.b (dotted line), asRFP (triangles), psRFP (solid line). Excitation was at 510 nm for fluorescence emission measurement at 600 nm. Light with 450/40 nm (center/bandwidth) was used for photoswitching irradiation with ~ 25 mW cm^{-2} (marked with arrows). At the starting point of the measurement all proteins were in their initial fluorescent on-state. After 5

min of data collecting additional blue light irradiation started for 5 min and again after 35 min of measurement for 5 min. The maximum remaining fluorescence reaches from 84% (asRFP.b) over 28% (asRFP) to 9% (psRFP), respectively.
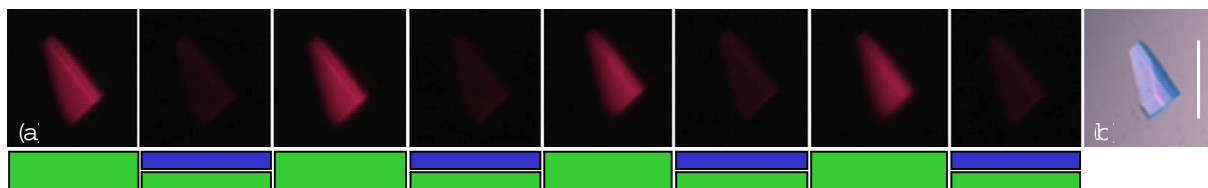

Figure 9. Reversible photoswitching of psRFP protein crystal under a fluorescence microscope. (a) psRFP crystals are considerably fluorescent in the on-state excited with 560 ± 50 nm (595 nm long-pass suppression filter, 645/75 nm transmission). Irradiation with blue light (470 ± 40 nm filter, 495 nm long-pass suppression filter, 525-575 nm transmission, 50 msec) causes quenching of the fluorescence in the off-state. The quenching also takes place while simultaneously irradiating with green light (required to survey the fluorescence) indicated by colored bars. (b) Brightfield image of the psRFP crystal (scale bar 200 μm).
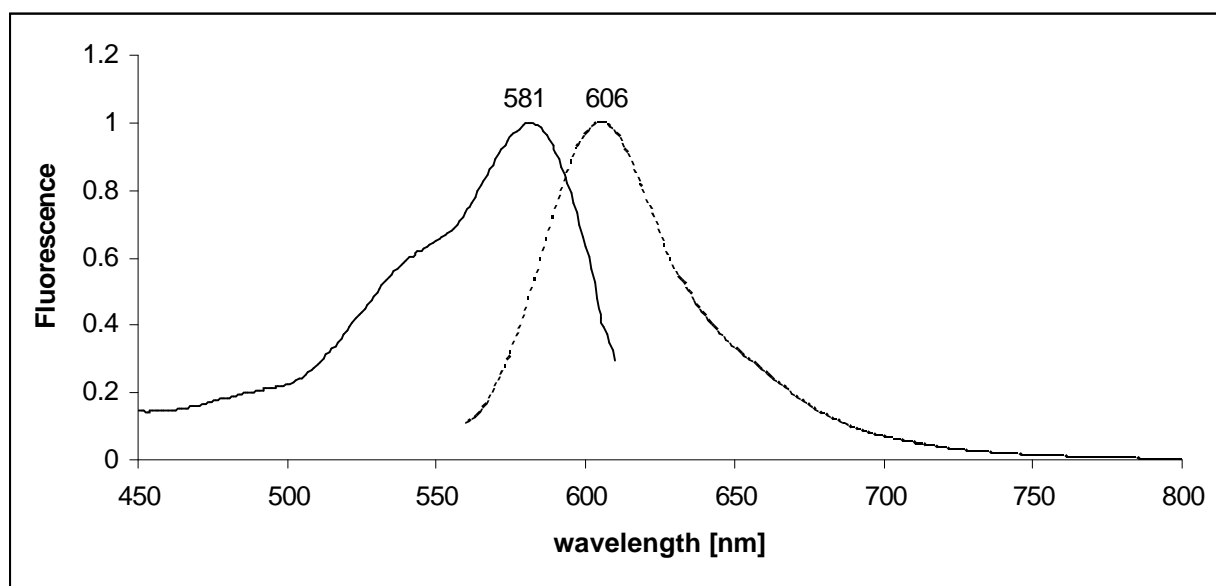

Figure 10. Excitation (solid line) and emission spectra (dashed line) of psRFP crystal (crystallized in buffer solution for structure determination of protein without illumination). For the excitation spectrum, the emission was measured at 640 nm; for the emission spectrum, fluorophores were excited at 510 nm.
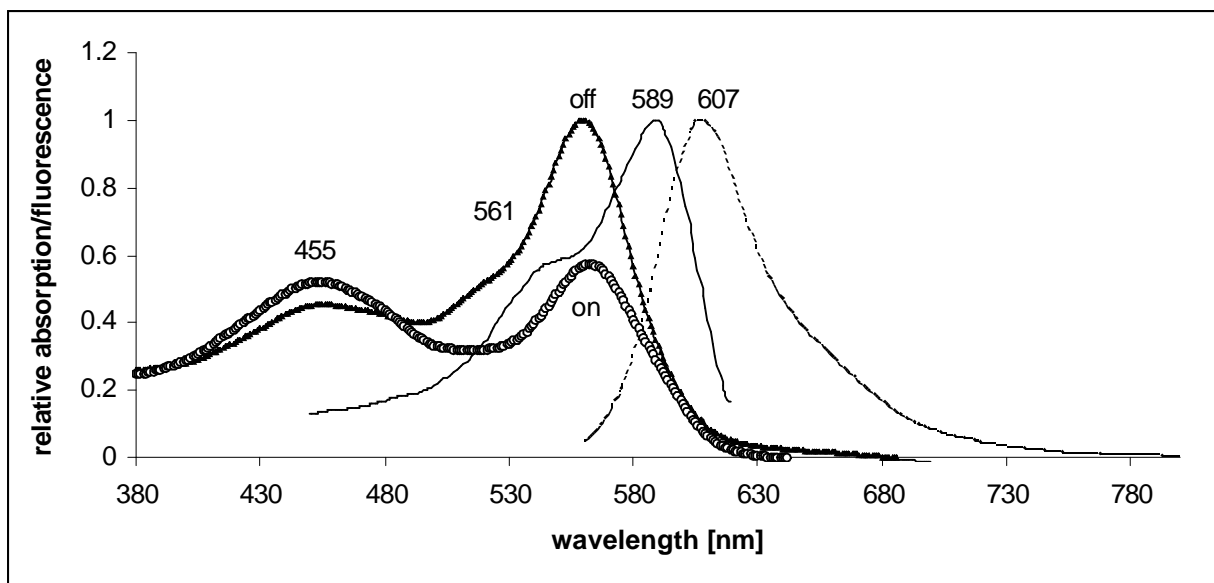
Figure 11. Absorption (on-state = line with circles; off-state = thick solid lines with triangles), excitation (solid line) and emission spectra (dashed line) of psRFP crystal (crystallized in buffer solution for structure determination of protein with illumination). For the excitation spectrum, the emission was measured at 635 nm; for the emission spectrum, fluorophores were excited at 510 nm. Illumination with 473 nm laser was used for photoswitching irradiation with ~ 65 mWcm^{-2} for measuring the absorption spectra.
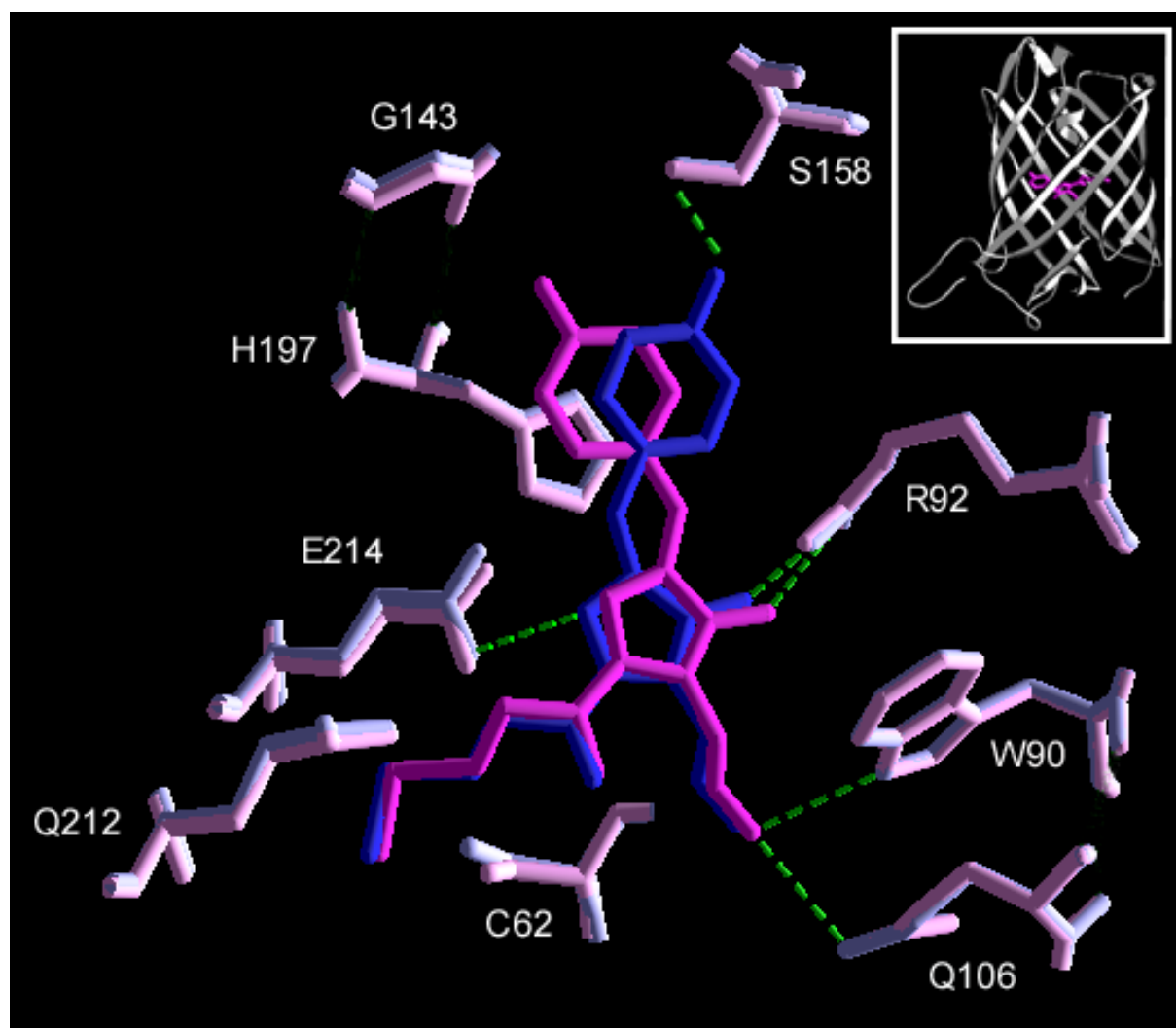
Figure 12. *Trans* (blue) and *cis* (magenta) conformation of the MYG chromophore in the off- and the on-state of psRFP (PDB accession code 3CFH, 3CFF) and environmental amino acids. Residues are shown in their major conformations. Hydrogen bonds are illustrated with dashed green lines. Inset shows a cartoon depiction of a monomeric subunit of the psRFP on-state crystal structure (PDB accession code 3CFF). The chromophore is highlighted in magenta.
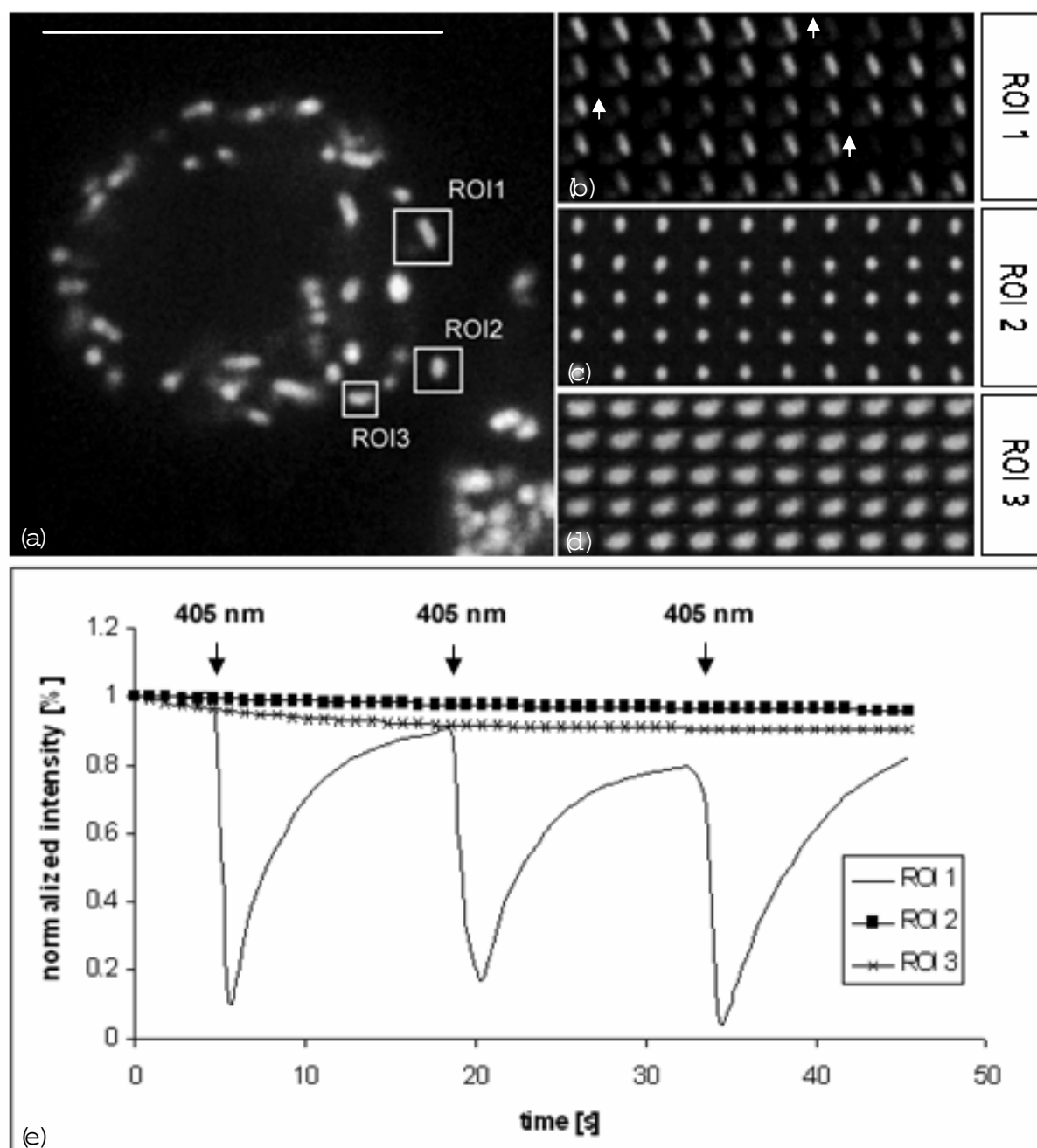
Figure 13. psRFP fused to mitochondrial localization signal (MLS) of subunit VIII of humane cytochrome c-oxidase and expressed in HEK293-cells. Pictures from living cells were taken 24 h after transfection. (a) Mitochondria of a transfected HEK293-cell are highlighted by the MLS-psRFP fusion protein (scale bar 5 μm). Three regions of interest were chosen (ROI 1-3) for analysis after the switching experiment. (b), (c), (d) every second a picture was taken at 532 nm excitation. Additional excitation with 405 nm laser at region of interest 1 (ROI 1) (marked with arrows) led to off-switching of psRFP. ROI 2 and 3 were not excited by 405 nm laser. (d) Normalized intensity [%] plotted per time from (b), (c) and (d). A single mitochondrion can be excited in ROI 1, which shows on- and off-switching of psRFP. It can be switched off to maximum ~ 5% of initial fluorescence and reaches ~ 80% of maximum fluorescence after measurement. ROI 2 and 3 only show negligible loss in fluorescence intensity at the end of the measurement.

Table

Table 1. Spectral properties of photoswitchable red fluorescent proteins

Protein name	Switching mode	Absorption maximum nm	Excitation maximum nm	Emission maximum nm	Maximum fluorescence (on-state)[a]	Maximum fluorescence (off-state)[a]	Ratio on-/off[a]	Extinction coefficient M^{-1} cm^{-1}	Quantum yield	Relative brightness (on-state)[b]
asRFP.b	-	572	575	597	100%	84%	1.2	38,000	0.33	0.81
asRFP	-	567	574	596	100%	28%	3.6	44,000	0.38	1.08
psRFP	-	562	582	601	100%	9%	11.1	~ 44,000[c]	0.35	1.0
KFP1 (kindled)[d]	+	n.m.	580	600	n.m.	n.m.	n.m.	59,000	0.07	0.27
rsCherry[e,f]	+	572	n.m.	610	32%[g]	15%[g]	2.1	80,000	0.02	0.10
rsCherryRev[e,f]	-	572	n.m.	608	8%[g]	5%[g]	1.6	84,000	0.005	0.03

[a] = data for asRFP.b, asRFP and psRFP transferred from Fig. 8
[b] = as compared to the brightness (extinction coefficient multiplied by quantum yield) of psRFP
[c] = transferred from data for relative brightness and quantum yield
[d] = Data are from ref. 28   [e] = Data are from ref. 19
[f] = Data are from ref. 30   [g] = determined relative to mCherry (see reference 30)
n. m. = data not measured

Online Supporting Information

Table S1. Data collection statistics

Data set PDB entry	psRFP without illumination 3CFF	psRFP with illumination 3CFH
Space group	C222$_1$	C222$_1$
Cell dimensions (Å)		
a	98.418	97.819
b	98.360	97.851
c	242.626	241.827
Wavelength (Å)	1.05	1.05
Resolution (Å)	20.0-1.80	20.0-1.75
	(1.83-1.80)	(1.78-1.75)
Completeness (%)	97.0 (95.6)	99.4 (99.5)
Redundancy	3.31 (3.31)	3.36 (3.35)
$<I/\sigma(I)>$	14.5 (4.5)	19.1 (4.0)
Rmerge[a]	0.073 (0.58)	0.073 (0.82)

Values in parentheses refer to data in the highest-resolution shell.

[a] Rmerge = $\Sigma |Iobs - <I>| / \Sigma <I>$.

Table S2. Refinement statistics

Data set	psRFP without illumination	psRFP with illumination
PDB entry	**3CFF**	**3CFH**
Resolution (Å)	12.3-1.80	12.3-1.75
No. reflections	100059	109836
Rcryst[a]	0.198	0.204
Rfree[a]	0.224	0.230
No. non-hydrogen atoms		
Protein	7376	7344
Solvent	920	918
Chromophore	4	8
Wilson *B* value (Å^2)	30.8	32.3
r.m.s. deviations from ideal geometry		
Bond lengths (Å)	0.021	0.022
Bond angles (^{o})	1.9	1.9
Ramachandran analysis		
Favored (%)	94.8	94.0
Allowed (%)	100.0	100.0

[a] R-factor = $\Sigma |Fobs - Fcalc| / \Sigma Fobs$.

Table S3. Chromophore geometries and hydrogen-bonding contacts

Data set PDB entry	psRFP without illumination 3CFF	psRFP with illumination 3CFH	psRFP with illumination 3CFH
State	on	on	off
Conformation	*cis*	*cis*	*trans*
Occupancy	1	0.7	0.3
Dihedral angle (˚)	9.3	4	18.7
H-bonds (Å)			
OH-S143OG			
OH-S158OG,A		3.09	2.49
OH-S158OG,B			
N1-C62O	2.17	2.33	2.15
N3-T60O	2.88	2.93	3.03
O2-R92NH2	2.61	2.55	2.83
O3-W90NE1	3.13		3.07
O3-Q106OE1	3.23		3.15
SD-Q212NE2	3.05	3.08	3.27
SD-E214OE1	3.17		

Analysis of fluorescent and non-fluorescent sea anemones from the Mediterranean Sea during a bleaching event

Alexandra Leutenegger [a], Simone Kredel [a], Silke Gundel [a], Cecilia D'Angelo [a], Anya Salih [b], Jörg Wiedenmann [a,c,*]

[a] *Institute of General Zoology and Endocrinology, University of Ulm, 89069 Ulm, Germany*
[b] *Electronic Microscopy Unit, University of Sydney, NSW 2006, Australia*
[c] *School of Ocean and Earth Sciences, National Oceanography Center, SO14 ZH, United Kingdom*

Abstract

We examined the physiological responses to bleaching of two shallow water anemones, *Anemonia sulcata* var. *smaragdina* and *A. rustica*, common to the Mediterranean Sea. The tentacle coloration of *A. sulcata* var. *smaragdina* is caused by proteins homologous to the green fluorescent protein (GFP) from *Aequorea victoria*. Minor amounts of the transcripts for the same GFP-like proteins were also detected in tentacles of the non-fluorescent *Anemonia rustica*. During a bleaching event observed in the Mediterranean Sea, representatives of both species lost ~90% of their zooxanthellae, indicating that the green fluorescent host pigmentation had no influence on the degree of bleaching of the two sea anemone species. Interestingly, the content of fluorescent proteins was also significantly reduced in bleached individuals of *A. sulcata*. The content of mycosporine-like aminoacids (MAAs) was essentially unaltered in bleached specimens. Bleached anemones were characterized by increased levels of superoxide dismutase activity, whereas the catalase activity in these animals was significantly reduced. The latter results indicate that oxidative stress might have been involved in the observed bleaching of *Anemonia* spp.
Crown Copyright © 2007 Published by Elsevier B.V. All rights reserved.

Keywords: Anthozoa; Bleaching; Fluorescent proteins; GFP; Photoprotection; Zooxanthellae

1. Introduction

The symbiosis with unicellular dinoflagellates, the zooxanthellae, allows anthozoans to thrive in oligotrophic waters. However, zooxanthellae are prone to light and temperature-mediated damage that results in oxidative stress harmful to the cnidarian host (Lesser, 1996, 1997; Lesser and Shick, 1989; Downs et al., 2002; Tchernov et al., 2004; Smith et al., 2005). Therefore, the animals adjust the number of zooxanthellae according to the light conditions (Brown et al., 2002). Moreover, the content of photosynthetic pigment per algal cell is adapted to the amount of available light (Shick and Dykens, 1985; Muller-Parker, 1985; Shick et al., 1995). During stressful conditions, zooxanthellae can be expelled and/or loose their pigments resulting in a bleaching of the host overall coloration (Coles and Jokiel, 1978; Brown et al., 1995; Gates et al., 1992;

Kleppel et al., 1989; Fitt et al., 2001; Coles and Brown, 2003; Rodolfo-Metalpa et al., 2006). The loss of symbionts can be associated with an increased mortality of the cnidarian host (Glynn and D'Croz, 1990). Mass bleaching events among scleractinian corals are considered a severe threat to the survival of coral reef ecosystems (Harvell et al., 1999; Pockley, 1999, 2000). Aside from abnormally high temperatures, other stress factors, such as cold shock, infections, reduced salinity, or unfavorable light conditions may cause bleaching (Muscatine et al., 1991; Wilson et al., 2001; Goreau, 1964; Lesser et al., 1990; Ben-Haim et al., 2003; Kushmaro et al., 1996, 1997, 1998). The majority of mass bleaching events have been reported in tropical regions as a result of elevated seawater temperatures and have been linked to the "El Niño" southern oscillation and global warming (Glynn, 1984, 1993; Glynn and D'Croz, 1990; Goreau and Hayes, 1994; Stone et al., 1999; Pockley, 2000). In the Mediterranean Sea, bleaching of the scleractinian coral *Oculina patagonica* has been reported in response to an infection with the bacterium *Vibrio shiloi*, promoted by elevated seawater temperature (Kushmaro et al., 1996, 1997, 1998; Banin et al., 2003). However, the latter species appeared resistant to bleaching in experiments featuring a short term increase of the water temperature (Rodolfo-Metalpa et al., 2006). With the exception of the latter reports, there is only scant information available about bleaching of anthozoans in temperate seas.

At the beginning of September 2001, we witnessed a bleaching event among a mixed population of the temperate sea anemones *Anemonia rustica* (Bulnheim and Sauer, 1984) and *Anemonia sulcata* (=*A. viridis*) var. *smaragdina* (Gosse, 1860; Wiedenmann et al., 1999) in the Mediterranean Sea next to Collioure, France. We found that ∼30% of the *Anemonia* spp. population (n_{total}= ∼900 individuals) in Collioure exhibited unusual white tentacles and pale oral discs. Although bleaching of single individuals within natural *Anemonia*-populations had been described previously (Gosse, 1860; Andres, 1881; Wiedenmann et al., 2000a), the 2001 bleaching appeared to be the most severe on record.

The two sea anemone species were initially described as color morphs of *A. sulcata* and recently taxonomically separated on the basis of their alloenzyme frequencies (Bulnheim and Sauer 1984). Both species can populate large areas in shallow water habitats by forming clones via longitudinal fission (Louis, 1960). Clone sizes can exceed 1200 individuals corresponding to a biomass (wet weight) of ∼40 kg (Wiedenmann

et al., 2000a, 2007). While *A. rustica* shows a uniform brown color, *A. sulcata* var. *smaragdina* is characterized by green tentacles with pink tips (Gosse, 1860). The color is derived from green fluorescent and pink host pigments (Wiedenmann et al., 1999). Differently colored pigments in both, zooxanthellate and azooxanthellate, non-bioluminescent anthozoa often belong to the family of GFP-like proteins (Wiedenmann 1997; Matz et al., 1999; Lukyanov et al., 2000; Wiedenmann et al., 2000a, 2002b, 2004; Shagin et al., 2004; Oswald et al., 2007). A photoprotective function was proposed for fluorescent host pigments (Kawaguti, 1944, 1969; Wiedenmann et al., 1999; Salih et al., 1998, Salih et al., 2000; Dove et al., 2001). In this context, the pigments were suggested to protect the animals from excess light by dissipation of energy via radiative and non-radiative pathways (Salih et al., 2000, 2006; Gilmore et al., 2003; Cox and Salih 2006; Cox et al., 2006; Salih et al., 2006). The stability of GFP-like proteins, indicated by the low turnover rate of ∼20 days measured *in vivo* and *in situ*, makes them suitable to fulfill such a function (Leutenegger et al., 2007). In contrast, the optical properties render some GFP-like proteins rather unsuitable for sun shielding by wavelength transformation (Mazel et al., 2003). Alternatively, it was suggested that FPs might exert a photoprotective function via an anti-oxidant activity (Mazel et al., 2003; Salih et al., 2006; Bou-Abdallah et al., 2006). The separate evolutionary history and the distinct tissue and species specific expression point to multiple functions of differently colored FPs (Ugalde et al., 2004; Field et al., 2006; Oswald et al., 2007). Such possible alternative functions include the attraction of prey (Matz et al., 2005; Haddock et al., 2005). In bioluminescent cnidarians as *Aequorea victoria*, *Renilla reniformis* or *Obelia geniculata*, green fluorescent proteins (GFPs) act as secondary emitters in the bioluminescent reaction (Morin, 1974; Prasher et al., 1992). The luminescence is thought to prevent predators from feeding either as a direct deterrent or by the attraction of top-predators that subsequently control the numbers of the predator of cnidarians (Burkenroad, 1943; Morin, 1974). Finally, fluorescent host pigments might act to enhance photosynthesis (Schlichter et al., 1986, Salih et al., 2000).

The natural bleaching incident among *Anemonia* spp. allowed us to study biomarkers of the adaptive status of the host–symbiont association considering the differing pigmentation of the two affected species. To this end, we showed that the green and red pigments of *Anemonia* spp. tentacles were GFP-like proteins and compared their content in the tentacle tissue of bleached

and non-bleached anemones. Moreover, we examined the zooxanthellae content of the tentacle tissue and the pigment content of the algal cells from both, bleached and non-bleached representatives of the two species. Finally, the levels of mycosporine-like amino acids (MAAs) and the activity of the anti-oxidant enzymes superoxide dismutase (SOD), peroxidase (POD) and catalase (CAT) in the tentacle tissue were measured.

2. Area description and methods

2.1. Description of the study site

The *Anemonia* spp. population is localized in a small bay (42°31′52″N, 3°04′68″E) sheltered by an ahead-lying rock formation close to Collioure, France (Fig. 1). An area of ~130 m^2 was demarcated and the number of animals was analyzed using the belt transect method as indicated in Fig. 1, area A. Water depths ranged from ~0.5 m to ~1.5 in the studied area. During the collection of animals for the present study in the afternoon of the 3rd of September 2001, water temperatures were determined. The temperatures reached 27 °C close to the shore and lowered to 25 °C in more sea exposed parts of the of the study site. It is interesting to note that day temperatures in the examined habitat were up to 3 °C higher than in nearby areas that were cooled to 24 °C by direct exposure to currents and wave action (Fig. 1). Similar temperature gradients were measured when the site was revisited in September in the years 2002–2004 and in 2006. Therefore, the micro-climate of the habitat is characterized by water temperatures that can be con-siderably increased in comparison to the regional costal water temperature.

2.2. Sample collection and preparation

Bleached and non-bleached individuals of *Anemonia* spp. from the studied site were collected from a depth of 0.8 m. In the sampling area, water temperatures of 27 °C were measured. Whenever a bleached animal was collected, the closest non-bleached individual from the same species found within a distance of <0.5 m was also sampled. Afterwards, the anemones were transferred promptly to aerated tanks with natural seawater in our field laboratory. Subsequently, ten tentacles were cut at the basis and immediately frozen at −20 °C for later analyses. The samples were homogenized in 5 ml sterile filtered artificial seawater using a glass Potter homog-enizer (Braun Biotech, Melsungen, Germany). An aliquot (1.8 ml) of each homogenate was centrifuged at 50,000 g for 30 min at 4 °C in order to remove zooxanthellae and cell debris. The protein concentra-tions of the supernatants were measured photometrically using the BCA™ Protein Assay (Pierce, Bonn, Germany). The supernatants were used to determine the concentration of green fluorescent protein, MAA levels, and the activity of anti-oxidant enzymes. Tentacle extracts clarified by 50,000 g-centrifugation obtained from non-bleached representatives both *A. sulcata* var. *smaragdina* and *A. rustica* were size-fractionated using a calibrated Superdex 200 HR 10/30 column attached to an Aekta Purifier (GE Healthcare Bio-Sciences, Uppsala, Sweden). The 0.5 ml fractions were frozen at −20 °C for later analysis of anti-oxidant enzymes. The content of zooxanthellae and their pigments was determined from the remaining primary homogenate.

2.3. RT-PCR analysis, cloning and sequencing of cDNA coding for GFP-like proteins

Total RNA was extracted from tentacle tissue accord-ing to Wiedenmann et al. (2000b). Subsequently, 1 μg of total RNA was reverse transcribed using the Superscript II™ Reverse Transcriptase and Oligo-d(T)$_{12–18}$ Primer Kit (Invitrogen, Karlsruhe, Germany). For semi-quanti-tative analysis of the transcript levels of GFP-like proteins in the different *Anemonia* species, PCR reactions with a final volume of 100 μl were prepared. The reaction mix contained 100 ng aliquots of cDNA, 2.5 units of Taq-polymerase (Bioline, London, UK) and 50 pmol of primers specific for the open reading frame of asFP499 and asCP562/asulCP (Wiedenmann et al., 2000b; 2002a;
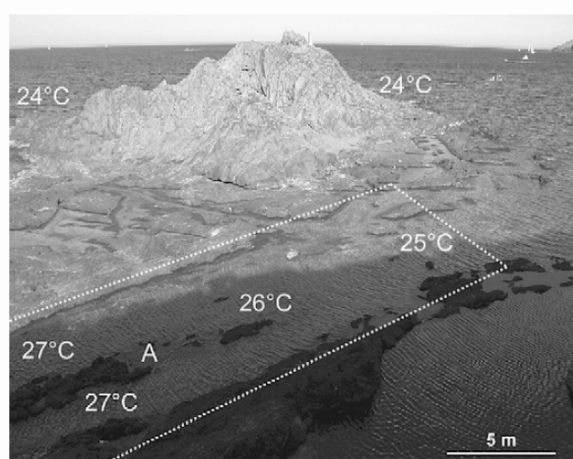

Fig. 1. The studied habitat of *Anemonia* spp. close to Collioure, France, marked by dotted lines and designate with an "A". The different water temperatures measured in the area on the afternoon of the 3rd Sept. 2001 are indicated in the picture.

Lukyanov et al., 2000). The transcript of the housekeeping gene glyceraldehyde-3-phosphate-dehydrogenase (GAPDH) (Pohjanvirta et al., 2006) was analyzed in parallel. After 30 and 35 PCR cycles 10 μl-aliquots were removed from the reaction mixes and analyzed by electrophoresis on ethidium bromide stained agarose gels. The amplicons were ligated in pQE-32 (Qiagen, Hilden, Germany) and cloned in *E. coli* XL1 Blue (Stratagene, La Jolla, CA, USA). Plasmids were isolated from pink and green fluorescent bacterial colonies and sent for sequencing by a commercial provider (MWG Biotech AG, Ebersberg, Germany).

2.4. Spectral analysis of GFP-like proteins and quantification of asFP499 contents

The GFP-like proteins were expressed in *E. coli* BL21 DE3 (Invitrogen, Karlsruhe, Germany) and purified by affinity and size exclusion chromatography as described (Wiedenmann et al., 2002b). Excitation and emission spectra of the green fluorescent protein were determined using a fluorescence spectrometer (Spex 1680 Double Spectrometer, Spex Industrie GmbH, Grasbrunn, Germany). The absorption spectrum of the chromoproteins was measured with a Cary 50 UV–VIS-spectrophotometer (Varian, Palo Alto, CA, USA). In order to estimate the relative content of green fluorescent proteins in the tentacle tissue of bleached and non-bleached individuals of *A. sulcata*, the excitation and emission spectra of diluted tissue extracts were measured as described above. Fluorescence emission at 499 nm was then normalized to the total protein content of the sample.

2.5. SDS-polyacrylamide gel electrophoresis

Proteins were denatured completely by adding 0.625 M Tris–HCl pH 6.8 supplied with 10% β-mercaptoethanol (14.3 mol/l), 1% SDS and 10% glycerol and heating at 99 °C for 5 min. Afterwards, SDS-polyacrylamide gel electrophoresis (PAGE) was performed as described (Laemmli, 1970). Gels were silver stained according to Blum et al. (1987).

2.6. Content of zooxanthellae and their pigments

To determine the number of zooxanthellae, 200 μl of tissue homogenate was centrifuged with 500 g for 10 min at 4 °C. The supernatant was removed and the pellet containing the algae was re-suspended in sterile filtered artificial seawater. The numbers of zooxanthellae were determined on a microscope using a haemo-

cytometer (Thoma, Germany). For each sample, the mean value was calculated from the results of counting zooxanthellae within three squares of the counting grid ($0.0025 \times 0.0025 \times 0.02$ mm). The numbers were normalized to the protein content of the homogenate.

The concentration of the zooxanthellae pigments chlorophyll *a*, *c* and peridinin in 1.5 ml tissue homogenate was determined. For this purpose, the samples were centrifuged with 5000 g for 10 min at 4 °C. The zooxanthellae were re-suspended in 350 μl bidistilled H_2O saturated with $MgCO_3$ (Lesser and Shick, 1989) and homogenized using a Sonifier (Branson Ultrasonic S.A., Trenton NJ, USA). Aceton (p.a.; Merck, Ulm, Germany) was added to a final concentration of 90% in order to extract photosynthetic pigments. After centrifugation at 20,000 g for 15 min at 4 °C, the absorption of the extracts was recorded with a Uvikon 820 spectrophotometer (Kontron, Eching, Germany). The concentrations of photosynthetic pigments were calculated using the equations of Jeffrey and Humphrey (1975).

2.7. Content of mycosporine-like amino acids

Methanol (HPLC grade; Merck, Ulm, Germany) was added to an aliquot of the tentacle extract to a final concentration of 97.5%. After incubation for 30 min on ice, the samples were centrifuged with 20,000 g for 15 min at 4 °C. The supernatants were transferred to a quartz cuvette and the absorption spectra were determined in a Beckmann DU-64 spectrophotometer (Beckman, München, Germany). The A_{334}-units were normalized to the protein content of the samples.

2.8. Activity of anti-oxidant enzymes

The activity of SOD in tentacle extracts was determined using the Superoxide Dismutase Assay Kit (Cayman Chemical Company, Ann Arbor, MI, USA) following the instructions of the manufacturer. Briefly, the activity of all three types of SOD (Cu/Zn-, Mn-, and Fe-SOD) in the samples is assessed by measuring the dismutation of superoxide radicals generated by xanthine oxidase and hypoxanthine. SOD standards serve as positive control.

POD activity was measured using the ECL™ Western Blotting Detection Reagents (Amersham International, UK). 50 μl of a 1:1 mixture of the ECL solutions A and B was automatically injected in a reaction tube containing 100 μl of tentacle extract in a Berthold Lumat LB 9507 luminometer (EG&G Berthold, Bad Wildbad, Germany). The luminescence intensity as a measure of the POD

activity was normalized to the protein content of the samples.

The CAT activity was determined using the floating paper assay (Gagnon et al., 1959). Filter paper squares (0.5×0.5 cm) (Schleicher and Schuell, Dassel, Germany) were soaked with 10 µl of tissue homogenate and dropped in a 1% H_2O_2 solution at 20 °C. Oxygen bubbles produced in course of the decomposition of H_2O_2 cause the filter paper to float to the surface after 10–40 s. The reciprocal value of the time required by the filter paper from entering the solution to reaching the surface again was used as a relative measure of the CAT activity. Seven replicates of a dilution series of one tentacle extract were measured to demonstrate that the method works accurately and reproducibly within the concentration range found in the samples (Fig. 2). Five replicates were measured per sample and normalized to the content of total protein in the tissue extracts.

2.9. Statistical analysis

The software ANALYSE IT for Microsoft Excel, Version 1.73 (Microsoft, Redmond, CA) was used for statistical analyses. Two-tailed P-values of <0.05 determined by the Mann–Whitney U-test (two independent groups) were considered statistically significant. Highly significant differences were assumed for P-values of =0.001. The significance of differences between the averaged fluorescence intensities of tissue extracts was determined with the t-test build into the Origin 6.1 software (OriginLab Corporation, Northampton, MA, USA). Significance levels were set as outlined above.
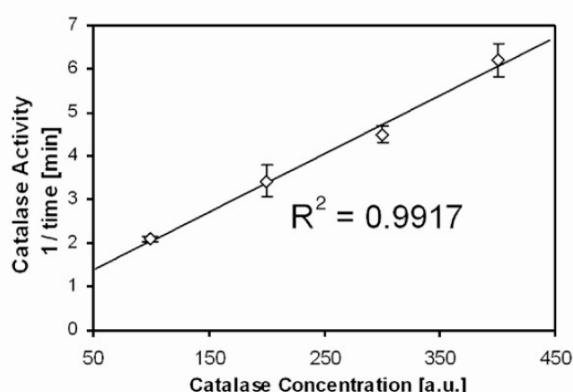

Fig. 2. Accuracy and reproducibility of the Gagnon-test of catalase activity shown for a dilution series of tentacle extracts. Values are the means of seven replicate measurements±standard deviation. The coefficient of determination R^2 of the linear fit is given in the figure.

3. Results

3.1. Color polymorphism among Anemonia spp.

The tentacle tips of the morph *A. sulcata* var. *smaragdina* contain a purple pigment while the color of the other parts of the tentacles is dominated by a green fluorescent pigment emitting at 499 nm (Figs. 3A–B and 4D). The green fluorescence is restricted to the ectoderm of tentacles (Fig. 3B–C). Molecular cloning and sequencing of a DNA fragment from a cDNA sample of *A. sulcata* var. *smaragdina* identified the 499 nm emitter as GFP-like protein with an amino acid sequence identical to asFP499 from *A. sulcata* var. *rufescens* (Wiedenmann et al., 2000b; Nienhaus et al., 2006) (Fig. 4A). The purple pigment also belongs to the family of GFP-like proteins. It has the same sequence as the chromoprotein asulCP (Lukyanov et al., 2000; Labas et al., 2002) cloned from a non-specified morph of *A. sulcata* (Lukyanov et al., 2000) and shares 97.4% identical amino acids with the chromoprotein asCP562 from the color morph *rufescens* (Wiedenmann et al., 2000b, 2002a). The recombinant protein shows an absorption maximum at 568 nm (Fig. 4B). The sequences were deposited in the GenBank under the accession numbers AF545827 and EF587182.

In *A. rustica*, green fluorescence was undetectable by visual inspection and by microscopic or spectroscopic analysis of tentacle extracts (Fig. 3D–E). A weak red fluorescence of the tentacles was attributed to chlorophyll of zooxanthellae (Fig. 3E).

Protein extracts of both *Anemonia* species were examined for the presence of GFP-like proteins by SDS-PAGE. The proteins asFP499 and asulCP are characterized by calculated molecular masses of 25.4 and 25.9 kDa, respectively. The polypeptide backbone of the latter protein splits into two fragments of ~6.8 and ~19.2 kDa during maturation of the chromophore (Martynov et al., 2001; Wiedenmann et al., 2002a; Wilmann et al., 2005). The subunits disassemble upon denaturation of the protein. Heat-treated tentacle extracts of *A. sulcata* var. *smaragdina* separated by SDS-PAGE consequently show clear bands at the heights expected for the full-length protein asFP499 and the subunits of asulCP (Inset Fig. 4A). In contrast, these bands are absent in extracts of *A. rustica*.

Using oligonucleotide primers specific for the 5′ and 3′ ends of the asFP499 and asulCP open reading frames, we performed a PCR analysis of cDNA samples to evaluate if the respective transcripts are absent in the non-fluorescent, non-colored *A. rustica* (inset Fig. 4B). Interestingly, cloning and sequencing of the amplified
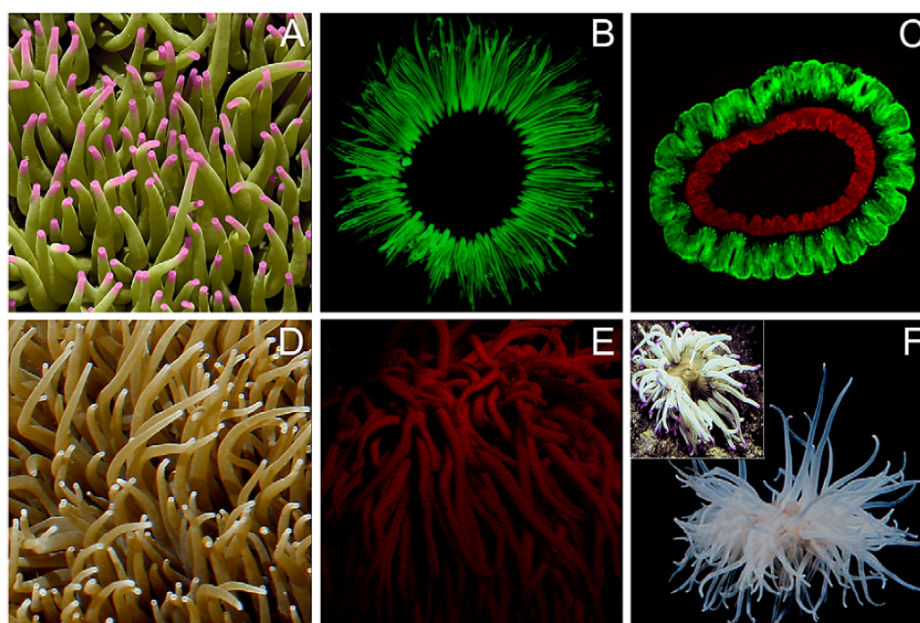
Fig. 3. Comparison of *A. sulcata* and *A. rustica*. (A) *A. sulcata* var. *smaragdina* showing the characteristic green tentacles with pink tips. (B) Fluorescence of *A. sulcata* var. *smaragdina* excited by UV light (366 nm). (C) Fluorescence image of a tentacle cross-section of *A. sulcata* var. *smaragdina* photographed under the fluorescence microscope. (D) Photography of *A. rustica*. (E) Chlorophyll fluorescence of the tentacles of *A. rustica* photographed under blue light excitation using a yellow longpass filter (Nightsea, Andover, MA). (F) Habitus of bleached *A. rustica* and of bleached *A. sulcata* var. *smaragdina* (inset).

~700 basepair long cDNA fragments revealed that asFP499 and asulCP transcripts are present also in non-fluorescent *A. rustica*. The sequences were submitted to the GenBank under the accession numbers EF587180 and EF587181. However, semi-quantitative PCR analysis (inset Fig. 4B) showed that transcript levels of asFP499 and asulCP were significantly lowered in *A. rustica* in comparison to *A. sulcata* var. *smaragdina*.

3.2. Reduction of GFP-content in bleached anemones

The fluorescence intensity at 499 nm was measured in tentacle extracts of *A. sulcata* var. *smaragdina* after zooxanthellae were removed by centrifugation. The content of asFP499 was deduced from a calibration curve of purified recombinant asFP499 with known protein content. We determined that asFP499 contributes ~5% to the total soluble cellular protein of non-bleached individuals. The comparison of the fluorescence spectra of the tissue extracts with those of the recombinantly expressed asFP499 shows the presence of minor amounts of a green fluorescent pigment with an excitation maximum at 511 nm and emission maximum at 522 nm (Fig. 4C–D). As in a previous study on *A. sulcata* var. *rufescens* (Wiedenmann et al., 2000b), it was not possible to clone the putative GFP-like protein. We found a

significant (emission maximum $P=0.0052$; excitation maximum $P=0.0021$) decrease by ~30% in tissue fluorescence in bleached individuals of *A. sulcata* (Fig. 4C–D). The ratio of the pigments emitting at 499 nm and 522 nm, however, remained unaltered in bleached individuals.

3.3. Analysis of symbiont pigments

The tentacles of both fluorescent and non-fluorescent *Anemonia* spp. hosted comparable numbers of zooxanthellae with similar contents of photosynthetic pigments (chlorophyll *a* and *c*, peridinin) (Fig. 5A–B). Bleaching of *Anemonia* spp. proceeds via the highly significant ($P<0.001$) loss of ~90% of the zooxanthellae and not by the reduction of their pigment content (Fig. 5B). No significant differences (Chl. a $P=0.0927$; Chl. c $P=0.0549$; Peridine $P=0.0592$) in the degree of individual bleaching are detectable between fluorescent and non-fluorescent *Anemonia* spp. (Fig. 5B).

3.4. Analysis of mycosporine-like amino acids

We determined the absorption of methanolic extracts of tentacle tissue of *Anemonia* spp. as an indicator of the content of MAAs (Stochaj et al., 1994). Both, extracts from
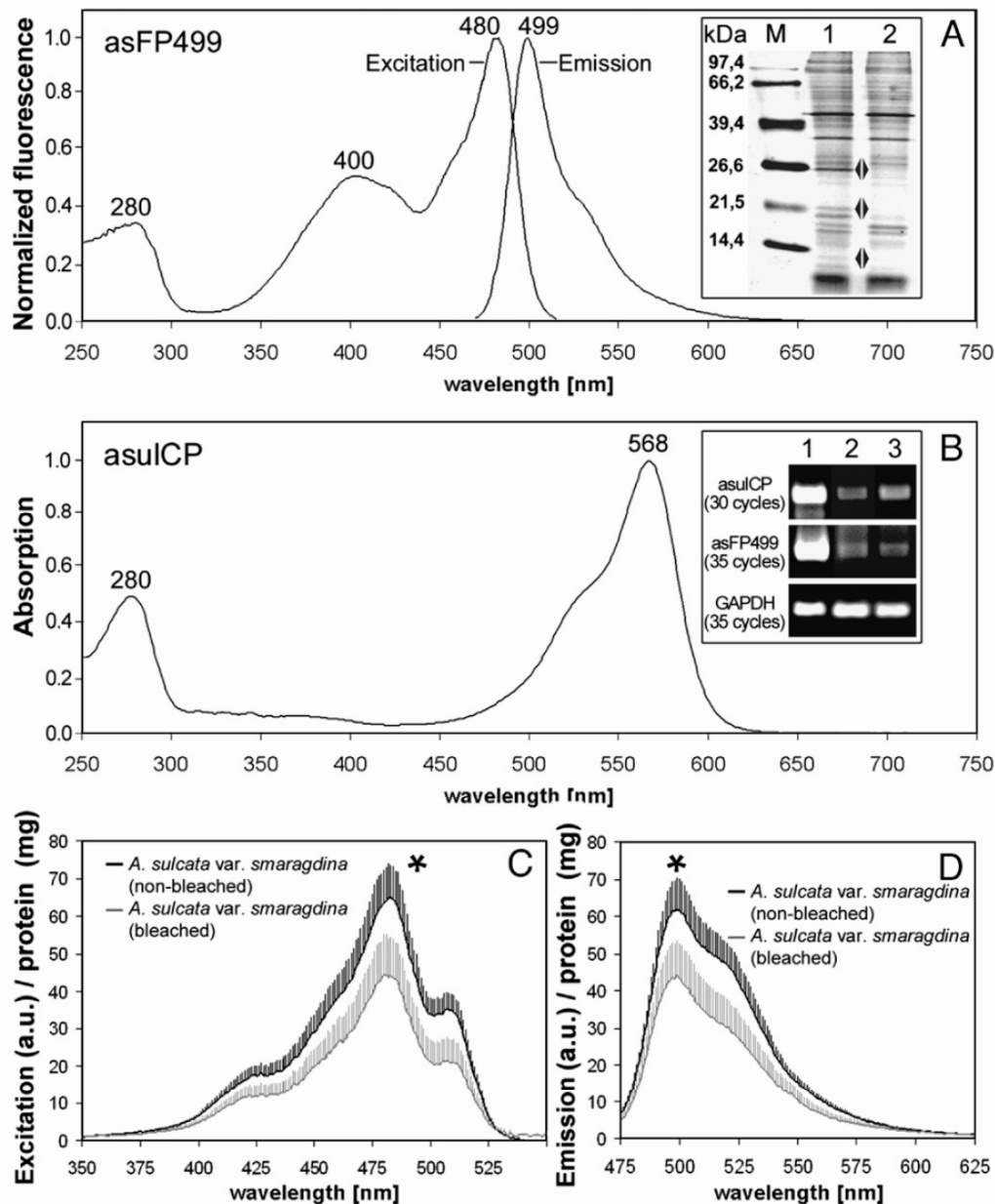
Fig. 4. Host pigments of *Anemonia* spp. (A) Excitation and emission spectra of asFP499 cloned from *A. sulcata* var. *smaragdina*. The numbers indicate the positions of excitation and emission maxima in [nm]. The inset in (A) shows a silver-stained SDS-polyacrylamide gel with protein extracts from tentacles of *A. sulcata* var. *smaragdina* (lane 1), *A. rustica* (lane 2) and a molecular weight marker (M) after electrophoretic separation. Bands corresponding to GFP-like pigments are highlighted by arrowheads. (B) Absorption spectrum of the pink pigment asulCP cloned from the tentacle tips of *A. sulcata* var. *smaragdina*. The peak position is given in [nm]. The inset in (B) displays ethidium bromide stained agarose gels showing the results of a RT-PCR analysis of tentacle tissue of *A. sulcata* var. *smaragdina* (lane 1) and two specimen of *A. rustica* (lanes 2–3). Using cDNA of *A. sulcata*, the PCR is saturated for asulCP after 30 cycles (upper row), for asFP499 after 35 cycles (middle row). After the same numbers of cycles, cDNA samples of *A. rustica* barely yield products. PCR products of the housekeeping gene GAPDH obtained after 35 cycles (lower row). (C–D) Excitation and emission spectra of the green fluorescent pigments in tentacle extracts of bleached and non-bleached representatives of *A. sulcata* var. *smaragdina*. The spectra represent the average values ($n = 10$) after normalization to the total protein content. Error bars indicate the standard deviation. Asterisks indicate significant differences ($P < 0.05$, *t*-test).

A. rustica and *A. sulcata* were characterized by a maximal absorption at 334 nm, suggesting the presence of the MAAs Porphyra-334 or Shinorine (Fig. 6A; Dunlap and Shick 1998). Compared to non-bleached *A. rustica*, non-bleached *A. sulcata* showed a highly significant increase ($P < 0.001$) of A_{334}-compounds by ∼17% (Fig. 6B). A
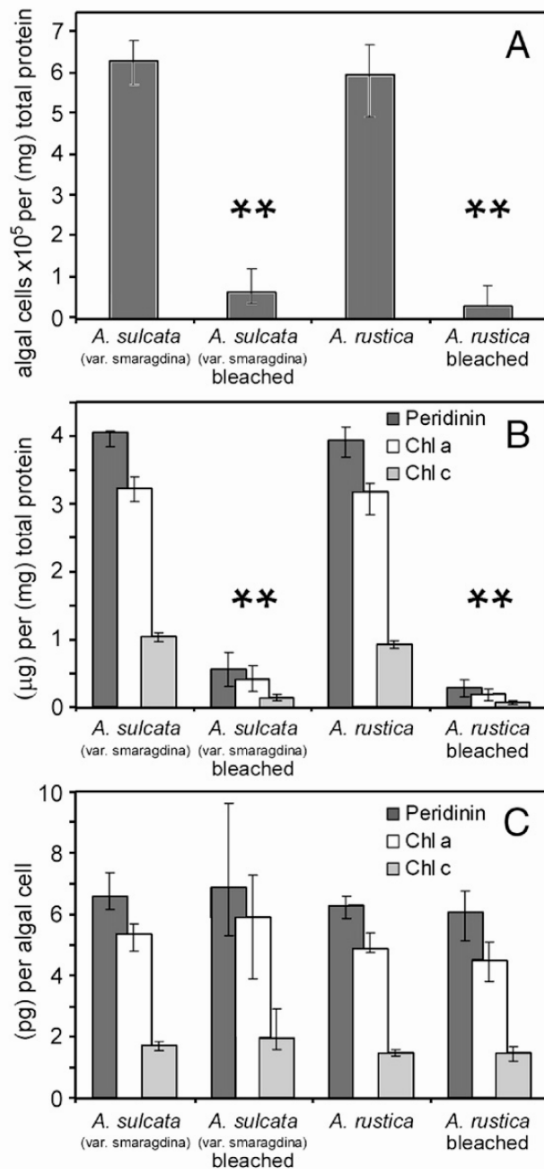
Fig. 5. Analysis of zooxanthellae from tentacles of bleached and non-bleached individuals of *A. sulcata* var. *smaragdina* and *A. rustica*. (A) Number of zooxanthellae in the tentacle tissue normalized to the protein content. (B) Contents of zooxanthellae pigments in the tentacle tissue normalized to the protein content. Concentration of the photosynthetic pigments chlorophyll *a* (chl a), chlorophyll *c* (chl c) and peridinin per algal cell. (C) Columns represent median values ($n=10$)±1st and 3rd quartiles. Asterisks indicate highly significant differences ($P<0.001$; Mann–Whitney *U*-test) between bleached and non-bleached representatives of one species.

significant increase ($P=0.0041$) of A_{334}-compounds by ~20% was determined for bleached *A. sulcata* compared to bleached *A. rustica* (Fig. 6B). The differences in A_{334}-levels between bleached and non-bleached individuals of each species remained non-significant (*A. sulcata* $P=0.0753$; *A. rustica* $P=0.1519$).

3.5. Analysis of anti-oxidant enzymes

Finally, we studied the activity of anti-oxidant enzymes SOD, POD, and CAT in tentacle tissue of *Anemonia* spp. (Fig. 7A–C). We analyzed protein fractions obtained from size exclusion chromatography of tentacle extracts of non-bleached *A. sulcata* and *A. rustica*. In the case of *A. sulcata*, also the presence of the green fluorescent proteins was monitored (Fig. 7A). The elution profile of proteins showing anti-oxidant activity was comparable between *A. sulcata* and *A. rustica*. SOD activity was detected in fractions containing proteins with apparent molecular weights of ~170, 72.9, 33.0 and 14.3 kDa. Proteins with POD or CAT activities eluted with apparent molecular weights of 33.0 and ~140 kDa, respectively. None of the elution maxima of anti-oxidant enzymes matched the elution peak of the green fluorescent proteins.
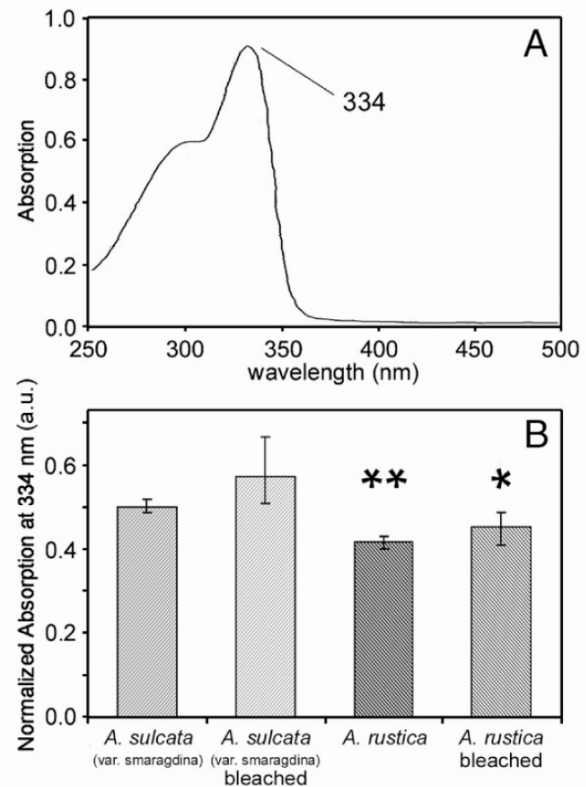

Fig. 6. Content of mycosporine-like amino acids of *Anemonia* spp. (A) Representative absorption spectrum of methanolic tissue extracts from *Anemonia* spp. The peak position [nm] is indicated by a number. (B) Absorption at 334 nm of methanolic tentacle tissue extracts after normalization to the protein content of the samples. Columns represent median values ($n=10$)±1st and 3rd quartiles. Significant differences ($P<0.05$, Mann–Whitney *U*-test) between the bleached representatives of each species are marked by an asterisk. Two asterisks indicated highly significant differences ($P<0.001$, Mann–Whitney *U*-test) between the non-bleached individuals of *Anemonia* spp.
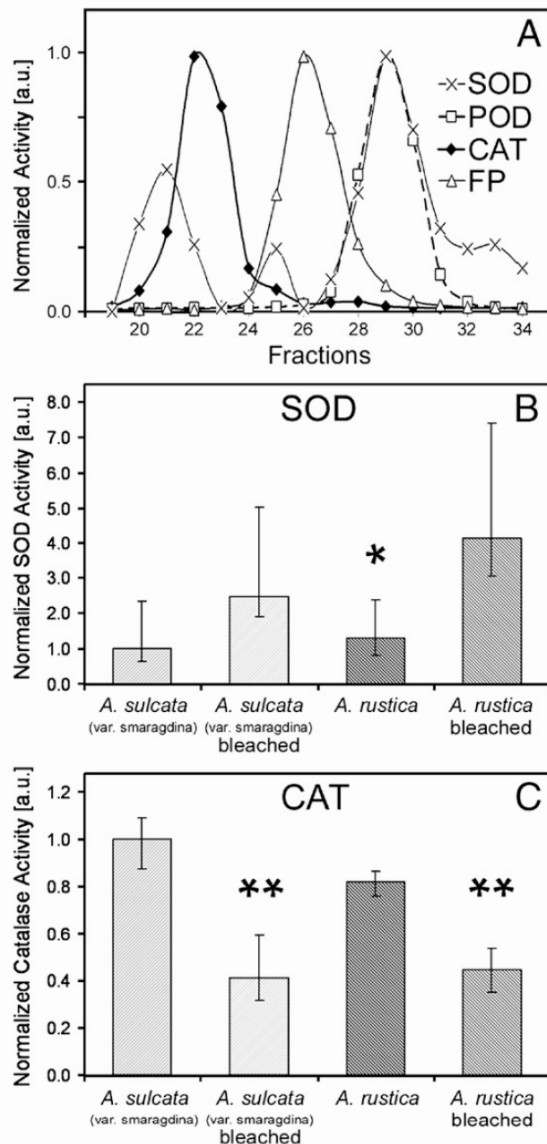
Fig. 7. Activity of anti-oxidant enzymes. (A) An elution profile of the anti-oxidant enzymes SOD, POD, CAT obtained from size exclusion chromatography representative of tentacle extracts of *Anemonia* spp. The pigments asFP499/522 (FP) can be detected only in samples of *A. sulcata* var. *smaragdina*. (B–C) Comparison of the activity of anti-oxidant enzymes in tentacle extracts of bleached and non-bleached *A. sulcata* var. *smaragdina* and *A. rustica*. (B) SOD activity. (C) CAT activity. All values were normalized to the protein content of the samples. Columns represent median values ($n=10$) ±1st and 3rd quartiles. Significant differences ($P<0.05$, Mann–Whitney U-test) between bleached and non-bleached individuals of a species are marked by an asterisk whereas two asterisks indicate highly significant differences ($P=0.001$; Mann–Whitney U-test).

The total SOD activity in tentacle extracts was determined (Fig. 7B). There were no significant differences ($P=0.2991$) between *A. sulcata* and *A. rustica*. The SOD activity of bleached representatives of both species

showed a clear tendency to be increased compared to the non-bleached counterparts. However, only the differences between bleached and non-bleached *A. rustica* were significantly different ($P=0.0140$), whereas the differences between bleached and non-bleached *A. sulcata* remained non-significant ($P=0.2238$).

No significant differences (*A. sulcata* $P=0.7577$; *A. rustica* $P=0.1932$) in the POD activity were detectable among non-bleached individuals of both species when compared to the bleached representatives (data not shown).

Fluorescent *A. sulcata* var. *smaragdina* showed a non-significant increase ($P=0.0513$) in CAT activity compared to *A. rustica* (Fig. 7B). Bleached individuals of both species were characterized by a highly significant ($P=0.001$) reduction in CAT activity.

4. Discussion

Bleaching among tropical anthozoans is a well studied phenomenon. In contrast, there are limited data available on bleaching of temperate anthozoans. Therefore, we documented a bleaching event among the two sea anemone species *A. rustica* and *A. sulcata* var. *smaragdina* in the Mediterranean Sea. The study included analyses of both host and symbiont pigments, MAA levels, and the activity of anti-oxidant enzymes.

4.1. Analysis of host and symbiont pigments

The present study confirmed by molecular analysis that the host pigments of *A. sulcata* var. *smaragdina* are proteins homologous to GFP from *A. victoria*. The amino acid sequences of the proteins are identical (asFP499) or highly similar (asulCP) to the pigments from the color morph *A. sulcata* var. *rufescens* (Wiedenmann et al., 2000b; 2002a). Both, macroscopic and fluorescence microscopic inspection and analysis of tentacle cross-sections show the exclusive expression of the GFPs in the ectoderm of the tentacles. The same localization was described for the green and red fluorescent proteins of *A. sulcata* var. *rufescens* (Wiedenmann et al., 2000b). In contrast, some fluorescent pigments of reef corals can be found in gastrodermal cells, partially in intimate proximity to the zooxanthellae (Salih et al., 2000; Brown et al., 2002; Mazel et al., 2003; Oswald et al., 2007).

In non-bleached representatives of *A. sulcata*, asFP499 contributes ~5% to the total soluble protein of tentacle tissue. Comparable amounts of FPs were already measured in the tissue of scleractinian corals (Oswald et al., 2007). We did not detect the presence of

GFP-like proteins in the tissue of *A. rustica* at the protein level using spectroscopy and SDS/PAGE analysis, however, RT-PCR analysis revealed the presence of minor amounts of asFP499 and asulCP transcripts. The difference in the coloration of the two closely related sea anemone species can therefore be attributed to altered expression levels of genes encoding at least two GFP-like proteins. Also, the green and red color morphs of *Montastrea cavernosa* both express the same set of GFP-like proteins and the characteristic colors of the animals result from differences in the expression levels of green and red pigments (Kelmanson and Matz 2003, Oswald et al., 2007). The two differently colored *Anemonia* species show a complete overlap in their depth distribution, with species specific maxima of abundance (Wiedenmann et al., 1999, 2007). Therefore, the altered expression levels of GFP-like proteins appear to be genetically fixed in adult anemones rather than a result of a dynamic adaptation to the environmental conditions in the habitat.

Anemonia spp. uniformly harbour the zooxanthellae strain 'temperate A', prevalent in cnidarians from the Mediterranean Sea and the southwest coasts of Europe (Savage et al., 2002; Visram et al., 2006). In the present study, we found that *A. rustica* and *A. sulcata* collected from 0.8 m depth hosted comparable numbers of zooxanthellae. Moreover, the amounts of the photosynthetic pigments chlorophyll *a*, *c* and peridinin per symbiont cell were similar. Bleaching of *Anemonia* spp. was caused by a loss of zooxanthellae. The individual content of the photosynthetic pigments of the algal cells remaining in the tissue was unchanged in the affected animals. This type of bleaching is also often found in scleractinian corals (Brown et al., 1995; Brown 1997). A release of zooxanthellae from *A. sulcata* was previously observed as a response to experimental heat stress (Miller et al., 1992; Richier et al., 2006). The individual degree of bleaching was comparable between non-fluorescent *A. rustica* and fluorescent *A. sulcata*. Contrastingly, some fluorescent corals showed enhanced resistance to bleaching during periods of heat stress (Salih et al., 2000, 2006). In yet another case, several color morphs of *Acropora aspera* containing GFP-like proteins were found to be more susceptible to thermal bleaching (Dove, 2004).

Most interestingly, the content of green fluorescent pigments was significantly reduced in bleached animals of *A. sulcata* var. *smaragdina*. This indicates that the loss of zooxanthellae is not exclusively responsible for the bleached appearance of the affected animals. Given the otherwise constitutive expression of the green fluorescent pigments in *A. sulcata*, the dramatical drop

in the pigment level reflects major derangements of physiological processes within the animals. It remains to be evaluated if the decreased contents of host pigments are a cause or a consequence of the loss of zooxanthellae.

4.2. Analysis of mycosporine-like amino acids

MAAs act as UV-screening compounds in many marine cnidarians including sea anemones (Dunlap and Shick, 1998). The tissue content is often positively correlated with the radiation intensity in the habitat (Shick et al., 1995). Methanolic tissue extract of *Anemonia* spp. showed an absorption maximum at 334 nm, pointing to the presence of the MAAs Porphyra-334 or Shinorine (Stochaj et al., 1994). These MAAs were previously identified in another sea anemone *Anthopleura elegantissima* (Stochaj et al., 1994). The animals from the studied habitat were all collected from 0.8 m depth and, therefore, experienced the same light climate. Nevertheless, *A. sulcata* showed MAA levels significantly increased by ~17% as compared to *A. rustica*. Bleached and non-bleached representatives of both species were characterized by comparable MAA levels. Therefore, a reduced MAA content can be likely excluded as cause for the bleaching.

The increased MAA levels in the fluorescent anemones might also contribute to the increased fitness of *A. sulcata* in shallow water (Wiedenmann et al., 1999, 2007). Similar to the present case, the green fluorescent morph of the reef coral *Porites asteroides* showed higher MAA levels in shallow water as compared to the non-fluorescent counterpart (Gleason, 1993).

4.3. Analysis of anti-oxidant enzymes

Under stressful conditions, anthozoans are confronted with cellular damage due to increased levels of reactive oxygen species (ROS) (Lesser and Shick, 1989; Downs et al., 2002; Tchernov et al., 2004; Smith et al., 2005). A particular role is attributed to H_2O_2. In contrast to other ROS, this molecule shows a relatively long lifetime and can cross organelle and cell borders by diffusion (Downs et al., 2002; Smith et al., 2005). The animals defend themselves against oxidative stress by a set of anti-oxidant enzymes including SODs, PODs and CATs. Experimentally increased water temperatures induced oxidative stress and release of zooxanthellae also in *A. sulcata* (Miller et al., 1992; Richier et al., 2006). The presence of the anti-oxidant enzymes SOD, CAT and glutathione POD was detected by immunocytochemical and functional tests in both, host and symbiont cells of *A. sulcata* (Hawkridge et al., 2000; Richier et al., 2003).

We compared the activity of the anti-oxidant enzymes SOD, POD and CAT from tentacle tissue of both, *A. rustica* and *A. sulcata* var. *smaragdina* after size fractionation of tissue extracts by gel filtration. SOD activity was detected in fractions containing proteins with apparent molecular weights of $\sim$ 170, 72.9, 33.0 and 14.3 kDa. Seven distinct SOD isoforms were already detected in the tissue of *A. sulcata* (=*A. viridis*) (Plantivaux et al., 2004; Richier et al., 2003). We found the major SOD activity to be caused by a $\sim$ 33 kDa protein. Minor amounts of SOD activity were found in fraction 25 containing also GFP-like pigments. However, the elution maximum of the SOD activity is shifted compared to the GFP peak. Consequently, under the present assay conditions, it appears unlikely that the GFP-like proteins in *Anemonia* sp. possess a significant SOD activity as suggested previously for GFP from *A. victoria* (Bou-Abdallah et al., 2006). Also, the major POD and CAT activities were found in fractions distinct from those containing the GFP-like host pigments.

Regarding the SOD, POD, and CAT activities, the non-significant differences between the unbleached representatives of the two species suggest a similar sensitivity of fluorescent and non-fluorescent *Anemonia* spp. to oxidative stress.

The average SOD activity was increased by a factor >2 in bleached individuals of each species. However, significant differences could only be detected between bleached and non-bleached representatives of *A. rustica*. An increase of the SOD activity by $\sim$ 20% was observed in the ectodermal tissue of *A. sulcata* after 24 h exposure to experimentally raised water temperatures (Richier et al., 2005).

We found that the level of CAT activity was significantly lowered in bleached individuals. Elevated H_2O_2 can mediate exocytosis of zooxanthellae via a mitogen-activated protein kinase signalling cascade (Smith et al., 2005). In the present case, the reduced CAT activity could have resulted in increased cellular H_2O_2 levels and, subsequently, exocytosis of the symbiotic algae. Merle et al. (2006) already demonstrated that an experimental inhibition of CAT results in bleaching of *A. sulcata* (=*A. viridis*). Therefore, the reduced CAT activity might be considered a direct cause for the observed bleaching among a natural sea anemone population.

Due to the micro-climate of the studied Mediterranean habitat, *Anemonia* spp. can experience higher water temperatures in comparison to the more exposed sites located nearby. During calm summer days, temperatures that cause the release of zooxantellae might have been reached (Miller et al., 1992; Richier et al., 2006). However, bleached anemones were always found in close proximity of non-bleached individuals, suggesting a reason affecting the animals more on the individual level, for example infections with microbes (Kushmaro et al., 1998).

5. Conclusions

The differences in the tentacle color of the two sea anemone species *A. sulcata* and *A. rustica* are due to altered expression levels of the asFP499 and asulCP genes. Bleaching of *Anemonia* spp. proceeds in the field via the loss of zooxanthellae. In bleached *A. sulcata*, also the level of green fluorescent host pigments was reduced. On the individual level, both *Anemonia* species were affected to the same extent by the loss of zooxanthellae. Therefore, the GFP-like proteins of *A. sulcata* did not offer protection from bleaching in the present case. However, to deduce further conclusions on the function of the host pigments, the exact reasons for bleaching of *Anemonia* spp. in the field remain to be elucidated.

Acknowledgements

References

Andres, A., 1881. Prodromus neapolitanae actiniarum faunae. Mitt. Zool. Stn. Neapel 2, 305–317.

Banin, E., Vassilakos, D., Orr, E., Martinez, R.J., Rosenberg, E., 2003. Superoxide dismutase is a virulence factor produced by the coral bleaching pathogen *Vibrio shiloi*. Curr. Microbiol. 46, 418–422.

Ben-Haim, Y., Thompson, F.L., Thompson, C.C., Cnockaert, M.C., Hoste, B., Swings, J., Rosenberg, E., 2003. *Vibrio coralliilyticus* sp. nov., a temperature-dependent pathogen of the coral *Pocillopora damicornis*. Int. J. Syst. Evol. Microbiol. 53, 309–315.

Blum, H., Beier, H., Gross, J., 1987. Improved silver staining of plant proteins, RNA and DNA in polyacrylamide gels. Electrophoresis 8, 93–99.

Bou-Abdallah, F., Chasteen, N.D., Lesser, M.P., 2006. Quenching of superoxide radicals by green fluorescent protein. Biochim. Biophys. Acta 1760, 1690–1695.

Brown, B.E., 1997. Coral bleaching: causes and consequences. Coral Reefs 16, 129–138.

Brown, B.E., Le Tissier, M.D.A., Bythell, J.C., 1995. Mechanisms of bleaching deduced from histological studies of reef corals during a natural bleaching event. Mar. Biol. 122, 655–663.

Brown, B.E., Dunne, R., Goodson, M., Douglas, A., 2002. Experience shapes the susceptibility of a reef coral to bleaching. Coral Reefs 21, 119–126.

Bulnheim, H.P., Sauer, K.P., 1984. *Anemonia sulcata*-zwei Arten? Genetische und ökologische Evidenz. Verh. Dtsch. Zool. Ges. 77, 264.

Burkenroad, M.D., 1943. A possible function of bioluminescence. J. Mar. Res. 5, 161–164.

Coles, S.L., Jokiel, P.L., 1978. Synergistic effects of temperature, salinity and light on the hermatypic coral *Montipora verrucosa*. Mar. Biol. 49, 187–195.

Coles, S., Brown, B., 2003. Coral bleaching — capacity for acclimatization and adaptation. Adv. Mar. Biol. 46, 183–223.

Cox, G., Salih, A., 2006. Confocal microscopy of GFP-like pigments in corals. In: Yu, H., Cheng, P.C., Lin, P.C., Kao, F.J. (Eds.), Multimodal Microscopy. World Scientific Publishing, Singapore, pp. 238–245.

Cox, G., Matz, M., Salih, A., 2006. Fluorescence lifetime imaging of coral fluorescent proteins. Microsc. Res. Tech. 70, 243–251.

Dove, S.G., 2004. Scleractinian corals with photoprotective host pigments are hypersensitive to thermal bleaching. Mar. Ecol. Prog. Ser. 272, 99–116.

Dove, S.G., Hoegh-Guldberg, O., Ranganathan, S., 2001. Major colour patterns of reefbuilding corals are due to a family of GFP-like proteins. Coral Reefs 19, 197–204.

Downs, C.A., Fauth, J.E., Halas, J.C., Dustan, P., Bemiss, J., Woodley, C.M., 2002. Oxidative stress and seasonal coral bleaching. Free Radic. Biol. Med. 33, 533–543.

Dunlap, W.C., Shick, J.M., 1998. Ultraviolet radiation-absorbing mycosporine-like amino acids in coral reef organisms: a biochemical and environmental perspective. J. Phycol. 34, 418–430.

Field, S.F., Bulina, M.Y., Kelmanson, I.V., Bielawski, J.P., Matz, M.V., 2006. Adaptive evolution of multicolored fluorescent proteins in reef-building corals. J. Mol. Evol. 62, 332–339.

Fitt, W.K., Brown, B.E., Warner, M.E., Dunne, R.P., 2001. Coral bleaching: interpretation of thermal tolerance limits and thermal thresholds in tropical corals. Coral Reefs 20, 51–65.

Gagnon, M., Hunting, W.M., Esselen, W.B., 1959. New method of catalase determination. Anal. Chem. 31, 144–145.

Gates, R.D., Baghdasarian, G., Muscatine, L., 1992. Temperature stress causes host cell detachment in symbiotic cnidarians: implications for coral bleaching. Biol. Bull. 182, 324–332.

Gilmore, A.M., Larkum, A.W.D., Salih, A., Itoh, S., Shibata, Y., Bena, C., Yamasaki, H., Papina, M., van Woesik, R., 2003. Simultaneous time resolution of the emission spectra of fluorescent proteins and zooxanthellar chlorophyll in reef-building corals. Photochem. Photobiol. 77, 515–523.

Gleason, D.F., 1993. Differential effects of ultraviolet radiation on green and brown morphs of the Carribean coral *Porites astreoides*. Limnol. Oceanogr. 38, 1452–1463.

Glynn, P.W., 1984. Widespread coral mortality and the 1982/83 El Niño warming event. Environ. Conserv. 11, 133–146.

Glynn, P.W., 1993. Coral-reef bleaching — ecological perspectives. Coral Reefs 12, 1–17.

Glynn, P.W., D'Croz, L., 1990. Experimental evidence for high temperature stress as the cause of El Niño-coincident coral mortalities. Coral Reefs 8, 181–191.

Goreau, T.E., 1964. Mass expulsion of zooxanthellae from Jamaican reef communities after Hurricane Elora. Science 145, 383–386.

Goreau, T.J., Hayes, R.L., 1994. Coral bleaching and ocean 'hot spots'. Ambio 23, 176–180.

Gosse P.H., (ed.) 1860. Actinologia Britannica: a history of the british sea-anemones and corals. Van Voorst, Paternoster Row London.

Haddock, S.H.D., Dunn, C.W., Pugh, P.R., Schnitzler, C.E., 2005. Bioluminescent and red-fluorescent lures in a deep-sea siphonophore. Science 309, 263.

Harvell, C.D., Kim, K., Burkholder, J.M., Colwell, R.R., Epstein, P.R., Grimes, D.J., Hofmann, E.E., Lipp, E.K., Osterhaus, A.D.M.E., Overstreet, R.M., Porter, J.W., Smith, G.W., Vasta, G.R., 1999. Emerging marine diseases — climate links and anthropogenic factors. Science 285, 1505–1510.

Hawkridge, J.M., Pipe, R.K., Brown, B.E., 2000. Localization of antioxidant enzymes in the cnidarians *Anemonia viridis* and *Goniopora stokesi*. Mar. Biol. 137, 1–9.

Jeffrey, S.W., Humphrey, G.F., 1975. New spectrophotometric equations for determining chlorophylls a, b, c_1 and c_2 in higher plants, algae and natural phytoplankton. Biochem. Physiol. Pflanzen 167, 191–194.

Kawaguti, S., 1944. On the physiology of reef corals VI. Study on the pigments. Palao Trop. Biol. Stn. Stud. 2, 617–674.

Kawaguti, S., 1969. Effect of the green fluorescent pigment on the productivity of reef corals. Micronesia 5, 313.

Kelmanson, I.V., Matz, M.V., 2003. Molecular basis and evolutionary origins of color diversity in great star coral *Montastraea cavernosa* (Scleractinia: Faviida). Mol. Biol. Evol. 20, 1125–1133.

Kleppel, G.S., Dodge, R.E., Reese, C.J., 1989. Changes in pigmentation associated with the bleaching of stony corals. Limnol. Oceanogr. 34, 1331–1335.

Kushmaro, A., Loya, Y., Fine, M., Rosenberg, E., 1996. Bacterial infection and coral bleaching. Nature 380, 396.

Kushmaro, A., Rosenberg, E., Fine, M., Loya, Y., 1997. Bleaching of the coral *Oculina patagonica* by *Vibrio* AK-1. Mar. Ecol. Prog. Ser. 147, 159–165.

Kushmaro, A., Rosenberg, E., Fine, M., Ben-Haim, Y., Loya, Y., 1998. Effect of temperature on bleaching of the coral *Oculina patagonica* by Vibrio AK-1. Mar. Ecol. Prog. Ser. 171, 131–137.

Labas, Y.A., Gurskaya, N.G., Yanushevich, Y.G., Fradkov, A.F., Lukyanov, K.A., Lukyanov, S.A., Matz, M.V., 2002. Diversity and evolution of the green fluorescent protein family. Proc. Natl. Acad. Sci. U.S.A. 99, 4256–4261.

Laemmli, K., 1970. Cleavage of structural proteins during the assembly of the head of bacteriophage T4. Nature 227, 680–685.

Lesser, M.P., 1996. Exposure of symbiotic dinoflagellates to elevated temperatures and ultraviolet radiation causes oxidative stress and inhibits photosynthesis. Limnol. Oceanogr. 41, 271–283.

Lesser, M.P., 1997. Oxidative stress causes coral bleaching during exposure to elevated temperatures. Coral Reefs 16, 187–192.

Lesser, M.P., Shick, J.M., 1989. Effects of irradiance and ultraviolet radiation on photoadaptation in the zooxanthellae of *Aiptasia pallida*: primary production, photoinhibition, and enzymic defenses against oxygen toxicity. Mar. Biol. 102, 243–255.

Lesser, M.P., Stochaj, W.R., Tapley, D.W., Shick, J.M., 1990. Bleaching in coral reef anthozoans: effects of irradiance, ultra-violet radiation, and temperature on the activities of protective enzymes against active oxygen. Coral Reefs 8, 225–232.

Leutenegger, A., D'Angelo, C., Matz, M.V., Denzel, A., Oswald, F., Salih, A., Nienhaus, G.U., Wiedenmann, J. 2007. It's cheap to be colorful: Anthozoans show a slow turnover of GFP-like proteins. FEBS J. 274, 2496–2505.

Louis, C., 1960. Modalités et déterminisme expérimental de la scissiparité chez l'actinie *Anemonia sulcata*. C. R. hebd Séances Acad Sci, Paris 251, 134–136.

Lukyanov, K.A., Fradkov, A.F., Gurskaya, N.G., Matz, M.V., Labas, Y.A., Savitsky, A.P., Markelov, M.L., Zaraisky, A.G., Zhao, X., Fang, Y., Tan, W., Lukyanov, S.A., 2000. Natural animal coloration can be determined by a nonfluorescent green fluorescent protein homolog. J. Biol. Chem. 275, 25879–25882.

Martynov, V.I., Savitsky, A.P., Martynova, N.Y., Savitsky, P.A., Lukyanov, K.A., Lukyanov, S.A., 2001. Alternative cyclization in GFP-like proteins family. The formation and structure of the chromophore of a purple chromoprotein from *Anemonia sulcata*. J. Biol. Chem. 276, 21012–21016.

Matz, M.V., Fradkov, A.F., Labas, Y.A., Savitsky, A.P., Zaraisky, A.G., Markelov, M.L., Lukyanov, S.A., 1999. Fluorescent proteins from

nonbioluminescent Anthozoa species. Nat. Biotechnol. 17, 969–973.

Matz, M.V., Labas, Y.A., Ugalde, J., 2005. Evolution of functions and color in GFP-like proteins. In Green Fluorescent Protein: Properties, Applications and Protocolls, In: Chalfie, M., Kain, S.R. (Eds.), 2nd ed. Wiley-Liss, New York, pp. 110–129.

Mazel, C.H., Lesser, M.P., Gorbunov, M.Y., Barry, T.M., Farrell, J.H., Wyman, K.D., Falkowski, P.G., 2003. Green-fluorescent proteins in Caribbean corals. Limnol. Oceanogr. 48, 402–411.

Merle, P.L., Sabourault, C., Richier, S., Allemand, D., Furla, P., 2006. Catalase characterization and implication in bleaching of a symbiotic sea anemone. Free Radic. Biol. Med. doi:10.1016/j.freeradbiomed. 2006.10.038.

Miller, D., Brown, B.E., Sharp, V.A., Nganro, N., 1992. Changes in the expression of soluble proteins extracted from the symbiotic anemone *Anemonia viridis* accompany bleaching induced by hyperthermia and metal stressors. J. Therm. Biol. 17, 217–223.

Morin, J.G., 1974. Coelenterate bioluminescence. In: Muscatine, L., Lenhoff, H. (Eds.), Coelenterate biology: reviews and new perspectives. Academic Press, New York, pp. 397–438.

Muller-Parker, G., 1985. Effect of feeding regime and irradiance on the photophysiology of the symbiotic sea anemone *Aiptasia pulchella*. Mar. Biol. 90, 65–74.

Muscatine, L., Grossman, D., Doino, J., 1991. Release of symbiotic algae by tropical sea anemones and corals after cold shock. Mar. Ecol. Prog. Ser. 77, 233–243.

Nienhaus, K., Renzi, F., Vallone, B., Wiedenmann, J., Nienhaus, G.U., 2006. Chromophore–protein interactions in the anthozoan green fluorescent protein asFP499. Biophys J. 91, 4210–4220.

Oswald, F., Schmitt, F., Leutenegger, A., Ivanchenko, S., D'Angelo, C., Salih, A., Maslakova, S., Bulina, M., Nienhaus, G.U., Matz, M.V., Wiedenmann, J., 2007. Contributions of host and symbiont pigments to the coloration of reef corals. FEBS J. 274, 1102–1122.

Plantivaux, A., Furla, P., Zoccola, D., Garello, G., Forcioli, D., Richier, S., Merle, P.L., Tambutté, E., Tambutté, S., Allemand, D., 2004. Molecular characterization of two Cu–Zn superoxide dismutases in a sea anemone. Free Radic. Biol. Med. 37, 1170–1181.

Pohjanvirta, R., Niittynen, M., Linden, J., Boutros, P.C., Moffat, I.D., Okey, A.B., 2006. Evaluation of various housekeeping genes for their applicability for normalization of mRNA expression in dioxin-treated rats. Chem. Biol. Interact. 160, 134–149.

Prasher, D.C., Eckenrode, V.K., Ward, W.W., Prendergast, F.G., Cormier, M.J., 1992. Primary structure of the *Aeqourea victoria* green fluorescent protein. Gene 111, 229–233.

Pockley, P., 1999. Global warming could kill most coral reefs by 2100. Nature 400, 98.

Pockley, P., 2000. Global warming identified as main threat to coral reefs. Nature 407, 932.

Richier, S., Merle, P.L., Furla, P., Pigozzi, D., Sola, F., Allemand, D., 2003. Characterization of superoxide dismutases in anoxia- and hyperoxia-tolerant symbiotic cnidarians. Biochim. Biophys. Acta 1621, 84–91.

Richier, S., Furla, P., Plantivaux, A., Merle, P.L., Allemand, D., 2005. Symbiosis-induced adaptation to oxidative stress. J. Exp. Biol. 208, 277–285.

Richier, S., Sabourault, C., Courtiade, J., Zucchini, N., Allemand, D., Furla, P., 2006. Oxidative stress and apoptotic events during thermal stress in the symbiotic sea anemone, Anemonia viridis. FEBS J. 273, 4186–4198.

Rodolfo-Metalpa, R, Richard, C., Allemand, D., Bianchi, C.N., Morri, C., Ferrier-Pagès, C., 2006. Response of zooxanthellae in symbiosis with the Mediterranean corals *Cladocora caespitosa*

and *Oculina patagonica* to elevated temperatures. Mar. Biol. 150, 45–55.

Salih, A., Hoegh-Guldberg, O., Cox, G., 1998. Photoprotection of symbiotic dinoflagellates by fluorescent pigments in reef corals. In: Greenwood, Hall (Ed.), Proc Aust Coral Reef Society, vol. 75, pp. 217–230. Anniv Conference.

Salih, A., Larkum, A., Cox, G., Kühl, M., Hoegh-Guldberg, O., 2000. Fluorescent pigments in corals are photoprotective. Nature 408, 850–853.

Salih, A., Cox, G., Coles, S., Baird, A., Dunstan, A., Mills, J., Larkum, A.W.D., 2006. Role of coral host-based fluorescent pigments in reducing coral bleaching stress. 2004 10th International Coral Reef Symposium. Okinawa, Japan. 12 pages.

Savage, A.M., Goodson, M.S., Visram, S., Trapido-Rosenthal, H., Wiedenmann, J., Douglas, A.E., 2002. Molecular diversity of symbiotic algae at the latitudinal margins of their distribution: dinoflagellates of the genus *Symbiodinium* in corals and sea anemones. Mar. Ecol. Prog. Ser. 244, 17–26.

Schlichter, D., Fricke, H.W., Weber, W., 1986. Light harvesting by wavelength transformation in a symbiotic coral of the Red Sea twilightzone. Mar. Biol. 91, 403–407.

Shagin, D.A., Barsova, E.V., Yanushevich, Y.G., Fradkov, A.F., Lukyanov, K.A., Labas, Y.A., Semenova, T.N., Ugalde, J.A., Meyers, A., Nunez, J.M., Widder, E.A., Lukyanov, S.A., Matz, M.V., 2004. GFP-like proteins as ubiquitous metazoan superfamily: evolution of functional features and structural complexity. Mol. Biol. Evol. 5, 841–850.

Shick, J.M., Dykens, J.A., 1985. Oxygen detoxification in algal–invertebrate symbioses from the Great Barrier Reef. Oecologia 66, 33–41.

Shick, J.M., Lesser, M.P., Dunlap, W.C., Stochaj, W.R., 1995. Depth-dependent responses to solar ultraviolet radiation and oxidative stress in the zooxanthellate coral *Acropora microphthalma*. Mar. Biol. 122, 41–51.

Smith, D.J., Suggett, D.J., Baker, N.R., 2005. Is photoinhibition of zooxanthellae photosynthesis the primary cause of thermal bleaching in corals? Glob. Chang. Biol. 11, 1–11.

Stochaj, W.R., Dunlap, W.C., Shick, J.M., 1994. Two new UV-absorbing mycosporine-like amino acids from the sea anemone *Anthopleura elegantissima* and the effects of zooxanthellae and spectral irradiance on chemical composition and content. Mar. Biol. 118, 149–156.

Stone, L., Huppert, A., Rajagopalan, B., Bhasin, H., Loya, Y., 1999. Mass coral reef bleaching: a recent outcome of increased El Niño activity? Ecol. Lett. 2, 325–330.

Tchernov, D., Gorbunov, M.Y., de Vargas, C., Yadav, S.N., Milligan, A.J., Häggblom, M., Falkowski, P.G., 2004. Membrane lipids of symbiotic algae are diagnostic of sensitivity to thermal bleaching in corals. Proc. Natl. Acad. Sci. U.S.A. 101, 13531–13535.

Ugalde, J.A., Chang, B.S., Matz, M.V., 2004. Evolution of coral pigments recreated. Science 305, 1433.

Visram, S., Wiedenmann, J., Douglas, A.E., 2006. Molecular diversity of symbiotic algae Symbiodinium (Zooxanthellae) in Cnidarians of the Mediterranean Sea. J. Mar. Biol. Assoc. UK 86, 1281–1283.

Wiedenmann, J., 1997. Die Anwendung eines orange fluoreszierenden Proteins und weiterer farbiger Proteine und der zugehörenden Gene aus der Artengruppe *Anemonia* sp. (*sulcata*) Pennant, (Cnidaria, Anthozoa, Actinaria) in Gentechnologie und Molekularbiologie. Offenlegungsschrift DE 197 18 640 A1. Deutsches Patent-und Markenamt, pp 1–18.

Wiedenmann, J., Röcker, C., Funke, W., 1999. The morphs of *Anemonia* aff. *sulcata* (Cnidaria, Anthozoa) in particular consideration of the

ectodermal pigments. In: Pfadenhauer, J. (Ed.), Verhandlungen der Gesellschaft für Ökologie, Band, vol. 29. Spektrum Akademischer Verlag, Heidelberg Berlin, pp. 497–503.

Wiedenmann, J., Kraus, P., Funke, W., Vogel, W., 2000a. The relationship between different morphs of *Anemonia sulcata* PENNANT (Anthozoa, Actinaria) evaluated by DNA fingerprinting. Ophelia 52, 57–64.

Wiedenmann, J., Elke, C., Spindler, K.D., Funke, W., 2000b. Cracks in the β-can: fluorescent proteins from *Anemonia sulcata*. Proc. Natl. Acad. Sci. U.S.A. 97, 14091–14096.

Wiedenmann, J., Elke, C., Spindler, K.D., Funke, W., 2002a. Correction for vol. 97, pp 14091–14096. Proc. Natl. Acad. Sci. U.S.A. 99, 13357, 2002.

Wiedenmann, J., Schenk, A., Röcker, C., Girod, A., Spindler, K.D., Nienhaus, G.U., 2002b. A far-red fluorescent protein with fast maturation and reduced oligomerization tendency from Entacmaea quadricolor (Cnidaria, Anthozoa, Actinaria). Proc. Natl. Acad. Sci. 99, 11646–11651.

Wiedenmann, J., Ivanchenko, S., Oswald, F., Nienhaus, G.U., 2004. Identification of GFP-like proteins in non-bioluminescent, azoox-anthellate Anthozoa opens new perspectives for bioprospecting. Mar. Biotechnol. 6, 270–277.

Wiedenmann, J., Leutenegger, A., Gundel, S., Schmitt, F., D'Angelo, C., Funke, W., 2007. Long-term monitoring of space competition among fluorescent and nonfluorescent sea anemones in the Mediterranean Sea. J. Mar. Biol. Assoc. UK. 87, 851–852.

Wilmann, P.G., Petersen, J., Devenish, R.J., Prescott, M., Rossjohn, J., 2005. Variations on the GFP chromophore: a polypeptide fragmentation within the chromophore revealed in the 2.1-A crystal structure of a nonfluorescent chromoprotein from *Anemonia sulcata*. J. Biol. Chem. 280, 2401–2404.

Wilson, W.H., Francis, I., Ryan, K., Davy, K., 2001. Temperature induction of viruses in symbiotic dinoflagellates. Aquat. Microb. Ecol. 25, 99–102.

Long-term monitoring of space competition among fluorescent and nonfluorescent sea anemones in the Mediterranean Sea

Jörg Wiedenmann*‡, Alexandra Leutenegger*, Silke Gundel*, Florian Schmitt*, Cecilia D'Angelo* and Werner Funke†

*Institute of General Zoology and Endocrinology, University of Ulm, 89069 Ulm, Germany.
†Institute of Experimental Ecology, University of Ulm, 89069 Ulm, Germany.
‡Corresponding author, e-mail: joerg.wiedenmann@uni-ulm.de

The competition for space among fluorescent and nonfluorescent *Anemonia* species was monitored in the Mediterranean Sea in order to see whether the fluorescent species *A. sulcata* var. *smaragdina* was a better competitor in shallow water habitats. Over a period of 11 years, *A. sulcata* var. *smaragdina* convincingly out competed the nonfluorescent *A. rustica*. We thereby found support for the notion that the GFP-like pigments may increase competitive ability in anthozoans.

Many sea anemones, such as *Anemonia sulcata* (= *A. viridis*), use acrorhagi when competing for space (Francis, 1973; Ayre, 1982; Bigger, 1980; Sauer, 1986; Wiedenmann, 2000). These globular structures, located directly beneath the tentacles and loaded with nematocysts, are used in inter- and intraspecific aggression to sting the opponent (Figure 1). In such fights, the subordinate animal retreats. *Anemonia* spp. inhabit the rocky shores of the Mediterranean Sea and all the south-west coasts of Europe, with a northern distribution limit in mid-Scotland (Schmidt, 1972; Manuel, 1988). Due to light dependent symbiosis with zooxanthellae, *Anemonia* spp. are most abundant in shallow water, but can be found at depths of 25 m (Schmidt, 1972; Manuel, 1988). In depths down to 5 m, *Anemonia* spp. form large clones by asexual reproduction due to longitudinal fission (Louis, 1960; Wiedenmann et al., 2000a). Because their muscles are only weakly developed, species such as *A. sulcata* need to shelter in rock crevices to resist the wave action of their habitats (Schmidt, 1972; Manuel, 1988). Consequently, the risk of dislodgement and drift increases, if individuals are excluded from this preferred environment due to inter- or intraspecific aggression (Francis, 1973; Sauer & Füller, 1988).

The colour of different morphs of *Anemonia sulcata* is due to the different fluorescent and nonfluorescent protein pigment homologues of the green fluorescent protein (GFP) that is found in *Aequorea victoria* (Wiedenmann, 1997; Wiedenmann et al., 1999, 2000b). A photoprotective function has been suggested for these GFP-like pigments (Wiedenmann et al., 1999; Salih et al., 2000). In order to evaluate whether pigmented sea anemones possess a selective advantage in a bright light habitat, the competition for space between green fluorescent *Anemonia sulcata* var. *smaragdina* (Gosse, 1860; Wiedenmann et al., 1999) and nonfluorescent *A. rustica* (Bulnheim & Sauer, 1984; Wiedenmann et al., 1999) was monitored over 11 years in a shallow-water habitat in Le Dramont, France (Figure 2). The studied area was a sun-exposed rocky slope that extended from 0.5 to 2 m depth. The population of the anemones was restricted to this area by a quay wall (0–0.5 m depth) and by the sandy bottom (>2.0 m depth). The area of possible colonization was approximately 15 m². The first observation of colonization of the habitat was made in 1994 and consisted of 13 *A. rustica*. Over a period of four years, this number of individuals increased markedly to 209 with highest densities at a depth of 0.5–1.0 m. By 1998, a considerable number (137) of *A. sulcata* var. *smaragdina* had settled in depths between 1.0 and 2.0 m, with most individuals found at depths from 1.0 to 1.5 m. The formation of dense distinct clusters of each

species indicated that the increases in their populations were due to clone formation by asexual reproduction, because direct contact between individuals is only tolerated if the animals share the same genotype (Sauer, 1986; Wiedenmann, 2000). By 2002, the habitat was overrun almost completely by *A. sulcata* var. *smaragdina*. The population of *A. rustica* no longer increased and animals were settled mainly at depths from 1.0 to 2.0 m. A small increase in the number of *A. rustica* was again observed in 2005, due to the formation of a daughter colony away from the major area of settlement. By 2005, the colony of *A. sulcata* var. *smaragdina* consisted of 1281 individuals. The average wet weight of an individual member of each species from Mediterranean habitats was about 30 ±11 g (Wiedenmann, 1996). Therefore, the sea anemone biomass (wet weight) in 2005 in the studied habitat was about 38.5 kg for *A. sulcata* var. *smaragdina* and 3.4 kg for *A. rustica*. The rate of growth of the population of *A. sulcata* var. *smaragdina* was exponential, with a doubling time of approximately two years. However, the rate of increase in the population observed over the first four years suggests that the anemones divided at least once a year. These results indicate that individuals of *A. sulcata* var. *smaragdina* have increased fitness when competing for space in sun-exposed shallow-water habitats. The

Figure 1. Acrorhagial fighting among *Anemonia* sp. Members of *A. sulcata* (left) and *A. rustica* (right) were brought into direct contact. The dominant *A. sulcata* retracted its tentacles on the side facing the opponent, inflated the acrorhagi (arrow) and is ready to sting the combatant by bending its body.

852 J. Wiedenmann et al.   *Space competition of sea anemones*

data are in good agreement with the observations of Sauer (1986), who reported that pigmented individuals of *A. sulcata* from shallow-water habitats (1.0–4.0 m) in Banyuls, France, were dominant in experimental acrorhagial fights against *A. rustica* obtained from the same depth. In contrast, coloured anemones collected from depths greater than 4 m lost experimental battles against *A. rustica* obtained from the same depth. Moreover, the enhanced fitness of fluorescent *A. sulcata* var. *smaragdina* in shallow water is consistent with the observations that the fluorescent morphs *viridis* and *rufescence* of this species show maximal abundance close to the surface in other locations (Wiedenmann et al., 1999).

The correlation of enhanced fitness of *A. sulcata* in bright light habitats and the expression of GFP-like proteins in the tentacles could be interpreted as support for the view that these pigments have a photoprotective function. However, the enhanced fitness might be as well mediated by other variable components of the photoprotection system such as ultraviolet light-protectant mycosporine-like amino acids or various antioxidant enzymes (Shick, 1991; Furla et al., 2005). Therefore, further studies are required to establish the role of GFP-like pigments in the defence of sea anemones against the detrimental effects of sunlight.
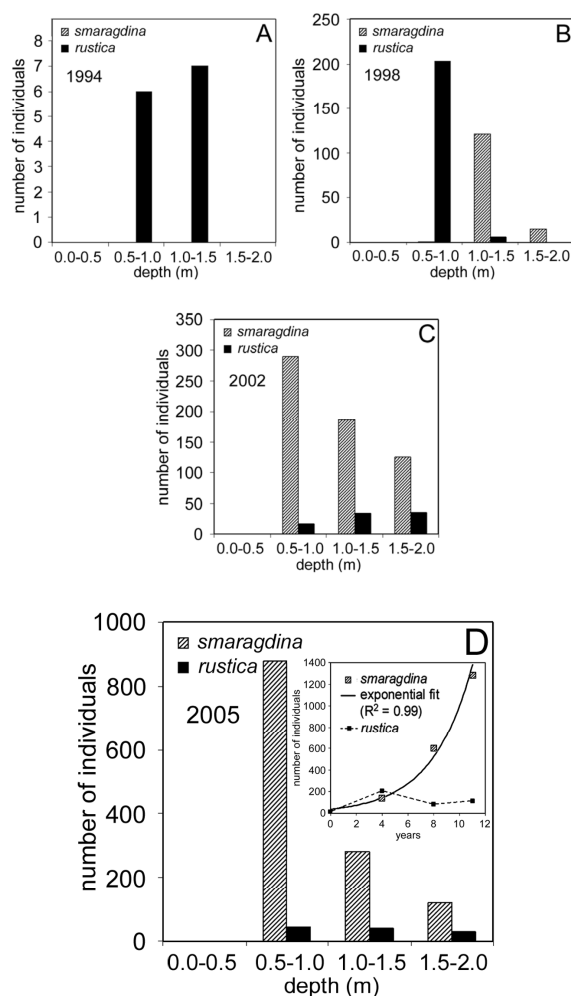

Figure 2. Competition for space among *Anemonia sulcata* var. *smaragdina* (*smaragdina*) and *A. rustica* (*rustica*) monitored in a shallow-water habitat in Le Dramont, France. (A–D) show the changes in population size and depth distributions of the two species. The inset in D shows the time-dependent increase in the number of individuals.

REFERENCES

Ayre, D.J., 1982. Inter-genotype aggression in the solitary sea anemone *Actinia tenebrosa*. *Marine Biology*, **68**, 199–205.

Bigger, C.H., 1980. Interspecific and intraspecific acrorhagial aggressive behavior among sea anemones: a recognition of self and not-self. *Biological Bulletin. Marine Biological Laboratory, Woods Hole*, **159**, 117–134.

Bulnheim, H.-P. & Sauer, K.P., 1984. *Anemonia sulcata* - two species? Genetical and ecological evidence. *Verhandlungen der Deutschen Zoologische Gesellschaft*, **77**, 264.

Francis, L., 1973. Intraspecific aggression and its effect on the distribution of *Anthopleura elegantissima* and some related sea anemones. *Biological Bulletin. Marine Biological Laboratory, Woods Hole*, **144**, 73–92.

Furla, P., Allemand, D., Shick, J.M., Ferrier-Pagès, C., Richier, S., Plantivaux, A., Merle, P.L. & Tambutté, S., 2005. The symbiotic anthozoan: a physiological chimera between alga and animal. *Integrative and Comparative Biology*, **45**, 595–604.

Gosse, P.H., 1860. *A history of the British sea-anemones and corals*. London: Van Voorst, Paternoster Row.

Louis, C., 1960. Modalité et déterminisme expérimental de la scissiparité chez l'actinie *Anemonia sulcata* PENNANT. *Comptes Rendus Hebdomaire de l'Académie des Sciences, Paris*, **251**, 134–136.

Manuel, R.L., 1988. *British Anthozoa. Synopses of the British fauna (New Series)* (ed. D.M. Kermack and R.S.K. Barnes), pp. 102–103. London: Brill & Backhuys.

Salih, A., Larkum, A., Cox, G., Kühl, M. & Hoegh-Guldberg, O., 2000. Fluorescent pigments in corals are photoprotective. *Nature, London*, **408**, 850–853.

Sauer, K.P., 1986. Strategies in generating temporally and spatially different niches. *Verhandlungen der Deutschen Zoologische Gesellschaft*, **79**, 11–30.

Sauer, K.P. & Füller, M., 1988. Reproductive strategies and differential predictability of environmental conditions. *Verhandlungen der Deutschen Zoologische Gesellschaft*, **81**, 260.

Schmidt, H., 1972. Prodromus zu einer Monographie der mediterranen Aktinien. In *Zoologica*. Vol. 42(2) (ed. F. Schaller). Stuttgart: E. Schweizerbart'sche Verlagsbuchhandlung (Nägele u. Obermiller).

Shick, J.M., 1991. *A functional biology of sea anemones*. London: Chapman & Hall.

Wiedenmann, J., 1996. *Zur Biologie der Ökotypen von* Anemonia sulcata *(PENNANT)*. Diploma thesis, University of Ulm, Germany.

Wiedenmann, J., 1997. *Die Anwendung eines orange fluoreszierenden Proteins und weiterer farbiger Proteine und der zugehörenden Gene aus der Artengruppe* Anemonia sp. *(*sulcata*) Pennant, (Cnidaria, Anthozoa, Actinaria) in Gentechnologie und Molekularbiologie*. Offenlegungsschrift DE 197 18 640 A1, Deutsches Patent- und Markenamt, 1–18.

Wiedenmann, J., 2000. *The identification of new proteins homologous to GFP from* Aequorea victoria *as coloring compounds in the morphs of* Anemonia sulcata *and their biological function*. PhD thesis, University of Ulm, Germany.

Wiedenmann, J., Kraus, P., Funke, W. & Vogel, W., 2000a. The relationship between different morphs of *Anemonia sulcata* PENNANT (Anthozoa, Actinaria) evaluated by DNA fingerprinting. *Ophelia*, **52**, 57–64.

Wiedenmann, J., Elke, C., Spindler, K.-D. & Funke, W., 2000b. Cracks in the β-can: fluorescent proteins from *Anemonia sulcata*. *Proceedings of the National Academy of Sciences of the United States of America*, **97**, 14091–14096.

Wiedenmann, J., Röcker, C. & Funke, W., 1999. The morphs of *Anemonia* aff. *sulcata* (Cnidaria, Anthozoa) in particular consideration of the ectodermal pigments. In *Verhandlungen der Gesellschaft für Ökologie*. Vol. 29 (ed. J. Pfadenhauer), pp. 497–503. Heidelberg, Berlin: Spektrum Akademischer Verlag.

VI. Presentation of results

Publications

Gundel, S., Kachalova, G. S., Bartunik, H. D., Fuchs, J., Nienhaus, G. U. & Wiedenmann, J. (2009a). Identification of key residues responsible for high fluorescence intensity in GFP-like proteins. *prepared for publication.*

Gundel, S., Kachalova, G. S., Bartunik, H. D., Fuchs, J., Nienhaus, G. U., Oswald, F. & Wiedenmann, J. (2009b). psRFP – a new photoswitchable red fluorescent protein from *Anemonia sulcata*. *prepared for publication.*

Wiedenmann, J., Leutenegger, A., Gundel, S., Schmitt, F. D'Angelo, C. & Funke, W. (2007) Long-term monitoring of space competition among fluorescent and nonfluorescent sea anemones in the Mediterranean Sea. *Journal of Marine Biological Association of the United Kingdom*, 87, 851-852.

Leutenegger, A., Kredel, S., Gundel, S., D'Angelo, C., Salih, A. & Wiedenmann, J. (2007). Analysis of fluorescent and non- fluorescent sea anemones from the Mediterranean Sea during a bleaching event. *Journal of Experimental Marine Biology and Ecology*, 353, 221-234.

Poster and oral presentations

Gundel, S., Gamber, M., Ivanchenko, S., Oswald, F.,Nienhaus, G.U. & Wiedenmann, J. *"Non-bioluminescent, azooxanthellate Anthozoa as source of green and red fluorescent marker proteins"* Conference on Calcium Regulated Photoproteins and Green-Fluorescent Proteins, Friday Harbor Labs, University of Washington, Posterpresentation/Abstract (2004).

Gundel S., Nienhaus, G. U. & Wiedenmann, J. *"Key residues responsible for red fluorescence in a GFP-like protein"* Conference on Genetically Engineered Probes for Biomedical Applications, San Jose, CA, USA, Oral presentation/Abstract (2006).

Gundel S., Nienhaus, G. U. & Wiedenmann, J. *"Functional relations between GFP-like chromoproteins and red fluorescent proteins"* Conference on Molecular Imaging/Probes for Contrast and Molecular Reporting I, Munich, Germany, Oral presentation/Abstract (2007).

VII. Danksagung

Herrn Prof. Dr. Klaus-Dieter Spindler gebührt mein aufrichtiges Dankeschön für die Übernahme des Erstgutachtens und die großartige Unterstützung v. A. bei der Fertigstellung der Dissertation, die freundliche Aufnahme in das Institut für Allgemeine Zoologie und Endokrinologie bereits zu Hiwi-Zeiten und die Möglichkeit nach dem Weggang meines Arbeitsgruppenleiters sowohl Labor- als auch Schreibplatz weiterhin nutzen zu dürfen.

Bei Herrn Prof. Dr. Wolfgang Weidemann möchte ich mich für sein Interesse am Thema und die Übernahme des Zweitgutachtens bedanken.

Das Thema der vorliegenden Arbeit wurde mir von Herrn Dr. J. Wiedenmann überlassen. Insbesondere wurden die Konzepte zur Herstellung reversibel schaltbarer Fluoreszenzproteine, deren Verbesserung durch Mutagenese sowie die biochemische und spektroskopische Charakterisierung der bearbeiteten Fluoreszenzproteine und deren Anwendung als zelluläre Marker von ihm erarbeitet. Herr Dr. J. Wiedenmann betreute die experimentellen Arbeiten, welche an der Universität Ulm durchgeführt wurden und trug zur Betreuung der Arbeiten der Strukturanalyse bei, die in Zusammenarbeit mit der AG Dr. H. Bartunik in Hamburg durchgeführt wurde.

Die Arbeiten an den Fluoreszenzproteinen wurden aus Mitteln der Landesstiftung Baden-Württemberg (Elite Postdoc Programm, Dr. J. Wiedenmann), der DFG (Wi1990/2-1 Dr. J. Wiedenmann) und aus Mitteln des Instituts Allgemeine Zoologie und Endokrinologie (Institutsmittel Dr. J. Wiedenmann) finanziert.

Darüber hinaus wurden mir große wissenschaftliche Freiheiten bei der Durchführung der Arbeit und Niederschrift der Dissertation gelassen. Nicht zu vergessen sind die Lehren fürs Leben, die ich aus der Zusammenarbeit ziehen konnte.

Wissenschaftlich fruchtbare Kooperationen sind nur mit Partnern zu verwirklichen, die sich mit entsprechendem Engagement und Herzblut für die Realisierung der gemeinsamen Projekte einsetzen. Für meine beiden wichtigsten Kooperationspartner Dr. Hans Dieter Bartunik und Dr. Galina Kachalova (Max-Planck-Arbeitsgruppe für strukturelle Molekularbiologie, AG Proteindynamik, DESY, Hamburg) trifft das glücklicherweise zu. Ohne die unkomplizierte, schnelle und unbürokratische Hilfe bei der Strukturaufklärung wäre ein bedeutender Anteil meiner Arbeit nicht realisierbar gewesen.

Ein großes Dankeschön geht an PD Dr. Franz Oswald und sein Team aus der Inneren Medizin I für die Unterstützung im Bereich der Zellkultur und Mikroskopie.

Im Weiteren möchte ich mich bei Herrn Prof. Dr. G. U. Nienhaus und den Mitarbeitern des Instituts für Biophysik für die Bereitstellung von Equipment und Know-how für die Experimente zur spektralen Charakterisierung bedanken. Ein spezielles Dankeschön geht hier an Jochen, den „Mess"-Fuchs, der mich an seinem großen Wissen über schaltbare FPs und deren Eigenschaften teilhaben hat lassen. Somit blieb mir manch stundenlange Recherche erspart!

Meinen beiden lieb gewonnenen Freundinnen und Laborkollegen Simone und Alex möchte ich für die lustige Zeit im Labor und in unserem „Massengrab" sowie die Unterhaltungen auf dem Raucherbalkon (obwohl ihr Nichtraucher seid!) und Euer fleißiges Korrekturlesen danken. Eure unermüdliche Diskussionsbereitschaft (nicht nur zum Thema fluoreszierende Proteine) hat mir immer weitergeholfen – saßen wir doch alle im selben Boot! Ich danke Euch für Eure wahre Freundschaft, in Zeiten, die sich sehr verändert haben.

Für die Übernahme unglaublich vieler Arbeiten im Labor (hektoliterweise Herstellung von 2xYT-Medium, Zentrifugation unzähliger Bakterienkulturen, Matrix-Regeneration im Marschtempo etc.), ihre gute Laune und ihr immer offenes Ohr gebührt Maja ein ganz herzliches Dankeschön.

Bei allen anderen Mitarbeitern des Instituts für Allgemeine Zoologie und Endokrinologie, allen voran der lieben, hilfsbereiten und fleißigen Heidi, möchte ich mich für die Unterstützung und das angenehme Arbeitsklima bedanken.

An Lars, den Retter in der Not bei versagenden Festplatten oder Laptops, geht ein besonderes Dankeschön für die unkomplizierte Bereitstellung von Rechenleistung und die vielen aufmunternden Worte bei diversen Kaltschalen.

Meinen Freunden Kordula, Nobbes, Steffi und Philipp, Christian und Gitti, Tanne und Alex, Malon und Serdar, Tom, Vivien und Robbie, Peter und all den anderen, die ich vergessen habe, danke ich dafür, dass sie immer für mich da waren, und mir gezeigt haben, dass es auch ein Leben außerhalb des Labors gibt.

Die allergrößte Dankbarkeit gebührt meiner Family!!! Und zwar dafür, dass sie immer hinter meinen Entscheidungen steht und mir unermessliche Geduld, unendliches Vertrauen und riesige Unterstützung schon während meines ganzen Studiums entgegengebracht hat – ohne Euch wäre ich nicht dort, wo ich heute bin!

Für drei Jahre finanzielle und darüber hinausgehende ideelle Unterstützung, die nur eine solche Institution vermitteln kann, möchte ich mich bei der Deutschen Telekom Stiftung bedanken. Mein ganz besonderer Dank gilt Herrn Dr. Klaus Kinkel, dem „Stiftungsmacher" und Wegbereiter, Herrn Dr. Ekkehard Winter meinem persönlichen Mentor und Förderer sowie Frau Christiane Frense-Heck, der Projektleiterin des Stipendiatenprogrammes und meine unmittelbare Ansprechpartnerin auf dem kurzen Dienstweg.

VIII. Curriculum vitae

Silke Gundel

■ Persönliche Daten

Geburtsdatum	14.02.1977
Geburtsort	Dillingen/Donau
Konfession	evangelisch

■ Ausbildung

1993	Mittlere Reife (Realschule Erbach)
1997	Allgemeine Hochschulreife (Gymnasium Ehingen)

■ Studium

10/1997 - 07/2004	Biologiestudium an der Universität Ulm
	Studienschwerpunkte: Zoologie, Mikrobiologie, Anthropologie, Mathematik Abschluss: Diplom

■ Promotion

seit 10/2004	Promotion (Dr. rer. nat.) an der Universität Ulm am Institut für Allgemeine Zoologie und Endokrinologie in Zusammenarbeit mit der Max-Planck-Arbeitsgruppe für strukturelle Molekularbiologie (AG Proteindynamik, Leiter: Dr. Bartunik) DESY (Deutsches Elektronen-Synchrotron), Hamburg sowie dem Institut für Biophysik, Leiter: Prof. Dr. Nienhaus und der Abteilung Innere Medizin I, AG Molekulare Transkriptionskontrolle, Leiter: PD Dr. Oswald, Universität Ulm

■ Stipendium

02/2005 – 01/2008	Deutsche Telekom Stiftung (Promotionsstipendium)

Ulm, den 27.07.09

Jeder Mensch bekommt nur die Hindernisse in den Weg gestellt, die er zu bewältigen und überwinden in der Lage ist.

Ingrid van Bergen